

ACTIVATION-DEPENDENT ENHANCEMENTS OF SYNAPTIC STRENGTH IN
PYRIFORM CORTEX EFFERENTS TO THE ENTORHINAL CORTEX.

by

CLIFTON ANDREW CHAPMAN, B.Sc.

A Thesis Submitted to the School of Graduate Studies
in Partial Fulfillment of the Requirements for the Degree

Doctor of Philosophy.

McMaster University

Copyright © 1995 by C.A.Chapman.

DOCTOR OF PHILOSOPHY (1995)
(Psychology)

McMASTER UNIVERSITY
Hamilton, Ontario, Canada

TITLE: Activation-dependent enhancements of synaptic strength in pyriform
cortex efferents to the entorhinal cortex.

AUTHOR: Clifton Andrew Chapman, B.Sc. (University of Toronto).

SUPERVISOR: Dr. Ronald J. Racine

NUMBER OF PAGES: xiii, 283

SYNAPTIC PLASTICITY IN THE ENTORHINAL CORTEX

ABSTRACT

The entorhinal cortex is reciprocally connected with both neocortical sensory areas and the hippocampal formation, and is thought to play a pivotal role in learning and memory. Changes in synaptic strength are thought to provide the major neurophysiological basis for memory formation, but little is known about synaptic plasticity in the entorhinal cortex. The objectives of this research were to provide a basis for the interpretation of evoked potentials recorded from the entorhinal cortex following pyriform (primary olfactory) cortex stimulation *in vivo*, and to determine the conditions under which synaptic enhancements in this pathway may occur and contribute to lasting changes in the processing of olfactory information. The synaptic currents which generate field potentials in the entorhinal cortex following pyriform cortex and medial septal stimulation were first localized to the superficial layers of the entorhinal cortex using current source density analysis techniques in the anesthetized rat. This allowed changes in the strength of these synaptic inputs to be monitored in the awake rat by measuring evoked field potential amplitudes at a single cortical depth. Long-term synaptic potentiation (LTP) in this pathway was reliably induced following stimulation of the pyriform cortex with either epileptogenic stimuli, or with prolonged subconvulsive high-frequency trains. Further, stimulation which results in short-term frequency potentiation effects, was found to increase the amount of LTP induced. Concurrent stimulation of the medial septum at a frequency similar to that of the endogenous theta rhythm also

resulted in a cooperative enhancement of the LTP produced. Computational modelling techniques were then used to formalize the heterosynaptic contribution of frequency potentiating medial septal inputs to Hebbian synaptic modification in entorhinal cortex. These results indicate that the frequency of rhythmic activity in sensory afferents and the activity of the medial septum may play critical roles in the regulation of synaptic plasticity in the entorhinal cortex.

ACKNOWLEDGEMENTS

I would like to thank Dr. Ronald J. Racine for supervising this Thesis and my other research efforts in his laboratory. The guidance of Dr. Susanna Becker was of great value to the modelling work in Chapter 5 and has also been highly appreciated. This thesis was supported by financial assistance from the Natural Sciences and Engineering Research Council of Canada, the Ontario Graduate Scholarship program, and the McMaster University Department of Psychology.

TABLE OF CONTENTS

Page	
Abstract.....	iii
Acknowledgements.....	v
List of Illustrations.....	viii
List of Abbreviations.....	xiii
Chapter 1. Introduction.....	1
1.1 Cortico-Hippocampal Interactions in Memory Formation.....	1
1.2 The Entorhinal Cortex and Memory.....	8
1.3 Memory and Synaptic Plasticity.....	20
1.4 Neuromodulatory and Temporal Factors Affecting LTP Induction.....	29
1.5 Synaptic Plasticity in Olfactory Inputs to the Entorhinal Cortex.....	41
Chapter 2. Spatial Distribution of Synaptic Currents in the Entorhinal Cortex Following Pyriform Cortex and Medial Septal Stimulation...	51
Chapter 3. Paired-Pulse and Frequency Potentiation of Synaptic Responses in the Entorhinal Cortex Following Pyriform Cortex and Medial Septal Stimulation.....	93
Chapter 4. Long-Lasting Potentiation of Synaptic Responses in the Entorhinal Cortex Following Pyriform Cortex Stimulation.....	146
4.1 Kindling-Induced Potentiation of Synaptic Inputs from the Pyriform Cortex to the Entorhinal Cortex	152
4.2 Long-Term Potentiation of Synaptic Inputs from the Pyriform Cortex to the Entorhinal Cortex	168
4.3 Enhancement of Long-Term Potentiation of Pyriform Cortex Efferents to the Entorhinal Cortex by Coactivation of the Medial Septum.....	192

Chapter 5. Hebbian Learning in a Neural Network Model Incorporating Frequency Potentiating Synapses.....	210
5.1 Synaptic Modelling.....	214
5.2 Network Modelling.....	221
Chapter 6. General Discussion.....	239
References.....	250

LIST OF ILLUSTRATIONS

<u>Figure</u>		<u>Page</u>
<u>Figure 2.1.</u>	Histological results for stimulating electrode placements.....	71
<u>Figure 2.2.</u>	Histological results for recording electrode placements and a photomicrograph of a representative section.....	72
<u>Figure 2.3.</u>	Frequency of following test for field potentials recorded in the entorhinal cortex following pyriform cortex stimulation.....	73
<u>Figure 2.4.</u>	Field potentials as a function of depth in the entorhinal cortex following single-pulse stimulation of the pyriform cortex.....	74
<u>Figure 2.5.</u>	Field potentials as a function of depth in the entorhinal cortex following double-pulse stimulation of the pyriform cortex.....	75
<u>Figure 2.6.</u>	Results of current source density analysis of the data shown in Figure 2.4.....	76
<u>Figure 2.7.</u>	Results of current source density analysis of the data shown in Figure 2.5.....	77
<u>Figure 2.8.</u>	Mean current source density analysis results for field potentials in the entorhinal cortex following pyriform cortex stimulation.....	78
<u>Figure 2.9.</u>	Field potentials as a function of depth in the entorhinal cortex following single-pulse stimulation of the medial septum.....	79
<u>Figure 2.10.</u>	Field potentials as a function of depth in the entorhinal cortex following double-pulse stimulation of the medial septum.....	80

<u>Figure 2.11.</u>	Results of current source density analysis of the data shown in Figure 2.9.....	81
<u>Figure 2.12.</u>	Results of current source density analysis of the data shown in Figure 2.10.....	82
<u>Figure 2.13.</u>	Mean current source density analysis results for field potentials in the entorhinal cortex following medial septal stimulation.....	83
<u>Figure 3.1.</u>	Histological results for the locations of stimulating and recording electrodes.....	115
<u>Figure 3.2.</u>	Field potentials in the entorhinal cortex evoked by pyriform cortex and medial septal stimulation during input/output testing.....	116
<u>Figure 3.3.</u>	Mean input/output curves for responses evoked by pyriform cortex and medial septal stimulation before and after paired-pulse and frequency potentiation testing.....	117
<u>Figure 3.4.</u>	Field potentials in the entorhinal cortex recorded during paired-pulse stimulation of the pyriform cortex.....	118
<u>Figure 3.5.</u>	Mean facilitation of entorhinal cortex responses during paired-pulse stimulation of the pyriform cortex.....	119
<u>Figure 3.6.</u>	Field potentials in the entorhinal cortex recorded during paired-pulse stimulation of the medial septum.....	120
<u>Figure 3.7.</u>	Mean facilitation of entorhinal cortex responses during paired-pulse stimulation of the medial septum.....	121
<u>Figure 3.8.</u>	Field potentials in the entorhinal cortex recorded in response to test-pulses delivered to the pyriform cortex following the delivery of conditioning-pulses to the medial septum.....	122

<u>Figure 3.9.</u>	Mean facilitation of entorhinal cortex responses to test-pulses delivered to the pyriform cortex following the delivery of conditioning-pulses to the medial septum.....	123
<u>Figure 3.10.</u>	Field potentials in the entorhinal cortex recorded in response to test-pulses delivered to the medial septum following the delivery of conditioning-pulses to the pyriform cortex.....	124
<u>Figure 3.11.</u>	Mean facilitation of entorhinal cortex responses to test-pulses delivered to the medial septum following the delivery of conditioning-pulses to the pyriform cortex.....	125
<u>Figure 3.12.</u>	The results of occlusion testing with low- and high-intensity stimulation pulses.....	126
<u>Figure 3.13.</u>	Field potentials in the entorhinal cortex recorded in response to the first and the last pulses in low-frequency trains delivered to the pyriform cortex and the medial septum.....	127
<u>Figure 3.14.</u>	Mean facilitation of entorhinal cortex responses during low-frequency pyriform cortex and medial septal stimulation as a function of stimulation train frequency.....	128
<u>Figure 4.1.</u>	Histological results for the locations of stimulating and recording electrodes.....	160
<u>Figure 4.2.</u>	Field potentials recorded during input/output testing before and after treatment in a control and a kindled animal.....	161
<u>Figure 4.3.</u>	Mean input/output curves for the control and kindled groups before and after treatment.....	162
<u>Figure 4.4.</u>	Mean evoked potential amplitudes as a function of days after the start of the kindling period for the control and kindled groups.....	163
<u>Figure 4.5.</u>	Histological results for the locations of stimulating and recording electrode placements.....	181

<u>Figure 4.6.</u>	The mean amplitude of entorhinal cortex field responses evoked by pyriform cortex test-pulses during three induction procedures.....	182
<u>Figure 4.7.</u>	Averaged evoked potentials obtained during three LTP induction procedures.....	183
<u>Figure 4.8.</u>	Two examples of field potentials in the entorhinal cortex evoked by pyriform cortex stimulation during input/output tests on the day before and the day after LTP induction.....	184
<u>Figure 4.9.</u>	Mean input/output curves before and after treatment for the three groups.....	185
<u>Figure 4.10.</u>	Mean evoked potential amplitudes as a function of days after LTP induction for the three groups.....	186
<u>Figure 4.11.</u>	Histological results for the locations of stimulating and recording electrode placements.....	199
<u>Figure 4.12.</u>	The mean amplitude of entorhinal cortex field responses evoked by pyriform cortex test-pulses during tests of the effects of medial septal stimulation on LTP induced by pyriform cortex stimulation.....	200
<u>Figure 4.13.</u>	Averaged evoked potentials obtained during tests of the effects of medial septal stimulation on LTP induced by pyriform cortex stimulation.....	201
<u>Figure 4.14.</u>	Field potentials in the entorhinal cortex evoked by pyriform cortex or medial septal stimulation during input/output tests on the day before and the day after LTP induction.....	202
<u>Figure 4.15.</u>	Mean input/output curves for pyriform cortex stimulation on the day before and the day after LTP induction, and the mean evoked potential peak amplitude as a function of days after LTP induction.....	203

<u>Figure 4.16.</u>	Mean input/output curves for medial septal stimulation on the day before and the day after LTP induction, and the mean evoked potential peak amplitude as a function of days after LTP induction.....	204
<u>Figure 5.1.</u>	The potential connection weight strength following a single input at $t=0$ in two synaptic models; one with and one without the slow hyperpolarizing component.....	228
<u>Figure 5.2.</u>	Frequency response characteristics of the two synaptic models.....	229
<u>Figure 5.3.</u>	Schematic representations of the two network architectures used in separate neural network simulations.....	230
<u>Figure 5.4.</u>	Changes in mean connection weights when pyriform cortex inputs were presented either constantly, or in synchrony with medial septal inputs.....	231
<u>Figure 5.5.</u>	Entorhinal cortex mean activation values in response to the four pyriform cortex input patterns during training of the network shown in Figure 5.3A.....	232
<u>Figure 5.6.</u>	Entorhinal cortex unit activation values in response to each of the four pyriform cortex input patterns following training of the network model shown in Figure 5.3B.....	233

LIST OF ABBREVIATIONS

AMPA	α -amino-3-hydroxy-5-methyl-4-isoxazolepropionate
ANOVA	analysis of variance
AP5	D-2-amino-5-phosphonopentanoate
APV	2-amino-5-phosphonovalerate
CA1	hippocampal area <i>cornu amonius</i> 1
Ca ²⁺	calcium
Cl ⁻	chloride
CNQX	6-cyano-7-nitroquinoxaline-2,3-dione
C-pulse	conditioning-pulse
CSD	current source density
EEG	electroencephalograph
EPSP	excitatory post-synaptic potential
GABA	gamma aminobutyric acid
I/O	Input/output
IPSP	inhibitory post-synaptic potential
K ⁺	potassium
LTP	long-term synaptic potentiation
Mg ²⁺	magnesium
Na ⁺	sodium
NMDA	N-methyl-D-aspartate
T-pulse	testing pulse

CHAPTER 1

GENERAL INTRODUCTION

1.1 CORTICO-HIPPOCAMPAL INTERACTIONS IN MEMORY FORMATION.

Both the neocortex and the hippocampal formation, an allocortical temporal lobe structure, appear to play important roles in learning and memory in the mammalian brain. The putative roles of these structures in memory formation are described below, and the contribution of the entorhinal cortex, which is reciprocally connected with the neocortex and hippocampal formation, is discussed in the following section.

The Role of the Hippocampus. The most striking evidence that the hippocampal region is critical to long-term memory formation was obtained in neuropsychological studies of human patients suffering bilateral lesions of the hippocampus and related inferior temporal lobe cortical structures (Scoville & Milner, 1957; Penfield & Milner, 1958). These patients displayed both retrograde and anterograde amnesia. Retrograde amnesia was expressed as an inability to recall memories formed over roughly a three year period prior to surgery, and anterograde amnesia as an inability to form new memories accessible to conscious retrieval after the lesion. The severity of the memory impairments were positively related to the extent of the hippocampal removal. While the patients could acquire new motor skills, and their intellectual and technical abilities were relatively unaffected, patients with these lesions could not maintain a conscious recollection of events experienced after the lesion for more

than a period of a few minutes (Scoville & Milner, 1957; Penfield & Milner, 1958; Corkin, 1968). These results suggest that the hippocampus is critical for the processing of memories that are normally accessible to conscious recollection (Press et al., 1989; Squire, 1992). Similar impairments have also been observed more recently in a patient suffering selective cell loss in the CA1 region of the hippocampus following a period of ischemia (Zola-Morgan et al., 1986).

These findings sparked a great interest in the role of the hippocampus in memory formation, and the use of animal models to further analyze deficits in memory performance following lesions of the hippocampal region (Mishkin, 1978). A common test used to assess memory in monkeys is the delayed nonmatching to sample test. In this task, the animal is first shown an object (the sample), and after a variable delay, the monkey is shown the same object paired with a second object. The monkey's task is to remember the sample for the duration of the delay, and then to obtain a food reward by choosing the novel object. At delays of only seconds between the sample and the test both control animals and animals with lesions to the hippocampal region perform correctly on about 90% of trials. However, at delays longer than 10 min, animals with damage restricted to the hippocampus, dentate gyrus and subiculum are impaired in this task (Zola-Morgan & Squire, 1986; Squire & Zola-Morgan, 1991; Clower et al., 1991; Zola-Morgan et al., 1992).

Hippocampal damage also results in memory impairments in other animals, and memory for spatial location is particularly affected in rats following hippocampal lesions. For example, memory for the location of a hidden platform is severely impaired in rats with hippocampal lesions in the Morris water maze task (Morris et al., 1982). In this task animals are placed in a

circular pool of opaque water at starting points which vary over successive trials, and the latency for the rat to escape the water by finding a submerged platform is recorded. While control animals can use available extramaze spatial cues to learn a representation of the location of the hidden platform, rats with bilateral hippocampal lesions perform poorly on this task (Morris et al., 1982). Rats with hippocampal lesions are also impaired on the radial arm maze task in which the animal must visit multiple arms of a dry maze in order to obtain food rewards. Because animals must remember which arms have already been visited in order to complete a given trial efficiently, the impairments in this task which follow hippocampal damage suggest that a form of short-term, "working memory" is mediated in part by the hippocampus (Olton et al., 1979; Olton & Feustle, 1981). Memory impairments in rats following hippocampal damage are not strictly spatial, however, since impairments are also observed in the ability to remember discriminations between simultaneously presented odours following fornix transections which disrupt hippocampal functioning (Eichenbaum et al., 1988).

The behavioural impairments which follow hippocampal lesions in experimental animals suggest that hippocampus contributes to the formation of lasting memories which require maintained representations of stimuli and the associations between them (O'Keefe & Nadel, 1979; Sutherland & Rudy, 1989; Squire & Zola-Morgan, 1991; Eichenbaum, 1992; Eichenbaum et al., 1992). The preservation of perception and short-term memory in humans following hippocampal damage (Scoville & Milner, 1957; Penfield & Milner, 1958), and the good performance of lesioned animals at short delays in the delayed nonmatching to sample task (Zola-Morgan & Squire, 1986), suggest that some other site in the brain must support perception and short-term memory.

Further, because retrograde amnesia following hippocampal damage in humans has a limited extent, up to about 3 years, before the lesion (Scoville & Milner, 1957), the hippocampus appears to be neither the permanent site of long-term memory storage, nor a structure required for the retrieval of long-term memory.

Cortico-Hippocampal Interactions. Access to sensory input and complexity in neural circuitry have made the neocortex the putative site for perception, short-term memory, and the storage of long-term memories. Various neocortical areas were targeted by Lashley (1950) in an attempt to localize the storage site of memories learned in visual discrimination and maze learning tasks in rats. The approach was to first train the animals on one of a variety of tasks, perform a lesion of a particular cortical area, and then to re-test the animal's performance on the same task. Cortical ablations did result in memory impairments, but the degree of the impairment depended not on the precise location of the lesion, but on its size (Lashley, 1950). Lashley's observations led to the conclusion that while limited regions of the cortex may be necessary for the acquisition and retention of a given task, the memory for the task is distributed throughout the cortical region. While the aim of these studies was the localization of the memory trace, or *engram*, the general conclusion which resulted was the principle of equipotentiality. This principle suggests that there is a functional equivalence of cortical tissue within a given region, and that memories have widespread or redundant representations in the cortex. The notion that long-term memory is stored in the neocortex is also consistent with the retrograde amnesia observed in the advanced stages of Alzheimer's Disease which is correlated with diffuse neuronal damage in neocortical areas (Terry & Davies, 1980).

The involvement of the hippocampus in memory formation, and the apparent role of the neocortex in the storage of long-term memory, has led to a number of theories regarding the ways that these structures may interact during learning and memory. Because hippocampal damage results in deficits in the ability to form and maintain new associations between environmental stimuli and events (Sutherland & Rudy, 1989; Squire & Zola-Morgan, 1991; Eichenbaum, 1992; Eichenbaum et al., 1992), it has usually been proposed that the hippocampus first combines distinct sensory features of environmental stimuli and events arriving from different cortical regions. Following the association or integration of these memory components by the hippocampus, the representation is then stored more permanently in the cortical regions which first supplied the sensory input.

An early view of this type was held by Marr (1971) who proposed that the hippocampus was responsible for forming associations between separate sensory inputs, and for the instantaneous but temporary storage of new information. By providing a temporary store for memory, the hippocampus could reduce the computational demands on the neocortex by transferring representations back to the cortex only if the information was later determined to be appropriate for long-term storage (Marr, 1971). This general idea of the hippocampus as a short-term store which can hold representations for later storage in the neocortex is a view still maintained by more recent authors (Eichenbaum & Otto, 1992; Squire & Zola-Morgan, 1991).

Teyler and DiScenna (1986) proposed that the hippocampus forms an integrated representation of a sensory event by creating an *index* of the cortical areas which are activated during the initial sensory input. Through projections from the hippocampus to the neocortex, the reactivation of a given hippocampal

index would lead to an appropriate spatio-temporal pattern of cortical activation, and the recall of the memory associated with the index. Similarly, recognition memory could result from the partial activation of some of the neural components of the hippocampal index by sensory input sharing some characteristics with the stored information. The index could then become fully activated through intrinsic hippocampal connections, and to lead to the stimulation of the cortical areas associated with the memory. While, in this theory, the hippocampus serves a critical role in recall and recognition, the associations between components of a memory which give it meaning are thought to be mediated by cortico-cortical connections linking the separate cortical areas. In addition, the repeated activation of a hippocampal index could lead to a strengthening of the connections between cortical areas so that the functions served by the index would become redundant to the linkages provided by the cortico-cortical connections. In this way, the storage and retrieval of memory could eventually become independent of the hippocampus (Teyler & DiScenna, 1986; Rolls, 1989).

Theories of this type explain why hippocampal damage results in only partial retrograde amnesia for memory. Because the hippocampus is thought to contribute to the reactivation of memories which are not yet fully consolidated in neocortical areas, damage to the hippocampus will interfere with the recall of recent memories, but not memories from the distant past. The most striking case of amnesia following bilateral hippocampal lesions, reported by Scoville and Milner (1957), showed global retrograde amnesia extending 19 months prior to surgery, and partial amnesia for up to 3 years. The period during which memory is consolidated in cortical areas may be shorter in the monkey since memories initially depending on the functioning of the hippocampal formation

gradually become insensitive to hippocampal damage over a period of weeks (Zola-Morgan & Squire, 1990). However, the time required for a memory to be consolidated may be reduced to the extent that circuitry supporting its storage in the neocortex is frequently reactivated (Teyler & DiScenna, 1986). Features of cortico-hippocampal interactions in memory function, then, are generally thought to include (1), a role for the hippocampus in the fast acquisition of associational information through a binding or indexing of discrete cortical components of sensory representations, (2), hippocampal mechanisms which maintain and retrieve recently formed memories through access to cortical memory elements, and (3) the eventual storage of memories in diffuse regions of the neocortex and their retrieval by mechanisms extrinsic to the hippocampus, likely through cortico-cortical associational pathways.

Because of the importance of the interactions between the hippocampus and the neocortex in memory formation, the cortical areas which likely mediate these interactions are of great theoretical interest. Memory studies in monkeys using the delayed nonmatching to sample test have indicated that inferotemporal cortical areas which link the neocortex and hippocampus (Witter et al., 1989), may contribute just as critically to the formation of long-term memory as does the hippocampus (Squire & Zola-Morgan, 1991). Early studies of the memory impairments in monkeys which follow hippocampal lesions indicated that the deficits were greatly exacerbated when the lesions included the amygdala, another subcortical temporal lobe structure (Mishkin, 1978). Direct surgical excision of these regions, however, also removed portions of the surrounding cortical areas, including the entorhinal, perirhinal, and parahippocampal cortices. More selective surgical techniques have recently been used to show that lesions restricted to the

hippocampus and amygdala do not result in impairments greater than those observed in animals with restricted hippocampal lesions alone (Zola-Morgan et al., 1989a). Further, only mild deficits in performance in a delayed nonmatching to sample test are observed following combined hippocampal and amygdalar lesions in rats (Mumby et al., 1992). However, when hippocampal lesions in monkeys are extended to include portions of the perirhinal, parahippocampal, and entorhinal cortices while sparing the amygdala, the memory impairments are just as severe as those which follow combined, unrestricted lesions of the hippocampus and the amygdala (Clower et al., 1990). Further, lesions which damage only the perirhinal and parahippocampal cortices without lesioning the hippocampus, entorhinal cortex or amygdala, result in impairments similar to animals with the more widespread damage (Zola-Morgan et al., 1989b). These results indicate that the extrahippocampal cortical areas in the temporal lobe may not only contribute to learning and memory by mediating communication between the neocortex and the hippocampus, but may also serve mnemonic functions additional to those supported by the hippocampus.

1.2 THE ENTORHINAL CORTEX AND MEMORY.

Inputs from widespread cortical regions reach the hippocampal formation through the perirhinal, parahippocampal and entorhinal cortices of the temporal lobe (Witter et al., 1989). The inputs to the hippocampal formation from the perirhinal and parahippocampal areas are not direct, however, and are mediated by synaptic connections in the entorhinal cortex. The entorhinal cortex is therefore anatomically well-positioned to play a pivotal role in the integration of multimodal sensory representations thought to be carried out by

the hippocampal formation. Further, because much of the output of the hippocampal formation reaches neocortical areas via the entorhinal cortex, this structure could also contribute to the way in which long-term memory is stored in the neocortex.

Anatomical Connections of the Entorhinal Cortex. The entorhinal cortex (Brodmann's area 28), is a 6-layered mesocortical region positioned on the caudo-ventral surface of the temporal lobe. The layering of the entorhinal cortex is similar to that of the neocortex but it has an additional cell-sparse layer called the lamina dissecans which partitions the superficial and deep layers. The medial and lateral portions of the entorhinal cortex can be differentiated both on cytoarchitectonic grounds and by the connections these regions have with the hippocampus and neocortical regions (Witter, 1993; Witter et al., 1989).

Layer I is the most superficial layer and is composed primarily of axonal fibers and very few cell bodies. Layer II contains the most densely-packed cells in the entorhinal cortex and contains mostly stellate cells, although pyramidal and other non-pyramidal neurons are also present (Germroth et al., 1989; Lingenhof & Finch, 1991). The cells of layer II tend to be grouped in small clusters or islands in the lateral entorhinal area, but the neurons in the medial entorhinal area are less densely packed and do not cluster distinctly. Layer III is relatively thick, contains mostly loosely packed pyramidal neurons, and is separated from the deep layers of the entorhinal cortex by the lamina dissecans. Layer IV is a thin layer of large, scattered pyramidal neurons while layer V is thicker and contains smaller pyramidal cells. Layer VI is the deepest layer and contains polymorphic non-pyramidal cells (Kohler, 1986; Amaral et al., 1987; Lingenhof & Finch, 1991). Intrinsic axonal projections originating in the superficial layers within both the medial and lateral entorhinal cortex tend to

project along the cortical plane, while axons of deep entorhinal cortex neurons have widespread termination fields in both deep and superficial layers (Kohler, 1986, 1988).

i) Reciprocal Connections with Cortical Areas. The entorhinal cortex receives inputs from both cortical and subcortical areas, and in turn, reciprocates many of these projections (Kosel et al., 1982; Van Hoesen, 1982; Swanson & Kohler, 1986; Witter et al., 1989; Lopes da Silva, 1990). The greatest amount of anatomical evidence for cortical projections to the entorhinal cortex has come from studies of the cat and monkey, but extensive projections have also been observed in the rat.

The perirhinal cortex receives inputs from widespread sensory cortical areas, and in turn, provides a large input to the superficial layers of the entorhinal cortex. These inputs are reciprocated by projections from layers II-IV of the entorhinal cortex (Van Hoesen & Pandya, 1975; Insausti et al., 1987; Witter et al., 1989, 1993; Lopes da Silva et al., 1990). Projections from multimodal association areas in the superior temporal lobe to the entorhinal cortex have also been described for the monkey (Amaral, 1983; Insausti et al., 1987). While many sensory inputs to the entorhinal cortex are mediated by the perirhinal cortex, the superficial layers of the entorhinal cortex also receive inputs from the pyriform cortex, and these inputs are reciprocated by projections from layers II-IV (Krettek & Price, 1977; DeOlmos et al., 1978; Wyss, 1981; Room et al., 1984).

Reciprocal connections are also formed with limbic cortical areas which project to the deep layers of the entorhinal cortex. These areas include the agranular insular cortex, the retrosplenial cortex (Deacon et al., 1983; Wyss & Van Groen, 1992), and the infralimbic cortex (White et al., 1990). Subcortical

inputs to the entorhinal cortex include projections from the thalamic nucleus reuniens (Wouterlood et al., 1990), the medial septum (Alonso & Kohler, 1984), the amygdala (Insausti et al., 1987) and brainstem nuclei (Krettek & Price, 1977; Beckstead, 1978; Witter et al., 1989).

ii) Reciprocal Connections with the Hippocampal Formation. The entorhinal cortex is also closely linked anatomically to the hippocampal formation (Amaral & Witter, 1989). The hippocampus itself is an allocortical structure containing a principal cell layer of pyramidal neurons with extensive dendritic arbour. The hippocampus is composed of areas CA1-CA4, with areas CA3 and CA1 being the largest and the most widely studied. The hippocampal *formation* contains the dentate gyrus, the hippocampal gyrus, and the subicular complex which are linked by a series of intrinsic excitatory projections (Rawlins & Green, 1977; Amaral & Witter, 1989). Axons of granule cells, the principal cells of the dentate gyrus, project to area CA3 of the hippocampus. CA3 pyramidal neurons form recurrent excitatory connections within CA3 and project to area CA1 via the Schaffer collateral system (Ishizuka et al., 1990). The final major intrinsic pathway of the hippocampal formation is the projection from CA1 pyramidal neurons to the subicular complex (Amaral et al., 1991). This general organization is maintained along the entire longitudinal (septo-temporal) axis of the hippocampal formation so that transverse cross-sections of the hippocampal formation display this same general pattern of connectivity. With the exception of the dentate gyrus to CA3 projection, a considerable divergence of these intrinsic pathways along the longitudinal axis of the hippocampal formation is also observed (Amaral & Witter, 1989).

The input from entorhinal cortex to the hippocampal formation is carried by the perforant path which contains mainly fibers of layer II stellate cells,

but also layer II non-stellate cells, and layer III pyramidal cells (Steward & Scoville, 1976; Germroth, 1989, 1991). Cells in the lateral portions of both the medial and lateral entorhinal area project more strongly to the dorsal aspect of the hippocampus, while the ventral hippocampal formation tends to receive more inputs from the medial entorhinal cortex (Witter & Groenewegen, 1984; Amaral & Witter 1989). Layer II entorhinal cortex neurons reach the dentate gyrus, areas CA3 and CA1, while layer III neurons terminate exclusively in area CA1 and the subiculum (Steward & Scoville, 1976; Witter, 1993). The dendritic termination fields within separate divisions of the hippocampal formation differ for the cells of the medial and the lateral entorhinal areas. Perforant path inputs from the medial entorhinal cortex terminate in the middle one third of the molecular layer of the dentate gyrus and the stratum lacunosum-moleculare of the CA3 and CA1 fields. In contrast, the lateral entorhinal area projects to the outer one third of these dendritic regions (Van Hoesen & Pandya, 1975).

The inputs to the hippocampal formation are reciprocated by projections from area CA1 and the subicular complex to both the medial and lateral entorhinal areas. The CA1 projections terminate in the deep layers of the entorhinal cortex, particularly in layer IV (Swanson & Cowan, 1977; Beckstead, 1978; Room & Goenewegen, 1986). Both deep and superficial layers are reached by the subicular complex, but the patterns of termination differ for each component of the subicular complex. The subiculum itself terminates in all layers of the entorhinal cortex with particularly prominent projections to layer IV of the medial entorhinal area (Sorensen & Shipley, 1979; Kohler, 1985). The presubiculum projects preferentially to the medial entorhinal area, terminating in all superficial layers (Kohler, 1984, 1985; Caballero-Bleda & Witter, 1993). The projections from the parasubiculum reach both the medial and lateral entorhinal

areas but the terminations are mostly restricted to layer II, with some terminals in layer III (Kohler, 1985; Van Groen & Wyss, 1990; Caballero-Bleda & Witter, 1993).

Anatomical data therefore indicate that the entorhinal cortex is reciprocally connected both with neocortical areas and with the hippocampal formation. In this way, the entorhinal cortex is both the major source of sensory input to the hippocampus and mediates much of the output of the hippocampal formation to cortical areas. In addition to these anatomical considerations, a variety of behavioural results have suggested that the entorhinal cortex contributes to learning and memory processes.

Entorhinal Cortex Involvement in Memory. Studies of the effects of lesions in both man and animals have provided most of the data indicating that the entorhinal cortex is involved in learning and memory. Damage to the entorhinal cortex necessarily interferes with input and output pathways of the hippocampus, however, so that the memory impairments that result from entorhinal cortex lesions may result from disrupted functioning of the entorhinal cortex, the hippocampus, or of both. However, there are some suggestive correlates between entorhinal cortex damage and human dementia, and some animal studies which point to differences in the contributions of the entorhinal cortex and the hippocampus to learning and memory.

Dementias in man associated with memory impairments are well correlated with entorhinal cortex damage. Although Alzheimer's disease results in widespread degeneration of neocortical areas and of neuromodulatory systems, the entorhinal cortex is invariably affected and is the most severely damaged cortical site (Van Hoesen et al., 1991). In fully developed Alzheimer's disease, damage to the entorhinal cortex is often apparent upon simple visual

inspection of the surface of the brain. Further, entorhinal cortex damage occurs very early in the disease, so that this damage may underlie early-developing memory impairments which include confusion and the inability to recall daily events (Jellinger et al., 1991; Van Hoesen et al., 1991). Entorhinal cortex damage also correlates better with the psychological status of aged and Parkinsonian patients than does hippocampal and neocortical damage (Jellinger et al., 1991). Damage in the entorhinal cortex can be specific to certain cell layers. In senile dementia, Down's syndrome, Parkinson's disease, and Alzheimer's disease, layer II is most strongly affected (Braak, 1990; Jellinger et al., 1991). In brains of patients with Alzheimer's disease, neurofibrillary tangles are consistently observed in layers II and IV and are observed less often in layers III, V, and VI (Hyman et al., 1986; Van Hoesen, 1991). In addition, neurofibrillary tangles appear in the dentate gyrus of brains of Alzheimer's patients in the terminal areas of the perforant path (Hyman et al., 1986).

Lesions of the entorhinal cortex in experimental animals are associated with memory deficits but it is unclear to what extent these deficits are due to an interruption of hippocampal inputs. For example, entorhinal cortex lesions have usually been performed in studies of olfactory learning in order to determine the effects of deafferenting the hippocampus. The results of damage to either the entorhinal cortex or the hippocampal system on odour discrimination have been interesting in that, depending on the demands of the task, odour discrimination can be either impaired or facilitated (Gauthier & Soumireu-Mourat, 1981; Eichenbaum, 1992). When animals must discriminate between two simultaneously presented stimuli, fornix lesions or entorhinal cortex lesions impair performance (Eichenbaum et al., 1988). However, when the animal must discriminate between sequentially presented stimuli, performance can be

enhanced following these lesions (Eichenbaum et al., 1988; Otto & Eichenbaum, 1991). Further, in entorhinal cortex lesioned animals, there are no retention deficits up to 65 days after learning (Otto et al., 1991). Concurrent discrimination, but not sequential discrimination, is also impaired in the visual modality following entorhinal or hippocampal lesions in monkeys (Moss et al., 1981). The deficits in concurrent discrimination may be due to a disruption of hippocampal formation-dependent memory processes required to construct representations of the relationships between stimuli, and to make a response choice based on these representations. Successive discriminations do not require simultaneous comparisons, and could be mediated by an extrahippocampal system capable of associating individual stimuli with an appropriate response choice. The facilitation of learning the successive discrimination tasks in animals with hippocampal or entorhinal cortex damage may be due to a tendency of *intact* animals to use the hippocampal-based memory system which may be less efficient than an extrahippocampal system for this task (Otto et al., 1991). This extrahippocampal system cannot involve the entorhinal cortex, however, since entorhinal cortex lesions do not impair successive discrimination performance. In addition to impairments in concurrent discrimination, olfactory learning in rats is impaired following lesions to the entorhinal cortex at long delays in an odour-guided delayed nonmatching to sample task (Otto & Eichenbaum, 1992). These lesions also included portions of the perirhinal cortex, and a comparison of performance deficits following *restricted* entorhinal cortex and hippocampal lesions has not been made.

Studies of performance on the delayed nonmatching to sample task in monkeys indicate that damage to the entorhinal cortex does not add as much to

the impairments which follow hippocampal formation damage as does damage to the perirhinal and parahippocampal cortices. The deficits observed in animals which either receive restricted hippocampal lesions, or lesions which also include the entorhinal cortex, are similar (Squire & Zola-Morgan, 1991; Clower et al., 1991). In addition, the spatial learning deficits in the Morris water maze task which follow entorhinal cortex lesions are similar to those which also follow damage to the hippocampal formation (Schenk & Morris, 1985). Knife-cuts of the perforant path also disrupt learning in the water maze (Skelton & McNamara, 1992), suggesting that the inputs to the hippocampus rather than independent processing within the entorhinal cortex itself is critical for this task. While animals with entorhinal cortex damage or knife cuts do show some improvement with continued training, this appears to be due to the development of procedural swimming strategies for finding the platform, rather than the learning of the spatial location of the platform (Schenk & Morris, 1985; Skelton & McNamara, 1992). Animals with entorhinal cortex lesions are also just as impaired as animals with hippocampal damage when tested on a short-term radial arm maze spatial location recognition task in which the animal must determine which of two arms was not just previously visited (Johnson & Kesner, 1994). Entorhinal cortex lesions also impair simple alternation in a T-maze (Loesche & Steward, 1977; Ramirez & Stein, 1984), and the ability to use short-term recollection of a cue to guide performance in a T-maze (Steward, 1981). The deficits in these tasks may also be due to reduced input to the hippocampus since recovery of alternation performance after unilateral lesions is correlated with reinnervation of the hippocampus by the contralateral entorhinal cortex (Loesche & Steward, 1977).

Animals with entorhinal cortex lesions are also impaired on the radial arm maze task which is thought to measure spatial working memory (Jarrard et al., 1984; Rasmussen et al., 1989; Johnson & Kesner, 1994). In this task, the animals are impaired in the use of the location of extra-maze cues to distinguish which arms have already been visited. The idea that these impairments are due to an interruption of hippocampal inputs is supported by the finding that entorhinal cortex lesions which spare the superficial layers do not interfere with performance (Bouffart & Jarrard, 1988). This further suggests that the deep layers of the entorhinal cortex, and the hippocampal efferents which project to these layers, do not contribute significantly to the performance of this task.

The similarities in the deficits in the previously mentioned tasks which follow entorhinal cortex or hippocampal damage could be due to factors including 1) the dependence of the hippocampal formation on inputs from the entorhinal cortex, 2) a close functional relationship between the memory processes mediated by both structures, or 3) a dependence of the memory processes supported by the entorhinal cortex on further processing by the hippocampus. There are some data, however, which indicate that the entorhinal cortex lesions can result in a somewhat different pattern of impairment in radial arm maze tasks than is observed following hippocampal formation lesions. The data come from cued versions of the radial arm maze in which the goal arms are distinguished not by their spatial location, but by a discriminative stimulus or cue. As indicated above, both hippocampal and entorhinal cortex lesions result in deficits in the performance of the place version of the task. However, performance in cued versions of the task tends to be more affected by entorhinal cortex lesions than by damage to the hippocampal formation (Jarrard et al., 1984; Rasmussen et al., 1989; Johnson & Kesner, 1994). This suggests

that the entorhinal cortex may support some types of non-spatial memory independently of the hippocampus. Further, Kesner's lab (Johnson & Kesner, 1994) has also shown that while hippocampal lesioned animals were able to solve a spatial location matching to sample task in the radial arm maze, animals with entorhinal cortex lesions were unable to learn the task. They interpreted these results to suggest that entorhinal cortex may be essential for guiding the selection of a simple spatial strategy for solving the task.

The most convincing evidence for different roles of the entorhinal cortex and the hippocampus in learning has come from studies in which either drug infusions or electrical stimulation have been applied to these structures at various times following passive and active avoidance training (Gauthier et al., 1982; Ferreira et al., 1992; Izquierdo et al., 1993). Deficits in passive avoidance in the mouse, and passive and active avoidance in the rat are observed following entorhinal cortex lesions (Entigh, 1971; Thompson, 1976; Gauthier & Soumireu-Mourat, 1981). Retention of passive avoidance is also inhibited following infusions into the entorhinal cortex or the hippocampus which either block NMDA receptor mediated glutaminergic transmission, or which enhance GABA_A-mediated inhibition with the drug muscimol. The timing of drug injections plays a critical role, however. When the drugs are infused into the hippocampus shortly after training there is an amnesic effect for habituation and step-down passive avoidance tasks when the animals are tested 18 hr later (Izquierdo et al., 1992). In contrast, when infused into the entorhinal cortex, amnesic effects are observed if the drug is applied 90 or 180 min after training, but not when given 0 or 360 min after training (Ferreira et al., 1992). Further, bilateral electrical stimulation of the entorhinal cortex in the mouse delivered 30 min after training, but not 30 sec or 3 hr, greatly improves 24 hr retention of

operant conditioning for food reward (Gauthier et al., 1982). Retention of a passive avoidance task 24 hr after training, however, is *impaired* when prolonged stimulation is delivered to the entorhinal cortex just after training, but is not impaired by similar stimulation during training (Collier & Routtenberg, 1978). In both the pharmacological and the electrical stimulation studies the experimental manipulation was effective when applied to the entorhinal cortex at some time after training, but not during or just after training. Taken together, these results suggest a role for the entorhinal cortex in the late consolidation of some types of memories, while the hippocampus has more immediate contributions.

Because of the close anatomical links between the entorhinal cortex and the hippocampus, the separate contributions of the entorhinal cortex to the interactions between the hippocampus and cortical areas in memory processes have been difficult to determine. Damage to either the hippocampus or the entorhinal cortex is associated with deficits in tasks which require the integration of sensory information and comparisons between multiple stimuli so that both structures are necessary for the performance of these tasks. The entorhinal cortex does appear to contribute, however, to the consolidation of some skills (Izquierdo et al., 1992; Ferreira et al., 1992) and to tasks requiring simple mnemonic functions (Johnson & Kesner, 1994; Jarrard et al., 1984), perhaps by partially integrating discrete cortical inputs. It is unknown to what extent such a function could contribute to further processing by the hippocampus. As described below, the main neurophysiological mechanism thought to mediate the formation of new memories is the modification of the strength of synaptic connections between neurons. A series of experiments described in this thesis was designed to further our understanding of the physiological mechanisms

which control synaptic plasticity in the entorhinal cortex, and the conditions under which the entorhinal cortex may contribute to learning-related synaptic modifications.

1.3 MEMORY AND SYNAPTIC PLASTICITY

Hebbian Cell Assemblies. The most important theoretical framework for the understanding of how neuronal tissue can serve to represent and store information for later use was provided by Hebb in 1949. Central to his theory was that a percept or memory could be instantiated in the pattern of activation within a neuronal "cell assembly" (Hebb, 1949). A given cell assembly was proposed to comprise a very large number of neurons within a given cortical region. A given percept or memory was proposed to result from a specific temporal pattern of activation within a cell assembly resulting from the pattern of sensory inputs and the synaptic connections between cell assembly elements. The same neurons could participate in multiple cell assemblies, and assemblies representing different elementary perceptual components could be linked together to form more complex multimodal percepts. A transient temporal pattern of sequential activation within a series of cell assemblies could therefore represent complex aspects of the environment.

In Hebb's theory, if the synaptic connections between neurons activated by the initial perception of a stimulus were strengthened, a new cell assembly could be formed to represent that stimulus. If enhancements also occurred in the synaptic connections between separate cell assemblies representing different aspects of a sensory scene, then more complex neural representations would be formed. By virtue of strengthened connections

between different cell assemblies, recall of a complex memory could then occur from the partial activation of some of its components. A second contribution to the development of this theory was Hebb's proposal of a physiological mechanism through which new cell assemblies could be formed during learning. He proposed that a new cell assembly could develop if the connections between its elements were strengthened by their repeated co-activation during and just after the initial perceptual experience. Therefore, to the extent that a given cell was able to repeatedly or consistently take part in activating another cell, the efficacy of that cell in firing the other cell would be enhanced. This mechanism of activity-dependent synaptic strengthening which depends on the temporal coincidence of activity in both pre- and post-synaptic cells, and which relies only on locally available information, has become known as the Hebbian synapse (Hebb, 1949; Brown et al., 1990).

The study of the behaviour of real cell assemblies in the mammalian nervous system has been limited by the techniques which are available to monitor the activity in large numbers of neurons. Single neuron recording techniques are seldom able to simultaneously record the activities of more than six or eight neurons, and electroencephalographic measures of field electrical activity, even within restricted brain regions, lack the spatial resolution necessary to isolate a given cell assembly. One way to study the potential ways in which cell assemblies may represent and store information is to construct computational models which incorporate model neurons with modifiable Hebbian synaptic connections (McClelland & Rumelhart, 1986).

There have been two major physiological approaches to the study of the mechanisms of cell assembly formation. One approach has been to examine changes in synaptic efficacy in identifiable neurons which accompany

forms of learning in simple, invertebrate nervous systems (Castellucci et al., 1978). The second approach, used here, has been to examine experimentally-induced changes in synaptic strength in complex nervous systems using model phenomena that possess characteristics similar to those of the Hebbian synapse. The most commonly used model is long-term synaptic potentiation (LTP), and the study of this phenomenon in a variety of neural pathways in the mammalian nervous system has provided some insights into the rules which may govern learning and memory processes in higher animals.

Long-Term Potentiation. Physiological evidence for the type of activity-dependent synaptic strengthening which could take part in the process of cell assembly formation described by Hebb was first reported in 1973 by Bliss and Lomo in the anesthetized rabbit. A companion paper described similar synaptic enhancements in the unanesthetized preparation (Bliss & Gardner-Medwin, 1973). The authors found that intense stimulation of the perforant pathway projection from the entorhinal cortex to the dentate gyrus could result in a long-term increase in the amplitude of post-synaptic responses evoked by single test-stimulations of the pathway. The strengthening, or potentiation, of the responses lasted between 30 min to 10 hr in the anesthetized preparation, and for up to 3 days in the unanesthetized preparation. Because these effects were much longer-lasting than other previously reported synaptic facilitation effects, the phenomenon was termed long-term synaptic potentiation (LTP). The discovery of LTP was significant because the duration of the effect suggested that LTP could reflect mechanisms which also support long term information storage. Later studies demonstrated that some LTP effects can last many weeks in the chronic preparation (Racine et al., 1983; Abraham et al., 1993).

A great deal of subsequent research on LTP focussed on the intrinsic pathways of the hippocampal formation, partly because of interest in the role of the hippocampus in memory, and partly because of the relative simplicity of hippocampal circuitry which makes this structure amenable to experimental analysis (Teyler & DiScenna, 1987; Bliss & Collingridge, 1993). LTP effects are not restricted to the hippocampal formation, however, and have been observed in a variety of limbic and neocortical regions (Racine et al., 1983, 1985*b*; Artola & Singer, 1987; Kirkwood & Bear, 1994). Further, while the long-lasting nature of LTP satisfies one of the first requirements of a memory processing mechanism, a number of other theoretically attractive properties of LTP have been demonstrated (Teyler & DiScenna, 1984; Bliss & Collingridge, 1993; Maren & Baudry, 1995). LTP can be induced rapidly using physiologically realistic stimulation parameters which result in levels of neuronal activation similar to those which may be present during learning and memory (Larson & Lynch, 1986; Larson et al., 1986; Ross & Dunwiddie, 1986; Buzsaki, 1989). For example, LTP may be induced with only 5 stimulation pulses in "primed-burst" stimulation protocols when a single pulse precedes a four-pulse, high-frequency train (Ross & Dunwiddie, 1986). LTP also demonstrates input-specificity, that is, only the inputs which are simultaneously activated during stimulation are potentiated and synapses which are not active during intense stimulation are not enhanced (Andersen et al., 1977). This is an attractive property since the brain's storage capacity should be much greater if the elementary unit of information storage is the modification of the strength of individual synapses rather than modification of the excitability of whole neurons.

LTP induction is also characterized by cooperativity between inputs. While low-intensity trains which stimulate a relatively small number of inputs may

not induce LTP, the same temporal parameters of stimulation applied to a larger number of inputs can be sufficient (McNaughton et al., 1978). The induction of LTP therefore requires the cooperative effects of the activation of multiple inputs to the same post-synaptic cells. A related characteristic of LTP induction is associativity in which cooperative interactions between separate input pathways can contribute to the induction of LTP. Associative LTP can be demonstrated by showing that, while stimulation of a "weak" input alone is not sufficient to induce LTP, the concurrent stimulation of the weak input with a strong input results in the strengthening of the weak input pathway (McNaughton et al., 1978; Levy & Steward, 1979; Barrionuevo & Brown, 1983). In the hippocampus, associative LTP has been observed during combined stimulation of subcomponents of the Schaffer collateral/commissural inputs to area CA1 (Barrionuevo & Brown, 1983; Kelso & Brown, 1986). Similarly, in the dentate gyrus, interactions between the medial and lateral portions of the perforant path (McNaughton et al., 1978) and between inputs from the ipsilateral and contralateral entorhinal cortex (Levy & Steward, 1979, 1983) produce associative enhancements in granule cell synaptic responses to the weak inputs.

The cellular and molecular mechanisms which mediate the induction of LTP have received much attention in an attempt to better understand the conditions which may govern synaptic plasticity (Madison et al., 1991; Malenka & Nicoll, 1993; McNaughton, 1993). The induction of LTP in the dentate gyrus and area CA1 of the hippocampus has both been found to be dependent on the activation of the N-methyl-D-aspartate (NMDA) glutamate receptor (Collingridge & Bliss, 1987; Zalutsky & Nicoll, 1990; Colino & Malenka, 1993). Other receptors for glutamate include the α -amino-3-hydroxy-5-methyl-4-isoxazolepropionate (AMPA), kainate, and metabotropic receptor subtypes. The

NMDA receptor is unique because the opening of its associated ionophore which is permeable to Na^+ , K^+ , and Ca^{2+} ions is dependent both on binding of glutamate and on post-synaptic depolarization (Ascher & Nowak, 1987). If glutamate is bound to the receptor in the absence of post-synaptic depolarization, the ion channel remains blocked by Mg^{2+} ions. Glutamate binding in the presence of post-synaptic depolarization which removes the Mg^{2+} block, however, results in the opening of the channel. The entry of Ca^{2+} into the post-synaptic cell through the NMDA receptor associated ionophore is thought to be the trigger for the induction of LTP through the activation of Ca^{2+} -dependent kinases (Malenka, 1994; Bliss & Collingridge, 1993). Because the activation of the NMDA receptor requires both neurotransmitter binding and high levels of post-synaptic depolarization, NMDA receptor activation provides a Hebbian mechanism for synaptic change which is dependent on both pre- and post-synaptic activity. The *expression* of increased post-synaptic responses is largely due to increased AMPA receptor-mediated responses although whether the synaptic modifications are pre- or post-synaptic or both is unresolved (McNaughton, 1993). While the NMDA receptor appears to be necessary for LTP induction in most sites, including cortical pathways outside the hippocampal formation (Artola & Singer, 1987; Alonso et al., 1990; Kirkwood & Bear, 1994), some pathways demonstrate LTP that does not require the NMDA receptor, notably the mossy fiber projection from the dentate gyrus to the CA3 region of the hippocampus (Johnston et al., 1992).

Although there has been considerable progress in understanding the cellular mechanisms which mediate the induction of LTP, conclusive evidence linking LTP to processes of learning and memory has been more difficult to obtain (Teyler & DiScenna, 1984; Racine & Kairiss, 1987; Maren & Baudry,

1995; Izquierdo & Medina, 1995). Some correlations between LTP and memory have been drawn, however, and there have been studies demonstrating interactions between learning and hippocampal LTP. The most intuitive approach has been to seek the spontaneous occurrence of LTP-like effects in the hippocampus during the performance of spatial learning tasks which require hippocampal functioning. While studies of this nature can be confounded by increases in post-synaptic responses due to motor activity and elevated brain temperature (Moser et al., 1993), a recent study has indicated that synaptic enhancements during exploratory learning can be measured even when the effects of temperature and movement are removed (Moser et al., 1994). In an alternative approach, attempts have been made to block the occurrence of learning-related synaptic modification by saturating LTP with electrical stimulation prior to training. The expectation is the induction of LTP could interfere with plasticity required during learning, and thereby impair performance. In accord with the presumed functioning of the hippocampus in the learning but not the storage of spatial memory it has been found that the induction of LTP in perforant path-dentate gyrus synapses impairs acquisition of spatial memory, but not in the retention of well-learned spatial memory (McNaughton et al., 1986). More recent studies, however, have failed to show similar effects of LTP saturation on spatial learning (Robinson, 1992; Sutherland et al., 1993).

Correlations have also been shown between the time-courses of the decay of LTP, and the forgetting of learned information. In aged animals, LTP in perforant path-dentate gyrus synapses decays more rapidly than in young animals, in parallel with the more rapid forgetting of a spatial task in older animals (Barnes 1979). Further, when high-frequency stimulation of the

perforant path is paired with foot-shock and is used as a conditioned stimulus for the suppression of lever pressing, a linear relationship is found between the decay of LTP and the forgetting of the learned association (Doyere & Laroche, 1992).

If LTP reflects mechanisms similar to those which take place during learning-related synaptic plasticity, then experimental manipulations that block LTP induction should also block learning and memory. Accordingly, the NMDA receptor antagonist D-2-amino-5-phosphonopentanoate (AP5) blocks spatial learning in the water maze when administered intraventricularly at doses similar to those which block LTP induction in the dentate gyrus (Morris et al., 1986; Morris, 1989; Davis et al., 1992). Similarly, mice in which the functioning of the NMDA receptor is disrupted by the absence of one of its subunits show impaired spatial learning and reduced LTP in area CA1 (Sakimura et al., 1995). Although these correlations are suggestive, it cannot be known to what extent the manipulations interfered with normally-occurring neuronal processes other than synaptic plasticity which may also be critical for memory formation.

The differences in the stimulation parameters which are required to induce LTP in the hippocampus and the neocortex are consistent with the different roles that plasticity may play in these sites during learning and memory. While the hippocampus is thought to rapidly acquire new information, the neocortex is thought to mediate the storage of information over a longer time period (Teyler & DiScenna, 1986; Rolls, 1989; Squire & Zola-Morgan, 1991; Eichenbaum et al., 1992). Accordingly, while hippocampal LTP in chronic preparations is rapidly induced by a single series of high-frequency trains, LTP in cortical afferents is not inducible on a single day even for a wide range of stimulus parameters (Racine et al., 1994). However, LTP can be reliably

induced in the neocortex of the awake rat when multiple stimulation sessions are spaced over 5 or more days (Racine et al., 1995b). This pattern of stimulation may mimic more closely the gradual transfer of representations for storage in the neocortex thought to occur during memory consolidation.

The resistance of the cortex to the rapid induction of LTP may be due to a greater relative contribution of inhibitory activity in the neocortex as compared to the hippocampus. Because post-synaptic depolarization is dependent on the balance of excitatory and inhibitory inputs, the concurrent activation of inhibitory systems during high-frequency stimulation may reduce post-synaptic depolarization and the degree of NMDA receptor-mediated Ca^{2+} influx. Although LTP effects in *in vitro* neocortical slice preparations have been observed frequently, these effects are routinely induced in the presence of agents which reduce GABA-mediated inhibition (e.g., Artola & Singer, 1987; Alonso et al., 1990). A striking exception to this has been demonstrated recently in the *in vitro* visual cortex slice preparation (Kirkwood & Bear, 1994). While the authors found that stimulation of deep white matter inputs to the cortex was not sufficient to induce LTP except in the presence of a GABA_A antagonism, they demonstrated that stimulation of layer IV *does* result in a lasting potentiation of responses in layer III, even in the absence of anti-inhibitory agents. It was proposed that inhibitory circuitry in layer IV usually acts to restrict the depolarization caused by white matter stimulation and that this inhibitory circuitry is bypassed by direct stimulation of layer IV so that LTP may be induced in the absence of pharmacological antagonism of GABAergic transmission (Kirkwood & Bear, 1994).

The strong role that inhibition appears to play in the gating of LTP in the neocortex suggests that inhibitory systems may normally serve to modulate

the induction of synaptic plasticity. The processes which may reduce inhibition in cortical areas during learning and memory are unknown. However, a variety of studies have shown that LTP in hippocampal and cortical regions can be enhanced by neuromodulatory agents, and by patterns of activation similar to those which occur naturally during periods of learning. These neuromodulatory and temporal factors, discussed below, may therefore contribute to learning-related synaptic plasticity by reducing the effects of neuronal inhibition.

1.4 NEUROMODULATORY AND TEMPORAL FACTORS AFFECTING LTP INDUCTION.

Neuromodulatory Systems. The activation of neuromodulatory systems during the occurrence of environmentally significant events may serve to enhance learning-related synaptic plasticity. For example, in the hippocampal indexing theory of Teyler and DiScenna (1986) neuromodulatory inputs activated during experience were postulated to determine whether or not LTP processes in the hippocampal formation would incorporate the incoming array of cortical activation into a hippocampal index. While multiple neuromodulatory systems, with variable contributions in different brain regions, are likely to contribute to memory processes, the effects on LTP of noradrenergic, dopaminergic, and cholinergic systems have been studied most extensively.

Dopaminergic modulation of LTP effects has been of interest because of the role that dopamine has been thought to play in reward and reinforcement (Wise, 1989). Systemic administration of the dopaminergic antagonist haloperidol in awake rabbits blocks the induction of LTP in the dentate gyrus,

but does not affect previously induced LTP (Jibiki et al., 1993). Further, dopamine release in the hippocampus is increased during high-frequency stimulation (Frey et al., 1990), and the presence of dopamine receptor antagonists, although not affecting the initial induction of LTP, results in a more rapid decay of LTP in area CA1 *in vitro* over a period of 2-3 hr (Frey et al., 1990; 1991). While some of the blocking of LTP by dopaminergic antagonists may be due to the inhibition of Ca²⁺-dependent kinases by these drugs (Dunwiddie et al., 1982; Mody et al., 1984), Frey et al. (1990) have shown that the blocking effect induced in CA1 by domperidone is reversed by the presence of the dopamine agonist apomorphine, suggesting that the effects of domperidone on LTP are mediated by an attenuation of dopaminergic transmission.

Noradrenergic systems which have been linked to learning and memory processes have also been shown to affect LTP in the hippocampus (Izquierdo et al., 1992, 1995; Hopkins & Johnston, 1984). Noradrenaline release in the hippocampus, induced either iontophoretically or by locus coeruleus stimulation, produces a facilitation of responses in the dentate gyrus for up to 11 hr *in vivo* (Neuman & Harley, 1983; Harley & Milway, 1986) and these effects appear to be mediated by the beta receptor subtype (Lacaille & Harley, 1985). In area CA3 of the hippocampus, LTP effects were larger and longer-lasting in the presence of noradrenaline, and noradrenaline enabled the induction of LTP in response to trains that were otherwise ineffective in inducing LTP (Hopkins & Johnston, 1984).

The contribution of cholinergic systems to synaptic plasticity is of particular interest with respect to the role of the entorhinal cortex in learning and memory because the entorhinal cortex receives a large cholinergic projection from the medial septum (Alonso & Kohler, 1984; Gaykema et al., 1990). In

separate studies, cholinergic drugs have been shown to affect both LTP induction and memory processes. Muscarine ($1 \mu\text{M}$), which alone does not affect either evoked EPSPs or cell firing, does facilitate the induction of LTP in the dentate gyrus (Burgard & Sarvey, 1990). The M_1 receptor antagonist pirenzepine blocks the facilitation, suggesting that this form of modulation is mediated by the M_1 receptor subtype (Burgard & Sarvey, 1990). Stimulation of the medial septum has also been shown to enhance LTP in the dentate gyrus induced by tetanizing the perforant path (Robinson & Racine, 1982; Robinson, 1986). LTP induction is also facilitated in area CA1 of the hippocampus by the muscarinic agonist carbachol (Blitzer et al., 1990), perhaps through the selective enhancement of NMDA-receptor-mediated currents (Markram & Segal, 1990). While cholinergic neuromodulation may affect plasticity in the entorhinal cortex and cortico-hippocampal interactions during memory formation, the effects of medial septal stimulation or cholinergic drugs on LTP in the entorhinal cortex has not been examined.

Anticholinergic drugs result in memory impairments in both man and animals and generally interfere with the initial acquisition of information, but not with subsequent recall. The administration of the cholinergic antagonist scopolamine in human subjects does not impair immediate recall or the recall of previously learned information, but does impair declarative memory when administered during acquisition (Drachman & Leavitt, 1974; Crow et al., 1975; Petersen, 1977; Flicker et al., 1990). Similarly, the administration of the cholinergic antagonist atropine to monkeys impairs performance of a visual, delayed non-matching to sample task at long intervals (Penetar & McDonough, 1983). Further, in a version of the task in which sample stimuli are first presented sequentially, and performance is tested in a subsequent test period,

scopolamine impairs performance when administered prior to the acquisition phase, but not when administered after the acquisition phase and prior the testing phase (Aigner et al., 1991).

Memory in both the radial arm maze and the water maze tasks is also impaired by anticholinergic drugs. In the radial arm maze, the performance of animals receiving scopolamine is impaired relative to controls over 15 days of training, but the same animals show improvements when trained later in the absence of scopolamine (Stevens, 1981; Watts et al., 1981; Rauch & Raskin, 1984). Morris water maze performance is also impaired following injections of scopolamine (Sutherland et al., 1982; McNamara & Skelton, 1992) or the M₁ receptor antagonist pirenzepine (Hagan et al., 1987). Although the performance of rats treated with atropine does improve, the improvements appear to be due to the adoption of swimming strategies similar to those used by blind rats and by rats that are tested with a new platform location on each trial (Sutherland et al., 1982). Atropine also impairs spatial navigation in a dry maze in which rats must search for buried food, although performance was enhanced in both this task and in the water maze by priming animals with experience of the motor demands of the task (Whishaw, 1989). The impairments observed in the Morris water maze, and the finding that animals that use non-spatial strategies in the radial arm maze are less affected by scopolamine treatment, suggests that some of the effect of anticholinergic treatments may be to affect spatial learning, a memory function associated with the hippocampal formation and related structures (Watts et al., 1981).

The effects of anticholinergics on maze tasks may be due to a disruption of activity in cholinergic projections from the medial septum to the hippocampus and entorhinal cortex (Kesner, 1988; Izquierdo, 1989; Hasselmo,

1995). Radial arm maze performance is impaired by reversible inactivation of the medial septum while a simpler, non-spatial goal cue recognition task is less affected by this treatment (Mizumori et al., 1990). Similar to the impairments which follow small dorsal hippocampal lesions, in a version of the radial arm maze task in which the animal must remember the location of the arms it visited during a study phase, small medial septal lesions impair memory for arms visited early in the study phase, but memory for the most recently visited arm is unaffected (Kesner et al., 1988). This suggests that the medial septum may act in concert with the hippocampus in the longer-term storage of spatial information (Gray & McNaughton, 1982). Medial septal lesions also impair spatial learning in the Morris water maze, but do not affect the ability of animals to find the platform based on a local goal cue (Kelsey & Landry, 1988). Further, cholinergic effects on water maze performance are more likely to be mediated by the medial septum than by the nucleus basalis cholinergic cell group since lesions of the medial septum and diagonal band impair performance (Hagan et al., 1988; Marston et al., 1993), while nucleus basalis lesions do not (Hagan et al., 1988).

The disruptions in maze performance caused by medial septal lesions also correlate with reductions in cholinergic markers. Medial septal lesions which disrupt radial arm maze and Morris water maze performance also reduce cholinergic staining in the entorhinal cortex and the hippocampus (Mitchell et al., 1982; Miyamoto et al., 1987). Further, learning rate in the Morris water maze is reduced when the GABA_A agonist, muscimol, is infused into the medial septum at doses which also significantly reduce high-affinity choline uptake in the hippocampus (Brioni et al., 1990). Recovery of function in the radial arm maze following septal lesions occurs only in animals in which there were

residual septohippocampal projections staining for acetylcholinesterase (Crutcher et al., 1983). While this suggests that cholinergic projections to the hippocampus are critical for this task, this study did not assess the correlation of residual cholinergic staining in the entorhinal cortex with performance.

Olfactory learning in rats is also impaired by scopolamine, although whether these effects are due to blocking cholinergic efferents from the medial septum has not been determined. Scopolamine impairs performance in a delayed match to sample task in which the animal must determine which arm of a T-maze contains a previously presented odour (Ravel et al., 1992). Scopolamine also reduces both habituation to odours, and the recognition of novel odours as measured by time spent sniffing (Hunter & Murray, 1989). Scopolamine attenuates habituation to the odour of juvenile conspecifics at 20 min inter-trial intervals (Soffie & Lamberty, 1988), and animals treated with arecoline, a cholinergic agonist, show a maintained habituation at 2 hr intervals which is not shown by control animals (Perio et al., 1989). This latter, enhancing effect of arecoline on memory is reversed by scopolamine and the habituation is not observed when novel rats are presented in the second trial. This suggests that the effect of arecoline is cholinergically mediated, and not due to non-specific behavioural impairments (Perio et al., 1989).

Temporal Processing and Oscillatory Activity. Oscillatory dynamics in populations of cells are striking features of neuronal activity which are reflected in electroencephalographic (EEG) recordings from brain regions including the entorhinal cortex and hippocampal formation. Neuronal oscillations are remarkable because they reflect not only the synchronization of massive numbers of cells, but also ordered temporal patterns of activation. These activities can result from the intrinsic membrane properties of neurons, and from

network interactions among populations of neurons (Freeman, 1978; Steriade et al., 1990; Lopes da Silva, 1991; Klink & Alonso, 1993). The temporal summation of EPSPs associated with oscillatory synchronization of neuronal inputs may contribute to Hebbian learning by enhancing levels of post-synaptic depolarization. Further, Singer (1993) has proposed that oscillatory activity may serve to increase the specificity with which use-dependent synaptic modifications occur. Because temporal correlations between inputs are critical to Hebbian synaptic modification, the determination of which synapses will be modified may be controlled by the phase of the oscillation at which different inputs arrive (Singer, 1993). Oscillatory activity may also contribute to the integration of the different elements of sensory stimuli into coherent perceptual representations. In the visual cortex, neurons fire at a frequency near 40 Hz in the gamma-frequency band, and correlations between the firing of units corresponding to separate aspects of visual stimuli increase with the perceptual integrity of the stimulus (Bressler, 1989; Gray & Singer, 1989; Gray, 1994). This suggests that gamma oscillations may serve to temporally "bind" elementary neuronal representations of stimulus elements.

i) Frequency Potentiation. The phenomenon of frequency potentiation has been used to show that rhythmic activity of afferents can contribute to the enhancement of the amplitudes of post-synaptic responses in a frequency-dependent manner. Frequency potentiation is a short-term enhancement in the amplitude of neuronal responses occurring when the low-frequency stimulation evoking the responses is applied within a given frequency range (Anderson & Lomo, 1967, 1968; Deadwyler et al., 1975; Creager et al., 1980; Nickell & Shipley, 1988). Because frequency potentiation tends to be optimal for somewhat different frequencies in different neuronal pathways, the

phenomenon suggests that different pathways may be preferentially responsive to different frequencies of spontaneous oscillatory activity. The first report of frequency potentiation following stimulation of intrinsic hippocampal pathways was provided by Andersen and Lomo in 1967. The authors observed frequency potentiation effects in the commissural and mossy fiber inputs to the CA3 region, and in the commissural and Schaffer collateral inputs to the CA1 region of the hippocampus. The stimulation was typically applied at a frequency of 10 Hz for 5 to 10 sec. The effects decayed within several hundred msec after termination of the train. It was also found that stimulation at 6 Hz or less resulted in maintained expression of IPSPs which appeared to impede the expression of frequency potentiation, while stimulation frequencies higher than 15 Hz tended to result in large but short-lived enhancements which rapidly became depressed with continued stimulation (Andersen & Lomo, 1967).

Later studies demonstrated frequency potentiation effects throughout the hippocampal formation. Frequency potentiation can be evoked by stimulation of the perforant path and commissural inputs to the dentate gyrus (Bliss & Gardner-Medwin, 1973; Dudek et al. 1976; Krug et al., 1985; Munoz et al., 1991), mossy fiber inputs to CA3 (Yamamoto, 1972; MacVicar & Ducek, 1979), and the Schaffer collateral inputs to CA1 (Schwartzkroin, 1975; Creager et al., 1980; Pitler & Landfield, 1987). However, although frequency potentiation has been shown to be a common property of synapses onto principal cells of the hippocampal formation, and appears to coincide with reduced inhibition (Andersen & Lomo, 1968), very little is known about the underlying cellular mechanisms.

Frequency potentiation effects are also observed in structures in the olfactory system and in non-olfactory inputs to the entorhinal cortex. Field

responses generated in the granule cell layer of the olfactory bulb by stimulation of the horizontal limb of the diagonal band are enhanced after about 14 sec of stimulation at 10 Hz (Nickell & Shipley, 1988). Frequencies as low as 5 Hz can then maintain the potentiation but responses to single pulses decay within about 3 to 4 sec after the end of the train. The potentiated field potentials are associated with enhanced activity in inhibitory neurons and are associated with *reduction* in the activity of the principal output neurons of the olfactory bulb, the mitral cells (Nickell & Shipley, 1988). The pyramidal cells of the pyriform cortex show frequency potentiation in response to lateral olfactory tract and intrinsic associational fiber stimulation (Hasselmo & Bower, 1990; Mokrushin & Emel'yanov, 1991). While 10 Hz lateral olfactory tract stimulation, and 20 Hz associational fiber stimulation have been shown to be sufficient for frequency potentiation in this site, the precise frequency tuning of the effects have not been determined. Amygdalar and hippocampal inputs to the entorhinal cortex support frequency potentiation (Deadwyler, 1975; Racine & Milgram, 1983; Finch et al., 1986; Jones & Heinemann, 1991), as do inputs to the entorhinal cortex from the subicular complex of the hippocampal formation (Shipley, 1975; Jones, 1987; Caballero-Bleda & Whitter, 1993). Effective frequencies range between about 5 to 15 Hz, although frequencies as low as 2.5 Hz applied to the subiculum can induce frequency potentiation in the slice preparation (Jones & Heinemann, 1991). The precise frequency response characteristics of these different inputs to the entorhinal cortex have not been well described and differences across laboratories in the preparations used make comparisons of the results for different pathways difficult.

ii) Theta Activity. Another clue to the sort of temporal activity which may be important for learning-related synaptic plasticity is the occurrence of

rhythmic slow activity, also called the theta rhythm, in EEG recordings during periods of movement and learning (Vanderwolf, 1988, 1992; Bland & Colom, 1993). The theta rhythm is a large amplitude, near-sinusoidal oscillation with a frequency near 8 Hz in chronic preparations observed in the hippocampal formation, entorhinal cortex, and the septum (Green & Arduini, 1954; Adey et al., 1957; Mitchell & Rank, 1980; Bland, 1986; Alonso & Garcia-Austt, 1987a&b; Bland & Colom, 1993). Rhythmic slow activity in these sites can be distinguished, both behaviourally and pharmacologically, into type I and type II theta (Vanderwolf, 1969; Bland, 1986). Type I theta is atropine-resistant while type II theta is abolished by the administration of atropine (Kramis et al., 1975). Type I theta is observed during ambulatory movement, the manipulation of objects, movement and shifts of posture, while type II theta is observed during periods of immobility. While the cellular generators of the theta rhythm have been localized to the principal cells of the entorhinal cortex and hippocampus, the intrinsic membrane properties and network interactions which initiate and maintain theta activity have not been well established.

The relationship of theta activity to the neural mechanisms of learning and memory are not well-understood. One possibility is that theta can serve to rhythmically synchronize neural activity so that inputs to cell groups in the hippocampal formation, if occurring at an appropriate phase relationship to theta, arrive concurrently with large levels of activation. The presence of background levels of depolarization has been shown experimentally to be important for LTP induction (Alonso et al., 1990; Morris et al., 1990; Singer & Artola, 1991; Fox & Daw, 1993). Although the amplitude of electrically-evoked responses in the dentate gyrus and hippocampus tend to be smaller during theta activity while animals are running or active (Winson & Azbug, 1978;

Buzsaki et al., 1981; Hargreaves et al., 1990), a number of studies have suggested that the *phase* of theta activity during which afferent inputs arrive may affect their efficacy in producing a post-synaptic response. Buzsaki et al. (1981) found that the size of evoked cell discharge in the dentate gyrus during running varied with the phase of the theta rhythm, and was greatest during the negative phase recorded in the dentate gyrus molecular layer. Further, behavioural studies have indicated that animals time the sampling of sensory stimuli in order to maintain a consistent phase relationship between the sampling and the phase of theta activity. During operant conditioning tasks rats are more likely to depress a bar at a particular phase of the theta rhythm (Buno & Velluti, 1977; Semba & Komisaruk, 1978), and the movement of rats' vibrissae during exploratory sniffing is also synchronized with theta activity (Komisaruk, 1970). Macrides et al. (1982) measured theta activity in the hippocampus and monitored sniffing with sensors in the nasal cavity during an odour discrimination task. They found that animals sniffed so as to maintain a consistent latency between a particular phase of theta and the onset of the sniffing cycle. Further, this latency relationship was strongest during the initial acquisition of the odour discrimination task.

Because entorhinal cortex and hippocampal theta activity is thought to be dependent in part on cholinergic projections from the medial septum (Mitchell et al., 1982; Bland, 1986; Stewart & Fox, 1990; Konopacki et al., 1992), one explanation of the deficits in learning which follow anticholinergic drug treatments is an associated disruption of theta activity. Similarly, the learning deficits which follow medial septal lesions may also result from disrupted theta activity (Green & Arduini, 1954). While drug treatments and lesions may result in a general disruption of entorhinal cortex and hippocampal functioning, rather

than a specific impairment in learning-related synaptic plasticity, some correlations have been drawn between learning impairments and manipulations of the septum which affect theta activity. While large lesions of the medial septum disrupt both theta activity and spatial learning, smaller lesions which do not disrupt theta also do not result in spatial memory impairment (Winson, 1978). In a study employing reversible inactivation of the medial septum by local injection of the local anesthetic tetracaine, both theta rhythm disruption and impairments in radial arm maze performance were observed (Mizumori et al., 1990). Performance deficits occurred only when the medial septum was inactivated during study and test phases, but not when it was inactivated during an intervening delay period. An additional study (Mitchell et al., 1982) found a correlation between deficits in radial arm maze performance resulting from medial septal lesions and reductions in theta activity and cholinergic staining in the entorhinal cortex and hippocampus.

Phase-locking sensory inputs with theta activity may serve some computational purpose (Komisaruk, 1970; Macrides et al., 1982; Singer, 1993), perhaps by cooperatively enhancing the amplitude of post-synaptic responses associated with sensory inputs leading to an increase in the likelihood of Hebbian synaptic modifications. In accord with the notion that theta activity may contribute to synaptic plasticity (Lynch et al., 1990), LTP in the CA1 field of the hippocampus (Larson et al., 1986), and in the dentate gyrus (Greenstein et al., 1988) is induced most effectively when the trains used to induce LTP are delivered at theta frequencies. While studies of the relationship of theta activity to learning and memory have focussed almost exclusively on the hippocampal theta rhythm, little is known about the contribution of theta activity in the entorhinal cortex to synaptic plasticity. Theta activity is generated by superficial

neurons in the entorhinal cortex (Alonso & Garcia-Austt, 1987a), and is also dependent in part on medial septal inputs (Mitchell et al., 1982; Konopacki & Golebiewski, 1992; Konopacki et al., 1992). While a number of studies have shown that theta-related stimulation parameters are particularly effective in the induction of LTP in the hippocampus, similar studies in the entorhinal cortex have not been performed, and the contribution of the medial septum to the control of plasticity in the entorhinal cortex has also not been assessed.

1.5 SYNAPTIC PLASTICITY IN OLFACTORY INPUTS TO THE ENTORHINAL CORTEX.

In the series of studies reported in the following chapters, changes in synaptic strength in olfactory inputs from the pyriform cortex to the entorhinal cortex have been examined in an investigation of temporal and neuromodulatory factors which control synaptic plasticity in this pathway. While the computational role of synaptic plasticity in the entorhinal cortex during memory formation is unknown, it is of great theoretical interest given the pivotal role this structure is thought to play in mediating interactions between hippocampal and neocortical areas. Synaptic plasticity in sensory afferents to the entorhinal cortex could contribute significantly to the alteration of processing of sensory inputs by the entorhinal cortex and the hippocampal formation. One possibility is that plasticity in synaptic inputs from the pyriform cortex could contribute to the storage of olfactory representations in the entorhinal cortex. It has been suggested that the pyriform cortex supports a form of associative memory mediated by extensive recurrent excitatory connections between the principal cells of this region (Hasselmo & Bower, 1993; Barkai et al., 1994).

Although the entorhinal cortex does not contain similarly extensive recurrent excitatory connections, cells in the superficial layers do display considerable axonal arbourizations (Kohler, 1986; Lingenhohl & Finch, 1991) which could contribute to the recruitment of restricted populations of entorhinal cortex neurons into stimulus-specific patterns of neuronal activity. Further, because the entorhinal cortex is a major site of convergence for sensory inputs from multiple modalities, plasticity in its afferent and intrinsic synapses may contribute, along with the hippocampal formation, to the formation of coherent multimodal sensory representations.

Synaptic enhancements in sensory afferents to the entorhinal cortex could also play a role during learning by enhancing the transmission of sensory representations from cortical areas to the hippocampal formation. A long-term, activity-dependent synaptic enhancement in inputs from a cortical area which is involved in the representation of a particular sensory stimulus could lead to a selective increase in the response of neurons in the entorhinal cortex to that stimulus. In turn, because sensory inputs primarily terminate in the superficial layers of the entorhinal cortex which contain the cells of origin of the perforant path (Room et al., 1984; Lopes da Silva et al., 1990; Witter et al., 1993), plasticity in these afferents could lead to an increase in the degree to which the representations they carry reach the hippocampus. In addition, if the entorhinal cortex also performs the sort of multimodal associative memory function mentioned above, the representations reaching the hippocampus may also contain related, associational information.

Behavioural studies have not clearly defined the mnemonic functions performed by the entorhinal cortex, and the coding and processing of neuronal representations by the entorhinal cortex are not amenable to direct physiological

examination. However, an understanding of the factors which affect experimentally-induced synaptic plasticity in its sensory inputs might provide some insights into the mechanisms which control the processing of sensory stimuli by the entorhinal cortex during learning and memory. In the following experiments, the inputs from the pyriform cortex to the entorhinal cortex were selected for study. This pathway provides an attractive model for plasticity in sensory inputs to the entorhinal cortex for a number of reasons. Anatomical and behavioural data suggests that the entorhinal cortex, in association with the hippocampus, is likely to contribute significantly to olfactory learning. Lesions of either the hippocampus or entorhinal cortex block olfactory learning (Gauthier & Soumireu-Mourat, 1981; Eichenbaum et al., 1988; Otto et al., 1991; Eichenbaum, 1992; Otto & Eichenbaum, 1992), and the acquisition but not the retention of olfactory discriminations is blocked by interrupting olfactory projections to the hippocampus (Staubli et al., 1984, 1986). Further, the pyriform cortex input to the entorhinal cortex is not only one of its largest inputs, but in contrast to other inputs from perirhinal and neocortical associational areas, it carries putatively unimodal sensory information (Witter et al., 1989; Lopes da Silva et al., 1990). This allows a less ambiguous interpretation of the types of sensory information that could be affected by plasticity in this pathway during learning and memory. Further, although the pyriform cortex input has been less well characterized anatomically than other links in the olfactory system, some anatomical data do exist to aid in the interpretation of electrophysiological recordings from this pathway (Krettek & Price, 1977; Beckstead, 1978; Boeijinga et al., 1982; Luskin & Price, 1983; Room et al., 1984).

The olfactory system is unique in that it is the only sensory modality which projects to cortical areas without passing through the thalamus. Afferents from receptors in the olfactory mucosa project to the olfactory bulb where they terminate on mitral cells from which the lateral olfactory tract originates (Shepherd, 1972). The lateral olfactory tract runs caudally on the ventro-lateral surface of the brain, projecting to the pyriform cortex which also lies on the ventrolateral surface of the brain, subjacent to the rhinal fissure. Lateral olfactory tract projections terminate in layer Ia of the pyriform cortex onto the apical dendrites of the densely packed layer II pyramidal neurons (Carmichael et al., 1994). Within the pyriform cortex, pyramidal neurons which receive lateral olfactory tract input project recurrent excitatory connections onto the dendrites of other pyramidal neurons in layer Ib (Haberly & Price, 1978; Luskin & Price, 1983; Haberly & Bower, 1984). Olfactory bulb afferents also project more caudally to the three most superficial layers of the lateral entorhinal area, and a smaller projection reaches the medial entorhinal area (Kerr & Dennis, 1972; Kosel et al., 1981; Wouterlood & Nederlof, 1983; Schwedtfeger et al., 1990).

The large projection from layers II and III of the pyriform cortex to the entorhinal cortex terminate exclusively in the superficial layers. The lateral entorhinal area receives inputs from both layers II and III of the pyriform cortex, while inputs to the medial entorhinal cortex arise mainly from layer II (Krettek & Price, 1977; Beckstead, 1978; Room et al., 1984). Most fibers terminate in layer I of both the lateral and medial entorhinal cortex (Beckstead, 1978), and smaller numbers of fibers reach layer II, and layer III of the lateral entorhinal area (Luskin & Price, 1983; Room et al., 1984; Boeijinga et al., 1982).

Factors Which May Affect Plasticity of Olfactory Inputs. There have been two reports of long-term potentiation effects in pyriform cortex inputs to the

entorhinal cortex in *in vitro* preparations. LTP effects were observed in both the isolated guinea-pig brain (Alonso et al., 1990; de Curtis & Llinas, 1993), and in the rat entorhinal cortex slice preparation (Alonso et al., 1990). In both preparations the induction and expression of LTP was NMDA-dependent. In the slice preparation, both Hebbian and non-Hebbian LTP were induced, either by stimulating synaptic inputs, or by rhythmic post-synaptic depolarization with no presynaptic stimulation, respectively (Alonso et al., 1990). While LTP effects lasted for hours in these preparations, it is not known if this pathway supports synaptic enhancements that are as long-lasting as LTP effects in the hippocampal formation which can last for weeks to months in chronic preparations. In chronically prepared animals, however, LTP in this pathway has not been readily induced. Racine et al., (1983) attempted the induction of LTP in 5 animals but reported the successful induction of LTP in only one of these as measured 24 hr after train delivery.

The apparent resistance of this pathway to the induction of LTP in chronically prepared animals may be due to the strong inhibitory circuitry in the entorhinal cortex which exerts a tight control over the excitability of entorhinal cortex neurons (Finch & Babb, 1980; Colino & Fernandez de Molina, 1986a&b; Finch et al., 1988; Jones & Heinemann, 1991; Jones, 1993). LTP in *in vitro* preparations may be a more reliable due to reduced inhibition. In the slice preparation, picrotoxin was used to reduce GABA_A-mediated inhibition (Alonso et al., 1990), and some reduction in inhibitory activity is also likely to have occurred in the isolated *in vitro* guinea-pig brain preparation (de Curtis et al., 1993). Inhibitory activity in the entorhinal cortex which is strongest in the superficial layers may, therefore, play a significant role both in restricting plasticity in sensory afferents, and in gating the normal transmission of sensory

input to the hippocampal formation (Jones, 1993). Jones (1987, 1993) and others (Shipley 1975; Finch et al., 1986; Caballero-Bleda & Witter, 1993), however, have reported results which indicate that there is a shift in the balance of excitation and inhibition during appropriate frequencies of input to the entorhinal cortex. Responses of superficial entorhinal cortex neurons can be enhanced when inputs are stimulated at frequencies between 2.5 and 10 Hz. Lower frequencies of stimulation are ineffective in producing these frequency potentiation effects, and the frequencies which are effective are similar to the frequency of theta activity expressed in the slice and acute preparations used (Konopacki & Golebiewski, 1992). Because plasticity in pyriform cortex inputs are dependent on levels of post-synaptic depolarization and NMDA receptor activation (Alonso et al., 1990; de Curtis & Llinas, 1993) these results suggest that the temporal pattern of background activity occurring in this pathway may be critical for LTP induction in chronic preparations in which inhibitory mechanisms are intact. Further, an examination of the optimal frequencies of stimulation for frequency potentiation effects in this pathway might suggest which frequencies of spontaneous input contribute to learning-related synaptic plasticity most strongly.

The types of stimulation sufficient to induce and enhance synaptic plasticity in the olfactory inputs to the entorhinal cortex were examined in a number of the experiments reported here. It had previously been demonstrated that 400 Hz, 8-pulse trains are insufficient for the reliable induction of LTP in chronic animals (Racine et al., 1983), so longer, 16-pulse 400 Hz trains were used in the present study in order to provide a more intense drive at excitatory synapses. The contribution of frequency potentiating stimuli to the induction of LTP was assessed by delivering high-frequency trains during the application of

frequency potentiating stimuli. Because the medial septum contributes significantly to the temporal nature of neuronal activity in the entorhinal cortex, and may therefore affect the susceptibility of entorhinal cortex synapses to LTP induction (Mitchell et al., 1982; Lynch et al., 1990; de Curtis & Llinas, 1993), the effects of theta-frequency stimulation of the medial septum on LTP in entorhinal cortex afferents were also assessed. Previous *in vitro* studies have shown that theta-frequency stimulation is sufficient for the induction of LTP in the pyriform cortex inputs to the entorhinal cortex (Alonso et al., 1990, de Curtis & Llinas, 1993), but whether the medial septum may contribute heterosynaptically to similar effects and provide a neural system which may control plasticity in the pyriform to entorhinal cortex pathway has not been assessed.

Determination of the stimulation parameters sufficient to induce plasticity in the entorhinal cortex under conditions in which normal inhibitory mechanisms are present requires the use of a chronic experimental preparation. The chronic implantation of field electrodes to monitor synaptic strength has a number of advantages for the study of the factors which may influence plasticity in this pathway. First, normal neuromodulatory and inhibitory processes remain intact so that there is a greater likelihood that some of the same mechanisms which support observed experimental effects could also contribute to learning-related synaptic plasticity. Second, neuromodulatory systems in areas of the brain which are not preserved in slice preparations may be selectively activated to test their effects on normal and potentiated synaptic transmission. Third, chronic preparations allow an assessment of the durability of LTP effects because reliable recordings can be obtained for months after the induction of LTP.

Electrophysiological recordings from chronically-implanted electrodes monitor the electrical field around the electrode which reflects the spatial and temporal summation of electric currents generated by synaptic activity. When an afferent pathway is stimulated, field activity can sum temporally to result in a discrete, evoked field potential, the amplitude of which can be used as an index of the strength of the connectivity in the synapses mediating the response. Because field potentials can be affected by activity of currents generated some distance from the electrode, the mapping of a particular evoked field potential onto a particular synaptic population depends in part on a knowledge of the anatomy and physiology of the pathway under study. While the pyriform cortex projection to the entorhinal cortex has been characterized well anatomically in a number of species including the rat (Luskin & Price, 1983; Room et al., 1984), *in vivo* physiological studies of this projection have been conducted almost exclusively in the cat and the use of chronic preparations to examine this system in the rat has remained undeveloped (Van Groen et al., 1987; Boeijinga & Van Groen, 1984). Similarly, while the medial septal projection to the hippocampal formation has been well-characterized both anatomically and physiologically (Andersen et al., 1961; Mosko et al., 1973; Chandler & Crutcher, 1983; McNaughton & Miller, 1984; Amaral & Kurz, 1985; Robinson & Racine, 1986), the anatomy of the septal projection to the entorhinal cortex has been well-described more recently (Alonso & Kohler, 1984; Insausti et al., 1987; Gaykema et al., 1990), and there is no available information on its physiological properties for any species.

The first experiments, reported in Chapter 2, were conducted to provide a sound interpretive basis for the analysis of field potentials in the entorhinal cortex following stimulation of either the pyriform cortex or the medial

septum. The technique of current source density analysis (Haberly & Shepherd, 1973; Nicholson & Freeman, 1975; Mitzdorf, 1985) was used to spatially localize the synaptic currents in the entorhinal cortex which result from electrical stimulation of the two input pathways, and the results were compared to the known anatomical distribution of the terminations of these pathways. This analysis allowed changes in field potentials recorded from chronically-implanted electrodes to be interpreted in terms of changes in the efficacy of identified synaptic populations.

Additional preliminary experiments were required to determine the optimal frequencies for frequency potentiation effects in pyriform cortex afferents to the entorhinal cortex because one of the hypotheses to be tested in later experiments was that frequency potentiation could contribute to the induction of LTP. In addition to the measurement of frequency potentiation in pyriform cortex inputs, the effect of low-frequency stimulation of the medial septal projection was also assessed to determine if frequency potentiation might occur in response to theta-frequency stimulation. The neural mechanisms which mediate frequency potentiation have been studied most extensively in peripheral nervous system preparations and little is known about the mechanisms which lead to frequency potentiation at central synapses (Magelby, 1973a; Magelby & Zengel, 1982; Magelby, 1987; Applegate & Landfield, 1988; Zucker, 1989; Hess & Kuhnt, 1992; Landfield, 1993). Therefore, a series of paired-pulse tests (Racine & Milgram, 1983) were used to examine the time course of facilitatory and inhibitory mechanisms in the entorhinal cortex which follow pyriform cortex and medial septal stimulation and which may also contribute to frequency potentiation effects.

The final chapter of the thesis reports the application of computational modelling techniques to the formalization of one set of neural mechanisms which could result in synaptic frequency potentiation, and to the simulation of the cooperative LTP effects in the entorhinal cortex. In addition to providing an explicit, quantitative description of neuronal mechanisms proposed to mediate experimentally observed phenomena, this approach allows an exploration of the possible forms which representations of sensory information may take in neural networks, a line of inquiry not possible with the sole use of current neurophysiological methods.

CHAPTER 2
SPATIAL DISTRIBUTION OF SYNAPTIC CURRENTS IN THE ENTORHINAL
CORTEX FOLLOWING PYRIFORM CORTEX AND MEDIAL SEPTAL
STIMULATION.

Available anatomical data describing the projections from the pyriform cortex to the entorhinal cortex comes primarily from work on the cat (Krettek & Price, 1977; Boeijinga et al., 1982; Room et al., 1984), but these projections have also been observed in the monkey (Van Hoesen et al., 1972; Van Hoesen & Pandya, 1975) and in the rat (Beckstead, 1978; Krettek & Price, 1977; Luskin & Price, 1983). Using horseradish peroxidase injections in the lateral and medial entorhinal areas, Beckstead (1978) found retrograde cell labelling in the pyriform cortex only after lateral entorhinal area injections, suggesting that the pyriform cortex projects most strongly to the lateral division of the entorhinal cortex. However, a pyriform cortex projection to the medial entorhinal area in the rat has also been described by Room et al. (1984) using ^3H -leucine anterograde tracing methods. They found that the lateral entorhinal cortex receives inputs from neurons in layers II and III of the pyriform cortex, and that the medial entorhinal cortex receives a somewhat less dense projection from cells in layer II (Room et al., 1984).

The inputs from the pyriform cortex terminate exclusively in the three most superficial layers of the entorhinal cortex. The inputs to layer I of the medial and lateral entorhinal areas are the most prominent (Beckstead, 1978), but somewhat lower fibre densities are also observed in layers II and III of the

lateral entorhinal cortex (Luskin & Price, 1983; Room et al., 1984), and in layer II of the medial entorhinal cortex (Boeijinga et al., 1982).

Extracellularly-recorded field potentials in the entorhinal cortex evoked by stimulating pyriform cortex inputs have been described for the cat (Van Groen et al., 1987; Boeijinga & Van Groen, 1984), and in the isolated guinea pig brain *in vitro* (Alonso et al., 1990; de Curtis & Llinas, 1993), but there are no reports for the rat. In the isolated guinea pig brain (de Curtis et al., 1991, 1994) a negative field potential is evoked at the surface of the entorhinal cortex by pyriform cortex stimulation, and there is a simultaneous depolarization of layer II entorhinal cortex neurons (de Curtis & Llinas, 1993). Because excitatory synaptic transmission results in a local region of negativity outside the neuronal membrane due to the net flow of positive current into the post-synaptic cell, this field potential component is consistent with the dendritic activation of many neurons in the superficial layers of entorhinal cortex. The field potential is almost completely abolished by perfusion with 6-cyano-7-nitroquinoxaline-2,3-dione (CNQX, a non-NMDA glutamate receptor antagonist), indicating that much of the response is mediated by glutaminergic neurotransmission. The application of the NMDA receptor antagonist 2-amino-5-phosphonovalerate (AP-5) results in a much smaller attenuation of field responses (about 10%) which is most pronounced during the later phases of intracellular EPSPs. These results suggest that the early and the late phases of the evoked field potentials are respectively mediated primarily by non-NMDA, and NMDA glutamate receptors on layer II neurons (de Curtis & Llinas, 1993).

In the cat, stimulation of the anterior pyriform cortex also results in a surface negative field potential which reverses in polarity near layer II (Boeijinga & Van Groen, 1984). Posterior pyriform cortex stimulation, however, results in a

surface *positive* field potential which also reverses near layer II and is attributable to synaptic activation of dendritic processes in layer III. Both anterior and posterior pyriform cortex stimulation results in unit responses primarily in layers I and II. Although stimulation of these regions results in field potentials in both the lateral and medial entorhinal areas, the evoked potentials are strongest in the lateral entorhinal area (Boeijinga & Van Groen, 1984).

Current source density (CSD) analysis has been used to study the synaptic inputs to the entorhinal cortex from the olfactory bulb and pyriform cortex in the cat (Van Groen et al., 1987). CSD analysis is a method for spatially localizing the membrane current sources and sinks which result from evoked neuronal activity in lamellar cortical tissue (Haberly & Shepherd, 1973; Nicholson & Freeman, 1975; Mitzdorf, 1985). Experimentally, the one-dimensional CSD is obtained by recording evoked field potentials at intervals spanning the depth of a cortical structure, and by then calculating the second derivative of the measured voltage gradient (Freeman & Nicholson, 1975; Rodriguez & Haberly, 1989; Ketchum & Haberly, 1993a). In this way, the membrane currents responsible for components of the evoked potentials may be localized in order to provide greater insight into the functional properties of cortical synaptic transmission *in vivo*. CSD analysis has been used to examine the activation of intrinsic circuitry in the pyriform cortex following stimulation of olfactory bulb efferents (Haberly & Shepherd, 1973; Rodriguez & Haberly, 1989; Ketchum & Haberly, 1993a&b), and has been used to study hippocampal long-term potentiation (Taube & Schwartzkroin, 1988; Leung et al., 1992) and the sources of theta activity (Buzsaki et al., 1986; Brankack et al., 1993).

The study by Van Groen et al. (1987) indicated that both olfactory bulb and pyriform cortex stimulation in the cat results in an early current sink in the

superficial layers of the ventrolateral entorhinal cortex which first develops in layer I before reaching layer II. Their results are consistent with the activation of dendritic processes of layer II neurons and a resulting depolarization of cell bodies in layer II. Further, shortly after the layer II sink, there was a large reduction in layer II unit activity, and the delivery of two pulses at a 40 msec interpulse interval resulted in a paired-pulse depression effect. These observations suggest that, in addition to the activation of principal neurons, pyriform cortex stimulation also results in the activation of inhibitory mechanisms.

While the above studies have provided a considerable amount of information about the synaptic responses in the entorhinal cortex induced by the stimulation of olfactory structures, there is no report of the analyses of field potentials in the entorhinal cortex of the rat following pyriform cortex stimulation. Similar data and analyses are needed for the rat because of possible species differences in the physiology of this pathway, and because of the usefulness of this species in the experimental study of olfactory learning and synaptic plasticity. Therefore, in the present study, CSD analysis of field potentials in the entorhinal cortex following pyriform cortex stimulation was performed in order to gain insight into the evoked synaptic events, and to facilitate the interpretation of components of field potentials recorded at single depths in chronically-prepared animals.

In these same experiments, medial septal inputs to the entorhinal cortex were also stimulated to provide field potentials which were also analyzed using CSD techniques. Both cholinergic and non-cholinergic efferents from the medial septum project to the entorhinal cortex via the dorsal fornix and the fimbria (Segal, 1977; Alonso & Kohler, 1984; Insausti et al., 1987; Gaykema et

al., 1990). Lateral aspects of the medial septum project heavily to the medial entorhinal cortex while cells in the medial aspect innervate more lateral parts of the entorhinal cortex (Gaykema et al., 1990). Septal inputs terminate most heavily in layer II and IV of the medial and lateral entorhinal areas, and also terminate in layer III to a lesser degree (Alonso & Kohler, 1984; Witter et al., 1989; Gaykema et al., 1990).

The medial septal area is of interest with respect to neuromodulation and temporal processing in the entorhinal cortex, in part, because of its contributions to oscillatory activity in the hippocampus. Cholinergic and non-cholinergic medial septal and diagonal band fibers project to the dentate gyrus and the CA fields of the hippocampal formation (Mosko et al., 1973; Chandler & Crutcher, 1983; McNaughton & Miller, 1984), and these projections are thought to contribute to the hippocampal theta rhythm (Green & Arduini, 1954; Petsche et al., 1962; Stewart & Fox, 1990; Bland & Colom, 1993). Some cells in the medial septum and nucleus of the diagonal band fire bursts in phase with the hippocampal theta rhythm, and maintain their rhythmic bursting even after fimbrial connections with the hippocampus are cut (Petsche et al., 1962; McLennan & Miller, 1976). In the entorhinal cortex, theta-frequency activity reverses in phase between the superficial and deep layers (Mitchell & Ranck, 1980; Alonso & Garcia-Austt, 1987a) indicating that this activity is not volume conducted from the hippocampus. The entorhinal cortex also contains neurons in layers II and III which fire either rhythmically or non-rhythmically with a constant phase-relationship to the theta rhythm (Alonso & Garcia-Austt, 1987b). The superficial layers of the entorhinal cortex therefore both receive septal inputs and contain neurons which are the source of entorhinal cortex theta activity. Lesions of the medial septum block theta activity in both the

hippocampus and in the entorhinal cortex (Green & Arduini, 1954; Mitchell et al., 1992), and carbachol induces theta-like activity in hippocampal (Konopacki et al., 1987) and entorhinal cortex slices (Konopacki & Golebiewski, 1992; Konopacki et al., 1992). These similarities further suggest that cholinergic efferents from the septum contribute to theta-frequency activity in both the hippocampal formation and the entorhinal cortex.

Although some studies have described field responses in the hippocampus following septal stimulation, there have been no reports describing entorhinal cortex responses to septal stimulation. Field potentials in the dentate gyrus following medial septal stimulation have been reported by some authors as being rather weak, but the same stimulation can result in strong facilitatory effects on field potentials evoked a short time later by stimulation of the perforant path (Alvarez-Leefmans & Gardner-Medwin, 1975; Fantie & Goddard, 1982). Other researchers have reported stronger field potentials, and similar facilitation effects which appear to result from the activation of granule cell neurons near their soma (Andersen et al., 1961; Robinson & Racine, 1982; McNaughton & Miller, 1984).

In order to facilitate the study of medial septal projections to the entorhinal cortex using field potential recording techniques in chronic animals, CSD analysis was used in the present study to localize the synaptic populations in the entorhinal cortex activated by medial septal stimulation. Further, because both pyriform cortex and medial septal inputs have been shown anatomically to terminate in the superficial layers of the entorhinal cortex, it was of interest to determine to what degree electrophysiologically localized synaptic events might also overlap near the same neuronal populations. Evoked field potential recordings for CSD analysis were therefore obtained in response to separate

stimulations of the pyriform cortex and the medial septum in the same animals. In addition, the synaptic events associated with short-term facilitation in these input pathways were examined by delivering pairs of pulses at an interpulse interval which leads to a facilitation of the evoked potentials. Some of these results have been reported in abstract form (Chapman & Racine, 1995a).

METHODS

Surgery. Adult male Long Evans hooded rats were anesthetized with urethane (1.5 g/kg, i.p.) and placed in a stereotaxic frame with bregma and lambda on the horizontal plane. The temperature of the animal was monitored with a rectal probe, and kept within 36.5 to 37.5°C during the course of the experiment by adjusting a heating lamp. Bipolar twisted wire teflon-coated stainless steel stimulating electrodes were lowered into the right pyriform cortex (3.6 mm posterior and 6.5 mm lateral to bregma, and 0.5 mm above the base of the brain), and the right medial septum (0.2 mm anterior, 0-0.2 mm lateral and 6.0 mm ventral to bregma). One tip of each of the bipolar stimulating electrodes extended 0.5 mm beyond the other. The stereotaxic instrument was grounded, and a stainless steel jeweler's screw placed above the left frontal cortex served as a reference electrode.

Monopolar recording electrodes were stainless steel 00 insect pins insulated with EpoxyLite with a flat exposed tip 40 to 60 μm in diameter. In three animals, teflon-coated tungsten wire electrodes cut blunt to a diameter of 50 to 80 μm were used. In order to record field potentials at multiple intervals in the plane perpendicular to the surface of the medial entorhinal cortex, the electrodes were placed in a Narishige mechanical micromanipulator and

advanced on the sagittal plane 5.2 mm lateral to the midline at an angle 40° above horizontal. This angle of electrode penetration was used by Mitchell and Ranck (1980) and by Alonso and Garcia-Austt (1987a) in a study of phase reversals in theta-frequency activity across lamina in the rat entorhinal cortex. Interaural coordinates for the surface of the entorhinal cortex were 0.2 mm anterior to the interaural line, 5.2 mm lateral to the midline (ipsilateral to the stimulating electrodes), and 2.6 mm dorsal to the interaural line. Warmed mineral oil was applied to the exposed cortex following electrode penetration to prevent drying. Although glass electrodes are preferable to metal electrodes because of their reduced junctional capacitance and better response to high-frequency potential changes, stiff insect pin electrodes were used in this experiment to limit bending of the electrode over the approximately 12 mm trajectory to the entorhinal cortex.

Stimulation and Recording. Electrical stimuli were generated with a Grass S88 stimulator, and photoelectric stimulus isolation units (Grass SIU6B) were used to deliver 0.1 msec biphasic constant current pulses to the pyriform cortex and medial septum. Evoked field potentials were analog filtered (.3 Hz high-pass, and 3 kHz low-pass at half-amplitude), and amplified using a Grass (Model 12) amplifier. Evoked field potentials were digitized at 10 kHz with a 12-bit A/D board and stored on computer hard disk.

The recording electrode was slowly advanced to the superficial layers of the entorhinal cortex, and the vertical positions of the pyriform cortex and medial septum electrodes were then adjusted to optimize the current thresholds for low-intensity test-pulses delivered at 0.1 Hz. Test-pulse intensities were then adjusted to levels which evoked entorhinal cortex responses approximately 75% of the asymptotic response amplitude. Test-pulse intensities ranged between

475 and 725 μA for pyriform cortex sites, and between 500 and 1000 μA for medial septal sites. The recording electrode was again slowly advanced while monitoring responses evoked by pyriform cortex stimulation until the electrode was prevented from advancing by contact with the skull underlying the surface of the entorhinal cortex. A 20 min period preceded subsequent testing. In most experiments, evoked field potentials were recorded at each of 41 depths spaced at 50 μm intervals as the recording electrode was retracted to a 2.0 mm distance from the surface of the cortex. When tungsten electrodes were used, however, the electrodes were not first placed at the surface, and field potentials were recorded as the electrode was advanced from a coordinate 2.0 mm distant from brain surface. This prevented damage to these more fragile electrodes prior to recording which could occur during surface determination.

During experiments with the first few animals it was found that when two identical pulses were delivered to either the pyriform cortex or medial septum at an interpulse interval of 70 msec, the response evoked by the second pulse was enhanced relative to that evoked by the first pulse. Field potentials were therefore recorded in response to paired-pulse stimulation of either the pyriform cortex or the medial septum at each recording depth to characterize synaptic events associated with the facilitation effects. Ten paired-pulse responses were recorded at each depth, one every ten sec, and later averaged.

Polysynaptic evoked potentials are less reliably evoked than monosynaptic responses due to variability in monosynaptically-induced firing, and in a resulting variability in the summation of disynaptic responses (Berry & Pentreath, 1976). Polysynaptic responses therefore tend to fail at frequencies of stimulation above 50 Hz, while monosynaptic responses usually follow frequencies closer to 100 Hz or more. In order to test whether the evoked

responses in the entorhinal cortex are due to monosynaptic connections from the pyriform cortex, frequency of following tests were conducted in three animals (after depth recordings) by delivering 1.0 sec trains of stimulation pulses at frequencies between 60 and 125 Hz. In one animal (#4), responses to five trains at each stimulation frequency were recorded at a depth of 250 μm and averaged at each frequency. Frequency of following tests were inconclusive for medial septal evoked responses due to the presence of large field components not generated in the entorhinal cortex (see below).

Histology After recordings were completed, anodal current (50 μA) was passed through the recording electrode relative to the right stereotaxic earbar for 15 sec. The location of the resulting iron deposits was later identified using the Prussian Blue reaction to confirm the depths at which recordings were obtained. In some animals, current was also passed between the tips of each bipolar stimulating electrode to aid in the localization of placements in the pyriform cortex and medial septum. Animals were perfused through the heart with 0.9% saline followed by a 10% formalin solution, and the brains were removed and stored in a solution of 20% glucose in 10% formalin. Brains were usually divided on the coronal plane so that coronal sections containing the stimulating electrodes tracks, and saggital sections containing the recording electrode tracks could be obtained. In a few early animals, all electrode locations were examined on saggital sections. The frozen, 40 μm thick sections were cut using a cryostat and placed on gelatin-coated slides for staining. Following the Prussian blue reaction (5% KFeCN in 1% HCl), sections were counterstained with Neutral red. Locations of stimulating electrodes were plotted on sections taken from the Atlas of Paxinos and Watson (1986). Light photomicrographs of recording electrode tracks were obtained with a Zeiss

Axioskop microscope using a green interference filter and 400 ASA black and white print film.

Current Source Density Analysis. Extracellularly-recorded field potentials result from the volume averaging of many small membrane currents resulting from neuronal activity. The extracellularly recorded field potential (ϕ) is related to the membrane current (I_m , in units A/cm³) by the equation

$$I_m = -\nabla\sigma \cdot \nabla\phi \quad (1)$$

where σ is a tensor describing the conductivity of the extracellular space, and ∇ is a divergence operation which determines the rate of change in the potential and conductivity gradients per unit volume for all coordinates in extracellular space (Nicholson & Freeman, 1975; Mitzdorf, 1985). I_m is negative for current sinks, and positive for sources. The validity of this equation depends on the assumptions that the electrical field in the extracellular space obeys Ohm's law, and is quasistatic (i.e. negligibly affected by capacitive, inductive, and magnetic effects of membrane currents) for physiologically relevant frequencies ($\approx 0-1$ kHz, Mitzdorf, 1985). Error induced on the basis of these assumptions is estimated to be less than 10% (Nicholson & Freeman, 1975; Mitzdorf, 1985; Holsheimer, 1987).

In laminar structures which are isotropic (conductivity is not different in different directions), and homogeneous (σ does not vary with position) so that there is negligible current flow in the planes perpendicular to the recording track, and an invariant conductivity gradient in the directions perpendicular to the lamina, a one-dimensional CSD can be computed by

$$I_m = -(\sigma_z \cdot d^2\phi/dz^2) \quad (2)$$

where z is the direction perpendicular to the cortical plane (Mitzdorf, 1985).

Because the potential gradient is proportional to the amount of current flow by

Ohm's law ($V=I \cdot R$), changes in the potential gradient at a given point indicate a change in the amount of membrane current flow. The second derivative of the voltage gradient ($d^2\phi/dz^2$) therefore reflects the location of induced membrane currents, and is employed alone to calculate the CSD when gradients in conductivity (σ_z) are likely negligible (Rodriguez & Haberly, 1989; Van Goen et al., 1987; Leung et al., 1992; Ketchum & Haberly, 1993a).

Because the second derivative greatly exaggerates high-frequency noise it is a conventional practice to perform a preliminary smoothing of the evoked potentials in the spatial dimension (e.g., Rodriguez & Haberly, 1989). In the present study, high-frequency noise component contributions to the depth profiles with periods of less than 250 μm were digitally smoothed at each time point by convolving the data with weights derived from a Blackman window. Smoothing at this frequency did not mask nor alter the location of consistently observed sink-source distributions. The second derivative of the smoothed evoked potentials was computed with respect to cortical depth for all sampled time points to yield an estimate of the CSD by differentiating a polynomial interpolated through the data points. Because the conductivity of the entorhinal cortex is unknown, data were expressed in arbitrary units. CSD analysis results were displayed using both three-dimensional and topographical plots.

RESULTS

Experiments were performed on 18 animals. Data from three animals were excluded from analysis because of excessive variability in field potential recordings during the course of the experiments. Reliable evoked potentials and CSD results indicating sink-source pairs in the entorhinal cortex were

obtained in all of the 15 remaining cases for pyriform cortex stimulation, but in only 9 cases for medial septal stimulation. More reliable results for medial septal stimulation were obtained in the later experiments once the field potential component corresponding to an induced entorhinal cortex sink was identified, and maximized during stimulating electrode placement.

Stimulation and Recording Sites. The positions of the tips of the effective stimulating electrodes are indicated in Figure 2.1. The stimulation sites which evoked current sinks in the entorhinal cortex were closely associated with the medial septum. However, the high stimulation currents needed to evoke septo-entorhinal evoked potentials suggest that currents from the medial septum electrodes may have spread ventrally to activate the nucleus of the diagonal band, and caudally to low threshold substrates in the anterior commissure and/or the fornix-fimbria. The positions of the pyriform cortex stimulating electrodes were distributed to some extent in the rostrocaudal and mediolateral directions, but all electrodes were positioned near the dense layer of pyramidal cells in layer II, and in most cases the bipolar stimulating electrode tips straddled the pyramidal cells.

Figure 2.2A shows the locations of the recording electrode trajectories on tracings of representative saggital sections. Electrode tracks typically passed through the caudal hippocampal formation, including the subiculum, prior to entering the ventral aspect of the medial entorhinal cortex which is approximately 950 μm thick at these coordinates. A photomicrograph of an electrode track through the entorhinal cortex illustrating the layering of the entorhinal cortex in these sites is also shown in Figure 2.2B. Electrode penetrations were nearly perpendicular to the surface of the cortex, and the recording sites which extended 2.0 mm from the cortical surface included the

subicular region, molecular layer of the dentate gyrus, and sometimes the granule cell layer of the dentate gyrus.

Pyriiform Cortex Stimulation: Field Potentials. Field potentials evoked in the superficial layers of the entorhinal cortex by pyriform cortex stimulation contained a prominent negative deflection. The superficial negativity was clearly observed to follow pulse train frequencies of 80 Hz, consistent with a monosynaptic response (Figure 2.3). Because of stimulus artifacts and a merging of consecutively-evoked field potentials during 90 Hz and 100 Hz pulse trains, individual responses were less apparent except for relatively discrete negative deflections which were observed at appropriate latencies after the last pulse in the trains. Similar deflections were not observed following the 125 Hz train, suggesting a failure of the synaptic response between frequencies of 100 and 125 Hz (Figure 2.3).

An example of field potentials recorded at 50 μm intervals to a depth of 2.0 mm below the cortical surface is shown in Figure 2.4 (where, for clarity, only the response to the first pulse is shown). In all animals, the surface-negative component was maximal in layers I and II, at depths between 150 to 350 μm below the surface, and averaged 0.55 mV in amplitude (range 0.16 to 1.1 mV). Onset latencies averaged 10.4 msec (range 6 to 15 msec), and the mean latency to peak was 18.4 (range 16.5 to 23 msec). This field potential component tended to reverse to a positive deflection as the recording electrode was moved from the superficial layers to the deeper layers (Figures 2.4 & 2.5).

A second negative-going potential was sometimes superimposed on the positivity in the deep layers of the entorhinal cortex, and when observed (12 of 15 cases), it tended to become stronger in the molecular layer of the dentate gyrus (Figure 2.5). There was considerable variability in the latency of this field

potential component relative to that of the negativity in entorhinal cortex layers I and II (range -3.0 to 3.5 msec).

Paired-pulse testing in all animals, in which two identical stimulation pulses were delivered at an interval of 70 msec, resulted in responses to the second pulse which were enhanced compared to the responses evoked by the first pulse. The peak amplitude of the superficial negativity was enhanced by 146% on average (range 112 to 174%), compared to the response evoked by the first pulse. The negativity recorded in the dentate gyrus was also enhanced, and usually doubled in amplitude.

Following the surface negative component, at latencies greater than 25 msec, the pyriform cortex response usually displayed a weaker, and more long-lasting surface positive component. This component reversed at depths between 450 and 550 μm into a negative deflection recorded in the deep layers of the entorhinal cortex.

Pyriform Cortex Stimulation: CSD Analysis. The results of CSD analyses of field potentials evoked in the entorhinal cortex by pyriform cortex stimulation were remarkably consistent across animals. The typical CSD profile included a superficial sink-deep source configuration which peaked around 18 msec. This was followed at longer latencies by a deeper sink accompanied by a source in the superficial layers. The CSD results for the field potential data of Figure 2.4 are shown in Figure 2.6, and the corresponding data for the double-pulse results of Figure 2.5 are shown in Figure 2.7. In addition, because the depths and latencies of the sink-source distributions were very similar across animals, it was possible to average the CSD results. The average was derived from individual CSD plots normalized to the amplitude of the superficial sink, which afforded a more equal weighting of the individual results (Figure 2.8).

The spatial peak in the superficial sink ranged between 250 and 350 μm below the cortical surface, corresponding to layer II and the superficial parts of layer III. This was somewhat deeper than the depths at which the maximal field potentials were recorded. The associated current source was centered about 750 μm deep in layers V and VI. The onset- and peak latencies of the superficial sink corresponded very closely to those of the surface negativity in field potential recordings. Animals showing the shortest field potential onset latencies also tended to display an earlier, more superficial sink near the border between layer I and II (e.g., Figures 2.4 and 2.6). This small sink was associated with a weak source in layer III, and merged with the larger sink in layer II. This result, observed in 7 of the 15 cases, is expressed in the averaged CSD topographical plot as a slightly descending sink that precedes the development of the main superficial sink (Figure 2.8).

At depths near 1.8 mm below the cortical surface in the dentate molecular layer, an early current sink was observed in 11 cases. The mean latency to peak for this sink was 17.6 msec and it was associated with a negativity superimposed on the positive field potentials recorded at these depths. The relationship between the sink and the deep negativity in the field potentials can be seen in the results for animal #8 which are shown in Figures 2.5 and 2.7. The negative deflection, while decaying gradually through the subiculum, was strongest at the deepest recording sites, and the resulting sink was centered in the outer regions of the dentate molecular layer (Figures 2.7 & 2.8). The responses to the second pulse of the stimulation pulse-pairs were enhanced for both the superficial sink-source pair, and for the deep sink-source pair when it was observed, in accord with the enhanced negativities observed in the field potentials.

A long-latency sink-source pair was observed in 12 of 15 experiments. The late sink peaked in layers IV and V of the entorhinal cortex, and typically had an onset latency near 30 msec, and a latency to peak of between 45 and 50 msec (Figure 2.8). The current source associated with the sink was centered in layer II, at a depth 50 μm more superficial than the early sink. This late sink-source pair was not markedly enhanced by paired-pulse stimulation at the inter-pulse interval used.

Medial Septal Stimulation: Field Potentials. The field potentials evoked by stimulation of the medial septum were more variable in morphology compared to those evoked by pyriform cortex stimulation, and there were five field potential components observed in most animals. The five components varied in amplitude with recording depth, but not all displayed reversals in polarity.

The earliest component observed was deep-positive, brief, and was typically observed at latencies of 2 to 4 msec. This spike-like component, observed in 10 of 15 cases (e.g.s Figures 2.9 & 2.10), was largest in the molecular layer of the dentate gyrus, and sometimes appeared to reverse into a slight negative deflection near the hippocampal fissure.

A longer-duration positive component, peaking at latencies of 5 to 8 msec was observed in all animals, and followed the offset of the early spike-like component when present. The positive component was usually maximal in the molecular layer of the dentate gyrus, decreasing steadily in amplitude towards the cortical surface (e.g., Figure 2.9), and in some animals toward the granule cell layer (e.g., Figure 2.10).

A negative component, peaking with a mean latency of 15.6 msec, was observed at the deepest recording sites. The amplitude of the negativity was

always greatest near the dentate gyrus except for three animals in which the negativity was reduced over the last few hundred μm as the recording electrode passed into the granule cell layer. Figure 2.9 illustrates a case in which the negativity was reduced at depth between 1750 μm and 2000 μm below the surface, and Figure 2.10 illustrates the more typical result.

The weakest of the field potential components was a surface positive component which peaked at latencies near 20 msec and reversed into a shallow negative deflections at depth of roughly 300 to 350 μm (Figures 2.9 and 2.10). This component was less reliable than the earlier components, and was clearly discriminable in only 6 animals. After reversal, this negative deflection tended to merge with the stronger negativity described above.

The longest latency component was surface negative, reversed, in the deeper layers of the entorhinal cortex, and peaked at a mean latency of 29.3 msec (Figures 2.9 & 2.10, arrows). Although a clear surface negativity was observed in only 5 cases, a deep positivity peaking at this latency was observed in 4 additional cases. When observed, the shallow surface negativity peaked at a mean depth of 230 μm in layer II, and reversed at depths of approximately 350 μm in the superficial region of layer III. Both the surface negativity and the deep positivity had post-stimulus offset latencies near 50 msec.

Paired-pulse stimulation tended to enhance all components in the field potentials, but the effect on the early spike-like component was small (Figure 2.10). The distinctness of the two longest-latency components in the field potentials was often greatly enhanced in response to the second pulse compared to rather weak initial responses.

Medial Septal Stimulation: CSD Analysis. CSD analysis of entorhinal cortex field potentials following medial septal stimulation indicated clear sink-

source distributions in the entorhinal cortex of only 9 of 15 animals. In the remaining cases, observed sink-source pairs were restricted to regions outside the entorhinal cortex. Because the sink-source distributions in the subiculum and dentate gyrus are well-represented by animals in which sinks were also observed in the entorhinal cortex, and because septal stimulating electrodes in these animals were better placed, only the CSD results for experiments in which entorhinal cortex sinks were observed are reported here. In these nine animals, the CSD results were sufficiently similar to allow averaging of the profiles which were normalized to the amplitude of the superficial sink.

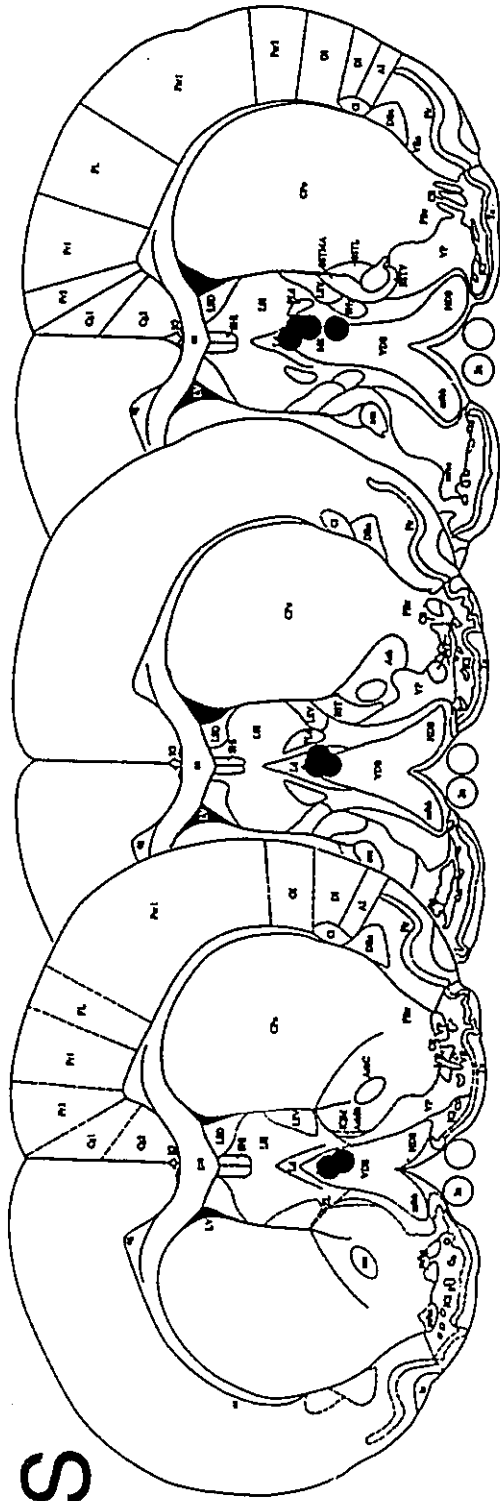
The entorhinal cortex sink evoked by medial septal stimulation had mean onset- and peak latencies of 14.1 and 30.3 msec, respectively. The sink began in superficial portions of layer III, and then rose into layer II near the border with layer III (Figure 2.13). This sink peaked in layer II at a depth of 350 μm , 50 μm deeper, on average, than the superficial sink induced by pyriform cortex stimulation. The current source associated with the sink was located in layers V and VI. The superficial sink evoked by septal stimulation corresponded to the late, surface negative component in the field potentials which occurred at the same latency and reversed at depths near 350 μm (Figures 2.11 & 2.12).

The superficial sink evoked by septal stimulation was often preceded by a shallow source at similar depths (Figure 2.11). The field potential correlate of this source was the weak, surface positive component. Both this source and following sink were enhanced by paired-pulse stimulation (Figures 2.12 & 2.13). The current source was more clearly localized to deep layer III following paired-pulse stimulation. Similarly, paired-pulse stimulation resulted in focussing of the peak of the superficial sink to more intermediate regions of layer III, and its onset became associated with a brief current source in layer I (Figure 2.13).

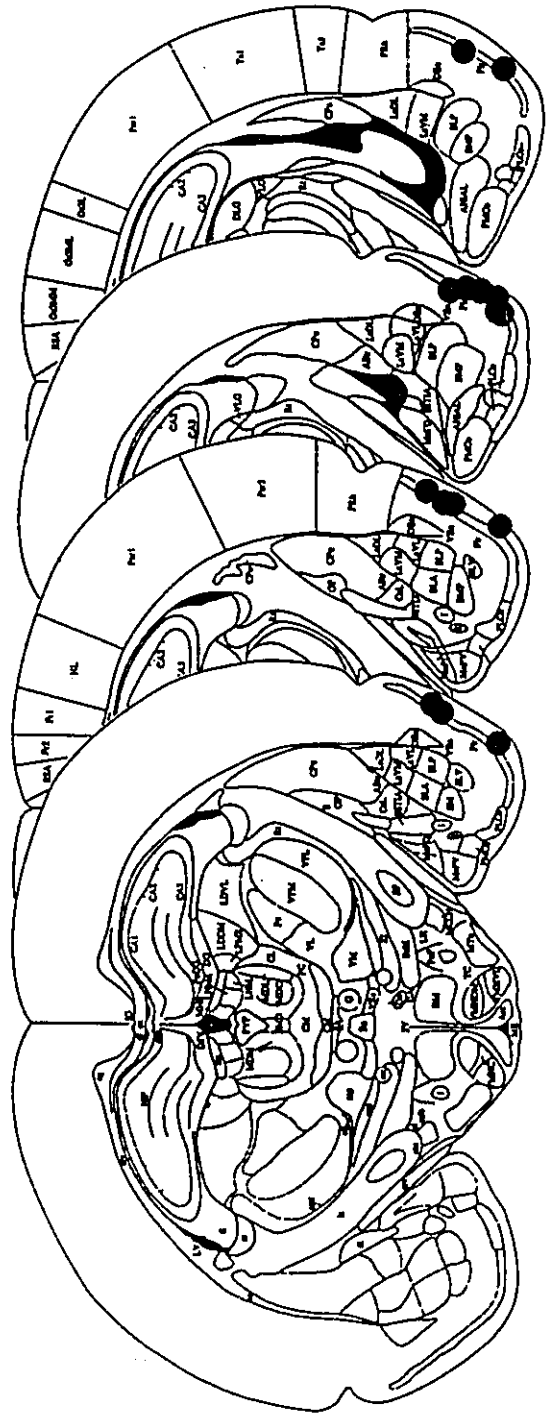
Short-latency current sources and sinks in the subiculum and hippocampal formation corresponded to the early spike-like, deep positive, and deep negative components of the field potentials observed at these depths. The spike-like component in the field potentials corresponded to a current sink of the same latency and duration at a depth of 1400 to 1700 μm which was accompanied by a current source close to the dentate gyrus granule cell layer. Following the spike, a strong current sink developed in the dentate molecular layer near the hippocampal fissure. This component, which peaked at a mean latency of 15.6 msec, corresponded to the strong deep negative component of the field potentials (Figure 2.13). The prominent deep positive-going component in the field potentials was not associated with marked effects in the CSD results. The only CSD correlate observed at similar latencies was a small current source at a depth of 1300 to 1500 μm . This source was more prolonged than the deep positive component, and was associated with a current sink in the subicular-angular bundle region, 900 to 1200 μm below the cortical surface. This source was observed in 7 of the 9 animals (see Figure 2.12 for one exception). After a single stimulation pulse, the peak latency of the sink tended to match that of the deeper source, but after the second stimulation pulse it tended to precede this source (Figure 2.13).

Figure 2.1

Figure 2.1. The locations of stimulating electrodes aimed at the medial septum (MS) and pyriform cortex (PY) are shown on representative coronal sections taken from the atlas of Paxinos and Watson (1986).



MS



PY

Figure 2.2

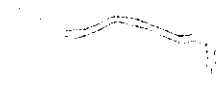
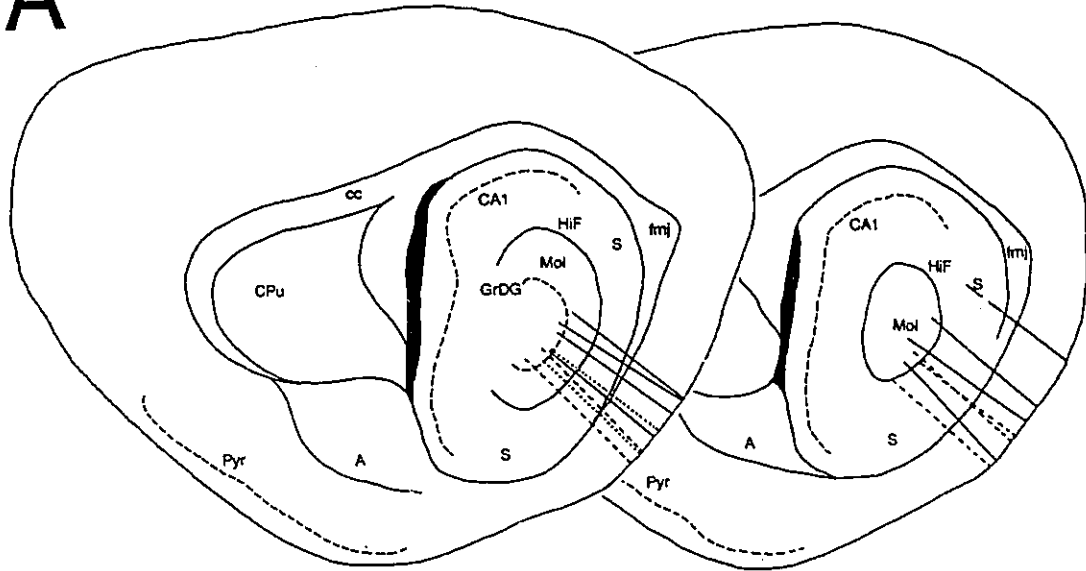
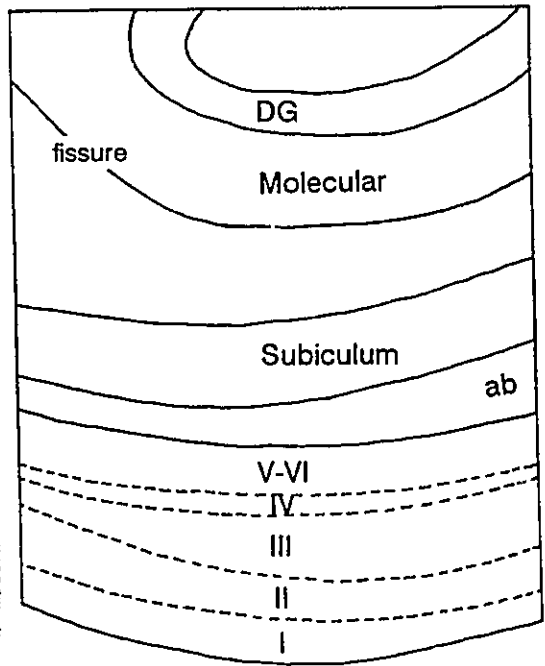
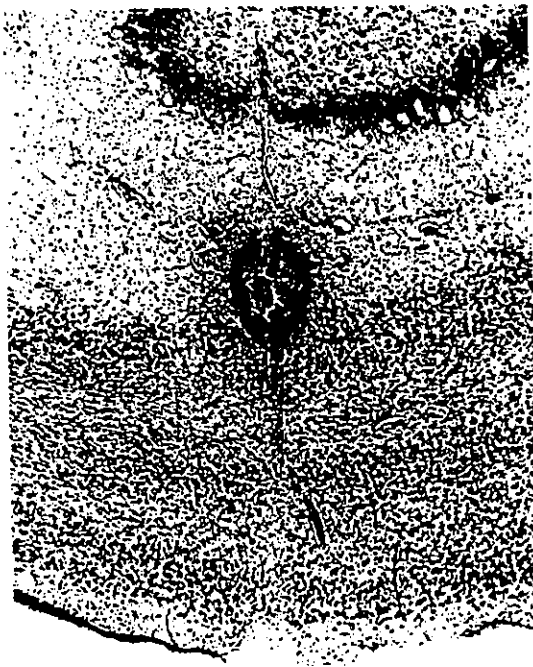


Figure 2.2. **A**, The 2.0 mm trajectories of recording electrodes through the entorhinal cortex are indicated on camera lucida tracings of representative saggital sections. **Solid lines** indicate tracks from which field potentials evoked by both pyriform cortex and medial septal stimulation were recorded. **Dashed lines** indicate tracks from which only pyriform cortex-evoked field potentials were recorded. **Dotted lines** indicate tracks from which representative recordings shown in subsequent figures were obtained. Subsequent figures based on responses only to the first stimulation pulse were based on data obtained from the more dorsal of these tracks. **B**, Photomicrograph of a representative saggital section. Cortical divisions and layers are indicated schematically to the right.

A



B



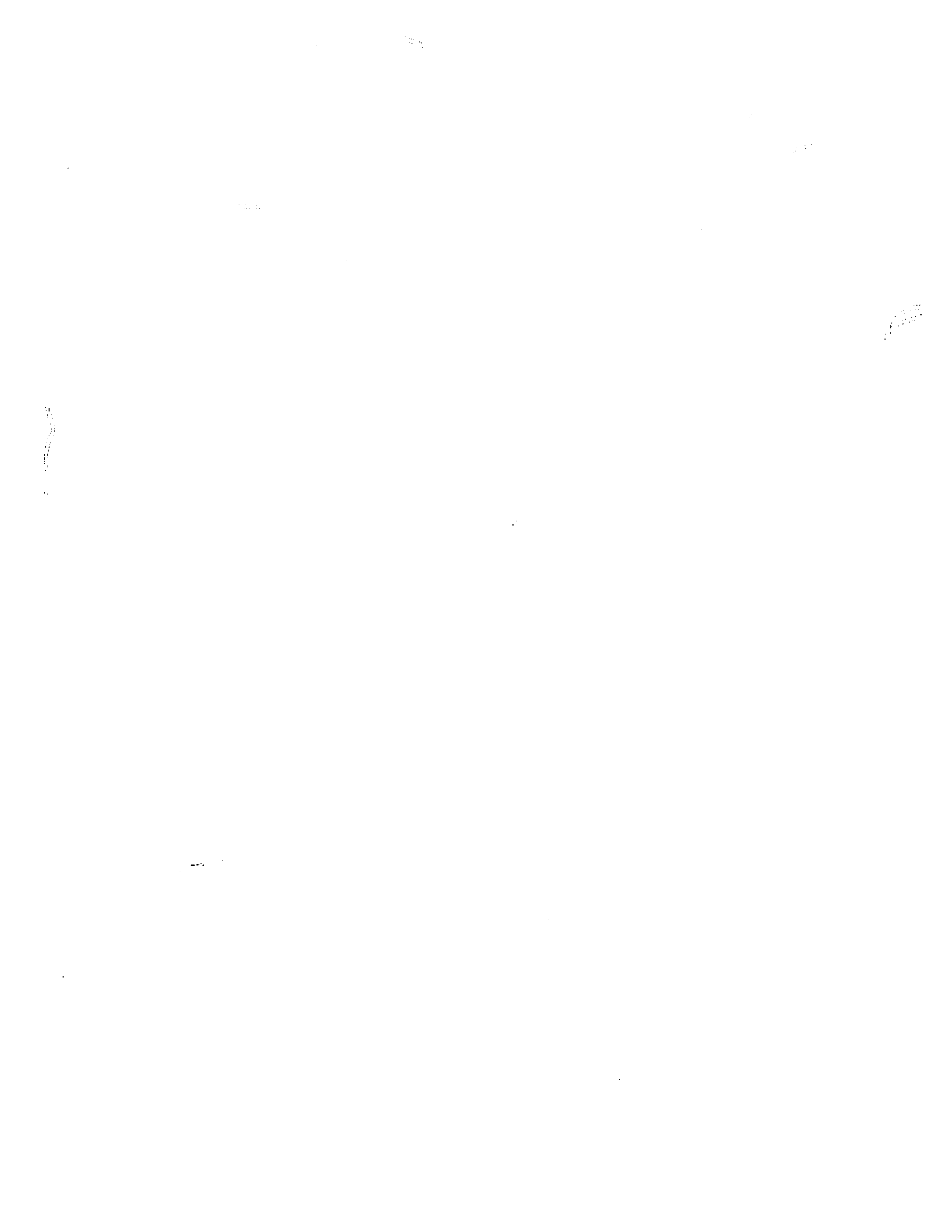


Figure 2.3

Figure 2.3. Frequency of following test for field potentials recorded in the entorhinal cortex following pyriform cortex stimulation. Stimulation trains at the indicated frequencies were 1.0 sec in duration. Recordings were made at a depth of 250 μm (Animal #4). Individual responses to each stimulation pulse are less distinct at stimulation frequencies above 80 Hz, and are not observed during 125 Hz stimulation. Stimulus artifacts have been reduced in size by low-pass filtering to improve clarity. Horizontal calibration, 25 msec; vertical calibration 0.25 mV.

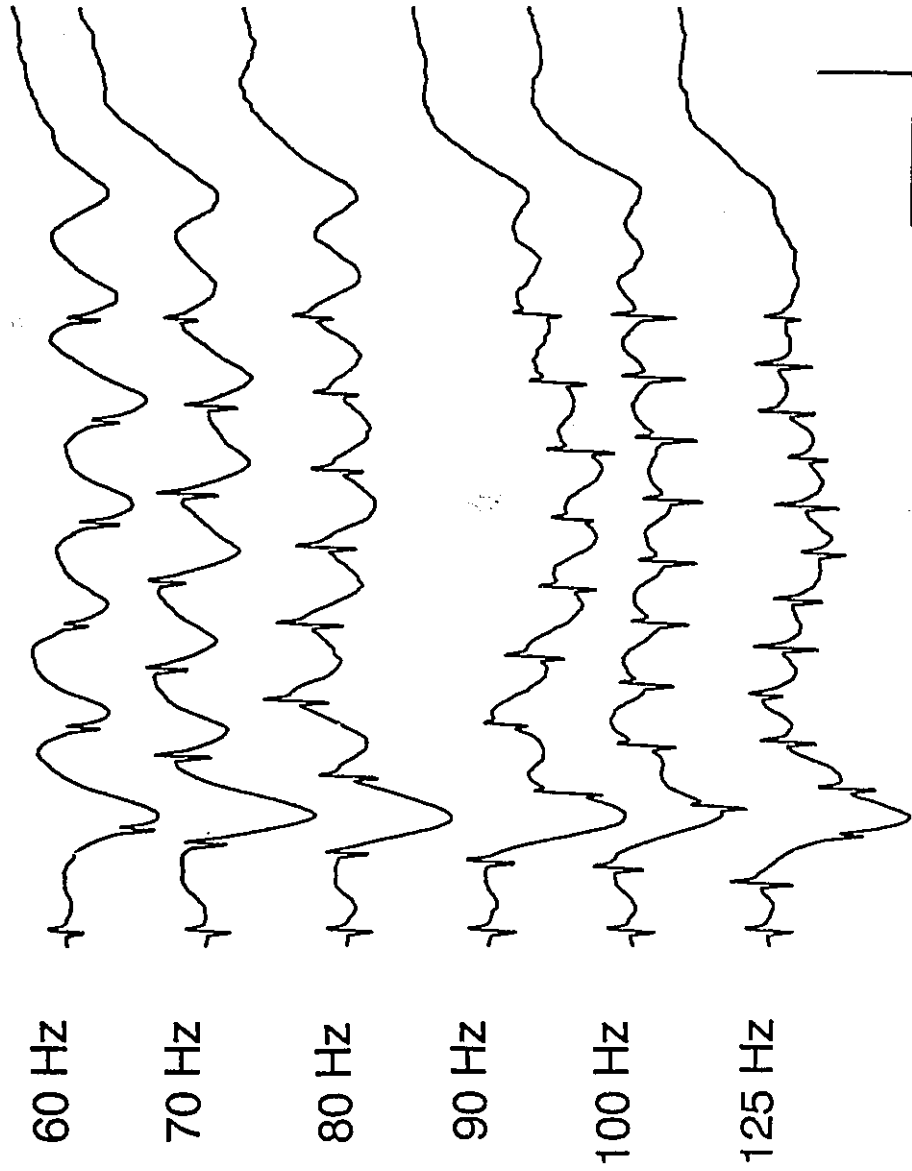


Figure 2.4

Figure 2.4. Averaged, un-smoothed evoked field potentials following pyriform cortex stimulation are shown for recordings made at 50 μm intervals between 0.0 mm and 2.0 mm from the surface of the entorhinal cortex in animal #16. The response to only the first of a pair of stimulation pulses is shown to enhance clarity. Stimulus intensity was 500 μA . Downward deflections are negative in polarity in this and all subsequent Figures. Horizontal calibration, 10 msec; vertical calibration, 1.0 mV.

PYRIFORM STIMULATION

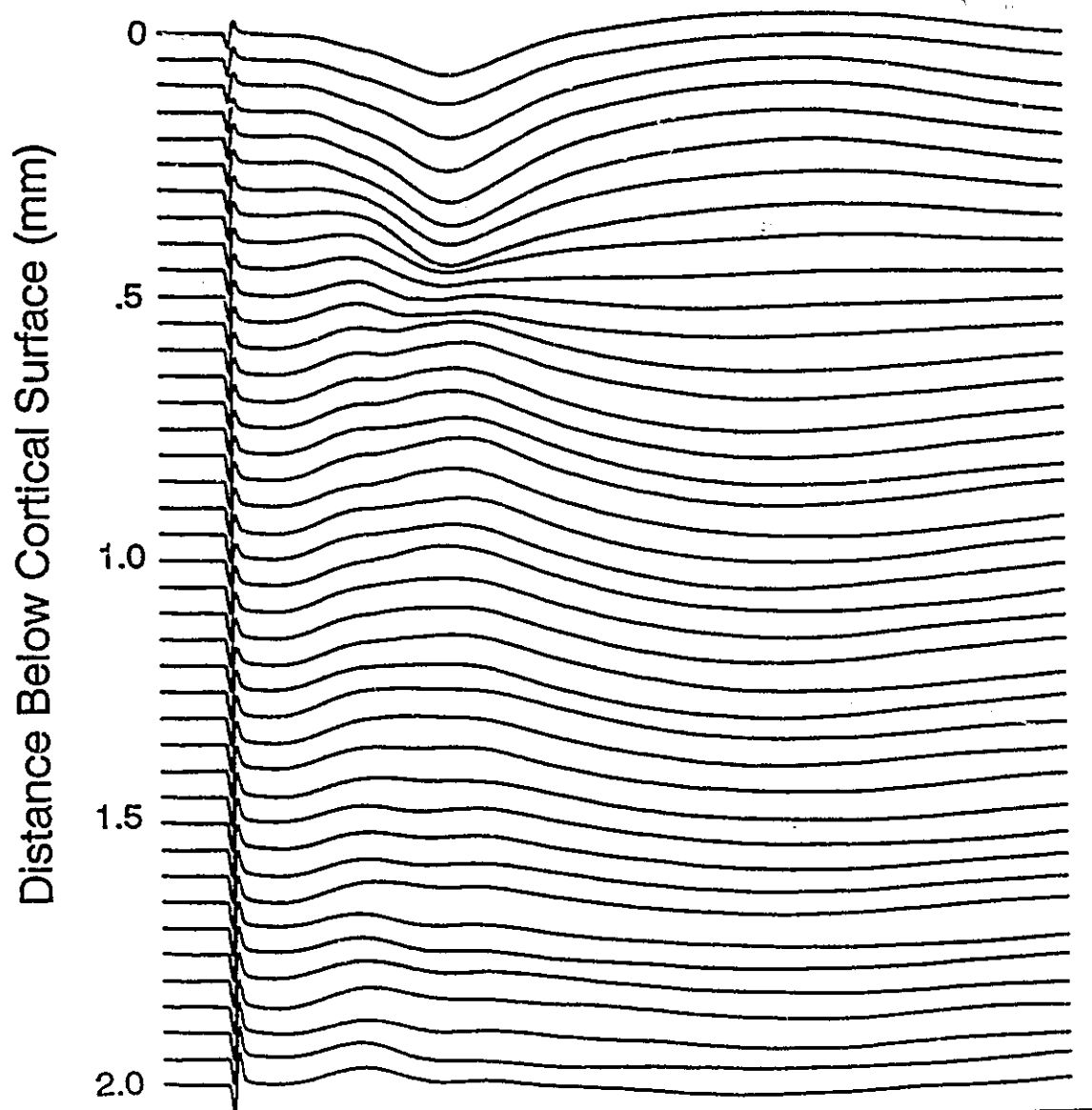


Figure 2.5

Figure 2.5. Averaged, un-smoothed evoked field potentials following paired-pulse pyriform cortex stimulation are shown for recordings obtained from animal #8. The interpulse interval was 70 msec. Stimulus intensity was 650 μ A. Horizontal calibration, 20 msec; vertical calibration, 1.0 mV.

PYRIFORM STIMULATION

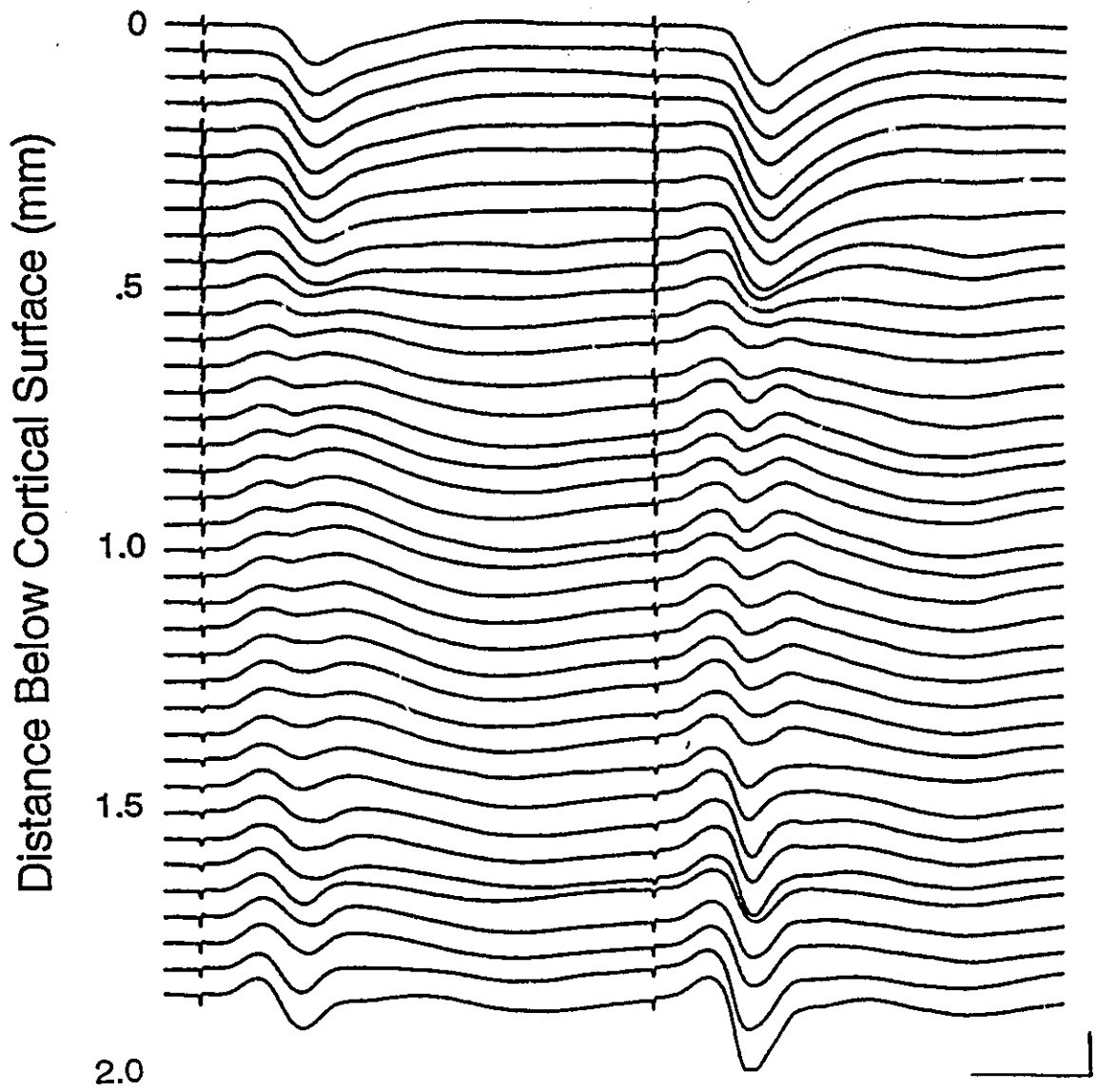
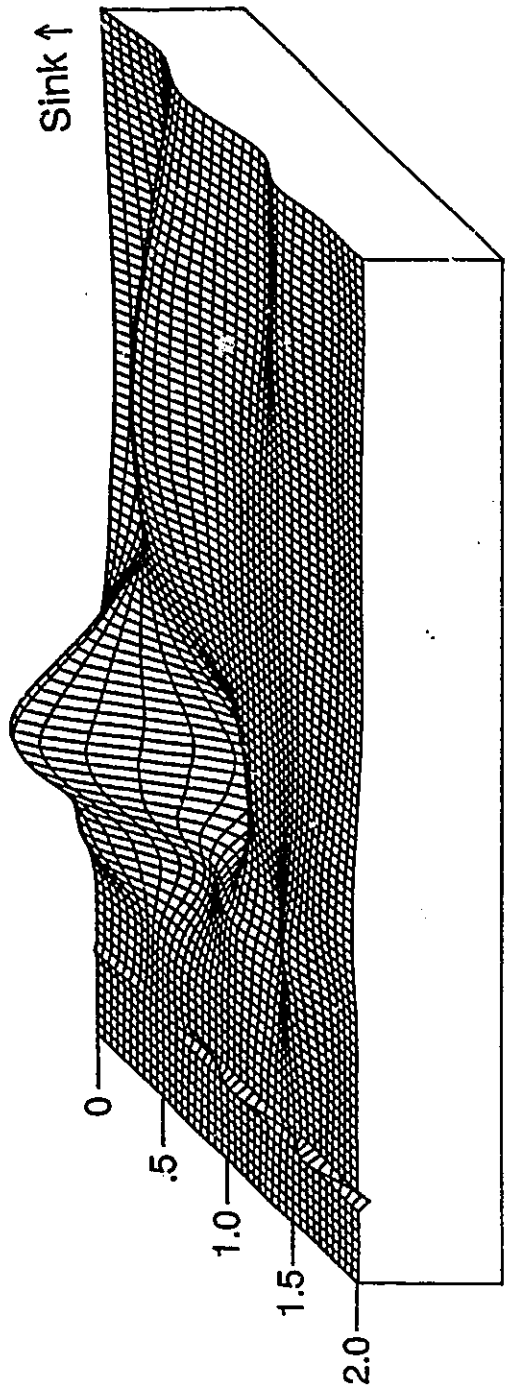


Figure 2.6

Figure 2.6. Current sinks and sources in the entorhinal cortex following pyriform cortex stimulation in animal #16 represented in both a surface plot and a topographical plot. Data are derived from the field potentials shown in Figure 2.4. The cortical layers and divisions are indicated to the right of the topographical plot in which the dotted line indicates transitions between current sinks and sources. Note that the major current sink is preceded by a weaker, more superficial sink.



Distance Below Cortical Surface (mm)

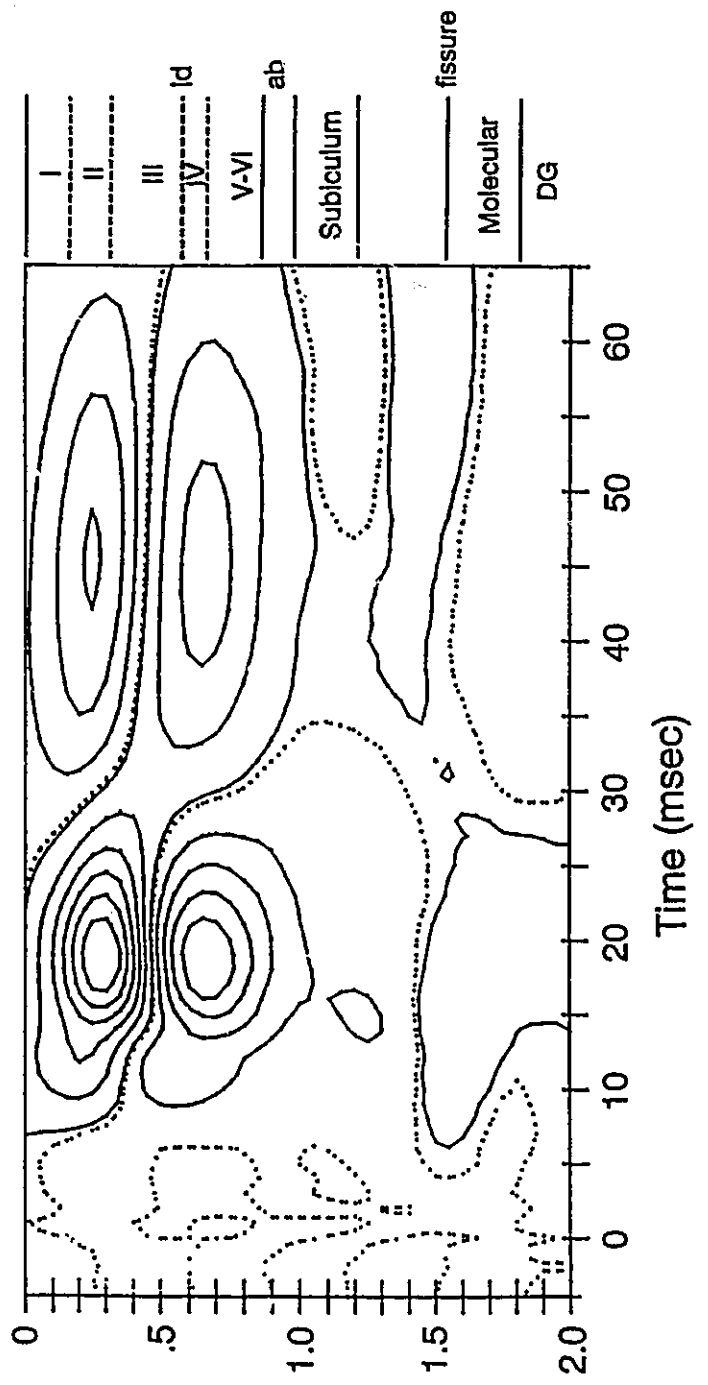


Figure 2.7



Figure 2.7. Current sources and sinks evoked in the entorhinal cortex following paired-pulse stimulation of the pyriform cortex in animal #8. Data are derived from the field potentials shown in Figure 2.5, and the electrode track shown in Figure 2.2B.

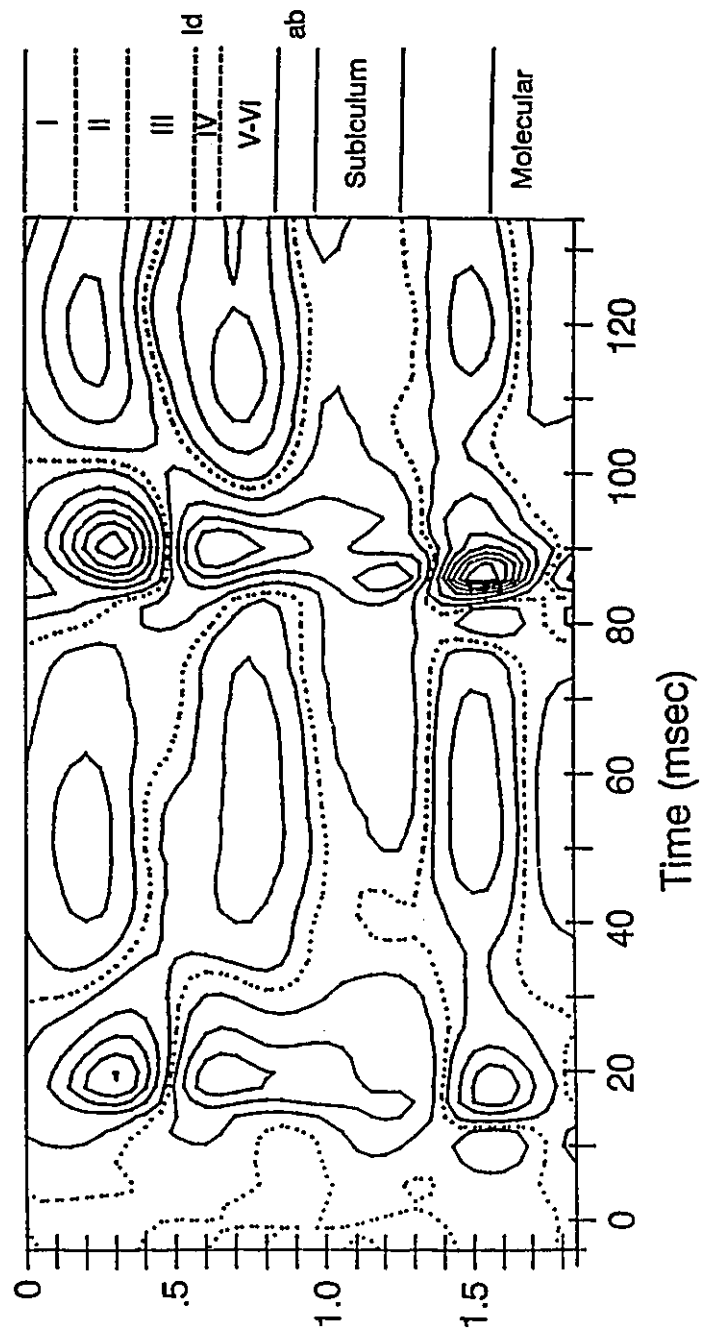
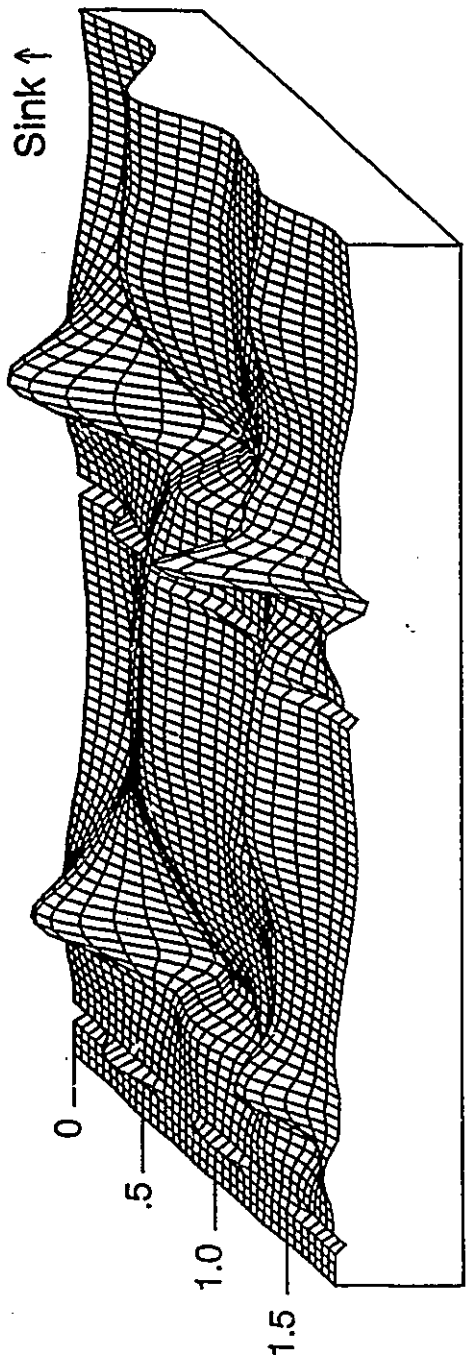
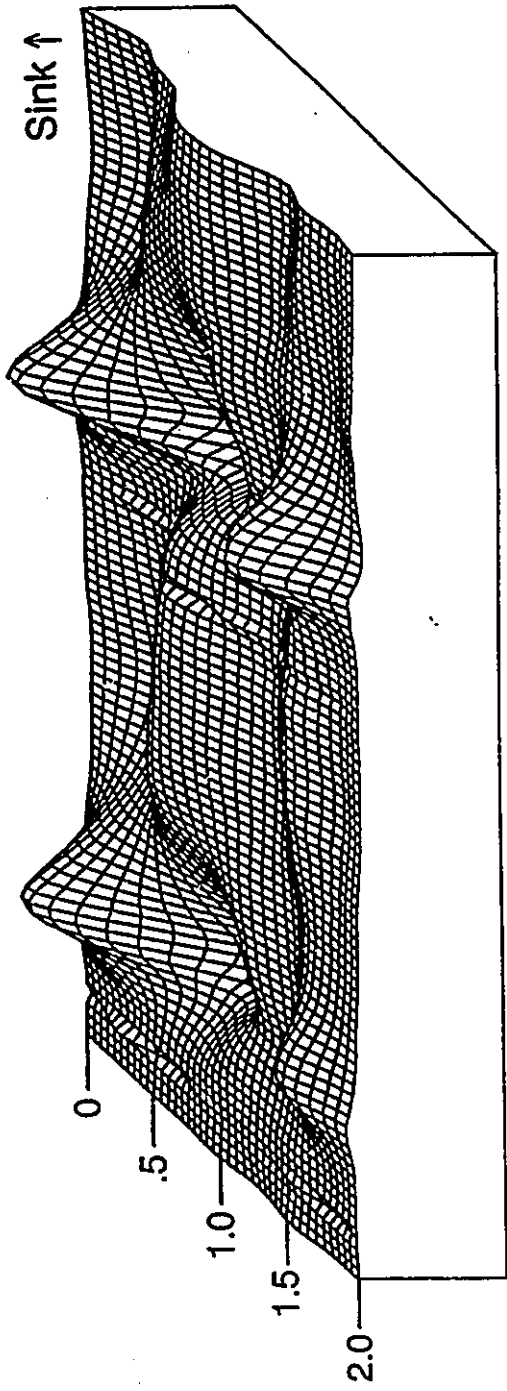


Figure 2.8

Figure 2.8. The average across CSD results for 15 animals indicating the location of membrane current sources and sinks in the entorhinal cortex following pyriform cortex stimulation. Data were standardized to the peak amplitude of the superficial sink prior to averaging.



Distance Below Cortical Surface (mm)

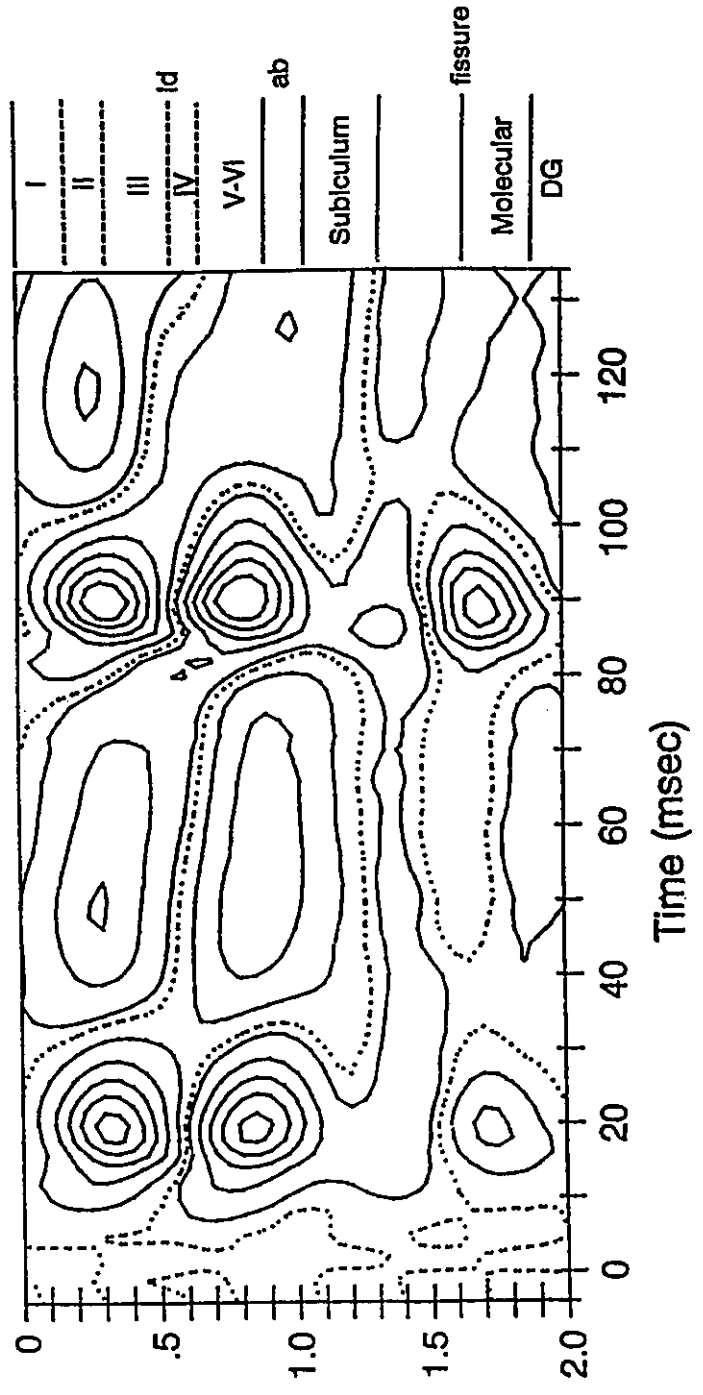


Figure 2.9

Figure 2.9. Averaged, un-smoothed field potentials evoked by medial septal stimulation are shown for recordings made at 50 μm intervals between 0.0 mm and 2.0 mm from the surface of the entorhinal cortex in animal #16. An arrow indicates a late surface negative component. Stimulus intensity was set to 500 μA . Horizontal calibration, 10 msec; vertical calibration, 1.0 mV.

SEPTAL STIMULATION

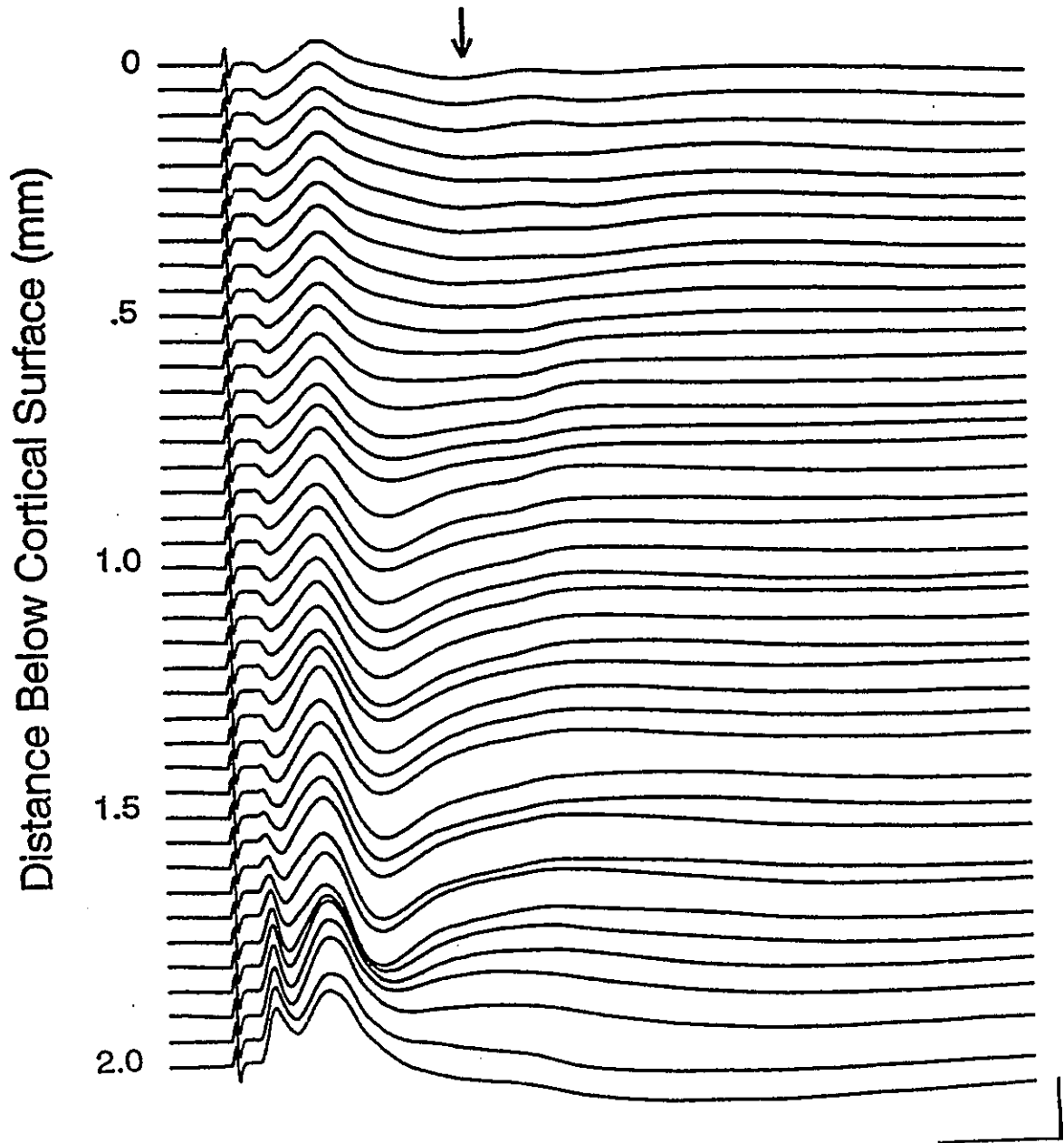


Figure 2.10

Figure 2.10. Averaged, un-smoothed field potentials evoked by paired-pulse stimulation of the medial septum are shown for recordings obtained from the electrode track of animal #8. Stimulus intensity was 650 μA . **Arrows** indicate a late surface negative component which is enhanced following the second pulse. Also, note the small spike-like field component superimposed on the deep negativity in response to the second pulse. Horizontal calibration, 20 msec; vertical calibration, 1.0 mV.

SEPTAL STIMULATION

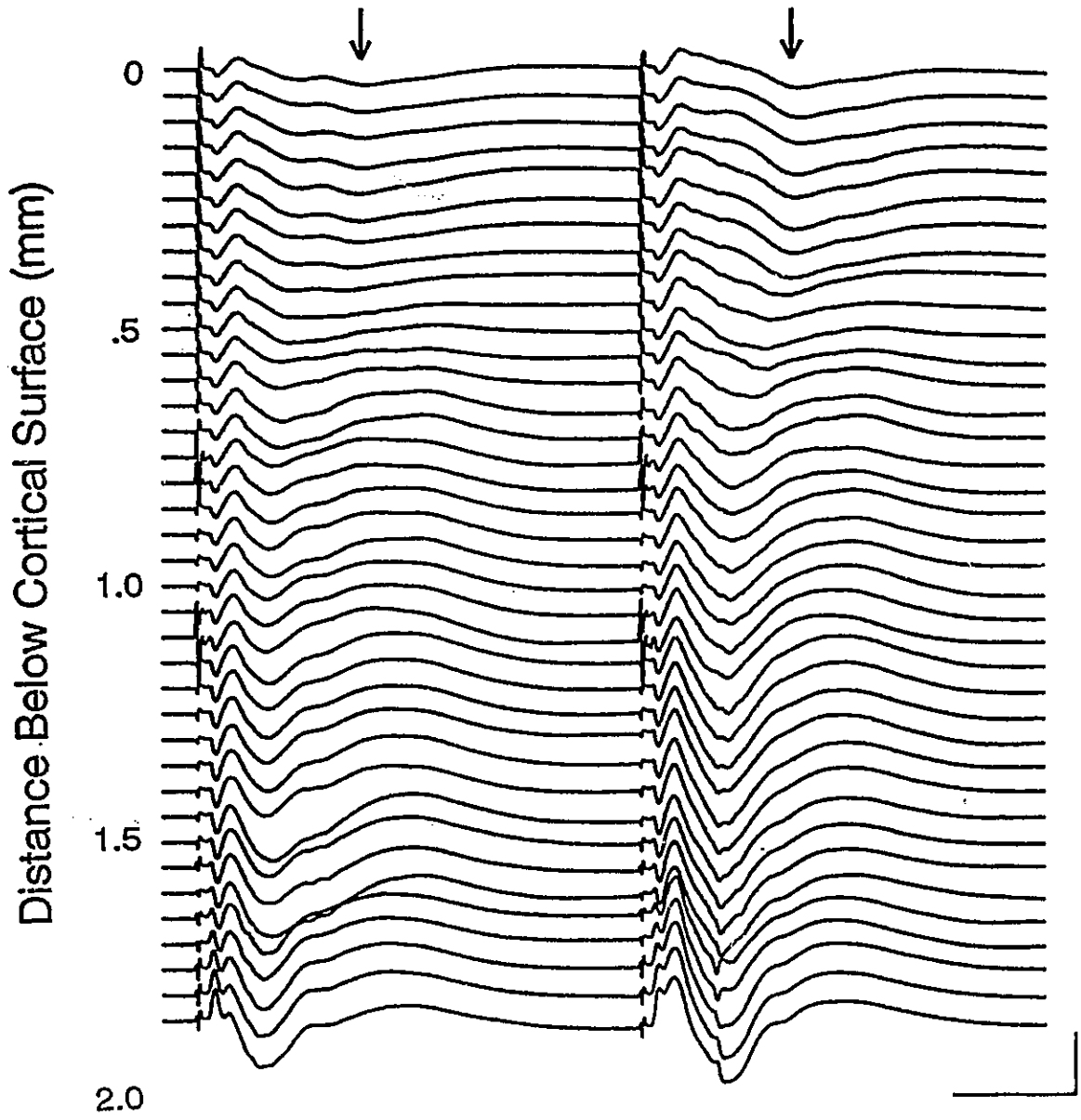
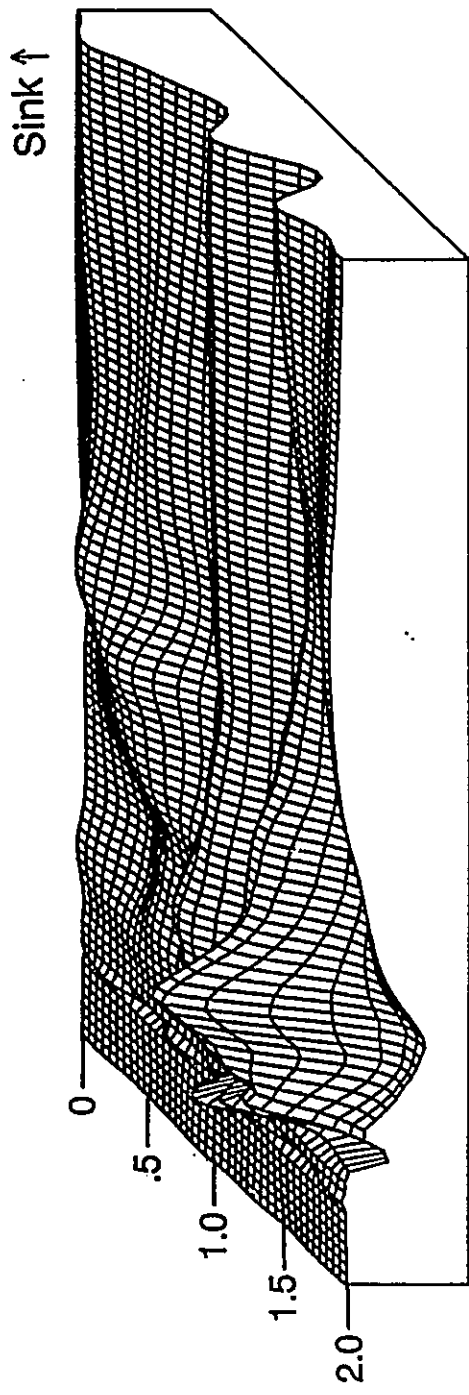


Figure 2.11

Figure 2.11. Current sinks and sources in the entorhinal cortex following medial septal stimulation in animal #16. Data are derived from the field potentials shown in Figure 2.9.



Distance Below Cortical Surface (mm)

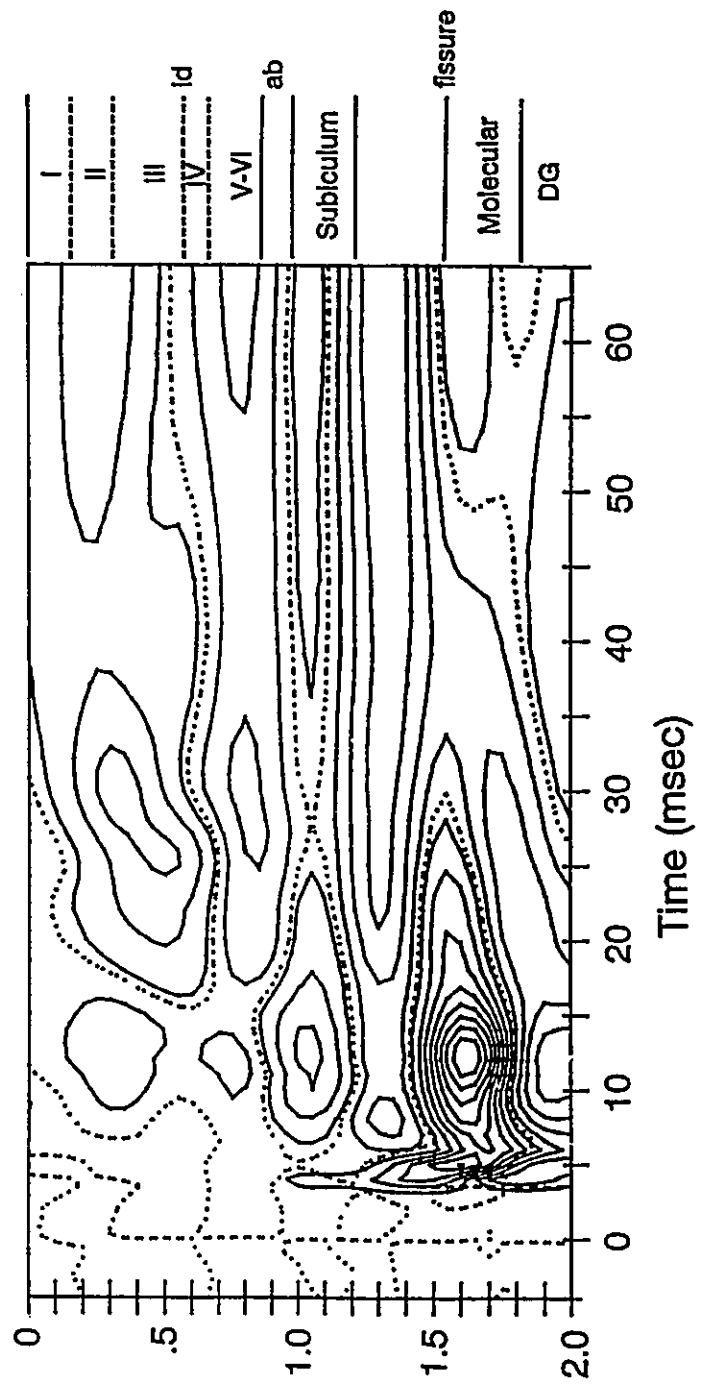


Figure 2.12

Figure 2.12. Current sources and sinks evoked in the entorhinal cortex following paired-pulse stimulation of the medial septum in animal #8. Data are derived from the field potentials shown in Figure 2.9.

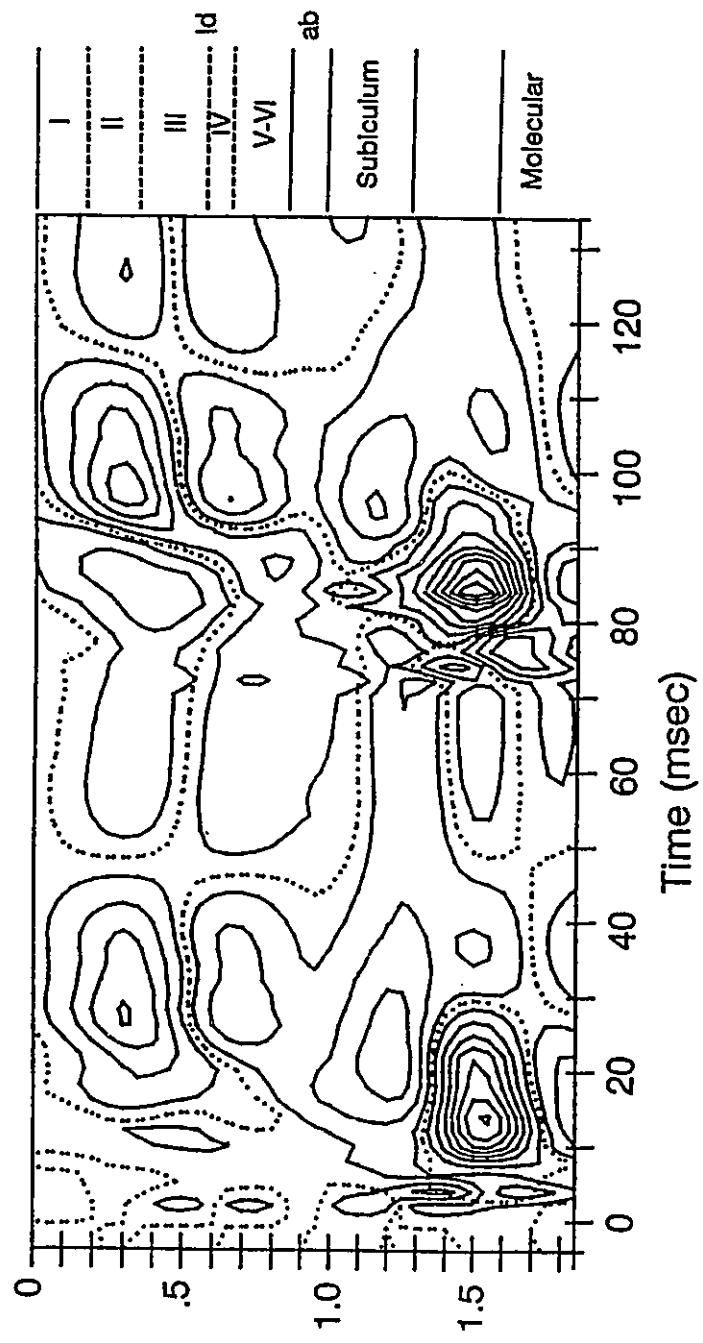
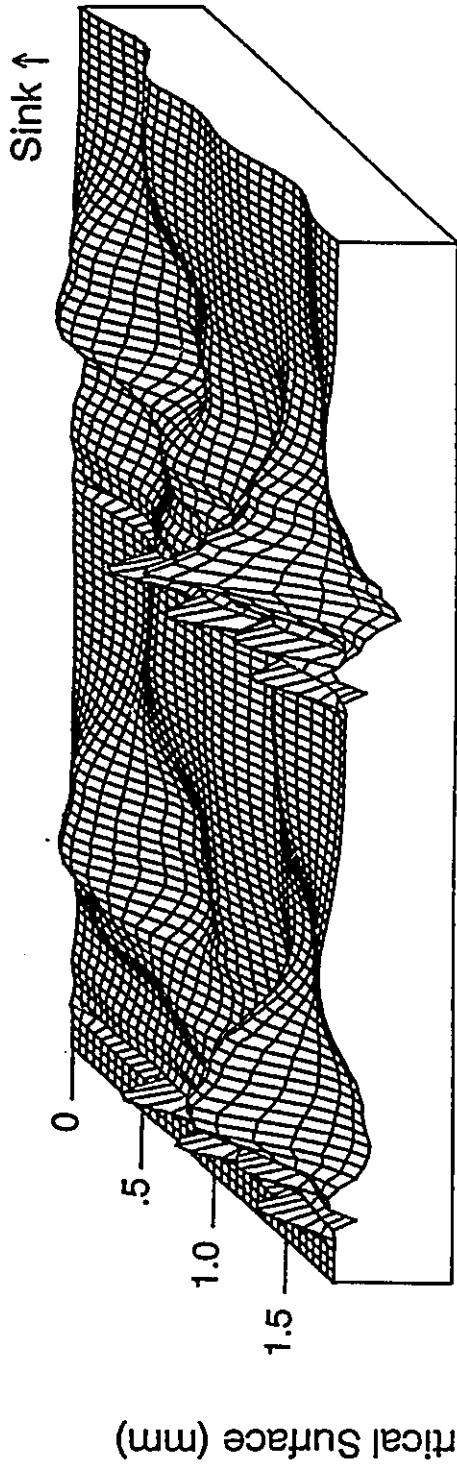
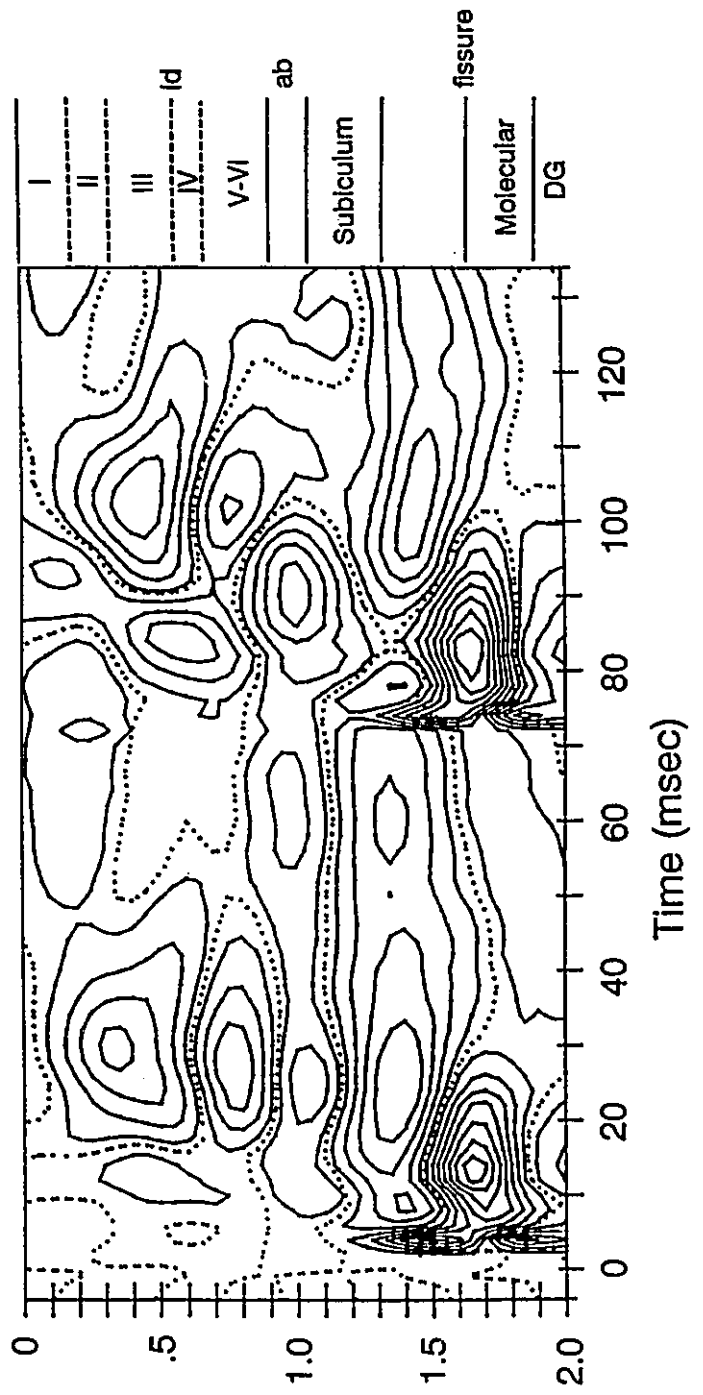
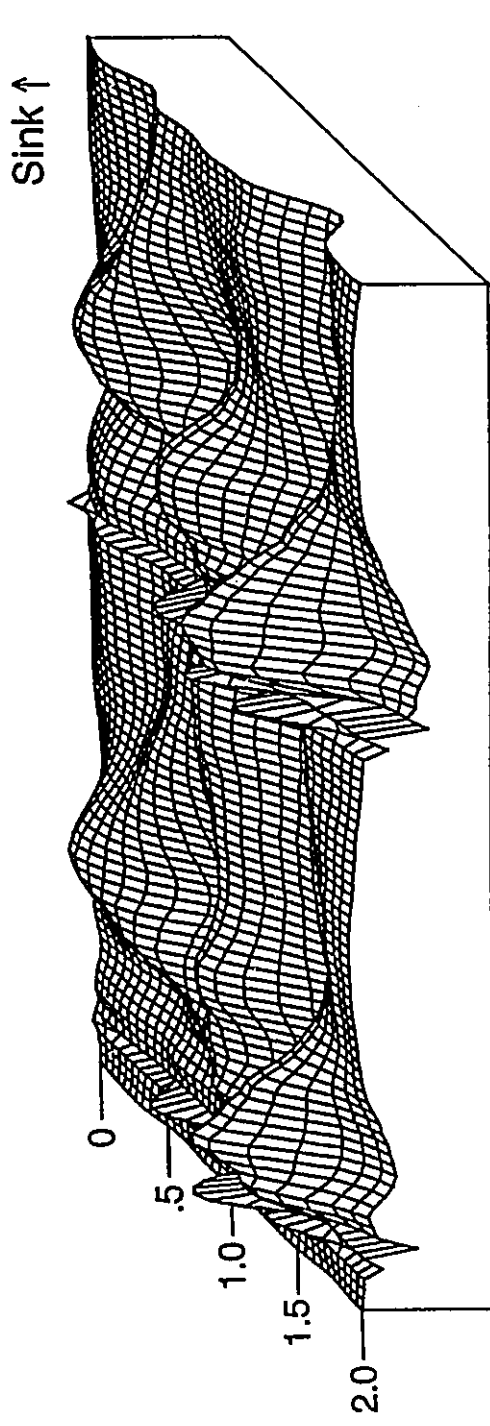


Figure 2.13

€

Figure 2.13. The average across CSD results for 9 animals indicating the location of membrane current sources and sinks in the entorhinal cortex following medial septal stimulation. Data were standardized to the peak amplitude of the superficial sink prior to averaging.



DISCUSSION

The CSD analyses described here indicate the location of the current sinks and sources in the medial entorhinal cortex which result from pyriform cortex and medial septal stimulation. Stimulation of either the medial septum or the pyriform cortex resulted in current sinks in layer II of the entorhinal cortex, although the sink induced by septal stimulation was more distributed and was centered close to the border between layers II and III. Current sources and sinks resulting from the activation of hippocampal formation structures were also observed. These data indicate the field potential components which are generated by synaptic activity in the superficial layers of the entorhinal cortex following stimulation of the pyriform cortex and medial septum. This information allows field potentials recorded in chronic preparations to be interpreted in terms of evoked synaptic activity these layers.

An important assumption of one-dimensional CSD analysis is that current flow within cortical lamina in directions perpendicular to the electrode penetration is negligible (Mitzdorf, 1985). Invariant field potential amplitude across a cortical region is consistent with this assumption, and has been observed for field potentials recorded in restricted regions of the entorhinal cortex following pyriform cortex stimulation in the cat. Boeijinga & Van Groen (1984) found that the amplitude of the early surface negativity in cat ventrolateral entorhinal cortex decreased gradually in the rostro-caudal direction, and that there was a smaller gradient in the mediolateral direction. Van Groen et al. (1987) also compared medial and lateral recording penetrations in the cat and found that amplitudes varied by a factor of only about 1.5 while field potential amplitudes varied much more with cortical depth. In the present study the

maximal amplitude of the entorhinal cortex field potential following pyriform cortex stimulation were compared to the mediolateral and dorsoventral positions of the recording electrodes. Although there was considerable variability in the amplitudes of responses across preparations (0.16 to 1.1 mV), there was not a clear gradient in either the dorsoventral or mediolateral directions. CSD profiles were also remarkably consistent across animals, suggesting a negligible contribution of lateral current flow to these profiles.

CSD analysis can also be affected by variations in the conductivity of the extracellular space (Mitzdorf, 1985). Conductivity in cortical tissue tends to be reduced in areas where somata are tightly packed (Holsheimer, 1987), and where there are many myelinated fibers (Haberly & Shepherd, 1973). Variations in cell density are most marked in the entorhinal cortex at the coordinates studied here between layer I and II (Figure 2.2B). However, in the pyriform cortex the conductivity gradient has only small effects on the results of CSD analyses near the border of layers Ib and II (Haberly & Shepherd, 1973). Further, the location of sources and sinks is not affected by corrections in the CSD method which account for reduced conductivity in the pyramidal cell layer of the CA1 region of the hippocampus (Holsheimer, 1987). For the results reported here, conductivity is most likely to be reduced to the greatest degree in the white matter regions between the subicular cell layers and the dentate gyrus, distal to recording sites in the entorhinal cortex.

Pyriform Cortex Inputs. The time-course and spatial location of the early sink in the entorhinal cortex following pyriform cortex stimulation (Figure 2.5) suggest that the negative field potential component results from excitatory synaptic activation of the dendritic arbour of cells in layers II, and possibly upper layer III. This superficial sink is consistent with anatomical findings indicating

that pyriform cortex efferents terminate exclusively in layers I-III of the entorhinal cortex (Room et al., 1984; Boeijinga et al., 1982). It is therefore assumed that the source in the deep layers of the entorhinal cortex, observed at the same latency, is passive. In some cases, the evoked current sink was first observed in the deep portions of layer I before centering in layer II. This may be due to the activation of the dendrites of layer II neurons which both extend upwards into layer I and arborize heavily in layer II (Lingenhohl & Finch, 1991). The ability of the corresponding field potential component to follow frequencies greater than 80 Hz is also consistent with the direct monosynaptic activation of layer II entorhinal cortex neurons by pyriform cortex efferents (Figure 2.3).

Given a distance of approximately 5.2 mm between the stimulating and recording electrodes, the fastest fibers mediating the response are estimated to have conduction velocities of 0.50 m/sec. Similarly slow conduction velocities for the anterior (0.7 m/sec) and posterior (0.4 m/sec) pyriform cortex inputs to the entorhinal cortex were estimated by Boeijinga and Van Groen (1984) on the basis of unit firing latencies.

A strong surface positive component, similar to that observed by Boeijinga and Van Groen (1984) in the cat following posterior pyriform cortex stimulation, was never observed in the present study. This may be due to the anterior stimulation sites used in this study, which were chosen to reduce the possibility of amygdalar stimulation, and it is not known if a similar early surface positive component may be observed in the rat.

A later source in layer II, peaking at latencies near 45 msec and accompanied by a deep sink, was associated with a surface-positive, deep-negative field potential component at similar latencies. A similar source in layer I and II accompanied by a sink in layers II and III was observed in the cat by Van

Groen et al. (1987). These authors also recorded a marked reduction in unit activity, and a paired-pulse depression effect at these same latencies, and suggested that the source may be due to active outward membrane currents induced in part by feedback inhibition of dendrites of layer II neurons. Finch and Babb (1980) have recorded IPSPs in principal cells of the entorhinal cortex at similarly long latencies following stimulation of the fornix and hippocampus, and have also recorded simultaneously from a putative inhibitory cell near the border of layers II and III whose firing was associated with strong inhibition of a nearby principal neuron. GABA containing processes of neurons which may mediate these effects are found in the superficial layers of the entorhinal cortex within the dendritic domains of layer II neurons (Kohler et al., 1985). Also, fast-spiking interneurons with extensive basket-like axonal arbourizations in layer II have been identified and suggested to play an important role in regulating the activity of stellate neurons in layer II (Jones & Buhl, 1993; Jones, 1993).

Some evidence suggests that a feedforward inhibition may be the most common form of inhibition in the entorhinal cortex. Following stimulation of a number of entorhinal cortex inputs, the latencies of EPSPs and of subsequent IPSPs are strongly correlated, consistent with feedforward inhibition (Finch et al., 1988). In addition, a lack of correlation between antidromic responses and IPSPs is inconsistent with feedback inhibitory mechanisms (Finch et al., 1988). Anatomical evidence for feedforward inhibition of lateral olfactory tract inputs to the entorhinal cortex was reported by Wouterlood et al. (1985) who demonstrated that axonal projections from the olfactory bulb terminate on layer I neurons which are immunoreactive for glutamic acid decarboxylase (a synthetic enzyme for the inhibitory neurotransmitter GABA), and appear to synapse onto the dendrites of non-immunoreactive neurons with cell bodies in layers II and III.

The current sink in the molecular layer of the dentate gyrus is consistent with prior reports of hippocampal activation following pyriform cortex stimulation in both the cat (Habets et al., 1980) and the rat (Woolley & Barron, 1968). Pyriform cortex stimulation results in a negative field potential component in the dentate gyrus which reverses to a positivity and reaches its maximal amplitude in the hilus (Woolley & Barron, 1968). The latency of this hilar field potential component (10 msec) agrees well with the negativity observed in this study which was also observed informally to reverse as recording electrodes in a few animals were retracted through the hilar region. Similar evoked potentials reversing in the region of the molecular layer of the dentate gyrus are also observed in the ventral hippocampal formation of the cat (Habets et al., 1980).

Although there are no known direct projections to the dentate gyrus from the pyriform cortex, and hippocampal activation by olfactory inputs is thought to be mediated by the entorhinal cortex (Wilson & Steward, 1978; Schwerdtfeger et al., 1990), the peak latencies are similar for the entorhinal cortex layer II sink and the sink in the dentate molecular layer. However, stellate cells in entorhinal cortex layer II that project to the dentate gyrus are highly responsive to small depolarizations of only a few mV (Alonso & Klink, 1993). Consequently, these cells may fire and synaptically activate the dentate gyrus granule cells before the negative peak in entorhinal cortex field potentials is reached. During paired-pulse stimulation in the present study, using an interval exceeding the apparent duration of peak inhibition, a facilitation of the field potential negativity in the entorhinal cortex and the corresponding layer II sink was observed in association with a similar enhancement of the dentate sink (Figure 2.8). This suggests that the paired-pulse facilitation of synaptic currents

in layer II were also expressed in an enhanced disynaptic activation in the dentate gyrus.

Medial Septal Inputs. The septally-activated current sink in layers II and III of the entorhinal cortex was far more distinct than the corresponding surface negative-deep positive field potential components which were partially obscured by earlier field potential components. The spatial peak of the current sink changed with time and tended to first appear in mid-layer III before ascending towards layer II (e.g. Figure 2.11). The more distributed form of the current sink likely reflects the distributed pattern of synaptic terminations of medial septal inputs to the entorhinal cortex. These have been shown to be distributed through layers II-IV (Alonso & Kohler, 1984; Gaykema et al., 1990), although there was no evidence of a layer IV sink in these experiments.

The earlier onsets of induced current sinks in layer III suggest that the medial septal inputs to layer III may have faster conduction velocities than those to layer II. The earliest onset latency of the sink was 12 msec, and the mean onset latency was 14.1 msec. By adding 2.0 mm to the straight-line interelectrode distance of 8.2 mm between stimulating and recording electrodes to account for the curved paths from the septum via the fornix and fimbria (Alonso & Kohler, 1984; Gaykema et al., 1990), the fastest fibers mediating the responses were estimated to have rather slow conduction velocities of roughly 0.62 m/sec.

The superficial sink was usually preceded by a source in layer III, and both this early source and the following sink were enhanced by paired-pulse stimulation (Figures 2.12 & 2.13). Because paired-pulse stimulation also resulted in an enhancement of the layer II-III sink, it is difficult to interpret these sources as due to feedforward inhibition onto the dendrites of the same neurons

activated by septal stimulation. Some of this current source may therefore be due to passive current flow induced by the deeper sink in the subiculum which had a similar onset latency (Figure 2.13). A second current source, located in layer I, and concurrent with the onset of the layer II sink, was observed following paired-pulse stimulation (Figure 2.13). While this current source may be due to enhanced passive current flow due to the layer II-III sink, it may also represent feedforward inhibitory input onto dendrites in layers I and II similar to those discussed above for pyriform cortex inputs. The second possibility is supported by the observation that the layer II-III sink becomes more focussed in layer III in response to the second stimulating pulse (Figure 2.13).

At sites near the dentate gyrus, field potentials usually showed a positive component at latencies near 8 to 10 msec, which was followed by a negative waveform. These field potential components were reduced in amplitude with distance from molecular layer of the dentate gyrus. Although the negative waveform was associated with a large current sink in the outer molecular layer of the dentate gyrus, the positive component was not markedly reflected in the CSD results, consistent with its typically close to linear decay along the recording track. This positive-negative pattern in the field potentials is very similar to that observed in the dentate molecular layer following medial septal stimulation (McNaughton & Miller, 1984). McNaughton and Miller (1984) also found that dentate neurons fired during the negative wave which may explain the spike-like component during the negativity evoked by paired-pulse stimulation in animal #8 (Figure 2.7). The strongest spike-like component observed here, however, had a 2-4 msec latency. Early spikes have been observed in other studies of septal inputs to the dentate region, often superimposed on the positive field potential component (Andersen et al., 1961;

Robinson & Racine, 1982; Robinson, 1986). Consistent with synchronous activation of dentate granule cells, the spike is positive in the molecular layer where the associated current source is located. Since the presence of the spike does not predict either subicular or entorhinal cortex sink-source distributions (e.g, Figure 2.7), the associated current sink in the white matter near the subiculum, is interpreted to reflect passive current flow.

In seven of the nine animals showing an entorhinal cortex layer II-III sink, another, slightly shorter-latency sink was also observed in the subiculum (Figures 2.11 & 2.13). While the early part of this sink was enhanced by paired-pulse stimulation, it was depressed at longer latencies (Figure 2.13). This subicular sink may be mediated by neurons in the lateral part of the medial septum which innervate ventral parts of the subiculum (Gaykema et al., 1990).

Convergence of Pyriform and Septal Inputs. These data indicate that both pyriform cortex and medial septal stimulation result in current sinks in the superficial layers of the entorhinal cortex. While the sink which follows pyriform cortex stimulation is localized primarily to layer II, the sink evoked by medial septal stimulation peaks roughly 50 μm deeper, and is more diffuse, spanning both layer II and parts of layer III. This broader distribution suggests that in addition to activating layer II neurons, septal inputs to layer III provide a strong contribution to the associated field potential component (Alonso & Kohler, 1984; Gaykema et al., 1990).

While these data are not conclusive, they are consistent with the possibility that pyriform cortex and medial septal inputs terminate on the same cells in layer II. Although there have been no appropriate double labelling studies, this hypothesis is supported by anatomical observations indicating that inputs from both the pyriform cortex and medial septum terminate on layer II

neurons (Alonso & Kohler, 1984; Room et al., 1984; Gaykema et al., 1990). This raises the possibility that septal inputs may serve to modulate the activity of layer II neurons which also receive pyriform cortex input. Both the broad spatial distribution and long duration of the sink evoked by medial septal stimulation are consistent with such a neuromodulatory role.

CHAPTER 3
PAIRED-PULSE AND FREQUENCY POTENTIATION OF SYNAPTIC
RESPONSES IN THE ENTORHINAL CORTEX FOLLOWING PYRIFORM
CORTEX AND MEDIAL SEPTAL STIMULATION

Frequency potentiation is a short-term enhancement in the amplitude of neuronal responses which occurs during the delivery of low-frequency stimuli to afferent pathways (Anderson & Lomo, 1967, 1968; Deadwyler et al., 1975; Applegate & Landfield, 1988). Because the optimal frequencies for inducing frequency potentiation vary between different cortical regions (Nickell & Shipley, 1988; Munoz et al., 1991), frequency potentiation effects may be used to measure the responsiveness of a particular cortical region to different frequencies of rhythmic input. The temporal nature of activity in sensory inputs to the entorhinal cortex may play a significant role in affecting synaptic plasticity in the entorhinal cortex and the transmission of neuronal activity to the hippocampal formation (Jones, 1987, 1993; Yeckel & Berger, 1990; de Curtis & Llinas, 1993). However, frequency potentiation has not been examined in any sensory input to the entorhinal cortex. In the experiments reported here, frequency potentiation effects in the large olfactory input from the pyriform cortex to the entorhinal cortex of the awake rat are described. The results of paired-pulse tests, which reflect the time-courses of facilitatory and inhibitory mechanisms which may contribute to the tuning of the frequency potentiation effects, are also reported. In addition, frequency potentiation and paired-pulse tests were applied to the characterization of the responses in the entorhinal

cortex which follow medial septal stimulation, a structure thought to contribute to theta-frequency activity in the entorhinal cortex (Mitchell et al., 1982; Mitchell & Rank, 1980; Alonso & Garcia-Austt, 1987a).

The principal cells of the pyriform cortex itself are susceptible to frequency potentiation. The layer II pyramidal cells in this region show enhanced responses during low-frequency stimulation of the lateral olfactory tract inputs from the olfactory bulb, and in response to activation of the intrinsic associational fibers (Hasselmo & Bower, 1990; Mokrushin & Emel'yanov, 1993). Stimulation of the lateral olfactory tract inputs from the olfactory bulb to the pyriform cortex in an *in vitro* slice preparation results in a frequency potentiation of the population EPSP (Mokrushin & Emel'yanov, 1991, 1993). At least for this *in vitro* slice preparation, however, multiple trains of 10 Hz stimulation, separated by 4 to 5 sec were required to induce the emergence of frequency potentiation. Frequency potentiation was also observed during a study of short-term potentiation in the pyriform cortex *in vitro* by Hasselmo and Bower (1990). These authors found that 20 Hz stimulation of the associational fibers in layer Ib of the pyriform cortex, resulted in a pronounced frequency potentiation effect in layer II pyramidal cells. The same stimulation pattern applied to lateral olfactory tract inputs to layer Ia resulted in only a very small frequency potentiation effect (Hasselmo & Bower, 1990), in accord with the findings of Mokrushin and Emel'yanov (1991, 1993) who found that *repeated* low-frequency stimulation was necessary to induce frequency potentiation at this synapse.

Although there are no reports describing frequency potentiation in the entorhinal cortex following pyriform cortex stimulation, low-frequency stimulation of sites in the amygdala and hippocampal formation have been found to result in frequency potentiation in the entorhinal cortex (Deadwyler, 1975; Racine &

Milgram, 1983; Finch et al., 1986; Jones & Heinemann, 1991). Some of this work has focussed on inputs from the subicular complex of the hippocampal formation (Shiple, 1975; Caballero-Bleda & Whitter, 1993; Jones, 1987). Ten Hz, and sometimes 5 Hz, stimulation of the subiculum is sufficient to result in frequency potentiation of intracellular unit responses in layer II and III entorhinal cortex neurons *in vivo* (Finch et al., 1986). These EPSPs were rapidly enhanced and resulted after several pulses in action potentials. A prolonged hyperpolarization, thought to result from feedforward inhibition, was also recorded from these neurons during low-frequency stimulation (Finch et al., 1986). Intracellular responses evoked in layer II entorhinal cortex units by subicular stimulation show somewhat different properties *in vitro*. Lower stimulation frequencies of 2.5 Hz are sufficient to induce a frequency potentiation effect, but instead of the development of a prolonged hyperpolarization, EPSP growth is associated with a fading in both early and late IPSP responses (Jones & Heinemann, 1991).

Low-frequency stimulation of the hippocampal CA3 field also results in frequency potentiation of responses in the entorhinal cortex. Deadwyler et al. (1975) stimulated the commissural outputs of the CA3 region of the hippocampus and recorded field potentials in the contralateral entorhinal cortex and dentate gyrus of anesthetized rats. Stimulation of the CA3 region, which sends crossed projections via the hippocampal commissure to the contralateral CA3 region, resulted in the emergence of a long-latency (20-25 msec onset), polysynaptic, deep-positive entorhinal cortex field potential component. While frequencies of stimulation up to 15 Hz resulted in frequency potentiation, the amount of frequency potentiation was maximal during 4 to 7 Hz stimulation, showing increases in amplitude of up to five times the baseline response.

Because the response was polysynaptic, however, synapses other than those in the entorhinal cortex may have contributed both the potentiation effect and the tuning of the effect to frequencies of 4 to 7 Hz.

The significance of frequency potentiation for ongoing neural activity in the intact animal is unknown, but it is possible that frequency potentiation-like phenomena are commonly induced spontaneously when appropriate frequencies of spontaneous activity occur (or occur in a sufficient number of neurons). Andersen and Lomo (1967) suggested that frequency potentiation mechanisms could play some role in learning and memory by enhancing the transmission of signals within neuronal channels which are active at their optimal frequency. They further suggested that a sequential amplification of frequency potentiation effects could occur in polysynaptic neuronal chains, and that more long-lasting synaptic changes might occur in circuits activated in this way. With regard to neuronal signal transmission, there is some evidence that frequency potentiation in the entorhinal cortex can lead to enhanced polysynaptic responses in the dentate gyrus (Deadwyler et al., 1975). During low-frequency stimulation of area CA3 which results in the frequency potentiation of entorhinal cortex responses, an initially very small, long-latency dentate gyrus field potential component becomes strongly enhanced (Deadwyler et al., 1975). This dentate gyrus response appears to be mediated by the entorhinal cortex since it has a similar lamellar profile as components evoked by entorhinal cortex stimulation, is expressed only after entorhinal cortex responses become enhanced, and is abolished by entorhinal cortex lesions (Deadwyler et al., 1975).

More recent authors have echoed the suggestions that frequency potentiation-like effects may enhance polysynaptic signal transmission between

cortical regions (Jones, 1993; Munoz et al., 1991). In the entorhinal cortex, frequency potentiation effects may play a more critical role for inputs to the superficial layers than for inputs to the deeper layers since the activity of neurons in the superficial layers is more strongly regulated by inhibition (Jones, 1993). In contrast to the deeper layers of the entorhinal cortex, which provide some input to the CA1 and CA3 fields of the hippocampus (Steward & Scoville, 1976; Whitter et al., 1989), synaptically evoked responses in layer II are dominated by fast and slow IPSPs mediated by GABA_A and GABA_B receptors, respectively, and spiking is not commonly observed with single stimulations (Jones, 1990a; Jones & Heinemann, 1991). Therefore, activation of layer II in the entorhinal cortex may require input frequencies high enough to result in frequency potentiation-like effects. These effects would be sufficient to overcome the inhibition and result in polysynaptic activation of the hippocampal formation (Jones, 1993). In contrast, input to the deep layers, where inhibition is less pronounced, may still be effective in disynaptically activating sites in the hippocampus even if they are active only at low frequencies. Signal transmission via the perforant path to the CA3 and CA1 regions also appears to be frequency-dependent (Yeckel & Berger, 1990). While monosynaptic responses in CA3 and CA1 are evoked by perforant path stimulation at 0.2 Hz, the multisynaptic activation of these sites (distinguishable on the basis of response latencies), is only obtained at frequencies between 5 and 15 Hz. Together, these studies suggest that activity in cortical afferents to the superficial layers of the entorhinal cortex may have little effect on entorhinal cortex and hippocampal activity unless they occur at frequencies sufficient to induce frequency potentiation-like effects.

A link may be drawn between frequency potentiation effects and the frequency range of theta activity in the hippocampus and entorhinal cortex (Green & Arduini, 1954; Bland, 1986; Mitchel & Rank, 1980; Alonso & Garcia-Austt, 1987a). Frequency potentiation in the hippocampal formation is observed readily at frequencies near 8 Hz which corresponds roughly to the mean frequency of the theta rhythm, although higher frequencies of up to roughly 20 Hz are also effective (Andersen & Lomo, 1967; MacVicar & Dudec, 1979; Finch & Babb, 1980; Landfield, 1993). Further, both the frequency of theta activity and frequencies sufficient to induce frequency potentiation are lowered to about 4 Hz in urethane-anesthetized and *in vitro* preparations (Bland, 1993; Munoz et al., 1991; Jones & Heinemann, 1991).

Although theta activity correlates strongly with movement in the absence of any *overt* signs of learning, theta activity is also observed during exploration and learning tasks and is thought to play an important role in learning and memory processes (Winson, 1978; Buszaki, 1989; Otto et al., 1991). During periods of type I theta activity, when animals are active and exposed to a large amount of sensory stimulation, frequency potentiation-like effects may occur in the hippocampal formation where a large number of cells are rhythmically active at frequencies which are effective in the experimental induction of frequency potentiation. Frequency potentiation effects may therefore occur during the theta rhythm and play some role in the processing of sensory information during or preceding learning and memory consolidation.

Although there is much theoretical interest in the entorhinal cortex as a structure mediating the transfer of neocortical signals to the hippocampus, and in the role of temporal processing and theta-frequency activity in the entorhinal cortex, there are no reports in the literature of investigations of the optimal input

frequencies for activation of entorhinal cortex neurons by inputs from the sensory cortices. An early work by Cragg (1960), however, demonstrated a growth of hippocampal responses during stimulation of the olfactory bulb at frequencies between 8 and 20 Hz. Stimulation at frequencies below 8 Hz resulted in only a small augmentation, and 20 to 200 Hz stimulation produced no hippocampal response. The responses measured by Cragg (1960) may have been mediated via direct lateral olfactory tract inputs to the entorhinal cortex, or by the intermediate activation of the pyriform cortex (Price & Powell, 1971; Wilson & Steward, 1978; Schwerdtfeger et al., 1990), and the site responsible for the growth in the responses is not known.

In order to determine the optimal frequencies for activation of entorhinal cortex neurons via the monosynaptic connections from the pyriform cortex, the experiments reported here examined field potential responses in the entorhinal cortex during low-frequency stimulation of the pyriform cortex in chronically-prepared animals. Stimulation at frequencies between 4 and 30 Hz, a range which includes normally-occurring frequencies of the theta rhythm, were applied in order to determine the optimal frequency of stimulation for evoking frequency potentiation responses. Because the medial septum also sends inputs to the entorhinal cortex (Alonso & Kohler, 1984; Gaykema et al., 1990), and is thought to play some role in the pacing of the theta rhythm (Alonso & Garcia-Austt, 1987a; Mitchell & Ranck, 1980), frequency potentiation tests were also conducted on medial septal inputs to the entorhinal cortex. Frequency potentiation in entorhinal cortex responses during theta-frequency medial septal stimulation would suggest that rhythmic activity in medial septal efferents could contribute to the excitability of entorhinal cortex neurons during periods of theta activity.

Although very little is known about the neural mechanisms which underlie frequency potentiation, the response growth during stimulation likely reflects alterations in the strength of, and the balance between, facilitatory and inhibitory processes. Paired-pulse tests were used in the present study to examine the time courses of inhibitory and facilitatory mechanisms that could contribute to entorhinal cortex frequency potentiation. In paired-pulse tests, two stimulation pulses are delivered. The first pulse is the "conditioning" pulse, or C-pulse, and the second pulse is the "testing" pulse, or T-pulse. By varying the interpulse interval between C- and T-pulses, the time-courses of inhibitory and facilitatory mechanisms activated by the C-pulse can be inferred by comparing the amplitudes of the responses evoked by each pulse. For example, if a facilitatory process is maximally expressed 50 msec after delivery of the C-pulse, the amplitude of the response evoked by the T-pulse will be maximally enhanced at this interpulse interval relative to the response evoked by the C-pulse.

In addition to paired-pulse tests in which the two pulses were delivered to the same site, interactions between the pyriform cortex and medial septal inputs to the entorhinal cortex were investigated by using double-site paired-pulse tests. In these studies the C- and T-pulses were delivered to the two different sites at variable intervals in order to determine if facilitatory or inhibitory mechanisms evoked by the first pulse could affect the response subsequently evoked by stimulating the other input.

METHODS

Surgery. Male Long Evans hooded rats (320-460 g) were anesthetized with a combined dose of 0.9 mg/kg ketamine and 0.05 mg/kg xylazine (i.p.) and placed in a stereotaxic frame with the skull surface on the horizontal plane. The level of anesthesia was monitored closely, and 10 to 20% supplemental doses of anesthetic were administered when required. Bipolar, teflon-coated stainless-steel twisted-wire electrodes (190 μ m exposed tip diameter) were implanted in the right pyriform cortex (posterior 3.6 mm, lateral 6.5 mm, and 8.5-10 mm ventral to bregma), medial septum (anterior 0.2 mm, lateral 0.2 mm, and ventral 6.0 mm to bregma), and medial entorhinal cortex (posterior 8.8 mm and lateral 5.0 mm to bregma, and 0.1 to 0.2 mm above the skull). One tip of each of the bipolar stimulating electrodes in the pyriform cortex and the medial septum was 0.5 mm longer than the other, and the tip separation of the entorhinal cortex recording electrode was set to 1.0 mm. The vertical placements of the stimulating electrodes were adjusted to minimize the current thresholds for evoked field potentials in the entorhinal cortex. The vertical placement of the entorhinal cortex electrode was then adjusted slightly to maximize the amplitude of field potential components evoked by pyriform cortex and medial septal stimulation recorded by the ventral-most tip. The electrode leads were connected to gold-plated Amphenol pins which were mounted in a 9-pin connector, and the whole assembly was embedded in dental cement and anchored to the skull with stainless-steel jeweler's screws. One skull screw in the contralateral frontal bone served both as a ground electrode and as a reference electrode for monopolar recordings of entorhinal cortex field potentials. Animals were housed individually in 18 x 20 x 35 cm stainless-steel hanging cages on a 12 hr on, 12 hr off, light-dark cycle. A two week recovery

period, during which animals were monitored for wound infection, preceded experimental testing.

Design and Apparati. Before paired-pulse and frequency potentiation tests were conducted, single stimulation pulses were delivered to the pyriform cortex and medial septum at 10 stimulus intensities between 16 and 1259 μA . By plotting stimulus intensity versus evoked potential amplitude for each stimulation site, two input/output (I/O) curves were generated for each animal. Further I/O tests were conducted again 2 days later to ensure that evoked potentials were stable, and again 1 day after the completion of paired-pulse and frequency potentiation testing to determine if these tests resulted in long-term changes in synaptic strength.

Paired-pulse and frequency potentiation testing were conducted for each animal over a 4 day period and tests were conducted in the following order on consecutive days: paired-pulse tests with C- and T-pulses delivered to the same stimulation site, paired-pulse tests with C- and T-pulses delivered to different sites, occlusion testing, and frequency potentiation testing. Animals were placed in a 30 x 40 x 30 cm wooden chamber with a Plexiglas front and a wire-grid floor, and were tested after habituation to the chamber while in a quiet, resting state.

Electrical stimuli were generated with a Grass S88 stimulator, and photoelectric stimulus isolation units (Grass SIU6B) were used to deliver 0.1 msec biphasic constant current pulses to the pyriform cortex and medial septum. Evoked field potentials recorded in the entorhinal cortex were analog filtered (0.3 to 3.0 kHz), and amplified using a Grass (Model 12) amplifier. Field potentials were digitized at 10 kHz with a 12-bit A/D board and stored on computer hard disk. In all paired-pulse tests, there was an interval of 10 seconds between the delivery of consecutive pulse-pairs.

Input/Output (I/O) Tests. Single stimulation pulses at 10 intensities taken from a logarithmic scale were delivered to the pyriform cortex or medial septum and responses evoked in the entorhinal cortex were recorded. The intensities were 16, 32, 63, 100, 159, 251, 501, 794, 1000, and 1259 μ A. Ten evoked potentials were recorded at each intensity in ascending order with a 10 sec interval between each sample, and the 10 samples at each intensity were then averaged. I/O testing allowed the determination of the stability of the evoked potential measures, and the pulse intensities which were sufficient for each animal to evoke responses 50, 75, and 100% of the asymptotic response amplitude. These intensity levels were used during subsequent paired-pulse and frequency potentiation testing.

Single Site Paired-Pulse Tests. Two single-site paired-pulse tests were conducted by delivering stimulation pulses either to the pyriform cortex or to the medial septum at 14 different interpulse intervals (range= 5 to 1000 msec). The intensity of both the C- and the T-pulses was set to an intensity which resulted in a response amplitude approximately 75% of the asymptotic response amplitude observed during I/O testing. Ten responses were recorded and averaged for an initial single-pulse condition and then again for each interpulse interval in ascending order.

In order to assess the effect of C-pulses on the responses evoked by the T-pulses, the peak amplitudes of the averaged field potentials evoked by the T-pulses were expressed as a per cent increase from the mean response amplitude recorded during the single-pulse condition (Racine & Milgram, 1983). The response amplitudes were averaged across animals and plotted as a function of interpulse interval. The measured field potential components which followed pyriform cortex or medial septal stimulation were shown previously to

be due primarily to current sinks in layer II of entorhinal cortex (Figures 2.8 & 2.13). At interpulse intervals less than 30 msec, however, responses evoked by T-pulses delivered to the medial septum were uninterpretable due to interference from field potential components evoked by the C-pulses and volume conducted from the hippocampal formation.

Double-Site Paired-Pulse Tests. Double site paired-pulse tests were used to assess whether responses in the entorhinal cortex evoked by stimulating either the pyriform cortex or medial septum could be affected by the activity of inhibitory or facilitatory mechanisms induced by prior stimulation of the other site. Separate tests were conducted in which either the pyriform cortex or the medial septum was stimulated first. Data were collected in the same way as in single-site paired-pulse tests except that the interpulse intervals ranged from 30 to 1000 msec, and the C-pulse was set to an intensity which evoked an asymptotic response amplitude during I/O testing.

Occlusion Testing. Double-site stimulation was also used to assess whether pyriform cortex and septal inputs to the entorhinal cortex may activate the same cells. If the dendrites of the same neurons are innervated by both pyriform cortex and medial septal inputs, and if one input results in a close to maximal depolarization of those cells, then the simultaneous activation of the neurons by stimulating the other input cannot result in further depolarization, and the corresponding field potential will be masked, or *occluded*. Therefore, when using stimulus intensities which result in maximal field potential amplitudes, the field potentials resulting from simultaneous activation of neurons in the entorhinal cortex by pyriform cortex and medial septal inputs should not result in a response amplitude greater than the largest response observed when stimulating either input alone. Alternatively, when using lower intensities which

result in sub-maximal depolarization, the post-synaptic potentials may sum, and the resulting field potential should approximate the sum of the field potential amplitudes recorded when stimulating each input pathway alone. This second result is less conclusive, however, since it may also be expected if each input pathway activates separate neuronal populations in the same cortical region.

Separate occlusion tests were conducted so that the simultaneous activation of the entorhinal cortex by pyriform cortex and medial septal stimulation could be compared for pulse intensities that resulted in either asymptotic or 50% of asymptotic response amplitudes during I/O testing. Ten responses to single-pulse stimulation of either site were first recorded and averaged, and ten double-pulse tests were then performed at four different interpulse intervals. Because medial septal stimulation results in field potential components in the entorhinal cortex which have a longer latency to peak than those which follow pyriform cortex stimulation, and because peak response latencies also vary somewhat for each input across animals, the medial septum was stimulated 5, 10, 15 or 20 msec prior to the stimulation of the pyriform cortex. Ten samples were recorded for each interpulse interval, and recordings were made in ascending order with respect to interpulse interval.

Following occlusion testing, the single-pulse conditions were examined to determine the differences for each animal in the latencies to peak of the pyriform cortex and medial septal evoked responses. The latency difference was used to determine the most appropriate interpulse interval for the assessment of occlusion effects. The differences between the latencies to peak were usually close to 10 or 15 msec, and due to the broad peak of responses evoked by medial septal stimulation there was good overlap. The response evoked by single-pulse pyriform cortex stimulation was summed with the

response evoked by single-pulse medial septal stimulation which was adjusted by the latency difference. Then, the result was compared to the actual response observed during double-pulse stimulation at that interpulse interval. The difference between the expected maximum amplitude of the waveform derived from the sum of the two single-pulse conditions, and the observed double-pulse response was determined for both the strong and the weak stimulation conditions. The results for the two conditions were analyzed using a matched samples student's *t*-test, and results from four representative animals were plotted.

Frequency Potentiation. Frequency potentiation was induced using trains of 10 pulses delivered at one of 11 frequencies (4, 6, 8, 10, 12, 14, 16, 18, 20, 25 and 30 Hz), using pulse intensities which resulted in response amplitudes 75% of the asymptotic response observed during I/O testing. Preliminary testing indicated that there was little further growth in response amplitudes beyond that observed after the 10th pulse when using longer trains. One sample was taken at each frequency in ascending order and this was repeated until 8 samples at each frequency were obtained. The delivery of consecutive trains was separated by a 30 sec interval to allow the decay of short-term effects. The mean response to each pulse in each train was calculated by averaging across the eight samples obtained at each stimulation frequency.

The use of multiple train frequencies allowed the construction of tuning-curves for the frequency potentiation induced by either pyriform cortex or medial septal stimulation. The mean amplitudes of responses to the *first* pulse in each train were averaged, and the amplitudes of the remaining responses at each frequency were expressed as a per cent increase from the mean first-pulse

response amplitude. The resulting data were averaged across animals and illustrated by plotting the response amplitudes for the first, second, sixth and tenth responses as a function of stimulation frequency.

Histology. Animals were deeply anesthetized with chloral hydrate and perfused through the heart with 0.9% saline followed by 10% formalin. The brains were removed and stored in a solution of 20% glucose in 10% formalin. Frozen, 40 μm thick coronal sections were placed on gelatin-coated slides, dried, and stained with Neutral red. The locations of stimulating electrodes were plotted on sections taken from the atlas of Paxinos and Watson (1986).

RESULTS

Histology. The positions of stimulating and recording electrode tips are indicated in Figure 3.1. Medial septal stimulating electrodes were clustered within or close to the dorsal border of the medial septum. Stimulating electrode tips in the pyriform cortex were all located near the densely packed pyramidal neurons in layer II. Recording electrode tips were located in the ventral aspect of the medial entorhinal cortex. Most of the recording electrode tips were located near layer II, while some electrodes were found in layers I and III.

Input/Output Tests. Of the 15 animals in which electrodes were implanted, pyriform cortex stimulation at the highest test-pulse intensity resulted in reliable field potentials larger than 0.22 mV in 14 rats. Twelve of these animals also showed reliable entorhinal cortex field potential components following medial septal stimulation. Examples of field potentials recorded from a representative animal following either pyriform cortex or medial septal stimulation are shown in Figure 3.2. The amplitudes of the responses increased

with stimulation intensity, consistent with a larger synaptic response resulting from the activation of larger numbers of efferents to the entorhinal cortex. Although differential recordings between the two tips of the recording electrode can result in larger recordings if the two tips straddle an evoked current dipole, and can also reduce the contribution of stimulus artifacts, current dipoles were not commonly observed in the electrode trajectories used here. Monopolar recordings from the ventral-most electrode tips in the superficial layers of the entorhinal cortex were therefore used in this study.

Pyramidal cortex stimulation resulted in a negative-going field potential in the superficial layers of the entorhinal cortex similar to those observed in previous acute and *in vitro* studies (Figure 3.2 left; Van Groen et al., 1987; de Curtis & Llinas, 1993; Figure 2.4). The current thresholds for just-discriminable field potentials averaged 163 μA (range= 63 to 501 μA), and the currents required to evoke responses 50%, 75%, and 100% of the asymptotic response amplitude averaged 488 μA (range= 250 to 794), 796 μA (range= 501 to 1000), and 1180 μA (range= 794 to 1259), respectively. The onset latencies of the evoked potentials at high pulse intensities averaged 10.9 msec (range= 6.7 to 15.4 msec). The peak amplitude of the field potentials at asymptotic pulse intensities averaged 0.51 mV (range= 0.22 to 1.0) at a mean latency of 16.2 msec (range= 14.3 to 19.0 msec).

Medial septal stimulation during I/O testing resulted in field potentials with multiple components which peaked at different latencies (Figure 3.2 right). At latencies under 15 msec a positive-going component was followed by a negative-going component. This positive-negative field potential pattern is similar to that observed in the dentate molecular layer following medial septal stimulation (Andersen et al., 1961; Robinson & Racine, 1982; Robinson, 1986)

and its occurrence in the entorhinal cortex is attributable to volume conduction of currents generated in the dentate gyrus (McNaughton & Miller, 1984; Figure 2.13).

At longer latencies, a negative component in the field potentials evoked by medial septal stimulation was observed in 12 of the 15 animals (Figure 2.3 right, note arrow). This long-latency component usually had a gradual onset during single-pulse testing and a broad, low-amplitude peak (mean=0.29 mV, range= 0.1 to 0.87). The earliest latencies at which the component was clearly observed at the highest pulse intensities averaged 22.6 msec (range= 16.6 to 29.5), and the field recordings returned to baseline at a mean latency of 58.4 msec (range= 50 to 63 msec). The current thresholds for the responses averaged 125 μ A (range= 32 to 501 μ A), and the currents required to evoke responses 50%, 75%, and 100% of the asymptotic response amplitude averaged 218 μ A (range= 63 to 500 μ A), 529 (range= 250 to 1000 μ A), and 842 (range= 500 to 1259 μ A), respectively. The long-latency field potential component is generated by currents in layers II and the upper portions of III (Figure 2.13), and was therefore the focus of further analyses.

The amplitude of the field potentials evoked during I/O testing of the pyriform cortex and medial septal inputs did not change following paired-pulse and frequency potentiation testing. Figure 3.3 shows the mean I/O test results for the day preceding and the day following paired-pulse and frequency potentiation testing.

Paired-Pulse Stimulation of the Pyriform Cortex. Figure 3.4 shows samples of evoked potentials evoked by paired-pulse stimulation of the pyriform cortex. The largest paired-pulse facilitation effects were usually observed at C-T intervals of 30 and 40 msec. Although the amount of facilitation was reduced at

C-T intervals below 30 msec, the responses were still enhanced. The amount of facilitation fell off sharply as the C-T interval was increased to 50 msec, and then more gradually as the C-T interval was increased to 500 msec (Figure 3.5).

Paired-Pulse Stimulation of the Medial Septal. Paired-pulse stimulation of the medial septum had effects on the early positive and negative components of the field potentials volume conducted from the hippocampal formation. At intervals near 50 msec there was a facilitation of the positive component, and an apparent depression in the negative component (Figure 3.6). These effects are consistent with earlier studies of facilitation effects in the dentate gyrus following paired-pulse stimulation of the medial septum (Robinson & Racine, 1982).

The paired-pulse tests also resulted in a facilitation of the longer-latency entorhinal cortex responses, and the facilitation was greatest for C-T intervals near 70 msec (Figures 3.6 & 3.7). Positive shifts in the field potentials at latencies including the late component sometimes reduced the amplitude of this component as measured from the prestimulus baseline. The amplitude of the late component was therefore measured with reference to a point just prior to its onset. Facilitation of the late negative component increased from C-T intervals of 30 msec to 70 msec and then decreased from intervals of 70 msec to 500 msec. No facilitation was observed at C-T intervals larger than 500 msec. A depression in the response to the T-pulse was sometimes observed at the longest C-T intervals (e.g., Figure 3.6), but this depression effect was not consistent across animals nor expressed in the group average.

Double-Site Paired-Pulse Tests. When C-pulses were delivered to the medial septum, and T-pulses were delivered to the pyriform cortex, the responses to pyriform cortex stimulation were enhanced relative to the single-pulse condition. This heterosynaptic facilitation effect occurred at C-T intervals

between 100 and 300 msec (Figures 3.8 & 3.9), and differed from the facilitation observed when both the C- and T-pulses were delivered either to the medial septum or to the pyriform cortex (Figures 3.5 & 3.7). The heterosynaptic facilitation effect was smaller, more variable, peaked later, and was not reliably expressed at C-T intervals less than 100 msec.

When C-pulses were delivered to the pyriform cortex, and T-pulses were delivered to the medial septum, the responses to medial septal stimulation were facilitated at C-T intervals less than 500 msec. While the size of the facilitation effect was smaller, the shape of the interpulse interval curve was similar to that obtained for double-pulse stimulation of the pyriform cortex (Figure 3.5). The facilitation of medial septum evoked responses was greatest, on average, for C-T intervals of 30 and 40 msec (Figure 3.10 & 3.11).

Occlusion Testing. The results of double-site stimulation tests used to assess whether pyriform cortex and medial septal inputs could be activating the same cells in the entorhinal cortex are shown in Figure 3.12. When both sites were stimulated with weak pulses, which evoked responses roughly 50% of the asymptotic response amplitude in the single-pulse conditions, it was found that the responses to combined stimulation were almost equivalent to those expected on the basis of summing the single-pulse responses (Figure 3.12A). The medial septal evoked waveform was shifted to account for differences in the latency to peak for pyriform cortex and medial septal evoked responses. In contrast, combined stimulation of both sites, with pulses strong enough to evoke maximal evoked response amplitudes in the single-pulse conditions, resulted in field potentials which were smaller than those expected on the basis of summing the single pulse responses (Figure 3.12B). The differences between the observed and expected results when using strong stimulation

pulses were roughly equivalent to the amplitudes of the medial septal evoked responses during the single-pulse conditions, suggesting that pyriform cortex stimulation served to occlude the depolarization expected from medial septal stimulation by maximally depolarizing the same entorhinal cortex neurons. There were significantly greater differences between the observed and expected peak amplitudes expressed as a proportion of the observed amplitudes when strong stimulation pulses were used than when weak stimulation pulses were used ($t=4.80$, $p<0.001$).

Frequency Potentiation. The frequency potentiation caused by low-frequency, 10-pulse trains has been illustrated by superimposing the mean responses to the first and last pulses in each stimulation train (Figure 3.13). The field potentials evoked by both pyriform cortex and medial septal stimulation were enhanced during the trains, and the effects were strongest at stimulation frequencies between 10 and 20 Hz. Both the growth of response amplitudes during the trains, and the response amplitudes after the last pulse in each train are illustrated by the averaged "tuning-curves" shown in Figure 3.14. These curves show the average standardized amplitude of responses to the 2nd, 6th, and 10th pulses in each train as a function of train frequency. The mean responses to the 1st pulses are also shown to indicate the stability of single-pulse responses during testing.

Frequency potentiated responses evoked by pyriform cortex stimulation had onset latencies similar to those observed after the first pulse in each train (Figure 3.13 left). However, the frequency potentiated responses tended to have longer latencies to peak, and much of the increase in the amplitude of the responses was due to enhancements in the durations of the responses. The tuning curves for pyriform cortex stimulation were rather broad,

and peaked on average at 14 Hz (Figure 3.14 top). Responses to the second pulse in each train were similar to those which were observed at comparable C-T intervals during paired-pulse stimulation of the pyriform cortex (Figure 3.5). Stimulation at frequencies between 6 and 20 Hz resulted in evoked responses which continued to increase during the course of the train to amplitudes greater than those observed during the paired-pulse tests.

Frequency potentiation effects evoked by medial septal stimulation were weaker and more variable than those evoked by pyriform cortex stimulation. The evoked responses during low-frequency medial septal stimulation showed changes in both the later negative component due to synaptic currents in the entorhinal cortex, and in the early positive-negative components. As in the analysis of medial septum paired-pulse data, measurements of the late component amplitude were made relative to a point just prior to its onset. The late negative component usually showed a simple enhancement in amplitude, but two animals developed what appeared to be two distinct field components with similar amplitudes but different peak latencies (e.g., Figure 3.13 right). Frequency potentiation of the late negative component peaked on average at 10 Hz, although there was considerable variability across animals with some showing peak potentiation at frequencies up to 18 Hz. Although pyriform cortex stimulation resulted in enhanced responses at all frequencies, septal stimulation produced frequency potentiation within a frequency range of 8 to 20 Hz (Figure 3.14). Tuning curves fell off sharply at frequencies above 20 Hz during medial septal stimulation, and responses after 30 Hz stimulation were generally depressed.

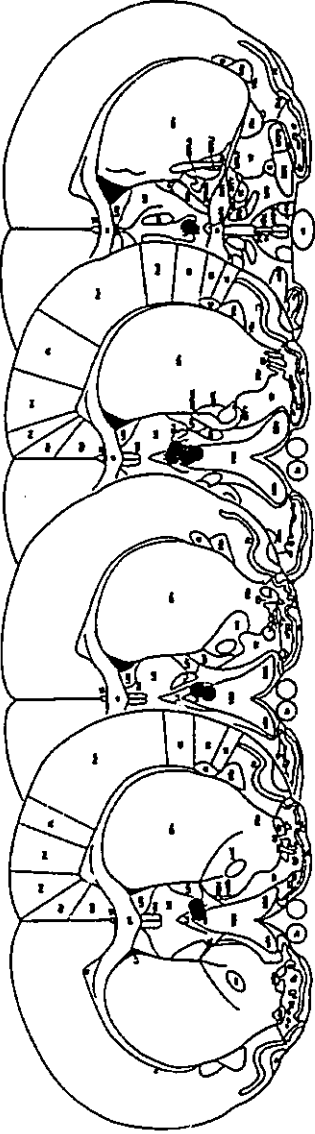
A depression in the negative component of the early positive-negative field potential pattern was observed in all animals during low-frequency

stimulation of the medial septum. This depression was observed at stimulation frequencies higher than 8 or 12 Hz, and tended to increase monotonically with stimulation frequency. An enhancement in the earlier positive component, which also increased with stimulation frequency, was also observed in some animals.

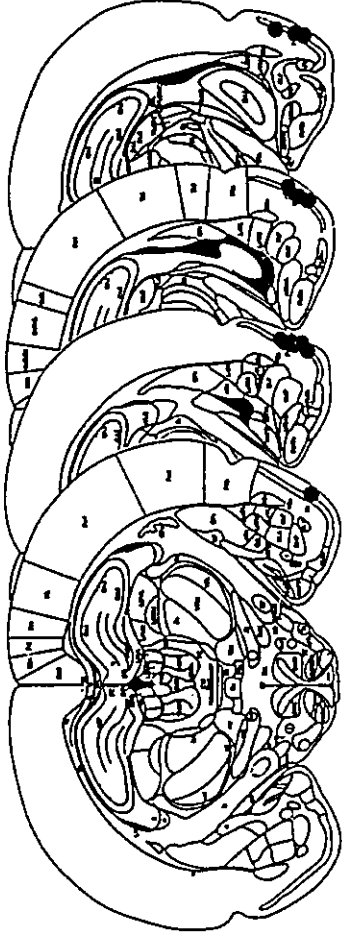
Figure 3.1

Figure 3.1. The locations of stimulating electrodes in the medial septum (MS) and pyriform cortex (PY), and of recording electrodes in the entorhinal cortex (EC) are shown on representative coronal sections taken from the atlas of Paxinos and Watson (1986).

MS



PY



EC

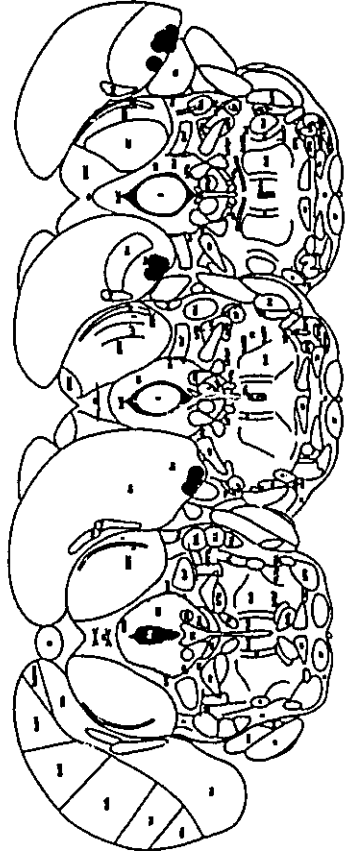
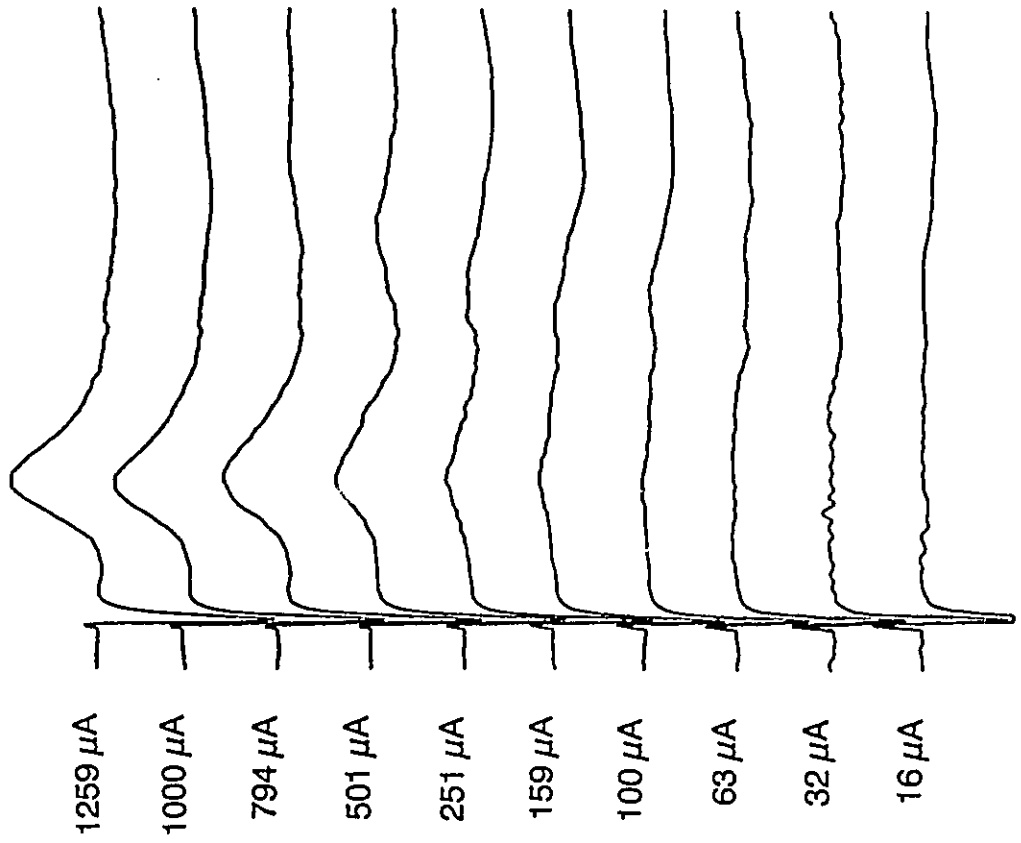


Figure 3.2

Figure 3.2. Field potentials in entorhinal cortex evoked by pyriform cortex (**left panel**) and medial septal (**right panel**) stimulation in a representative animal at the stimulation intensities indicated at left. An arrow indicates the peak latency for the field potential correlate of layer II-III activation following medial septal stimulation. Earlier components are volume conducted from the hippocampal formation. Upward deflections indicate negativity in this and all subsequent figures. Horizontal calibration, 10 msec; vertical calibration, 0.5 mV.

PYRIFORM STIMULATION



SEPTAL STIMULATION

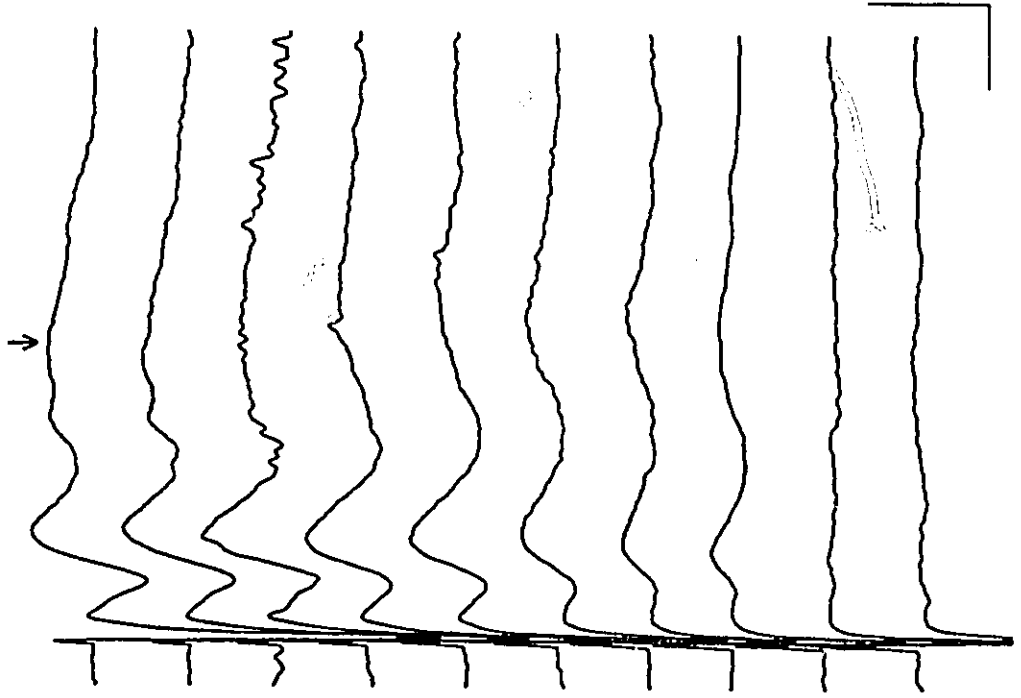


Figure 3.3

Figure 3.3. The mean peak amplitudes of field potential components evoked in the entorhinal cortex by pyriform cortex and medial septal stimulation are shown as a function of test-pulse intensity both before (**Pre-PP/FP**), and after (**Post-PP/FP**) paired-pulse and frequency potentiation testing. Data have been standardized to the response to the highest test-pulse intensity during the last pre-testing input/output test. Bars indicate twice the standard error of the mean in this and all subsequent figures.

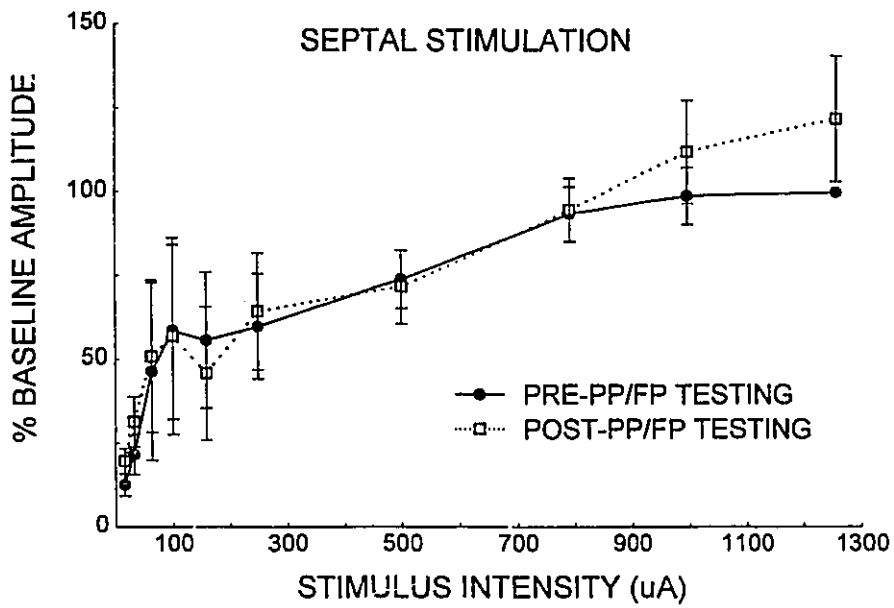
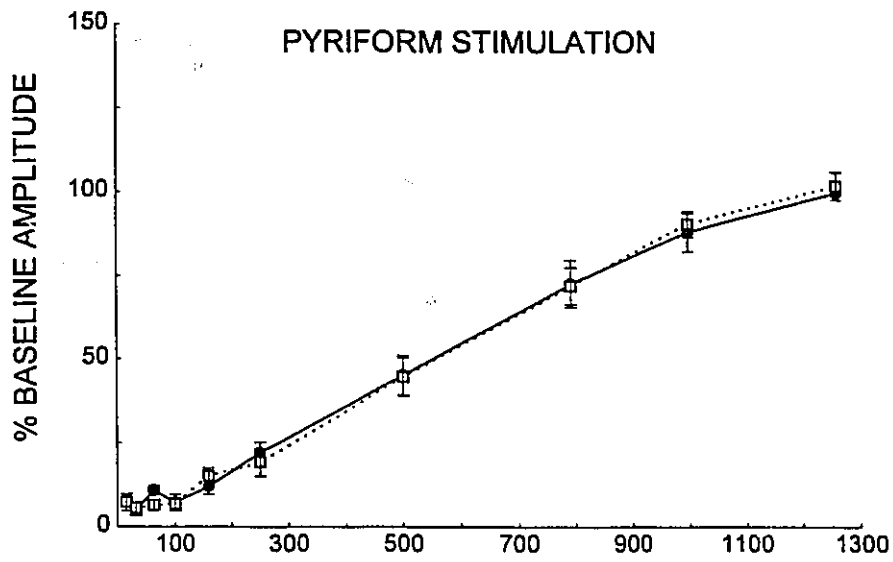


Figure 3.4

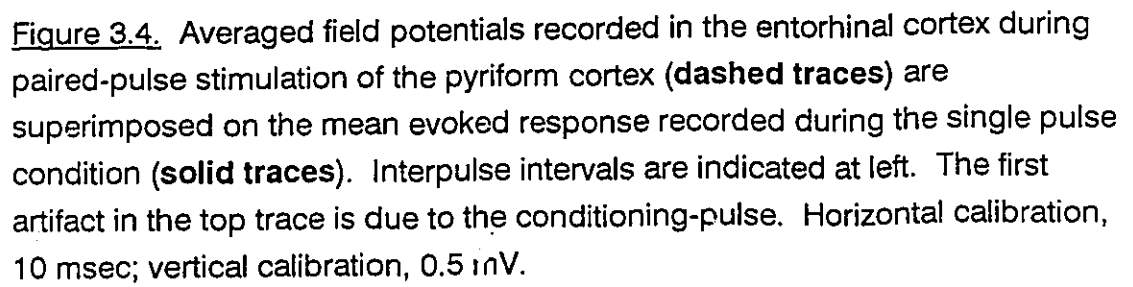


Figure 3.4. Averaged field potentials recorded in the entorhinal cortex during paired-pulse stimulation of the pyriform cortex (**dashed traces**) are superimposed on the mean evoked response recorded during the single pulse condition (**solid traces**). Interpulse intervals are indicated at left. The first artifact in the top trace is due to the conditioning-pulse. Horizontal calibration, 10 msec; vertical calibration, 0.5 mV.

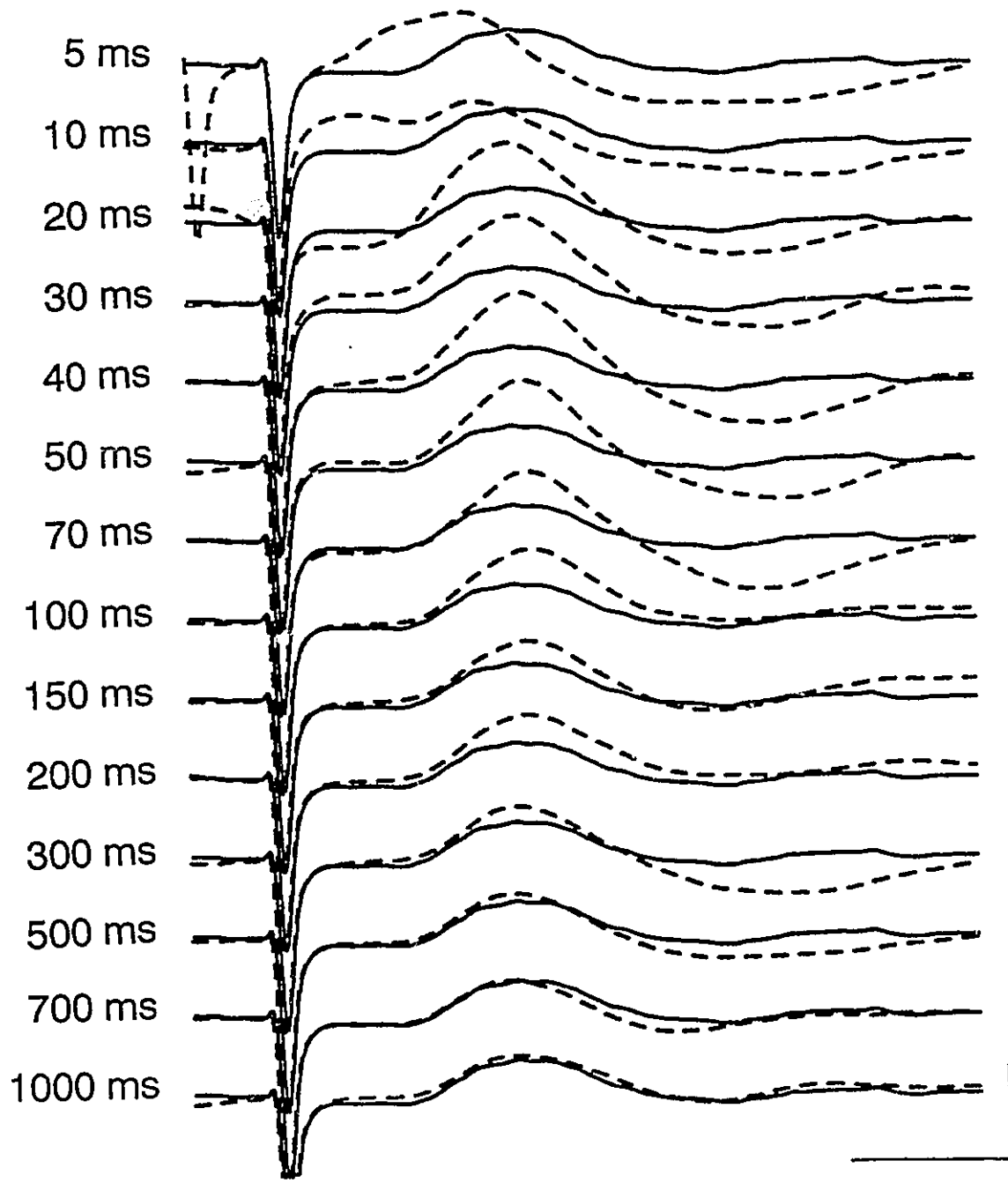


Figure 3.5

Figure 3.5. The average peak amplitudes of responses to test-pulses during paired-pulse stimulation of the pyriform cortex (**PY-PY**) are shown as a function of interpulse-interval. Data are expressed as a percent increase from the mean response amplitude recorded during the single-pulse condition. Note the sharp reduction in paired-pulse facilitation at interpulse intervals less than 30 msec.

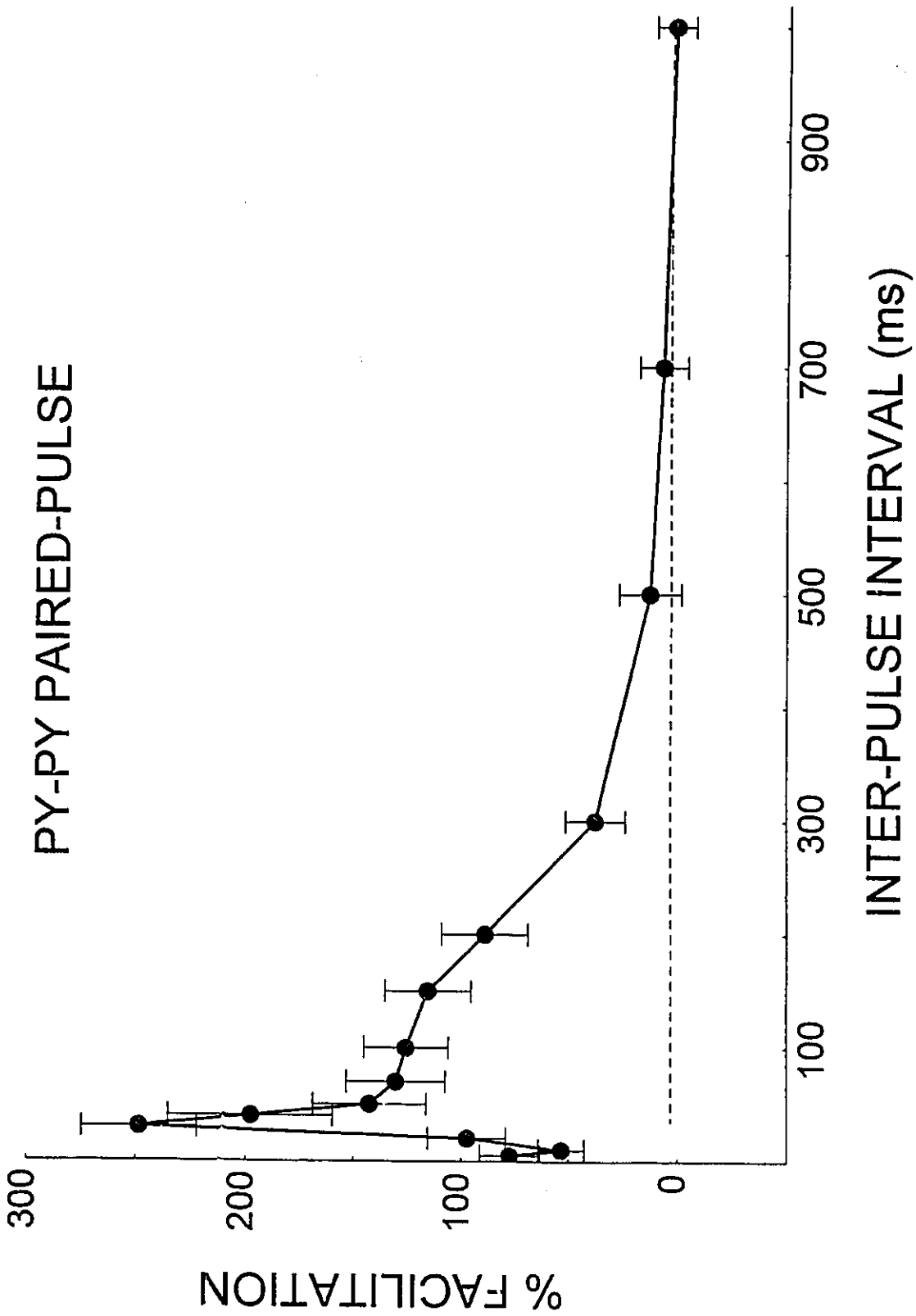


Figure 3.6




Figure 3.6. Averaged field potentials recorded in the entorhinal cortex during paired-pulse stimulation of the medial septum (**dashed traces**) are superimposed on the mean of the evoked responses recorded during the single pulse condition (**solid traces**). Interpulse intervals are indicated at left. The peak of the field component generated by evoked currents in layers II-III of the entorhinal cortex is indicated by an **arrow**. Horizontal calibration, 10 msec; vertical calibration, 0.5 mV.

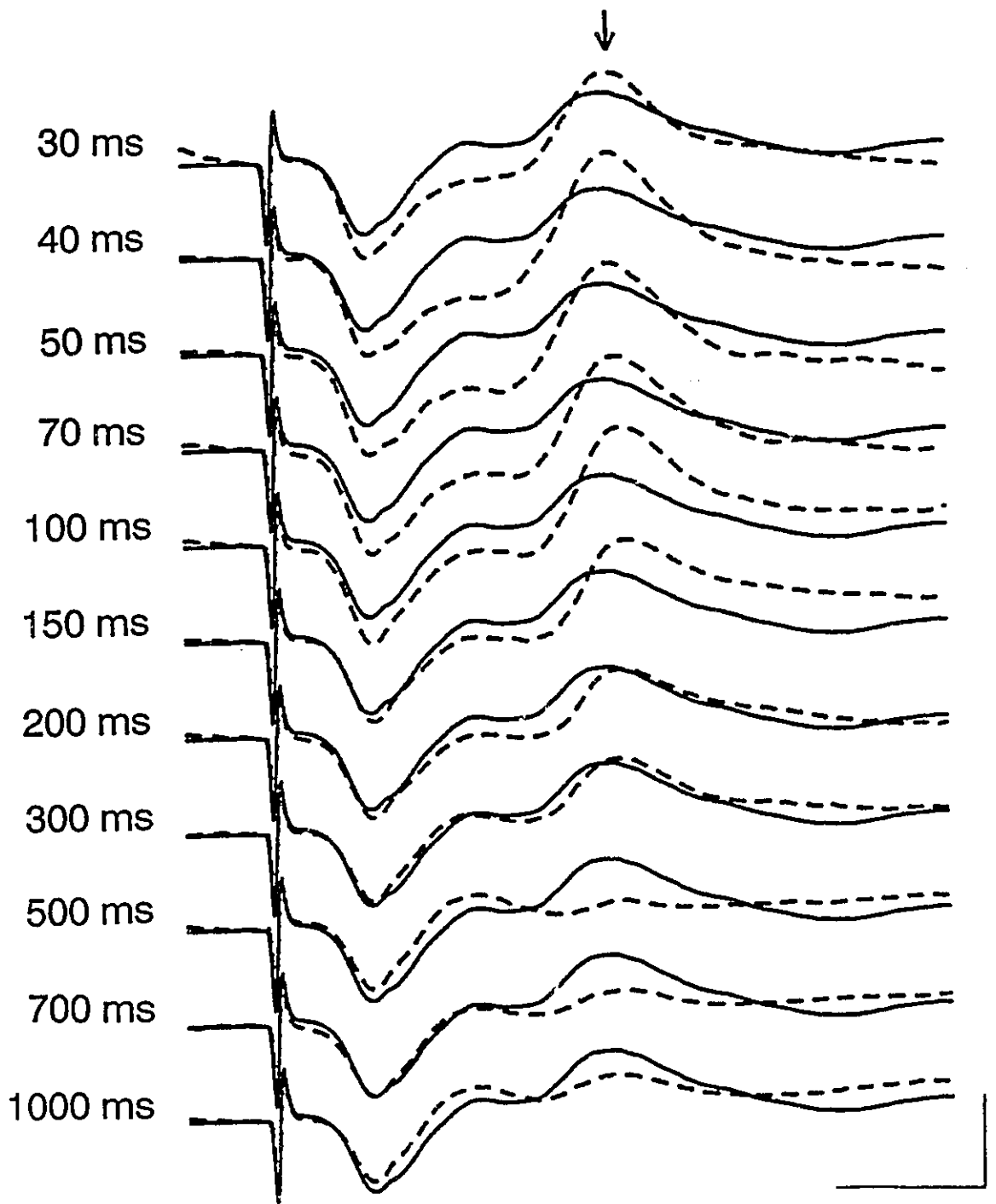


Figure 3.7

Figure 3.7. The average peak amplitude of field potentials in the entorhinal cortex evoked by test-pulses during paired-pulse stimulation of the medial septum (**MS-MS**) are shown as a function of interpulse-interval. Data are based on the field potential component indicated by an arrow in Figure 3.6. Data are expressed as a percent increase from the mean response amplitude recorded during the single-pulse condition.

MS-MS PAIRED-PULSE

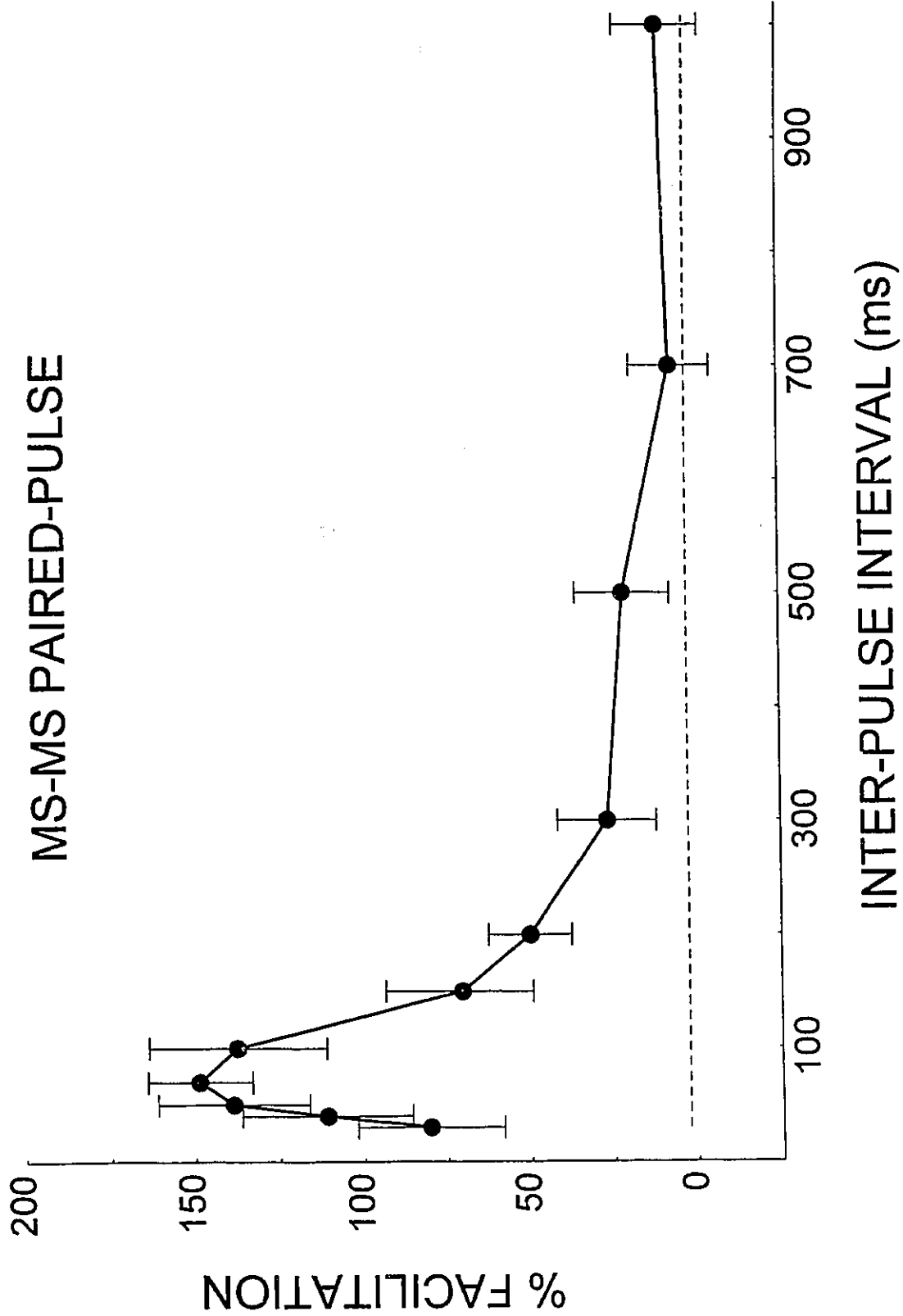


Figure 3.8

Figure 3.8. Responses to test-pulses delivered to the pyriform cortex (**dashed traces**) following delivery of conditioning-pulses to the medial septum at the interpulse intervals indicated at left. Responses evoked by test-pulses are superimposed on the mean of the responses evoked during the single-pulse pyriform cortex stimulation condition (**solid traces**). Horizontal calibration, 10 msec; vertical calibration, 0.5 mV.

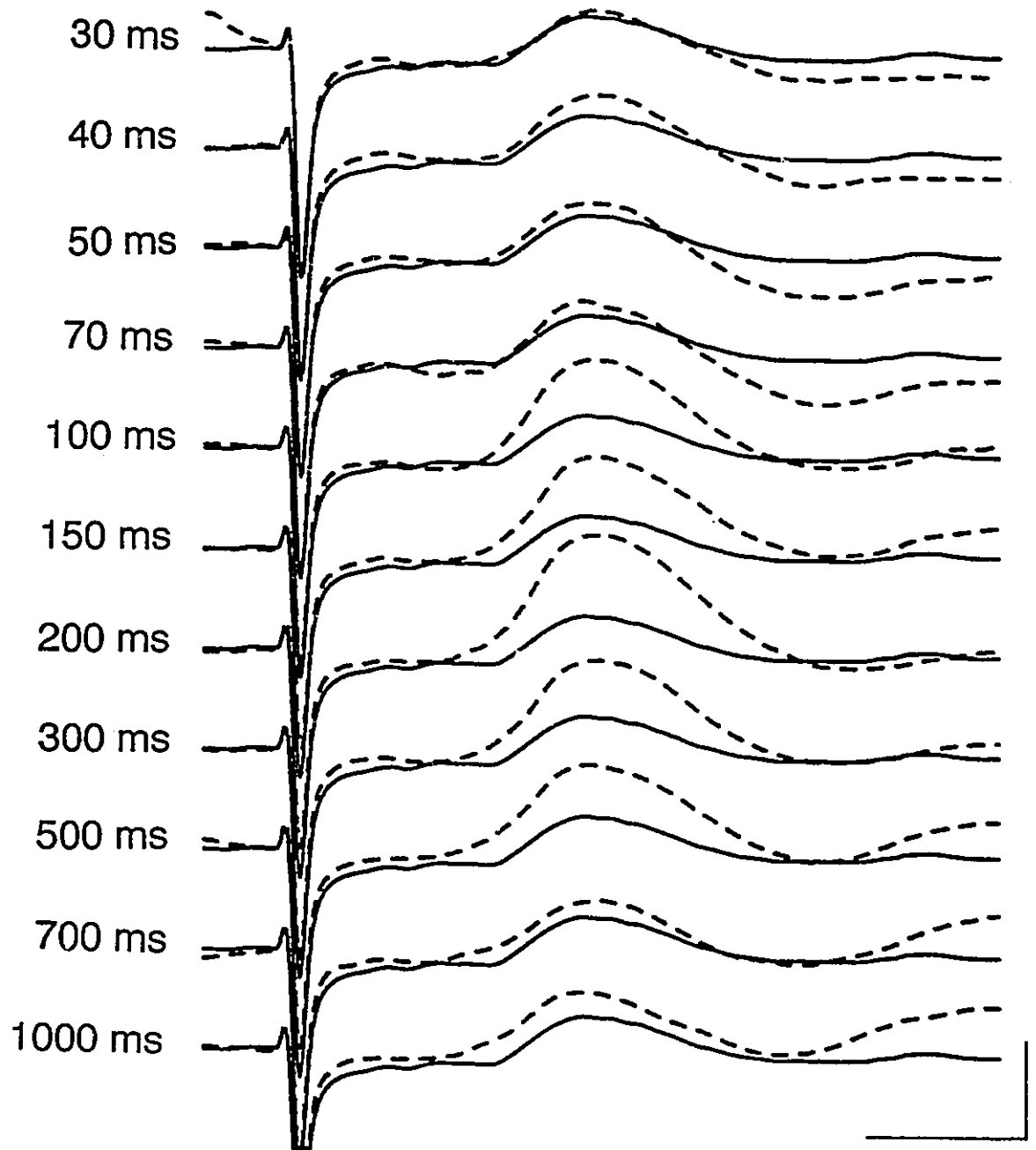


Figure 3.9

Figure 3.9. The average amplitude of responses to test-pulses delivered to the pyriform cortex following the delivery of conditioning-pulses to the medial septum (**MS-PY**). Data are expressed as a percent increase from the mean response amplitude recorded during the single-pulse pyriform cortex stimulation condition.

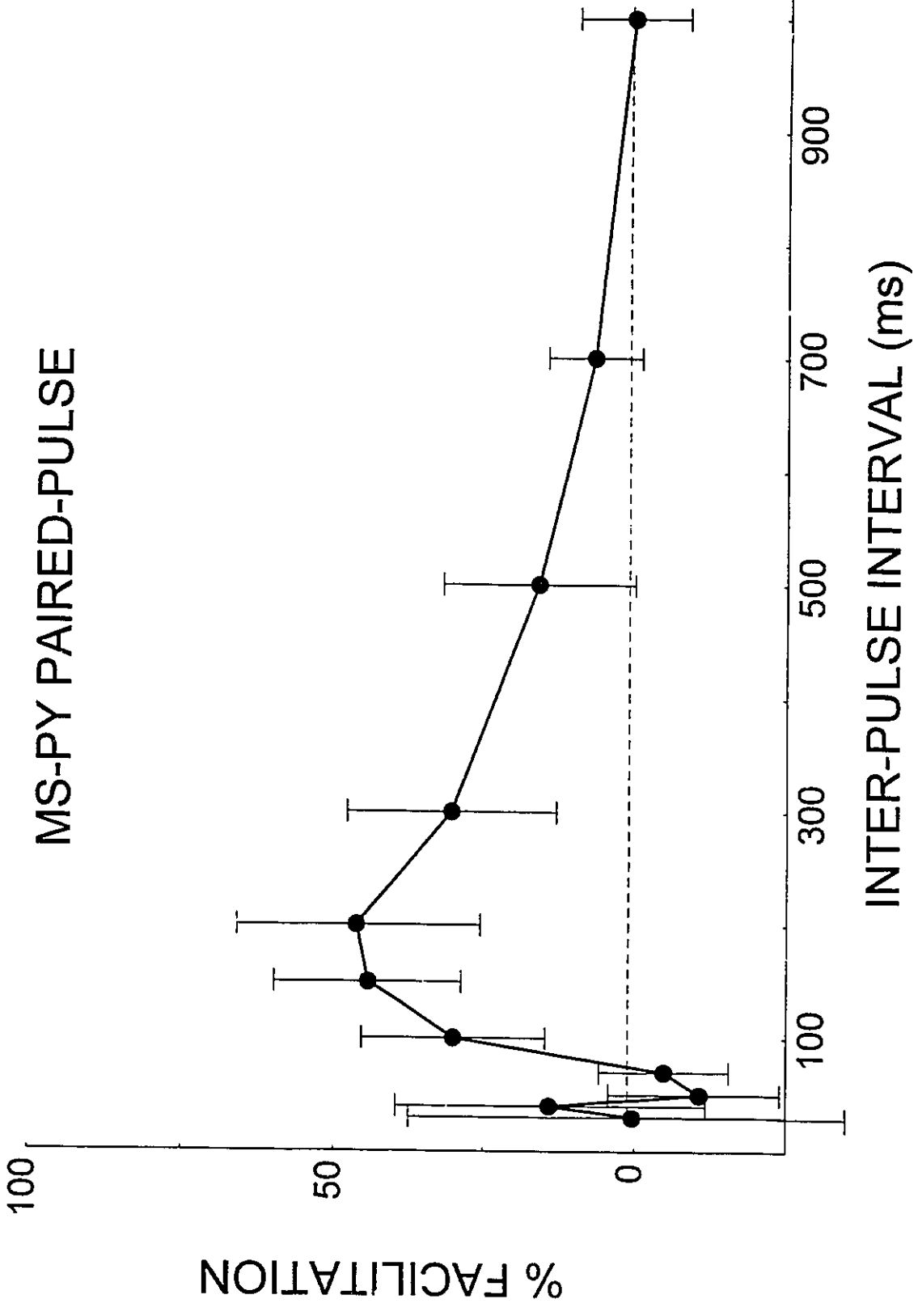


Figure 3.10

Figure 3.10. Responses to test-pulses delivered to the medial septum (**dashed traces**) following the delivery of conditioning-pulses to the pyriform cortex at the interpulse intervals indicated at left. Responses evoked by test-pulses are superimposed on the mean of the responses evoked during the single-pulse medial septum stimulation condition (**solid traces**). An **arrow** indicates the peak latency of the field potential component generated by currents in layers II-III. Horizontal calibration, 10 msec; vertical calibration, 0.5 mV.

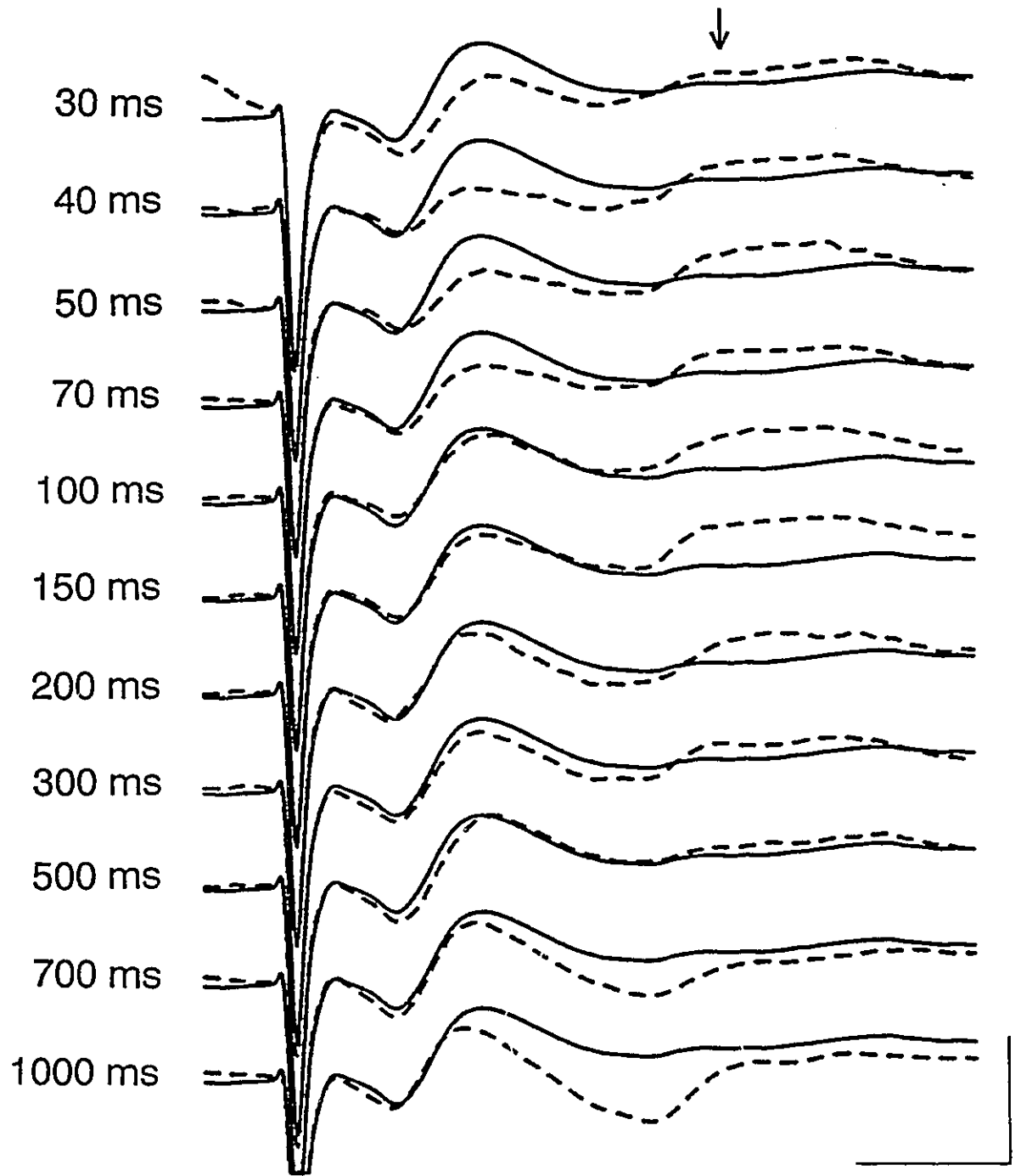


Figure 3.11

Figure 3.11. The average amplitude of responses to test-pulses delivered to the medial septum following the delivery of conditioning-pulses to the pyriform cortex (**PY-MS**). Data are expressed as a percent increase from the mean response amplitude recorded during the single-pulse medial septal stimulation condition. Data are based on the field potential component indicated by an arrow in Figure 3.10.

PY-MS PAIRED-PULSE

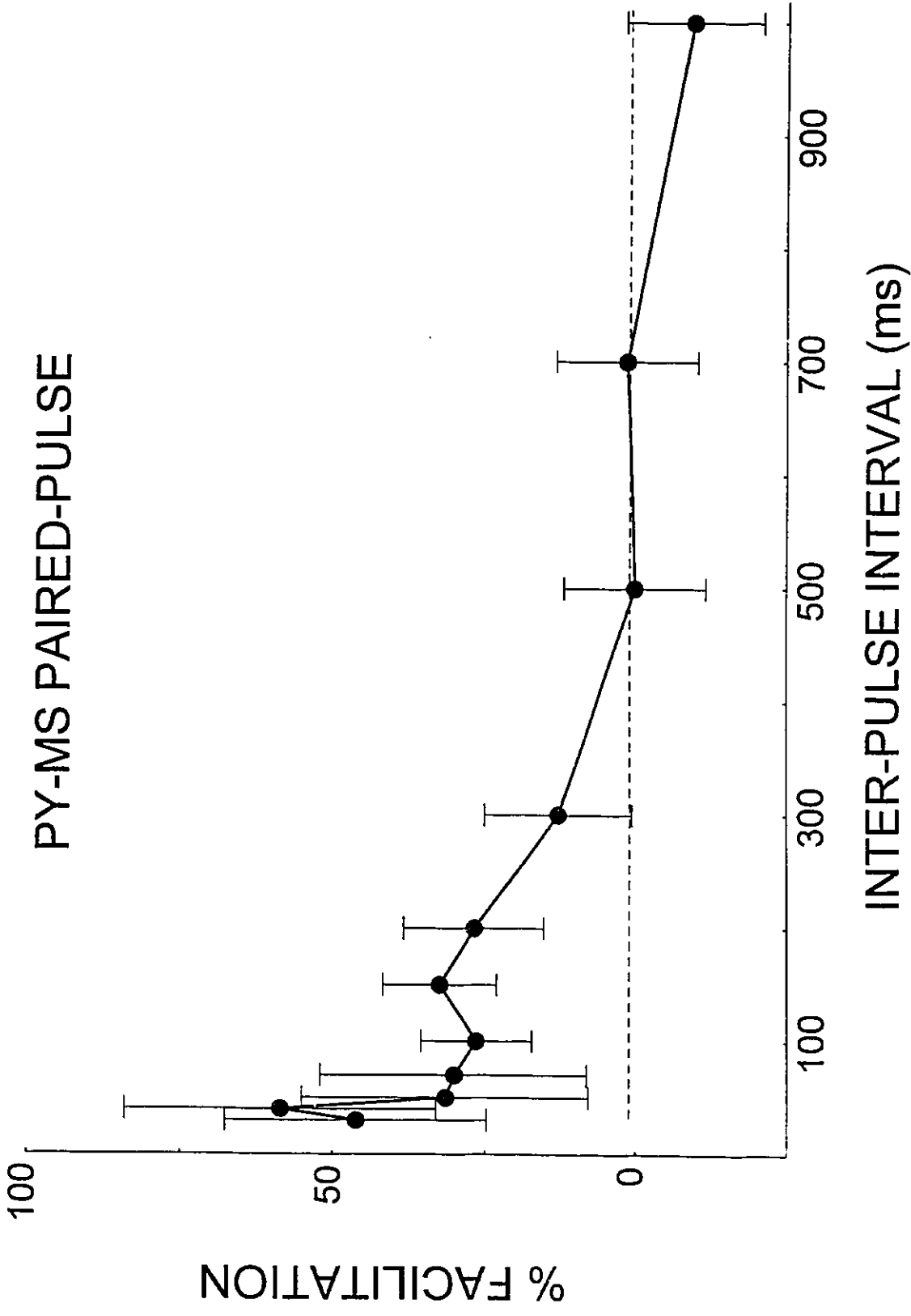
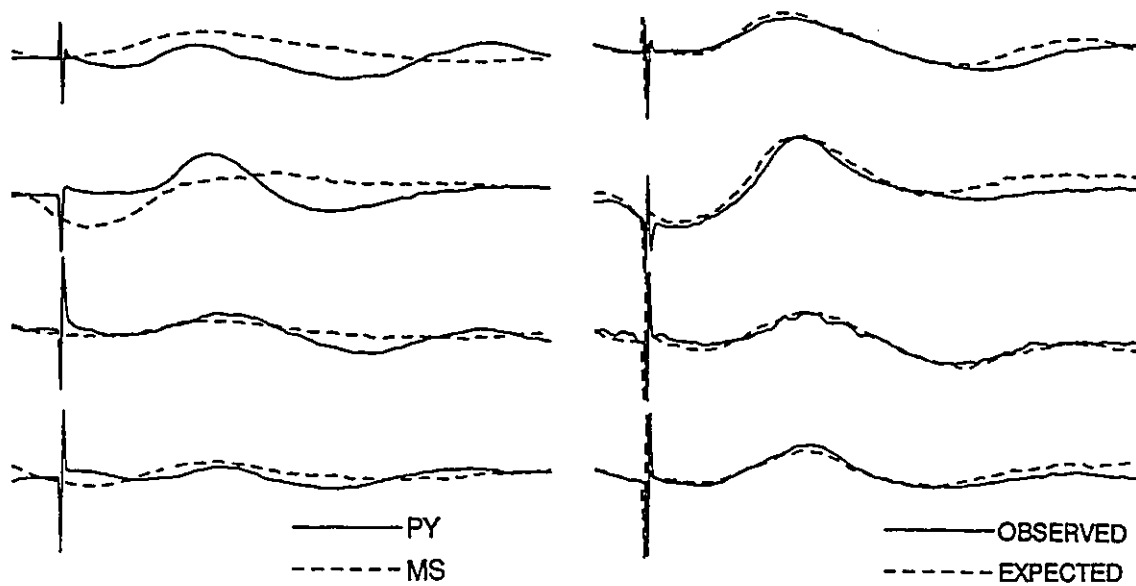


Figure 3.12

Figure 3.12. The results of occlusion testing with low (A), and high (B) intensity stimulation pulses are shown for four animals which are representative of the range of response morphologies observed. **Left panels** show the single-pulse responses to pyriform cortex (PY) and medial septal (MS) stimulation with the field potentials evoked by septal stimulation shifted to the left to match the peak latencies of the responses evoked by pyriform cortex stimulation. The **right panels** show the results of double-pulse stimulation recorded using an interpulse interval equal to the latency shift applied in the left panels (**observed**). The double-pulse responses expected on the basis of summing the single-pulse evoked field potentials using the same latency shift (**expected**) are also shown for comparison. Note that the observed double-pulse results are smaller in amplitude than the expected results for high-, but not for low-, intensity stimulation. Horizontal calibration, 10 msec; vertical calibration, 0.5 mV.

A LOW INTENSITY



B HIGH INTENSITY

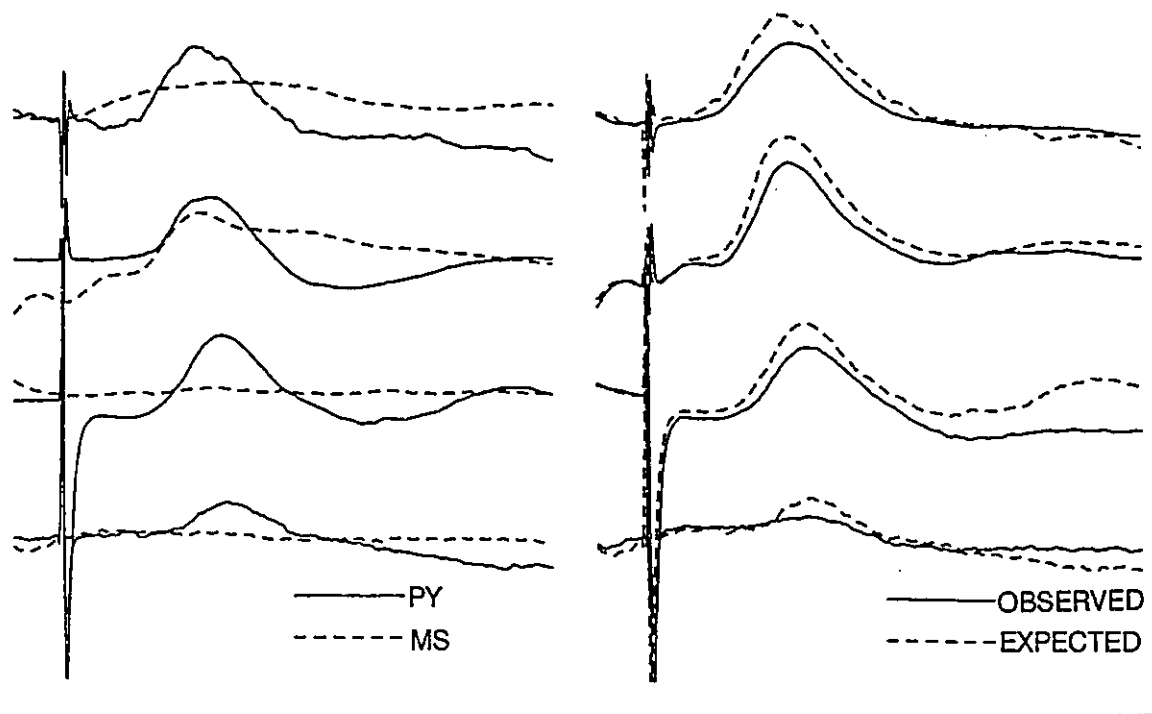
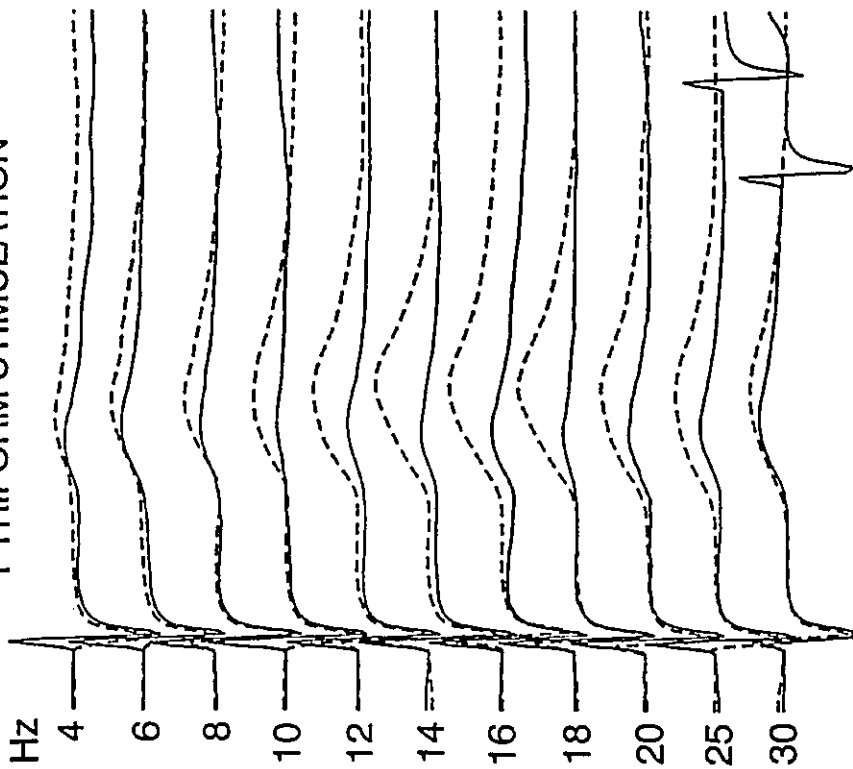


Figure 3.13

Figure 3.13. Averaged evoked field potentials recorded in the entorhinal cortex during stimulation of the pyriform cortex (**left panel**) and medial septum (**right panel**) with 10-pulse stimulation trains at the indicated frequencies. The average response to the first pulse (**solid traces**) and to the last pulse (**dashed traces**) in each train are superimposed. The stimulation artifacts due to the second pulses in the 25 and 30 Hz conditions are visible in the solid traces. Intermediate frequencies result in the greatest frequency potentiation. Horizontal calibration, 10 msec; vertical calibration, 0.5 mV.

PYRIFORM STIMULATION



SEPTAL STIMULATION

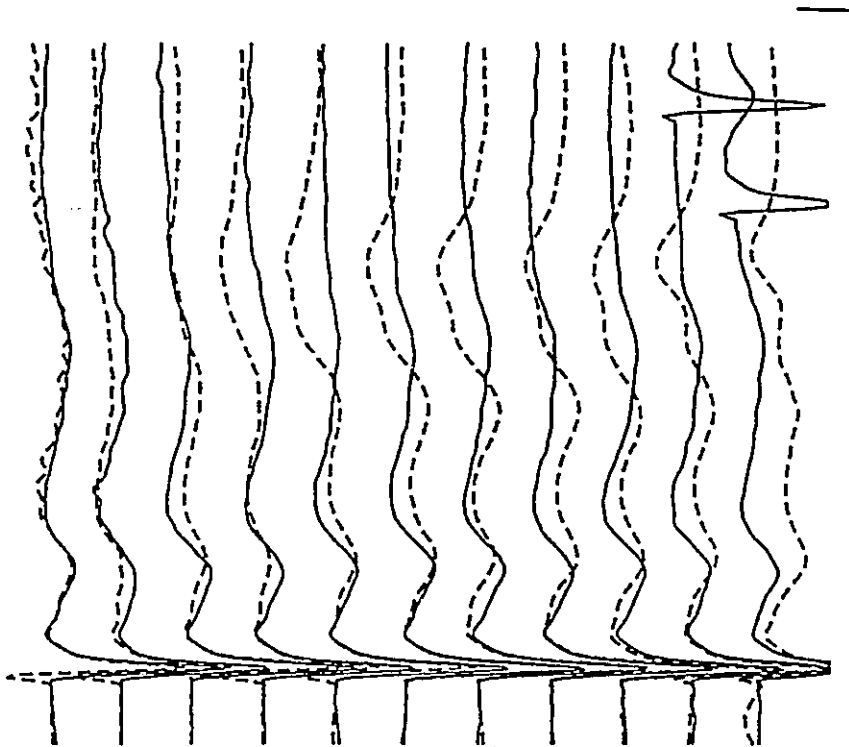
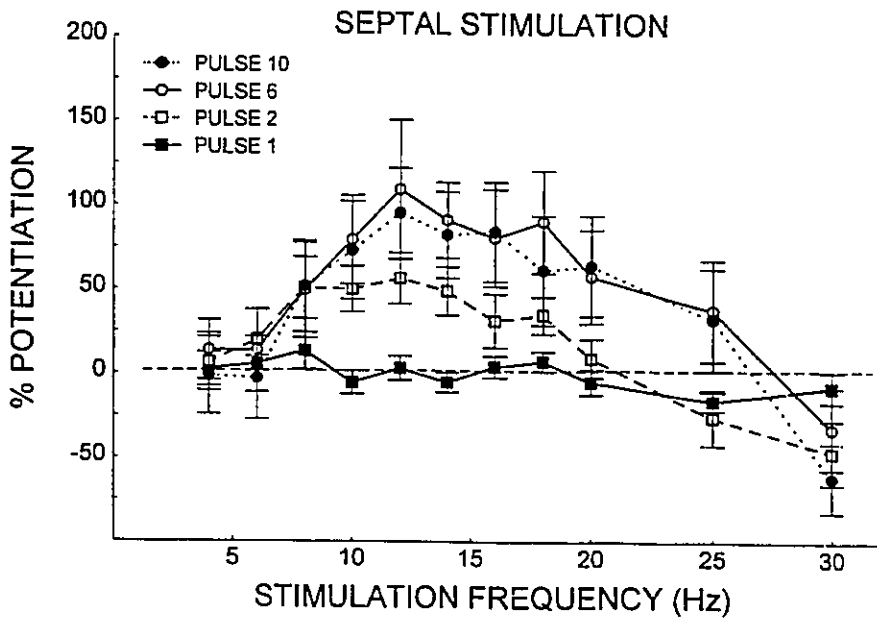
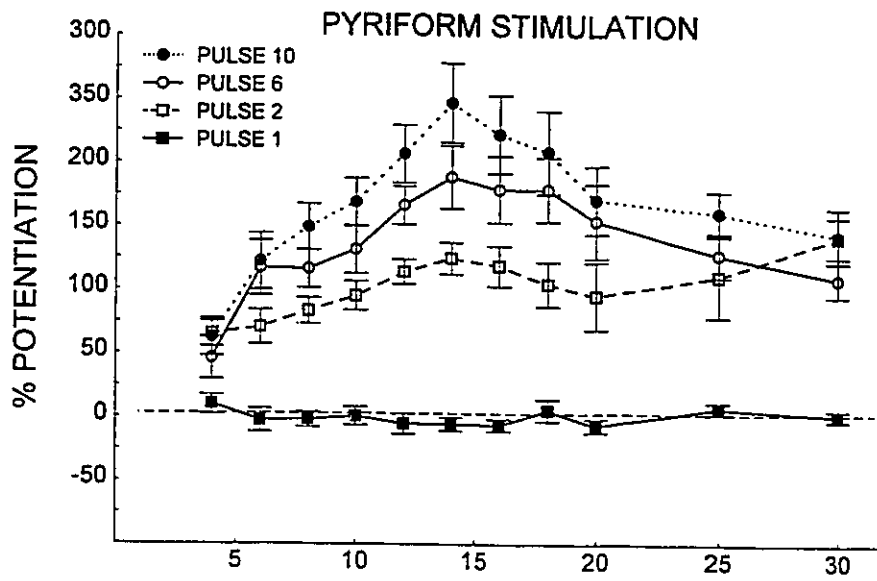


Figure 3.14

Figure 3.14. The mean amplitudes of responses in the entorhinal cortex during low-frequency pyriform cortex (**top panel**) and medial septal (**bottom panel**) stimulation are shown as a function of stimulation train frequency. Mean response amplitudes are shown for the first (**pulse 1**), second (**pulse 2**), sixth (**pulse 6**), and tenth (**pulse 10**) pulses in each train. Data are expressed as a percent increase from the mean amplitude of potentials evoked by the first pulse in each train, averaged across all stimulation frequencies.



DISCUSSION

The temporal parameters which govern frequency potentiation and paired-pulse facilitation effects have been examined here in the chronic preparation for pyriform cortex and medial septal inputs to the entorhinal cortex. The frequency potentiation tests were used to determine the optimal frequency ranges for the activation of the entorhinal cortex through these inputs. The strongest effects were observed in the 10 to 20 Hz range when using brief 10-pulse stimulation trains (Figures 3.13 & 3.14). These findings are consistent with the possibility that endogenous neuronal activity in these efferents are enhanced when occurring at, or somewhat above, frequencies of the theta rhythm.

Dual-site paired-pulse tests indicated that pyriform cortex and medial septal inputs to the entorhinal cortex can interact so that the prior activation of one input facilitates the responses subsequently evoked by the other input (Figures 3.10 & 3.11). Although these interactions may have been mediated by interneurons, the results of occlusion testing suggest that they may have also resulted from post-synaptic interactions in cells directly activated by both inputs. The occlusion tests showed that the depolarization expected from the activation of medial septal inputs to the entorhinal cortex was occluded, or masked, by strong, simultaneous activation of pyriform cortex inputs. These effects, which were not observed when weak, summing inputs were used (Figure 3.12), are thought to result from a ceiling effect on the amount of post-synaptic depolarization which can be induced, and suggest that the neuromodulatory inputs from the medial septum do indeed synapse onto the same neuronal populations as pyriform cortex efferents.

Although frequency potentiation was induced throughout most of the theta range, the largest effects were observed at frequencies near 12 Hz. Consequently, if frequency potentiation-like phenomena are induced during spontaneous theta activity they are likely to be larger during higher-frequencies of theta activity. The speed with which movements are initiated is positively correlated with the frequency of theta activity (Vanderwolf, 1969), and the frequency of theta activity tends to be somewhat higher during locomotor approach than during investigatory sniffing (Macrides et al., 1982). During periods of theta activity, when animals may be exposed to an increased amount of sensory information, the rhythmic discharge of medial septal neurons (Petsche et al., 1962), could collectively contribute to an enhancement via frequency potentiation mechanisms of rhythmic depolarization in the entorhinal cortex. Further, behavioural data suggests that pyriform cortex inputs to the entorhinal cortex are also active at theta-frequency during periods of odour sampling (Komisaruk, 1970; Macrides et al., 1982), so that frequency potentiation-like effects may also occur in pyriform cortex inputs to the entorhinal cortex during these periods. If an appropriate phase relationship were to exist between pyriform cortex and septal inputs to the entorhinal cortex so that the rhythmic inputs were synchronized, an even greater enhancement of transmission of sensory information carried by the pyriform efferents to the entorhinal cortex might occur.

Heterosynaptic interactions between medial septal and pyriform cortex inputs to the entorhinal cortex may also have some effect on the induction of long-term changes in synaptic efficacy. Septal inputs may both contribute to the induction of theta rhythmicity in layer II entorhinal cortex neurons, and result in a frequency potentiation of these neurons during rhythmic activity in septo-

entorhinal cortex efferents. The resulting increase in levels of post-synaptic depolarization could contribute to the induction of long-term potentiation of synaptic transmission in sensory afferents to the entorhinal cortex (Alonso et al., 1990; de Curtis & Llinas, 1993). Experiments addressing this possibility are described and discussed in Chapters 4 and 5 of this thesis.

Pyriiform Cortex Stimulation. Entorhinal cortex potentials were apparently evoked by activation of cell bodies or initial segments of pyramidal cell projection neurons in layer II. Although the stimulation electrodes were scattered to some extent both medio-laterally and rostro-caudally, they were all located near layer II of the pyriiform cortex and they all evoked field potentials with similar morphology. The dorsoventral positions of these stimulation sites had been optimized during surgery with respect to the current thresholds of the evoked responses.

Single-pulse stimulation of the pyriiform cortex resulted in a negative-going field potential similar to those observed in previous acute and *in vitro* studies in the superficial layers of the entorhinal cortex (Figures 2.4 & 3.2 left; Van Groen et al., 1987; de Curtis & Llinas, 1993). Previous current-source density analyses in the urethanized cat (van Groen et al., 1987), and rat (Figure 2.8) indicate that these field potentials result from membrane currents generated by layer II neurons.

The average distance between the stimulating and recording electrodes was estimated to be 5.2 mm, and the average onset latency for the evoked potentials was 10.9 msec, yielding a conduction velocity estimate of 0.48 m/sec for the fastest fibers mediating the response. Similar estimates have been made for fibers projecting from the pyriiform cortex to the entorhinal cortex for the cat (Boeijinga & Van Groen, 1984), and the anesthetized rat (Chapter 2).

Repetitive, low-frequency activation of the pyriform cortex resulted in very strong frequency potentiation effects in the entorhinal cortex. The effects were maximal for 14 Hz stimulation, but the tuning curves were rather broad, showing growth in response amplitudes during the train at frequencies ranging between 6 and 20 Hz (Figures 3.13 & 3.14). It is not known to what extent frequency potentiation effects rely on the abnormally high *synchrony* of activation of the input pathways by electrical stimulation. Consequently, it is not clear to what extent the tuning phenomenon mirrors the endogenous reactivity of the entorhinal cortex to inputs from the pyriform cortex. These results do, however, show that the entorhinal cortex may be preferentially activated by frequencies that fall within a normal physiological range.

The frequencies reported here for the induction of frequency potentiation in animals with chronically implanted electrodes are similar to those reported in other *in vivo* studies of frequency potentiation in the olfactory system and hippocampal formation (Cragg, 1961; Andersen & Lomo, 1967; Krug et al., 1985). Eight to 20 Hz stimulation frequencies are also effective in inducing facilitation of hippocampal responses by olfactory bulb stimulation (Cragg, 1961), but it is unknown to what extent the pyriform to entorhinal pathway studied here may have contributed to the frequency effects observed by Cragg. However, lateral olfactory tract inputs to the pyriform cortex, at least *in vitro* (Hasselmo & Bower, 1990), do not frequency potentiate well with 20 Hz stimulation, suggesting the effects observed by Cragg (1961) may have been due to a later link in the olfactory path; perhaps the inputs to the entorhinal cortex from the pyriform cortex studied here.

During low-frequency stimulation of the pyriform cortex, the evoked responses increased, not only in amplitude, but also in duration so that late

portions of the evoked responses were enhanced. This may reflect the enhancement of late NMDA receptor-mediated components of the evoked potentials (Jones, 1987; de Curtis & Llinas, 1993). Late components of field potential evoked by subicular stimulation are enhanced in Mg^{2+} -free medium (Jones & Heinemann, 1988), and frequency potentiation of the EPSP by stimulation of the parasubiculum *in vitro* is blocked by the NMDA receptor antagonist 2-AP5 (Jones & Heinemann, 1991). Because Ca^{2+} currents associated with NMDA receptor activation are necessary for long-term potentiation in pyriform cortex inputs to the entorhinal cortex in the *in vitro* guinea pig brain (Alonso et al., 1990), the enhanced late component observed here suggests that the entorhinal cortex could be more susceptible to the induction of long-term potentiation (LTP) during times when pyriform cortex inputs are highly active at frequencies between 6 and 20 Hz. The putative activation of NMDA currents by frequency potentiation effects, however, does not appear to be sufficient alone for the induction of LTP, since long-term changes in evoked potentials were not observed in this study (Figure 3.2). Bursts of synaptic activation occurring during the most depolarized phase of frequency potentiation might, however, result in sufficient NMDA-mediated Ca^{2+} currents to result in LTP (see Chapter 4).

Double-pulse stimulation of the pyriform cortex was used to examine paired-pulse facilitation effects which may have contributed to the frequency potentiation. The greatest paired-pulse facilitation was observed at C-T intervals of 30 and 40 msec which correspond to frequencies of 33 and 25 Hz (Figure 3.5). However, the peak frequency potentiation effects occurred for lower-frequency trains with interpulse intervals near 60 and 80 msec. Similarly, while frequency potentiation effects declined at stimulation frequencies above 14 Hz,

the decline would have been predicted to occur at frequencies above 30 to 50 Hz on the basis of reductions in paired-pulse facilitation at interpulse intervals between 5 and 20 msec. In addition, although there was no growth during the 4 Hz stimulation trains, paired-pulse facilitation effects were observed at C-T intervals of 200 and 300 msec, and in response to the second pulse during 4 Hz stimulation. However, although the shape of the paired-pulse facilitation curve does not entirely account for the tuning of frequency potentiation in this pathway, substantial paired-pulse facilitation was observed at interpulse intervals which resulted in the largest frequency potentiation effects.

Medial Septal Stimulation. Medial septal stimulation resulted in field potentials in the entorhinal cortex with multiple components which peaked at different latencies (Figure 3.3). Previous current source density analysis in the urethanized rat (Figure 2.13) has indicated that the late, weak negative component is the result of synaptic activation of entorhinal cortex neurons in layer II and in the upper portion of layer III. The earlier, positive and negative field potential components are volume conducted from sites in the hippocampal formation (Figure 2.13; Andersen et al., 1961; McNaughton & Miller, 1984). Although hippocampal activation could result in the polysynaptic activation of the entorhinal cortex, the amplitudes of the early and the late negative components were not well correlated, so that the late negativity is most likely mediated by the known monosynaptic projection from the medial septum to the entorhinal cortex (Alonso & Kohler, 1984; Gaykema et al., 1990). Based on the mean onset latency of the late negativity (22.6 msec) and the estimated distance between stimulating and recording electrodes, the fastest fibers mediating the response are estimated to have rather slow conduction velocities of roughly 0.45 m/sec.

Enhancements of entorhinal cortex responses during low-frequency stimulation of the medial septum were weaker, more variable, and occurred over a more restricted frequency range than during low-frequency stimulation of the pyriform cortex. A frequency-dependent growth in entorhinal cortex responses was observed during 8 to 25 Hz stimulation (Figure 3.14 bottom). In most of the animals, frequency potentiation of late negativity was expressed as an increase in amplitude with no change in the latency to peak. In two of the 12 animals, however, the late negativity appeared to separate into two distinct field potential components at higher stimulation frequencies (e.g., Figure 3.13 left). This may be due to a shift in the latency of responses in a subpopulation of the neurons directly activated by the medial septum, or to the multisynaptic recruitment of activity in an additional neural population.

Similar to the results for pyriform cortex stimulation, medial septum paired-pulse facilitation effects did not predict the entire form of the frequency potentiation tuning curve. Facilitation at a given C-T interval did not predict growth beyond the 2nd pulse during trains with corresponding interpulse intervals. While paired-pulse facilitation was observed at C-T intervals between 500 and 150 msec, frequency potentiation did not occur during 4 and 6 Hz trains (with interpulse intervals of 250 and 167 msec). There was, however, a reasonably good correspondence between the interpulse intervals which evoked maximal paired-pulse facilitation effects, and those which evoked optimal frequency potentiation effects. Peak paired-pulse facilitation effects were evoked with C-T intervals of 70 msec, and frequency potentiation was strongest on average for 12 Hz trains with an 83 msec interpulse interval.

Both paired-pulse and low-frequency stimulation of the medial septum result in changes in early components of the field potentials which are likely

generated in the dentate gyrus (Andersen et al., 1961; McNaughton & Miller, 1984; Chapter 2). Although these potentials are volume conducted over a distance of roughly 2 mm to the entorhinal cortex, and are therefore a less direct measure of dentate gyrus activity, repeated stimulation was observed to result in an enhancement in the positive component, and a reduction in the negative component (Figures 6 & 13 right). Others have recorded a similar time-course for facilitation of the positive component in the dentate gyrus which typically peaks at C-T intervals between 50 and 100 msec, and falls off to single-pulse levels at C-T intervals above 150 msec (Robinson & Racine, 1982, 1986; McNaughton & Miller, 1984).

Frequency Potentiation Mechanisms. Although the mechanisms of frequency potentiation in both central and peripheral nervous systems are not well understood, the facilitation of response amplitudes during both paired-pulse and frequency potentiation is generally thought to result largely from increased transmitter release due to a build-up of residual presynaptic Ca^{2+} (White et al., 1979; Turner & Miller, 1982; Applegate & Landfield, 1988). Katz and Miledi (1968) first proposed that a residual amount of presynaptic Ca^{2+} left over by incomplete sequestration or inactivation of the Ca^{2+} entering the presynaptic terminal after a first stimulation pulse could result in enhanced transmitter release in response to a second stimulation pulse. The Ca^{2+} entering in response to the second pulse could sum with residual Ca^{2+} remaining in the terminal after the first pulse, resulting in enhanced Ca^{2+} -dependent neurotransmitter release. A small amount of residual Ca^{2+} is thought to result in a large facilitation of transmitter release during paired-pulse stimulation due to a non-linear relationship between release and free intracellular Ca^{2+} concentration near release sites. Transmitter release varies with approximately the fourth

power of Ca^{2+} concentration so that small increments in the amount of intracellular Ca^{2+} can result in a much larger response (Barrett & Stevens, 1972; Zucker & Stockbridge, 1983; Zucker, 1989). Further, when a fourth power relationship is applied to the Ca^{2+} concentration within a 100 angstrom distance from the membrane, paired-pulse facilitation in the frog neuromuscular junction is well predicted by a model which also incorporates slow intracellular diffusion, active efflux of Ca^{2+} , and the inactivation of Ca^{2+} due to binding to cytoplasmic sites (Stockbridge & Moore, 1984).

Paired-pulse facilitation of synaptic transmission at the neuromuscular junction decays rapidly at first, with a time constant of roughly 20 to 35 msec, and then more slowly with a time constant of about 250 msec (Mallart & Martin, 1967; Barrett & Stevens, 1972; Magelby, 1973a&b). When trains of stimuli are used, a third, more slowly-decaying facilitatory component referred to as augmentation, with a time constant of 7 sec, is also observed (Magelby & Zengel, 1976; Zengel & Magelby, 1980, 1982). The decay of enhanced synaptic transmission following train delivery can be well fit by assuming that successive stimulation pulses add Ca^{2+} incrementally to an intracellular store of residual Ca^{2+} , and that the removal of Ca^{2+} from the store is governed by the sum of three decaying exponentials corresponding to the two components of facilitation and to augmentation (Zengel & Magelby, 1982; Zucker, 1989).

Short-term synaptic enhancements with time courses similar to those observed at the neuromuscular junction also occur in a number of pathways in the central nervous system, including intrinsic pathways of the hippocampal formation (Racine & Milgram, 1983; McNaughton, 1982). Paired-pulse facilitation effects at central synapses are also thought to result from the effects of residual presynaptic Ca^{2+} (Andreasen & Hablitz, 1994; Wu & Saggau, 1994).

Presynaptic Ca^{2+} transients consistent with the residual Ca^{2+} model are observed during paired-pulse facilitation of responses in area CA1 by stratum moleculare stimulation in the guinea pig hippocampal slice (Hess & Kuhnt, 1992). Further, Wu and Saggau (1994) have found that EPSP amplitude in CA1 is related to the fourth power of presynaptic Ca^{2+} as in the peripheral synapse, and that the amount of paired-pulse facilitation is roughly proportional to the amount of residual presynaptic Ca^{2+} measured. Response enhancements during frequency potentiation at central synapses is therefore also likely to be partly due to the build-up of residual presynaptic Ca^{2+} caused by repetitive stimulation.

In the present study, the frequency potentiation effects cannot be explained simply by facilitation due to the incremental addition of Ca^{2+} to an intracellular compartment since frequency potentiation does not increase monotonically with stimulus frequency, and is also not expressed at low stimulation frequencies with interpulse intervals that result in paired-pulse facilitation. Part of this discrepancy could be explained by stimulation-dependent changes in the effectiveness of presynaptic mechanisms which remove free intracellular Ca^{2+} . While Ca^{2+} uptake and extrusion processes likely have the greatest effect on the decay rate of augmentation, the time courses of the facilitation effects, which are likely responsible for most of the frequency potentiation, may be affected more by changes in faster processes of cytoplasmic binding and diffusion of Ca^{2+} (Zengel & Magelby, 1980; Zucker & Stockbridge, 1983; Zucker, 1989). At low frequencies of stimulation, frequency potentiation is likely absent due to a negligible accumulation of presynaptic Ca^{2+} due to long interpulse intervals since presynaptic Ca^{2+} transients approach baseline levels in central neurons after approximately 200 msec (Hess & Kuhnt,

1992). However, at both high and low train frequencies, enhanced Ca^{2+} removal during prolonged stimulation may reduce the amount of frequency potentiation expected on the basis of the facilitation observed during paired-pulse testing with similar interpulse intervals.

Enhancements in response amplitude during frequency potentiation may also be due to factors affecting the excitability of the post-synaptic cell. Creager et al., (1980) have suggested that frequency potentiation effects resulting from prolonged (>5-10 sec) low-frequency stimulation could result from an increase in extracellular K^+ which could increase the K^+ equilibrium potential and therefore neuronal excitability. They stimulated the Schaffer collateral projection to the CA1 region *in vitro* and found that the enhanced population spike and declining EPSP amplitude they observed during frequency potentiation could be simulated by adding increasing amounts of KCl to the bathing medium. Similar "ephaptic" effects in the extracellular field were found by Turner et al. (1983) to contribute to frequency potentiation by recruiting subthreshold neurons. They found that sharp depolarizing waves in the transmembrane potential of CA1 pyramidal neurons covaried with the amplitude and latency of extracellularly-recorded population spikes during both paired-pulse and frequency potentiation, and that these depolarizing waves sometimes resulted in action potentials. Similar alterations in the extracellular field are less likely to have played a role in the present study in which relatively brief stimulation was applied, clear population spikes were not observed, and the neuronal elements are less tightly packed than in CA1.

Frequency-dependent reductions in inhibitory mechanisms could also contribute to response growth during frequency potentiation (Andersen & Lomo, 1968). Reductions in inhibitory post-synaptic currents during paired-

pulse stimulation have been observed in the neocortex (Deisz & Prince, 1989) and in the hippocampus where the greatest depression is observed at interpulse intervals near 100 msec and effects can last up to about 4 sec (Davies et al., 1990; Nathan et al., 1990; Nathan & Lambert, 1991; Mott et al., 1993). This form of inhibition has been linked to the activation of GABA_B autoreceptors on the terminals of inhibitory neurons (Davies et al., 1990; Mott et al., 1993). In addition, conditions which reduce transmitter release in response to the first pulse also reduce the depression in the IPSCs, suggesting that reductions in transmitter available for release may contribute to the depression (Wilcox & Dichter, 1994). It is of interest that this form of depression of inhibition in the dentate gyrus has its most marked effects on signal transmission to the CA3 region when tested by delivering pairs of pulses at frequencies between 2.5 and 10 Hz (Thompson & Gahwiler, 1989; Mott et al., 1993). A similar frequency-dependent reduction in inhibition in the entorhinal cortex may contribute to frequency potentiation there.

Although reduced inhibition may play a role in enhancing the response of principal neurons during frequency potentiation, inhibitory mechanisms must play a strong role in *reducing* frequency potentiation effects at non-optimal stimulation frequencies. While response enhancements during paired-pulse or frequency potentiation are commonly thought to be due primarily to the build-up of residual presynaptic Ca²⁺, this mechanism alone does not explain why frequency potentiation effects do not increase monotonically with the frequency of stimulation. Inhibitory mechanisms are therefore needed to explain why maintained growth in response amplitude does not occur at stimulation frequencies below and above those which are optimal for inducing frequency potentiation, but which still produce paired-pulse facilitation effects.

At low stimulation frequencies inhibitory mechanisms with prolonged time-courses could prevent maintained response growth during frequency potentiation. Candidate mechanisms in the entorhinal cortex include both synaptically induced, long-duration IPSPs (Finch & Babb, 1980; Finch et al., 1988; Jones & Heinemann, 1991; Jones, 1990a; Colino & Fernandez de Molina, 1986), and afterhyperpolarizations following activation of principal neurons (Alonso & Klink, 1993). Synaptically-induced inhibitory effects in the entorhinal cortex, likely due to feedforward circuitry, have latencies ranging from about 5 to 25 msec, and a very slow decay which lasts for periods of 50 to 500 msec (Finch & Babb, 1980; Finch et al., 1988). Hyperpolarizations following single spikes in both stellate and non-stellate entorhinal cortex neurons also last for prolonged periods of several hundred msec, and the afterhyperpolarizations which follow trains of spikes in stellate cells can last for up to about 2 sec. Although long-lasting inhibitory processes were likely evoked in the present experiment, a net depression was not observed at any interpulse interval during double-pulse stimulation of either the pyriform cortex or medial septum. While inhibitory effects were therefore likely balanced by the decaying facilitation during double-pulse testing at long C-T intervals, they could, however, have limited the growth of frequency potentiation during repetitive stimulation at 4 to 8 Hz.

Reduced frequency potentiation at higher frequencies of stimulation is unlikely to be due to the depletion of a limited vesicular store of neurotransmitter since neurotransmitter depletion is usually associated with more prolonged stimulation (Del Castillo & Katz, 1954; Zucker, 1989). Synaptically-mediated inhibition, however, is likely to have contributed to limiting response growth at the higher frequencies of stimulation. Short-latency inhibitory mechanisms in

the entorhinal cortex appear to be induced following stimulation of either the pyriform cortex or the medial septum since the amount of paired-pulse facilitation was reduced at the shortest C-T intervals (Figures 3.5 & 3.7). In studies of frequency potentiation in the hippocampus (MacVicar & Dudek, 1979; Schwartzkroin, 1975; Pitler & Landfield, 1985), and the *in vitro* and *in vivo* entorhinal cortex (Finch et al., 1986; Jones, 1990b), sustained hyperpolarizations during stimulation have been a common observation. For example, MacVicar and Dudek (1979) stimulated mossy fibers and recorded EPSPs in CA3 pyramidal neurons which were superimposed on a sustained hyperpolarizing shift in membrane potential. A similar sustained hyperpolarization occurs in layer II entorhinal cortex neurons during 11 Hz stimulation of the presubiculum (Finch et al., 1986; Jones, 1990b). The sustained hyperpolarization during frequency potentiation in the entorhinal cortex is thought to be due to synaptic inhibition via feedforward inhibitory mechanisms (Finch et al., 1986, 1988). This may also be the mechanism in the hippocampus where the hyperpolarizing membrane shift is only observed in thicker hippocampal slices which maintain the diffuse circuitry of inhibitory neurons (Yamamoto, 1972). In CA1, the sustained hyperpolarization is correlated with K⁺-dependent glial membrane potentials, and is *not* blocked by bicuculline which blocks GABA_A mediated Cl⁻ conductances, suggesting that it is mediated by an increased K⁺ conductance. The latter could arise from the activation of GABA_B receptors or a Ca²⁺-dependent K⁺ conductance (Pitler & Landfield, 1987). Both a build-up of GABA_B-receptor mediated inhibition, and the repetitive activation of fast GABA_A-mediated inhibition (Jones & Heinemann, 1991; Jones, 1990b), may therefore have contributed to reductions in frequency potentiation at high stimulation frequencies. The reductions in paired-pulse facilitation at short C-T intervals, however, is likely to have been mediated largely

by GABA_A transmission since these fast IPSPs commonly have latencies in the range of 5 to 25 msec (Finch et al., 1988; Jones & Heinemann, 1991; Jones, 1990b).

Heterosynaptic Interactions. Double-site paired-pulse stimulation tests indicated that stimulation of either the medial septum or pyriform cortex leads to a facilitation of the field potential subsequently induced by stimulation of the other site. The time courses of the facilitation observed, however, differed for each test. The delivery of C-pulses to the pyriform cortex resulted in a facilitation of responses evoked by medial septal stimulation which had a time-course similar to the facilitation observed when both pulses were delivered to the pyriform cortex. Although the magnitude of the facilitation was smaller, the effects were strongest for interpulse intervals of 30 and 40 msec, and decayed as the C-T interval was increased to 500 msec (Figures 3.5 & 3.11). In contrast, when the C-pulse was delivered to the medial septum the facilitation persisted at C-T intervals of 500 msec, and there was no facilitation of pyriform cortex evoked responses at C-T intervals less than 100 msec (Figure 3.9). This heterosynaptic facilitation of pyriform cortex evoked responses induced by septal stimulation is similar in relative magnitude to the facilitation of perforant path evoked responses in dentate granule cells (Robinson & Racine, 1982).

The heterosynaptic nature of the facilitation effects indicates that they cannot be due to presynaptic mechanisms. Because medial septal and pyriform cortex efferents may synapse onto the same cells (Figure 3.12), postsynaptic mechanisms governing interactions between the two inputs could contribute to the facilitation effects. The heterosynaptic facilitation effects may be partially due to an enhancement of NMDA-mediated components of the EPSP if the first afferent volley at least partially removes the Mg²⁺ block on the

NMDA receptor. A second input to the same neurons could then result in a more complete depolarization of the cell (Thompson & Deuchars, 1994). This is a probable mechanism for pyriform cortex inputs to the entorhinal cortex which are known to evoke both NMDA- and non-NMDA-mediated EPSPs (de Curtis & Llinas, 1993). NMDA currents in area CA1 of the hippocampus are enhanced by cholinergic agonists (Markram & Segal, 1990). If a similar enhancement occurs in the entorhinal cortex following activation of cholinergic septal inputs (Alonso & Kohler, 1984), this could facilitate NMDA-mediated components of the pyriform cortex evoked responses. The facilitation of pyriform cortex inputs did not decay completely on average until over 700 msec after the septal C-pulse, consistent with the relatively prolonged action of cholinergic neurotransmission on the excitability of neurons (Cole & Nicoll, 1984). However, although the late, putatively NMDA-mediated component of the evoked potentials studied here was enhanced, the initial, presumably *non*-NMDA-mediated component was also enhanced (Figure 3.8).

If some of the same feedforward inhibitory neurons are activated by both medial septal and pyriform cortex inputs to the entorhinal cortex, then the early component of the field potentials could be enhanced if these neurons display a paired-pulse depression of GABA-ergic transmission as they do in the neocortex and hippocampus (Deisz & Prince, 1989; Davies et al., 1990; Mott et al., 1993). Such a reduction in inhibition could account for some of the facilitation of the responses during double-site stimulation tests, in addition to the potential contribution to the single-site paired-pulse tests as described above. It is unclear why, at C-T intervals under 100 msec, responses to septal T-pulses following pyriform cortex stimulation were enhanced, while responses to T-pulses in the pyriform cortex were not enhanced by prior stimulation of the

septum. Heterosynaptic facilitatory mechanisms evoked by septal stimulation may have a slower onset than those assessed in the other paired pulse tests, or the facilitation may have been masked by similarly powerful, fast inhibitory mechanisms.

CHAPTER 4

LONG-LASTING POTENTIATION OF SYNAPTIC RESPONSES THE ENTORHINAL CORTEX FOLLOWING PYRIFORM CORTEX STIMULATION

Long-term enhancements in synaptic strength are thought to contribute to the processes of learning and memory (Hebb, 1949; Bliss & Lomo, 1973; Teyler & Discenna, 1984; Racine & Kairiss, 1987; Maren & Baudry, 1995). Experimentally-induced long-term potentiation (LTP) of synaptic strength suggests that cortical areas affected may be capable of supporting the temporary or permanent storage of information during normal information processing. Most of the LTP research in chronic preparations has focussed on the intrinsic pathways of the hippocampal formation, but very little work has been directed to the entorhinal cortex. Because the entorhinal cortex receives inputs from primary and associational sensory cortical areas (Van Hoesen et al., 1972, Van Hoesen & Pandya, 1975; Krettek & Price, 1977; Beckstead, 1978; Witter et al., 1989; White et al., 1990), plasticity in sensory input pathways to the entorhinal cortex may contribute to the storage of multimodal sensory representations. For example, synaptic plasticity in the pyriform cortex inputs to the entorhinal cortex could contribute to the storage of representations of olfactory stimuli, and these representations could combine with other sensory inputs to become integrated into multimodal representations of sensory events.

Because the entorhinal cortex is the major source of cortical input to the hippocampal formation (Witter et al., 1989; Amaral & Witter, 1989; Witter & Groenewegen, 1984), enhancements of synaptic strength in inputs to the

entorhinal cortex may also enhance the transmission of the sensory information to the hippocampus for further processing. Pyriform cortex inputs to the entorhinal cortex terminate in layer II (Van Hoesen & Pandya, 1975; Beckstead, 1977; Krettek & Price, 1977; Boeijinga et al., 1982; Luskin & Price, 1983; Room et al., 1984) which contains the cells of origin of the perforant path projection to the hippocampal formation. An enhanced capacity of pyriform efferents to excite layer II entorhinal cortex neurons is likely to result in a greater effect of pyriform cortex activity in the hippocampus. Enhancements of synaptic strength restricted to neurons which participate in a particular neuronal representation in the entorhinal cortex could result in the selective enhancement of the transmission of that representation to the hippocampus. Because the hippocampal formation is thought to contribute to the processing of multimodal representations (Squire & Zola-Morgan, 1991; Eichenbaum, 1992), synaptic modifications in the entorhinal cortex could enhance the access of particular olfactory inputs to mnemonic processing by the hippocampus.

While synaptic enhancement may play an important role in information processing and learning, it has also been suggested to contribute to propagation of epileptiform activity originating in the temporal lobe (Racine et al., 1975; Racine & Burnham, 1984; Russel & Stripling, 1985; Matsuura et al., 1993). Synaptic potentiation resulting from epileptiform activity has been most widely examined using the kindling model of epilepsy in which the repeated induction of seizure activity leads to a growth in both electrographic and behavioural manifestations of seizures (Goddard, 1967; Goddard et al., 1969). Kindling-induced potentiation of synaptic strength in the neuronal populations involved in the seizure are thought to occur in part because of the high levels of synaptic activation which occur during epileptiform activity (Racine et al., 1975).

The pyriform cortex is particularly susceptible to the induction and growth of electrically-induced seizure activity, and the development of strong bursting discharges (Racine et al., 1988; McIntyre & Plant, 1989; Stripling & Patneau, 1990; Haberly & Sutula, 1992; Teskey & Racine, 1993). Structures to which the pyriform cortex projects, then, are likely to be strongly activated during seizure activity in the pyriform cortex, and the strength of the projections enhanced.

Although enhancements in the strength of pyriform cortex efferents to the entorhinal cortex could contribute to the spread of seizure activity to the entorhinal cortex, the effect of pyriform cortex seizure activity on the strength of synaptic inputs to the entorhinal cortex is unknown. The induction of seizure activity in the entorhinal cortex by epileptogenic foci in the pyriform cortex could be significant for the progression of epileptic activity because of the role the entorhinal cortex is thought to play with the hippocampus in maintaining seizure activity (Stringer & Lothman, 1992; Spencer & Spencer, 1994).

Neither kindling-induced potentiation in the pyriform cortex inputs to the entorhinal cortex nor reliable LTP effects in this pathway have been demonstrated previously in the chronic preparation. LTP effects have been observed, however, in both the isolated, perfused whole guinea-pig brain *in vitro* (Alonso et al., 1990; de Curtis & Llinas, 1993), and in the *in vitro* rat entorhinal cortex slice preparation (Alonso et al., 1990). The mechanical stability of these experimental preparations has allowed intracellular recordings of activity in entorhinal cortex neurons to be made, and has provided some insights into the cellular mechanisms which mediate LTP induction in this pathway.

Two patterns of stimulation have been used to induced LTP in the rat entorhinal cortex slice preparation: 1) bursts of high-frequency trains delivered at 5 Hz for 10 to 20 sec, and 2), 20 sec bursts of rhythmic, 10-20 mV post-

synaptic depolarizing current pulses delivered at 5 Hz. Both protocols, one caused by presynaptic stimulation and the other by direct postsynaptic activation, resulted in LTP effects, suggesting that both Hebbian and non-Hebbian LTP can be generated in the entorhinal cortex (Alonso et al., 1990). In both the perfused guinea-pig brain and the rat entorhinal cortex slice, the induction of LTP by stimulation of pyriform cortex efferents is blocked by the NMDA antagonist D-2-amino-5-phosphonovalerate (AP-5), and is therefore dependent on NMDA receptor activation. Further, in contrast to LTP effects in the hippocampal formation which are *expressed* via increased *non*-NMDA-receptor-mediated synaptic currents (Zalutsky & Nicoll, 1990; McNaughton, 1993), both the induction *and* expression of entorhinal cortex LTP effects were largely blocked by NMDA receptor antagonism (Alonso et al., 1990; de Curtis & Llinas, 1993).

In the *in vitro* preparations mentioned above, LTP was observed to last at least 2 hr, but testing in animals with chronically-implanted electrodes is needed to determine if these effects are longer-lasting, and not dependent on experimental conditions peculiar to these *in vitro* preparations. A previous attempt to induce LTP in this pathway in chronically prepared rats using 8-pulse, 400 Hz stimulation trains resulted in LTP in only a minority of the 5 animals tested (Racine et al., 1983). The LTP observed in the *in vitro* guinea-pig brain may have depended to some extent on the highly-artificial nature of this preparation (de Curtis et al., 1991, 1994). Conditions in the slice chamber are even more artificial because of the elimination of neuromodulatory inputs to the entorhinal cortex which may affect LTP induction. In addition, the investigators included picrotoxin in the bathing medium to reduce GABA_A-mediated inhibition (Alonso et al., 1990). Anti-inhibitory agents have also been used routinely in the

study of neocortical LTP effects *in vitro* (Artola & Singer, 1987; Kirkwood & Bear, 1994), but the neocortex of the awake adult rat, in which neuromodulatory and inhibitory mechanisms are intact, is strongly resistant to LTP induction in response to the stimulation parameters effective in the slice (Racine et al., 1994). Further, because the entorhinal cortex slice does not include pyriform cortex tissue, the synaptic induction of LTP has required placement of the stimulation electrode 0.5 mm from the recording site, so that inputs other than those arising from the pyriform cortex may also have been activated (Alonso et al., 1990).

In Chapter 2 of this thesis, current source density analysis was used to localize the synaptic generators of current sinks in the rat entorhinal cortex evoked by both pyriform cortex and medial septal stimulation. It was found that activation of either the pyriform cortex or medial septum resulted in field potentials generated by synaptic currents in the superficial layers of the entorhinal cortex. These results allow field potentials recorded from single cortical depths in chronically-prepared rats to be interpreted to result from synaptic activation in the superficial layers following pyriform cortex or medial septal stimulation. In the present study, changes in the amplitude of evoked field potentials in the entorhinal cortex were used to study activation-induced long-term changes in the efficacy of synaptic inputs from the pyriform cortex to the entorhinal cortex. Some of these results have been presented previously in abstract form (Chapman & Racine, 1994, 1995b).

In the first experiment, the effect of pyriform cortex kindling on field potentials evoked by pyriform cortex test-pulses was examined in order to determine if pyriform cortex kindling is associated with enhanced connectivity between these cortical sites. A series of experiments employing brief, high-frequency stimulation of the pyriform cortex was then conducted to determine if

LTP in this pathway can be reliably induced in the awake rat, and to explore the potential effects of frequency potentiating stimuli on LTP induction in the entorhinal cortex. In a third experiment, the effect of medial septal stimulation in cooperatively enhancing LTP in pyriform cortex efferents was assessed by delivering high-frequency trains to the pyriform cortex immediately following theta-frequency stimulation of the medial septum.

EXPERIMENT 4.1

KINDLING-INDUCED POTENTIATION OF SYNAPTIC INPUTS FROM THE PYRIFORM CORTEX TO THE ENTORHINAL CORTEX

Kindling is a progressive enhancement in behavioural and electrographic seizure activity which results from the repeated induction of initially subconvulsive seizure states (Goddard, 1969). Kindling effects are usually induced by the repeated (usually daily) delivery of intense, low-frequency (about 60 Hz) stimulation to specific regions of the brain of animals with chronically implanted electrodes. Days to weeks of daily kindling stimulation are usually required to induce fully-generalized behavioural seizures, and the fastest rates of kindling are observed following temporal lobe stimulation (Racine, 1978; Racine & Burnham, 1984).

During kindling-induced afterdischarges, electrographic recordings of field activity from indwelling electrodes reflect the synchronous, rhythmic discharge of large numbers of neurons which are similar to recordings obtained from human epileptic patients (Goddard, 1969; Duckrow & Spencer, 1992). The highly synchronous neuronal discharges are expressed electrographically as spike-like events in the EEG, and the afterdischarge is usually followed by a period of flattened EEG reflecting a period of reduced neuronal activity. Over the course of kindling, current thresholds for seizure induction are reduced, and the duration of afterdischarges, and the frequency and amplitude of spiking activity, are increased (Racine, 1972a&b). In addition to increased afterdischarge activity in the kindled site as kindling progresses, neuronal

populations in related brain sites also begin to participate in the afterdischarge and show enhanced epileptiform responses (Racine, 1972a&b). The generation of the afterdischarge appears to be critical for the development of kindling since repeated electrical stimulation which is subthreshold for seizure induction has little effect on the subsequent rate of kindling in response to suprathreshold stimulation (Racine, 1972a; Racine et al., 1975).

Behavioural seizure activity during the first few afterdischarges may be absent, but convulsive responses appear and are strengthened with repeated stimulation. The initial behavioural manifestations of kindling include immobility, and rhythmic movements of the mouth or vibrissae. With repeated stimulation convulsive activity is increased and fully generalized clonic seizures occur (Racine, 1972b). A similar progression of behavioural seizure activity is observed during kindling of many brain sites in the temporal lobe, suggesting that common motor systems become recruited into the afterdischarges induced by stimulating these sites (Racine, 1972b).

While the kindling phenomenon is most widely studied as an animal model of neuronal changes associated with human temporal lobe epilepsy (Racine & Burnham, 1984; Sato et al., 1990), it is also of interest with regard to the neural mechanisms of learning and memory (Racine & Cain, 1991). The progressive recruitment of neuronal populations in separate areas of the brain into kindled afterdischarges, although clearly pathological, is more akin to the general cell assembly concept put forth by Hebb (1949) than are the monosynaptic long-term potentiation (LTP) effects commonly used to study the hypothesized basis of cell assembly formation. Kindling is also attractive as a model for memory because it has often been associated with long-lasting increases in synaptic efficacy in efferent pathways of the kindled site (Racine et

al., 1972, 1975; Russel & Stripling, 1985; Sutula & Steward, 1986; Racine & Cain, 1991; Racine et al., 1995a). An interesting difference between LTP effects and kindling-induced potentiation is that kindling-induced potentiation effects can last much longer (de Jonge & Racine, 1987; Racine et al., 1983; Racine et al., 1991a), consistent with the notion that mechanisms activated by kindling could contribute to long-term memory formation (Racine & Cain, 1991). Further, a much smaller number of stimulations is required to induce a maximal seizure even after months of delay following the initial kindling (Racine et al., 1972), again suggesting that kindling induces extremely long-lasting neuronal changes.

While brainstem and neocortical sites show slow advancements in afterdischarge duration during kindling, temporal lobe cortical areas including the amygdala, perirhinal cortex, and pyriform cortex show rapid increases in behavioural and electrographic responses (Goddard, 1969; Racine, 1975). The olfactory bulb, pyriform cortex and perirhinal cortex show the most rapid kindling rates, and the pyriform cortex is an important locus for the generation of spontaneous epileptiform interictal spikes (Cain, 1977; Racine et al., 1988; McIntyre & Plant, 1989; McIntyre & Kelly, 1990). The involvement of pyriform cortex associational fibers in the kindled afterdischarge (Stripling & Patneau, 1990), and reduced levels of intrinsic inhibition (Haberly & Sutula, 1992), are thought to contribute to the rapid advancement of pyriform cortex kindling.

Although kindling-induced potentiation in the projection from the olfactory bulb to the pyriform cortex has received considerable study (Russel & Stripling, 1985; Racine et al., 1991a), the effect of pyriform cortex kindling on synaptic plasticity in the entorhinal cortex has not been examined. The induction of a single afterdischarge in the pyriform cortex by olfactory bulb

stimulation results in an enhancement of the population EPSP in the pyriform cortex resulting from olfactory bulb test-pulses (Russel & Stripling, 1985), and enhancements resulting from 12 afterdischarges last at least 3 months (Racine et al., 1991a). Synaptic enhancements in the pyriform cortex projection to the entorhinal cortex could contribute to the spread of seizure activity to the entorhinal cortex, and could also affect non-ictal neuronal transmission. In the present study, field potentials in the entorhinal cortex were recorded in response to test-pulses delivered to the pyriform cortex in order to determine the effect of pyriform cortex kindling on synaptic strength in the pyriform cortex efferents to the entorhinal cortex. Field potentials were monitored up to 3 weeks after the start of a rapid kindling procedure in which animals received three daily kindling stimulations.

METHODS

Design. Evoked potentials in the entorhinal cortex evoked by pyriform cortex test-pulses were recorded every two days over a five day baseline period. Ten animals were matched for field potential amplitude and morphology and randomly assigned to a control or a kindling group. A rapid kindling procedure, in which three kindling stimulations per day were delivered to the pyriform cortex until two consecutive stage 5 seizures were observed, began on the day after the last baseline evoked potentials were recorded. Animals required 5 or 6 days to reach this criterion. Evoked potentials were recorded before the second and fourth daily sets of kindling stimulations were delivered, and again on the day after animals had reached criterion. Control animals were run on an analogous schedule, but did not receive kindling stimulation. Evoked potentials were then

recorded every 2 days over the next week, and again, one week later. The general materials and methods used for surgery, stimulation, recording, and histology in this experiment were similar to those described in Chapter 3.

Surgery. Electrodes were chronically implanted in the pyriform cortex (AP-3.6mm; L6.4mm; V8.5-10mm), and the entorhinal cortex (AP-8.8mm; L5.0mm; V 8.5-9 mm). The vertical tip separation of the bipolar electrodes was 0.5 mm for both sites. A two week recovery period preceded further testing.

Evoked Potential Testing. On each evoked potential testing day, ten evoked field potentials were recorded in the entorhinal cortex and averaged for each of 10 pyriform cortex test-pulse intensities. The interpulse interval was 10 sec. The intensities of the 0.1 msec biphasic square wave pulses were set to 16, 32, 63, 100, 159, 251, 501, 794, 1000 and 1259 μA and field potentials in the entorhinal cortex were recorded monopolarly with reference to ground.

The peak amplitudes of averaged field potentials were measured and used for subsequent analysis. The magnitude of kindling-induced changes in evoked potential amplitudes was assessed by standardizing the values to the amplitude of the response evoked by the highest stimulus intensity during the last baseline test day. Standardized response amplitudes, averaged across animals, were plotted as a function of stimulus intensity to generate input/output (I/O) curves for both groups before and after the kindling procedure. Statistical analysis was performed using a mixed design repeated measures analysis of variance (ANOVA) to evaluate changes in the I/O curves before and after kindling. An ANOVA was also used to assess the decay of the potentiation effect, measured by the mean responses to the two highest stimulus intensities delivered during the I/O tests.

Kindling. Piriform cortex kindling stimulations were 1.0 sec, 60 Hz trains of 600 μ A, 1.0 msec biphasic square wave pulses. Electrographic seizure activity was recorded from both cortical sites on chart paper (15 mm/sec), and the durations of the afterdischarges were measured. Between 1.5 to 3.0 hr separated the induction of consecutive seizures on the same day. Behavioural seizure activity during the afterdischarge was rated on a 5 point scale commonly used to rate the behavioural manifestations of subcortical kindling stimulation (Racine, 1972*b*). Stage 1 of this scale is characterized by mouth and facial movements, stage 2 by head nodding, stage 3 by unilateral or bilateral forelimb clonus, stage 4 by clonic rearing, and stage 5 by rearing and loss of postural control or hindlimb clonus.

RESULTS

Histology. The positions of stimulating and recording electrode tips are indicated in Figure 4.1. Tips of the piriform cortex stimulating electrodes were located near layer II of the piriform cortex and the tips of the entorhinal cortex electrodes were all located within the superficial layers of the entorhinal cortex.

Kindling. The intensity of behavioural seizures progressed during the course of kindling stimulation. Following the first kindling stimulation one animal had a stage 1 seizure and one animal had a stage 2 seizure, but the other three animals showed no behavioural signs of seizure activity. There was no behavioural progression of seizure activity across the 5-point scale during the first day except in one animal who showed a stage 1 seizure after the 3 stimulations. After 2 days of kindling (6 stimulations) three animals had reached

stage 1, and 2 animals had reached stage 2. After 3 days of kindling (9 stimulations) three animals had reached stage 2, and two animals had reached stage 4. Between 13 and 18 stimulations were required to reach the criterion of two consecutive stage 5 seizures in all animals (mean = 15.4 stimulations).

Afterdischarge recordings showed an increase in the amplitude of rhythmic epileptiform spiking during the course of kindling. The occurrence of smaller spike-like events, superimposed on the dominant spiking activity at a frequency of about 4 to 5 Hz, also became more common, contributing to a more complex afterdischarge morphology. Afterdischarge durations were the same in both recording sites during all seizures with only few minor exceptions. On the first day of kindling mean afterdischarge duration increased on average only minimally from 11.8 sec after the first kindling stimulation (range = 11 to 13), to 13.4 sec after the third stimulation (range = 9 to 20). After 2 days of kindling mean afterdischarge duration roughly tripled to 34 sec (range = 17 to 52 sec). Although seizure duration increased only minimally from 49 sec after 3 days of kindling (range = 35 to 73), to 54 sec after two stage 5 seizures (range = 40 to 94), there were marked increases in the amplitude and complexity of the discharges.

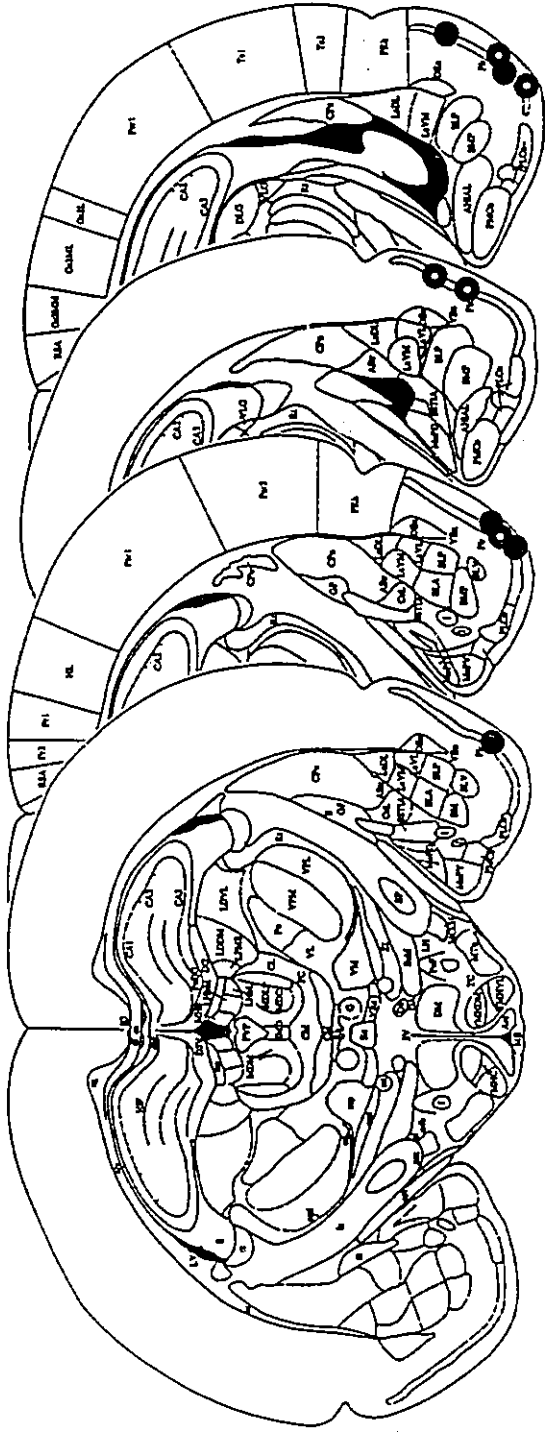
Evoked Potentials. The field potentials evoked in the entorhinal cortex by pyriform cortex test-pulses were similar in latency and morphology to those observed previously in chronically prepared rats (Figure 3.2 left), and are consistent with synaptic activation of dendrites of layer II neurons in the entorhinal cortex (Figure 2.8). The major field potential component was a negative deflection with an onset latency between 7 and 13 msec, and a peak amplitude near 0.5 mV during baseline with 1259 μ A test-pulses. Current thresholds for measurable responses were between 250 and 500 μ A.

The amplitude of the field potentials increased in all animals in the kindling group. Increases in the evoked potentials of kindled animals occurred both during the rising phase of the field potential, and at longer latencies. Figure 4.2 (right panel) shows examples of field potentials in a kindled animal in which enhancements at longer latencies were particularly distinct. Increases in the peak amplitude of evoked potentials with test-pulse intensity were associated with the enhancements at longer latencies. While the I/O curves in the control group were relatively stable, kindling stimulation resulted in strong enhancements in response amplitude at all suprathreshold test-pulse intensities (Figure 4.3). This was reflected in a significant group by pre/post treatment interaction ($F=16.17$, $p<0.01$).

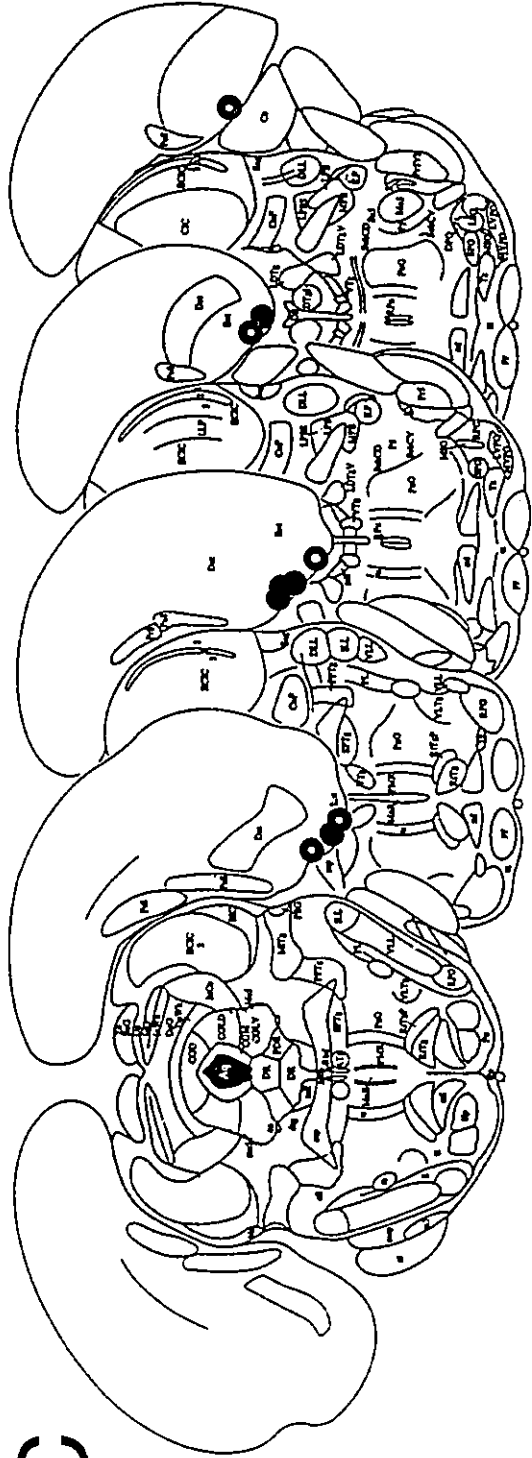
The amplitude of the responses to the two highest pulse intensities used in I/O tests was averaged for each animal and standardized to the average for the last baseline day to provide a measure of the amplitude of the field potentials over the course of the experiment. These pulse intensities resulted in close to asymptotic responses in all animals, and there was a significant group by days interaction ($F=4.07$, $p<0.001$). Although there was considerable variability in mean evoked potential amplitudes in the control group over the course of the experiment, there was no systematic increase over 26 days of testing (Figure 4.4 top). Baseline field potential amplitudes were more stable in the kindled group, and all animals in the kindled group showed large increases in field potential amplitude after only 3 kindling stimulations. An additional increment was observed after 9 kindling stimulations but further enhancements did not result from continued kindling. Decay of the evoked potential amplitudes occurred 3 and 5 days after the completion of the kindling procedure, but mean evoked potential amplitudes remained at potentiated values for the remainder of the testing period (Figure 4.4 bottom).

Figure 4.1

Figure 4.1. The locations of electrodes in the pyriform cortex (**PY**) and the entorhinal cortex (**EC**), are shown on representative coronal sections taken from the atlas of Paxinos and Watson (1986). **Open circles** indicate electrode positions for animals in the control group, and **closed circles** for animals in the kindling group.



PY



EC

Figure 4.2

Figure 4.2. Examples of field potentials in the entorhinal cortex evoked by pyriform cortex stimulation at the indicated pulse intensities are shown for a control and a kindled animal. Field potentials recorded on the day following the completion of the kindling protocol, and at the corresponding time for the control animal (**dashed traces**), are superimposed on field potentials recorded on the last baseline day (**solid traces**). Negativity is upward in this and all subsequent figures. Horizontal calibration, 10 msec; vertical calibration, 1.0 mV.

CONTROL

KINDLED

1259 μA

1000 μA

794 μA

501 μA

251 μA

159 μA

100 μA

63 μA

32 μA

16 μA

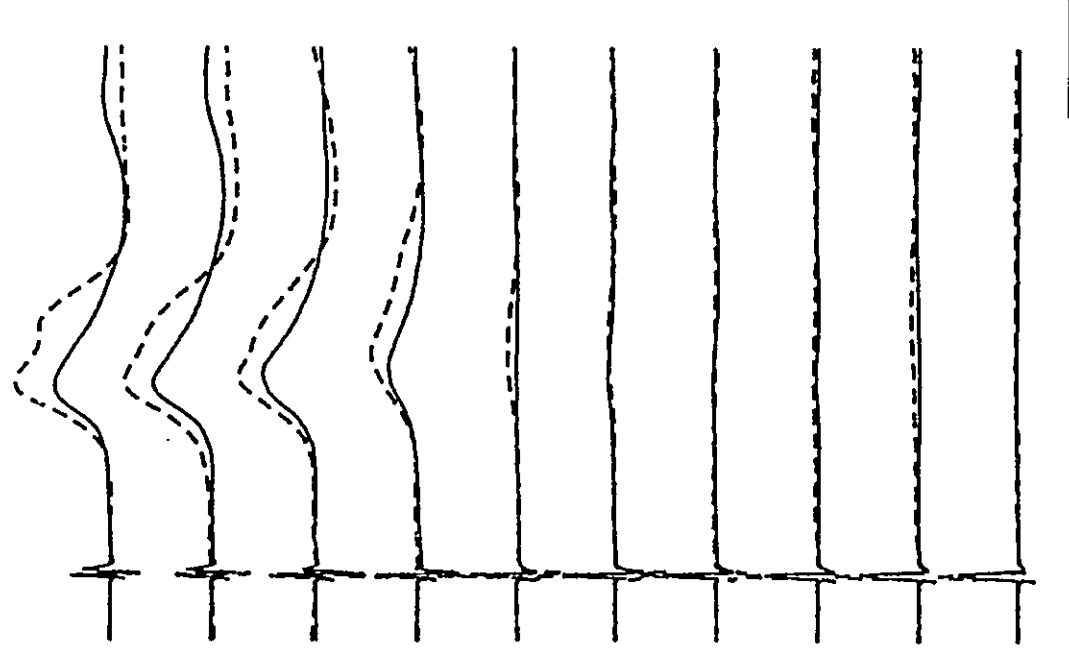


Figure 4.3

Figure 4.3. Mean evoked potential peak amplitude for the control and kindled groups is shown as a function of stimulus intensity one day before (**Pre**) and one day after (**Post**) either a control period or a 5-day kindling period. Response amplitudes were enhanced in the kindled group on the day after the last kindling stimulation. Data have been standardized to the amplitude of the response to the highest test-pulse intensity on the last baseline day. Bars indicate twice the standard error of the mean in this and all subsequent figures.

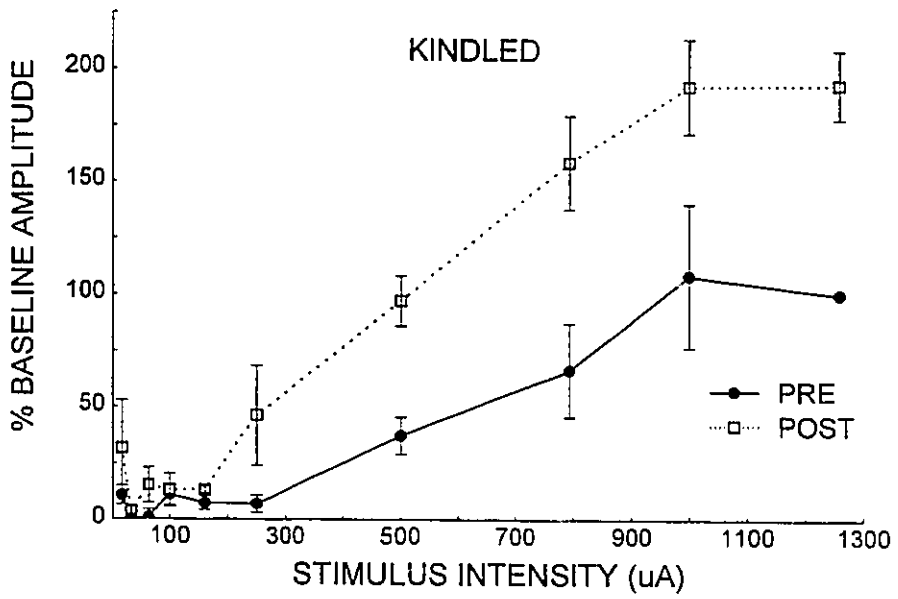
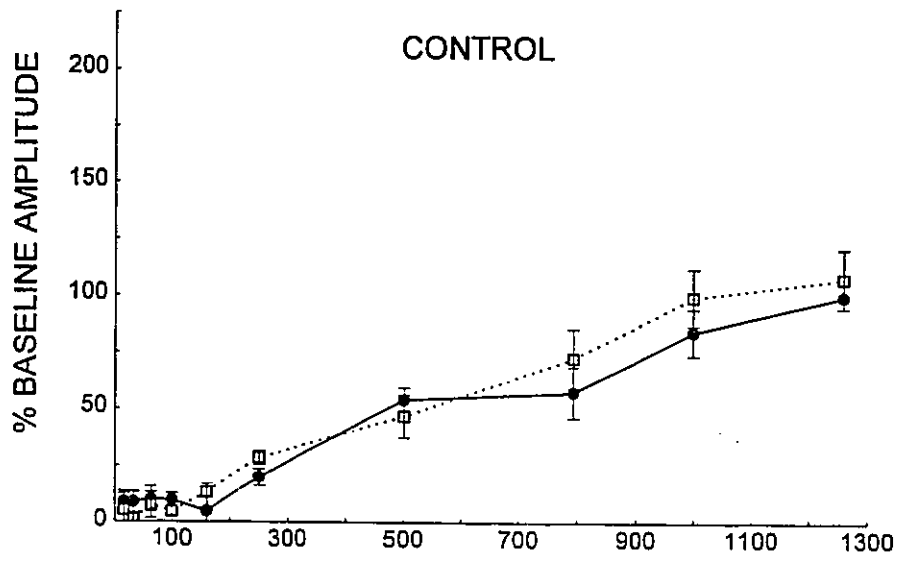
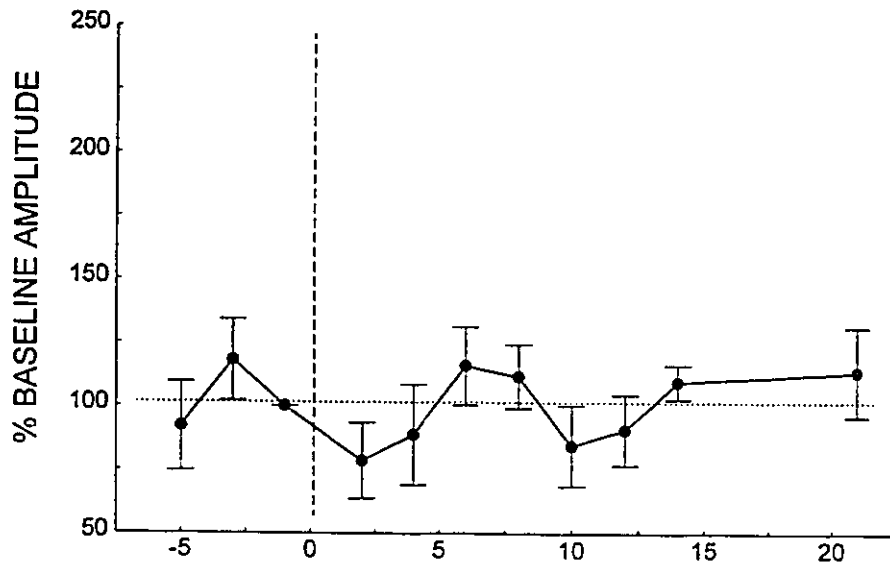


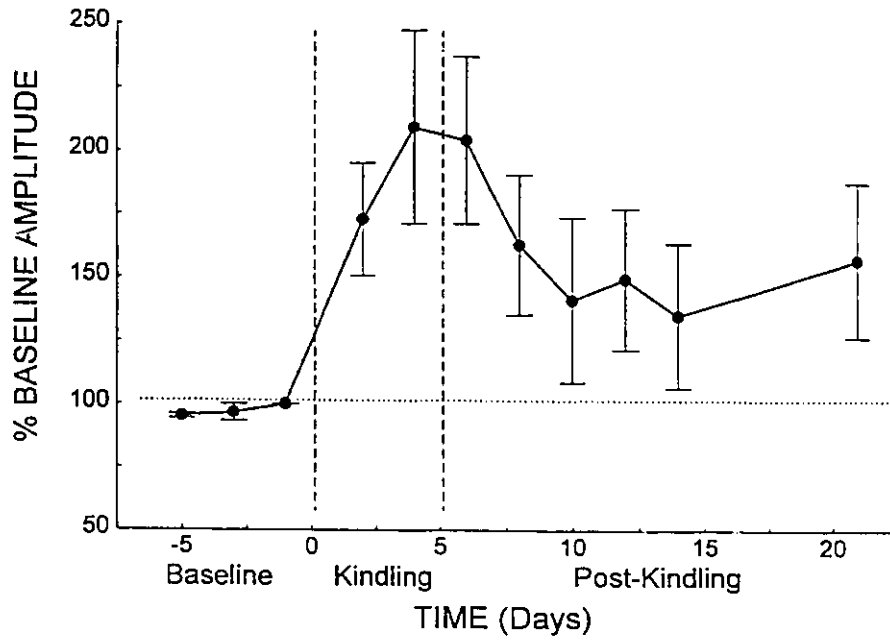
Figure 4.4

Figure 4.4. Mean evoked potential amplitudes are shown as a function of days after the start of the kindling period for the control and kindled groups. The responses to the two highest test-pulse intensities during input/output test were averaged, and the data were standardized to the results for the last baseline day. Evoked potentials recorded on the second and fourth days of kindling were recorded before administering kindling stimulation, and therefore reflect the maintained effects of the three, and nine kindling stimulations, respectively. In the lower panel, data for day six, recorded one day after animals had displayed 2 consecutive stage 5 seizures, include data from all animals irrespective of whether they required 5 or 6 days to reach this criterion.

CONTROL



KINDLED



DISCUSSION

Kindling stimulation delivered to the pyriform cortex resulted in afterdischarges in both the pyriform cortex and the entorhinal cortex, and also resulted in large increases in entorhinal cortex field potentials evoked by test-pulses delivered to the pyriform cortex. Both early and late portions of the field potentials were enhanced, and the peak amplitudes were doubled after 9 kindling stimulations (Figures 4.2 & 4.3). The field potentials shown here are generated by synaptic currents in the entorhinal cortex following activation of the monosynaptic pathway from the pyriform cortex to synaptic termination fields in layers I and II (Chapter 2; Beckstead, 1978; Krettek & Price, 1977; Luskin & Price, 1983; Room et al., 1984; Boeijinga et al., 1982). The increased field potentials therefore indicate that pyriform cortex kindling results in a long-term enhancement of the monosynaptically-evoked responses of neurons in the superficial layers of the entorhinal cortex, primarily neurons in layer II. Most of the enhancement in evoked potential amplitude decayed over a 5 day period after the completion of the kindling procedure but enhancements were maintained on average over the course of the 16 day testing period. Lasting enhancements of mean evoked potential amplitude of roughly the same magnitude have been observed for even longer periods in the pyriform cortex in response to olfactory bulb kindling (Racine et al., 1991a).

The growth of kindling-induced potentiation effects was not closely linked to the growth in the magnitude of the afterdischarges induced by kindling. Large enhancements in evoked field potentials were observed on the day after the first day of kindling, but there was only minimal progression in behavioural seizure activity and afterdischarge amplitude and duration, over the

course of these first three stimulations. Further, while kindling beyond the third day resulted in no further field potential enhancements (Figure 4.4), the duration and amplitude of afterdischarges in the pyriform and entorhinal cortices increased, and behavioural seizure activity became more intense. Therefore, the strength of the monosynaptic connection from the pyriform cortex to the entorhinal cortex was enhanced before there were marked increases in seizure activity. Also, seizure activity progressed both electrographically and behaviourally after the maximal enhancements in field potentials were observed.

These observations suggest kindling-induced potentiation effects in this pathway do not contribute substantially to the development of kindling-induced epileptiform activity in the entorhinal cortex. This is in accord with previous reviews suggesting that kindling-induced potentiation effects are not adequate alone as a kindling mechanism, partly because kindling effects have been observed in the absence of kindling-induced potentiation (Sato et al., 1990; Racine & Cain, 1991). The NMDA receptor appears to play an important role in entorhinal cortex seizure activity. Slices of rat entorhinal cortex maintained in a Mg^{2+} -free medium which removes the Mg^{2+} block of the NMDA receptor are particularly prone to seizure activity which is strongest in layers IV and V (Jones & Heinemann, 1988). Initially isolated seizure-like events occur, and later develop into recurrent tonic discharges. Both types of seizure activity are blocked by NMDA receptor antagonism with DL-2-amino-5-phosphonovalerate (2-AP5; Jones & Heinemann, 1988), while the recurrent seizures are insensitive to AMPA receptor antagonists (Jones & Heinemann, 1988; Heinemann et al., 1993). Blocking synaptic inhibition by GABA_A antagonism in the entorhinal cortex induces seizure activity, and seizures induced in this way can also be blocked by both NMDA and non-NMDA

receptor antagonists (Jones & Lambert, 1990). Increased bursting discharges, which are displayed by some deep entorhinal cortex cells (Heinemann et al., 1993) may also contribute to epileptogenesis.

The NMDA receptor, which is critical for the induction of long-term potentiation in the *in vitro* entorhinal cortex (Alonso et al., 1990, de Curtis et al., 1993), may also have contributed to the enhancements in field potentials observed here following kindling stimulations. In this study, kindling stimulation was delivered via the same pyriform cortex electrode used to deliver test-pulses during I/O testing so that NMDA receptor activation sufficient to result in synaptic enhancements could have occurred during the kindling stimulation itself, or during to the propagation of epileptiform activity during the afterdischarge. Depolarization of superficial neurons in the entorhinal cortex by intrinsic excitation in the entorhinal cortex and recurrent excitation from other structures involved in the afterdischarges (Stringer & Lothman, 1992; Heinemann et al., 1993; Spencer & Spencer, 1994) could also have induced heterosynaptic enhancements in the pyriform cortex inputs to the entorhinal cortex.

Kindling-induced potentiation effects were expressed in both early and late components of the field potentials, similar to long-latency enhancements in entorhinal cortex field potentials which follow amygdalar kindling (Matsuura et al., 1993). Alonso et al. (1990) found that the *expression* of LTP in the pyriform cortex projection to the rat entorhinal cortex *in vitro* was blocked by AP5, indicating that the response increments were primarily due to increased NMDA-receptor-mediated currents. Because activated NMDA-receptor channels close with a prolonged time-course, NMDA-receptor mediated Na^+ and Ca^{2+} currents may have contributed to the enhanced field potentials observed here. Unlike

the long-latency field potential correlate of NMDA receptor activation in the hippocampus which is induced by trains of pulses (Racine et al., 1991*b*), the enhancements in this study were induced by single test-pulses. Increased NMDA receptor responses to test-pulses could occur if the Mg^{2+} block was reduced by an alteration in resting membrane potential, or if fast, non-NMDA-mediated EPSPs were also potentiated, as is suggested by the enhanced early components in the field potentials (Figure 4.2).

The present results indicate that pyriform cortex stimulation which causes epileptiform activity in the pyriform and entorhinal cortices can lead to long-lasting increases in strength of synaptic connections from the pyriform cortex to the entorhinal cortex. In the following experiments, brief high-frequency stimuli were applied to the pyriform cortex to determine the effect of intense, non-epileptogenic stimuli on synaptic strength in this pathway. In addition, frequency potentiating stimulation of either the pyriform cortex or the medial septum was paired with the high-frequency trains to determine the possible effect of low-frequency activation of these structures on synaptic plasticity in this pathway.

EXPERIMENT 4.2

LONG-TERM POTENTIATION OF SYNAPTIC INPUTS FROM THE PYRIFORM CORTEX TO THE ENTORHINAL CORTEX

Because of the role the entorhinal cortex is thought to play in processes of learning and memory (Squire & Zola-Morgan, 1991), an animal model of synaptic plasticity in the entorhinal cortex of awake, behaving rats could contribute to the understanding of the neural mechanisms of learning and memory in the temporal lobe. The entorhinal cortex receives input from a variety of cortical areas (Van Hoesen et al., 1972; Van Hoesen & Pandya, 1975; Krettek & Price, 1977; Beckstead, 1978; Witter et al., 1989), and in turn, provides the major cortical input to the hippocampal formation (Witter et al., 1989; Amaral & Witter, 1989; Witter & Groenewegen, 1984). The perforant pathway has been thoroughly investigated and is known to support LTP, but plasticity in cortical efferents to the entorhinal cortex has not been investigated extensively in chronic preparations (Racine et al., 1983). The use of chronic preparations allows the determination of the durability of long-term potentiation (LTP) effects and of the potential effects of neuromodulatory systems on LTP under close to normal physiological conditions (Bliss & Gardner-Medwin, 1973; Racine & Milgram, 1983).

LTP effects in the pyriform cortex projection to the entorhinal cortex have been observed in both the isolated guinea-pig brain *in vitro* (Alonso et al., 1990; de Curtis & Llinas, 1993), and in the rat entorhinal cortex slice preparation (Alonso et al., 1990). In both preparations the induction and expression of LTP

effects were NMDA-dependent. In the rat entorhinal cortex slice, both Hebbian and non-Hebbian LTP may be induced either by stimulation of pyriform cortex afferents, or by rhythmic post-synaptic depolarization in the absence of induced cell firing (Alonso et al., 1990). A previous attempt to induce LTP in this pathway in chronically prepared rats showed potentiation only in a minority of the 5 rats tested (Racine et al., 1983). The apparent resistance of this pathway to the induction of LTP in awake animals may be due to the more normal operation of processes which mediate inhibition in the superficial layers of the entorhinal cortex (Jones, 1993; Jones & Heinemann, 1991; Colino & Fernandez de Molina, 1986; Finch & Babb, 1980; Finch et al., 1988). LTP in the entorhinal cortex slice was induced in the presence of picrotoxin to reduce GABA_A-mediated inhibition (Alonso et al., 1990). However, in the isolated guinea-pig brain (maintained at 32 °C), LTP was observed in the absence of anti-inhibitory agents, suggesting that LTP may be induced in this pathway in the presence of at least some intrinsic inhibitory activity (de Curtis et al., 1991; 1993).

Because inhibitory mechanisms in the awake rat at normal body temperature are likely to be more intact than in *in vitro* preparations, higher intensities of stimulation may be necessary in the chronic preparation to overcome inhibition which may impede LTP induction in this pathway. While the relatively strong series of trains used by Racine et al. (1983; 400 Hz, 8-pulse trains delivered once every 30 sec) were effective in a variety of other cortical and subcortical pathways, they were ineffective in inducing LTP in the projection from the pyriform cortex to the entorhinal cortex. In the present study, the effect of longer, 16-pulse, 400 Hz trains was assessed on LTP induction in chronically prepared rats.

Other temporal parameters of stimulation may also impact on LTP induction in the entorhinal cortex. In the *in vitro* studies, theta-frequency activation of pyriform cortex efferents was shown to be sufficient for inducing LTP in the pyriform cortex projection to the entorhinal cortex (Alonso et al., 1990, de Curtis & Llinas, 1993). Brief, 4-pulse 100 Hz trains were delivered at a train frequency of 5 or 7 Hz for up to 3 sec. The effectiveness of this stimulation pattern for LTP induction is interesting in light of the prominent spontaneous theta-band electroencephalographic (EEG) activity in the entorhinal cortex and hippocampal formation (Green & Arduini, 1954; Bland, 1986; Alonso & Garcia-Austt, 1987a), and because theta-frequency train delivery has also been found to be particularly effective in inducing LTP effects in the hippocampal formation (Larson et al., 1986; Staubli & Lynch, 1987; Greenstein et al., 1988).

Synaptic responses in the entorhinal cortex to single stimulation pulses delivered to the pyriform cortex in short, low-frequency 10-pulse trains were examined in Chapter 3. Theta-frequency stimulation resulted in frequency potentiation of synaptic responses in the entorhinal cortex, and higher frequencies near 16 Hz were even more effective. The results suggested that rhythmic activity in pyriform cortex efferents in the 8 to 18 Hz range may be particularly effective in exciting neurons in the entorhinal cortex. Further, the evoked potentials were enhanced at long latencies, consistent with the increased activation of NMDA-receptor-mediated currents (Flatman et al., 1983; Alonso et al., 1990; Racine et al., 1991b) which are necessary for LTP induction in this pathway (Alonso et al., 1990; de Curtis & Llinas, 1993). Although long-term enhancements in field potentials were not observed in response to the frequency potentiating stimuli, it was hypothesized that the NMDA-receptor-mediated currents induced by frequency potentiation might contribute to the induction of LTP when associated with more intense stimulation.

In a series of experiments described here, LTP effects in the pyriform cortex projection to the entorhinal cortex in conscious, behaving rats were examined. Because 8-pulse stimulation trains have been unreliable in the past in inducing LTP effects in this pathway (Racine et al., 1983), longer-duration trains were used in these experiments. Also examined were interactions between frequency potentiating stimuli and high-frequency stimuli in the induction of LTP. The objective was to determine if short-term frequency potentiation effects could enhance the LTP induced by high-frequency pyriform cortex stimulation. A procedure was used in which trains of high-frequency stimulation were first administered repeatedly until no further enhancements in responses to test-pulses were observed. After levels of LTP had saturated to the delivery of high-frequency trains, the same trains were then paired with 15 Hz stimulation of the pyriform cortex, and test-pulse responses were monitored for further increments in LTP.

METHODS

Surgery. The general materials and methods used for surgery, data acquisition and histology in this experiment were similar to those described in Chapter 3. Bipolar, teflon-coated stainless-steel twisted-wire electrodes (190 μ m exposed tip diameter) were implanted in the right pyriform cortex (posterior 3.6 mm, lateral 6.5 mm, and 8.5-10 mm ventral to bregma) and medial entorhinal cortex (posterior 8.8 mm and lateral 5.0 mm to bregma, and 0.1 to 0.2 mm above the skull). One tip of the bipolar stimulating electrode in the pyriform cortex was 0.5 mm longer than the other, and the tip separation of the entorhinal cortex recording electrode was 1.0 mm. The vertical placement of the

stimulating electrode was adjusted during surgery to minimize the current threshold for evoked field potentials in the entorhinal cortex. The vertical placement of the entorhinal cortex electrode was then adjusted slightly to maximize the amplitude of the field potentials. One skull screw placed above the contralateral frontal cortex served both as a ground electrode and as a reference electrode for monopolar recordings of entorhinal cortex field potentials.

Design. Evoked field potentials in the entorhinal cortex in response to pyriform cortex stimulation were recorded every 2 days over a 5 day baseline period in all animals. On the following day, multiple sets of trains of stimulation pulses were delivered to the pyriform cortex to induce LTP in the projection from the pyriform cortex to the entorhinal cortex. Test-pulse responses were recorded from the entorhinal cortex after the delivery of each set of trains to monitor the development of LTP effects. There were 5 animals in each of 3 groups. In each group, the stimulation trains consisted of either high-frequency 400 Hz trains, or 400 Hz trains combined with low-frequency, 15 Hz trains. Evoked potentials were recorded every two days over a 1 wk period beginning the day after LTP induction, and weekly thereafter for up to 10 weeks.

In the first group only high-frequency trains were delivered to the pyriform cortex. After at least a 10% enhancement in field potential amplitude was observed following train delivery, three more sets of trains of the same intensity were delivered to determine if there was a saturation of response increments for that train intensity. The intensity of the trains was then increased to determine if this would result in further response enhancements.

In the second and third groups, the effects of pairing low-frequency trains with 400 Hz stimulation of the pyriform cortex were assessed. In the first

experimental group, the effect of peak pyriform cortex frequency potentiation on LTP induction was assessed. Following the stable induction of LTP with high-frequency trains alone, 400 Hz trains were delivered in place of the 6th pulses in 15 Hz pyriform cortex frequency potentiating trains. Frequencies near 15 Hz result in maximal frequency potentiation effects in this pathway with no long-term effects on synaptic efficacy, and the effects reach near asymptotic levels by the 5th pulse (Figures 3.3 & 3.14 top). In the second experimental group, the high-frequency trains were delivered in place of the 2nd pulses in each 15 Hz train at a time when paired-pulse facilitation is observed but when frequency potentiation effects are still far from peak levels.

Evoked Potential Tests. On each of the baseline and follow-up testing days, 10 evoked field potentials were recorded in the entorhinal cortex and averaged for each of 10 pyriform cortex test-pulse intensities. The sets of ten pulses at each intensity were delivered in ascending order of intensity. The interpulse interval was 10 sec. The intensities of the 0.1 msec biphasic square wave pulses were set to 16, 32, 63, 100, 159, 251, 501, 794, 1000 and 1259 μ A and field potentials in the entorhinal cortex were recorded monopolarly.

Mean input/output (I/O) curves, showing response amplitude as a function of stimulus intensity, were compared between the days before and after LTP induction in each group. The peak amplitudes of evoked potentials during I/O tests were expressed as a proportion of the response to the highest test-pulse intensity recorded on the last baseline day.

LTP Induction. Animals were tested for LTP induction after habituation to the testing chamber while in a quiet, resting state. Responses to test-pulses which evoked responses roughly 50% of the asymptotic response during baseline I/O tests were used to monitor changes in field potential amplitude

within the period during which trains were delivered. The test-pulse intensities used ranged between 501 and 794 μA . Responses to each of 30 test-pulses were recorded during a baseline period, and again after each set of 10 stimulation trains. Within each series, test-pulses were delivered once every 20 seconds over a 10 min period.

Sets of 10 trains of 0.1 msec biphasic square wave pulses, with an inter-train interval of 60 sec, were delivered to induce LTP. High-frequency stimulation was delivered to the pyriform cortex, and consisted of 400 Hz trains of 16 pulses each (37.5 msec duration). Trains of 11 pulses at 15 Hz (667 msec duration) were applied to the pyriform cortex in two groups. Stimulation frequencies and the timing of train delivery were computer-controlled, and train-evoked responses were monitored on a digital oscilloscope. Frequency potentiation effects were observed in all animals in response to low-frequency stimulation, with some variability within animals in magnitude of the effects induced by each train. Field activity in the entorhinal cortex was recorded on chart paper during train delivery to confirm that epileptiform afterdischarges did not occur.

Following the baseline test-period, a set of high-frequency trains was delivered to the pyriform cortex using a pulse intensity shown to result in single pulse-evoked response amplitudes approximately 50% of asymptotic levels. Another series of test-pulses followed train delivery, and the amplitude of the average of the last 10 field potentials evoked was compared to corresponding amplitude observed during baseline testing. If the mean field potential amplitude was enhanced by at least 10 to 15%, a second set of high-frequency trains of the same intensity was delivered to determine if LTP had saturated for that train intensity. If further enhancements were apparent in subsequent test-

pulses, this process was repeated. If enhancements in field potential amplitude did not occur in response to the first set of trains, the intensity of the trains was increased by one increment on the logarithmic scale of test-pulse intensities used in the I/O tests. The intensity of the trains was increased in this way until enhancements in the field potentials were observed, after which trains were re-delivered at the same train intensity as described above to ensure that no further LTP was inducible at that train intensity. In two animals, response enhancements were not observed even in response to repeated delivery of trains at an intensity of 1259 μA . In these cases combined trains were then delivered as described below.

In the control group, the set of high-frequency trains was delivered twice more, separated by series of test-pulses. The train intensities used to show saturation in LTP in this group ranged from 501 to 1000 μA . Two more sets of high-frequency trains were then delivered at an intensity of 1259 μA to determine if the field potentials could be further enhanced by increasing the train intensity.

In the experimental groups, after saturation of LTP to high-frequency trains, two sets of combined high- and low-frequency trains were delivered to the pyriform cortex. Responses to test-pulses were recorded after each combined train set. The stimulation intensity used in the preceding set of high-frequency trains was also used for the combined trains. In one experimental group, 16-pulse, 400 Hz trains replaced the 6th pulse in 11-pulse, 15 Hz trains. In the other experimental group, 400 Hz trains replaced the 2nd pulses in the low-frequency trains.

Analysis. Evoked potential peak amplitudes were expressed as a percentage of the average response amplitude during the baseline period. The

amplitudes of each consecutive set of three responses were then averaged to provide 10 measures of responses amplitude for each of the 10 min testing periods. The data were averaged across animals within each group and the standard errors of the mean were calculated.

In order to compare the effects of the different LTP induction procedures, a repeated measures ANOVA was conducted on the mean peak amplitudes of responses to the last three test-pulses in three LTP induction phases. Mean responses at the end of the baseline period, after the second set of 400 Hz trains, and after the second set of combined trains (or increased-intensity trains in the control group) were analyzed. Separate ANOVAs were also used to analyze changes in the I/O curves, and the decay of LTP across days.

RESULTS

Histology. The spatial distributions of histologically-verified electrode tip locations in the pyriform cortex and entorhinal cortex are shown in Figure 4.5. The three groups showed a similar distribution of electrodes; stimulating electrodes were located near pyramidal cell soma in layer II of the pyriform cortex, and recording electrodes were positioned in the superficial layers of the ventromedial aspect of the medial entorhinal cortex.

LTP Induction. All animals showed enhancements in response amplitude during LTP induction procedures. There were two cases, however, in which the animals did not respond to delivery of 400 Hz trains at any intensity, but later showed lasting enhancements in responses after combined train delivery.

Once the train intensity was increased to a level which induced field potential enhancements, the degree of potentiation in the group which received only 400 Hz pyriform cortex stimulation remained stable even after delivery of 3 more sets of trains at the same intensity (Figure 4.6A). The average baseline response was 0.24 mV (range= 0.20 to 0.28 mV), and there was an average increase to 149% of baseline response amplitudes (range= 22 to 70%). The train intensities used to induce these initial potentiation effects ranged between 501 and 794 μA (mean=658 μA).

When the train intensities were increased to 1259 μA , however, only two animals showed further response enhancements, and the mean evoked response amplitude increased by only 8% to 157% of baseline amplitudes (Figure 4.6A). A matched samples student's *t*-test indicated no significant enhancement in the response amplitudes following the delivery of increased-intensity trains ($t=1.77$, $p=0.15$). Evoked responses recorded at the end of the three major phases of the LTP induction procedure are shown in Figure 4.7. For the control group (400 Hz only), field potentials recorded at the end of the baseline period, after repeated train delivery, and after the intensity of the trains was increased, are shown in the left panel. Field potential amplitudes were enhanced, but marked enhancements at longer latencies in the field potentials were only observed in one control animal.

In the group which received combined trains in which 400 Hz trains replaced the 6th pulse in the low-frequency trains, all but one animal showed enhanced field potentials after delivery of 400 Hz trains alone (Figure 4.7 middle). Considerable variability in mean test-pulse response amplitudes following the initial potentiation (Figure 4.6B) was due in part to a highly variable response in one animal. This animal, however showed increases in the mean of

test-pulse responses following train delivery similar to the other animals in this group. The average baseline response was 0.31 mV (range= 0.14 to 0.21 mV), and there was an average increase to 200% of baseline response amplitudes (range= 95 to 368%). Train intensities used to induce these initial potentiation effects ranged between 501 and 1259 μA (mean=870 μA). Following *combined* train delivery, test-pulse response amplitudes were increased in all animals to between 162 and 449% of baseline response levels (mean=298%; Figure 4.6B). These large increases tended to be expressed in response enhancements both during the rising and late phases of the field potentials (Figure 4.7 middle).

Enhancements in field potentials in response to high-frequency trains alone and in response to the later delivery of combined trains also occurred in the group in which 400 Hz trains replaced the 2nd pulse in the low-frequency trains. The average baseline response was 0.26 mV (range= 0.20 to 0.42 mV), and there was an average increase to 177% of baseline response amplitudes following delivery of high-frequency trains alone (range= 109 to 278%; Figure 4.6C; Figure 4.7 right). The train intensities used to induce these initial potentiation effects ranged between 501 and 1259 μA (mean=644 μA). Response enhancements following *combined* train delivery occurred in all animals in this group, but the enhancements were smaller on average than those observed when the 400 Hz train replaced the 6th pulse. Test-pulse response amplitudes were increased in all animals to between 136 and 352% of baseline levels (mean=245%; Figure 4.6C). Again, the increases tended to be expressed during both the early and late phases of the field potentials (Figure 4.7 right).

Statistical analysis of the changes in response amplitudes in the three groups during LTP induction indicated a significant interaction between the

phase of LTP induction and group ($F=3.74$, $p<0.05$). A post-hoc Newman-Keuls test indicated no significant differences between groups after saturation of LTP with 400 Hz trains alone. The amount of LTP induced in the experimental group in which 400 Hz trains replaced the 6th pulse in the 15 Hz trains, however, was significantly greater than the LTP induced in the other groups after either combined trains or after repeated delivery of high-frequency trains in the control group ($p<0.01$). The amount of LTP induced after combined trains in which 400 Hz trains replaced the 2nd pulses in the 15 Hz trains was statistically not significantly greater than that induced after repeated high-frequency train delivery in the control group ($p=0.052$).

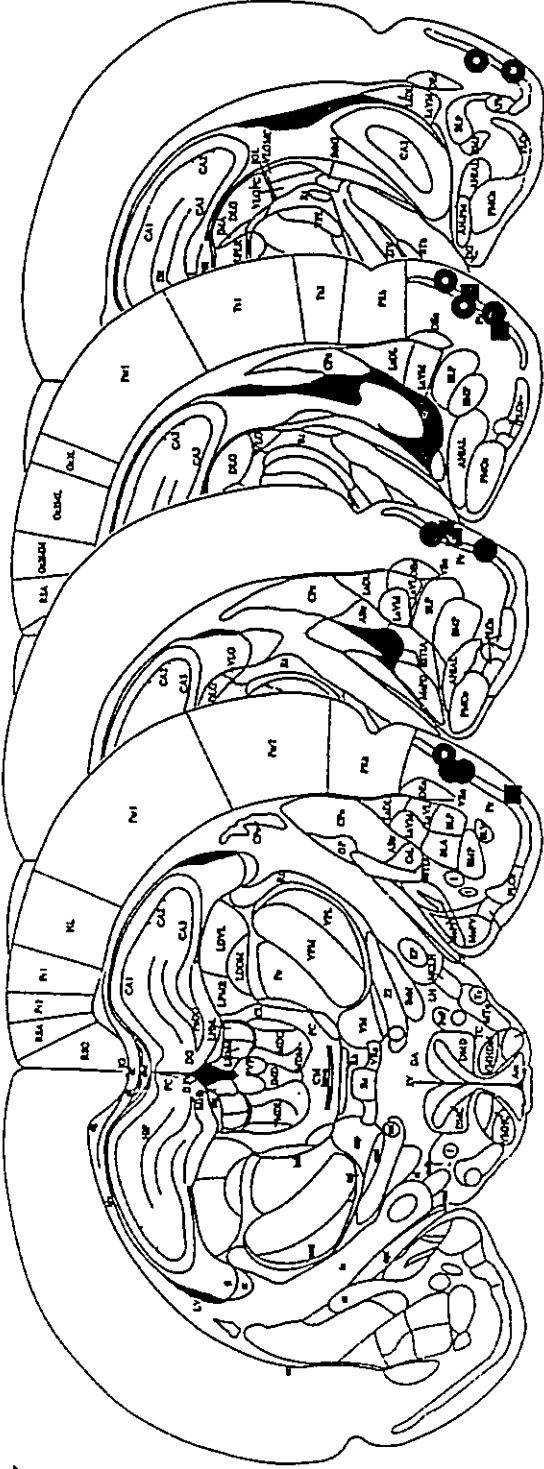
Input/Output Tests. The effects of LTP induction on the field potentials evoked by a range of stimulus intensities were assessed by comparing field potentials recorded during I/O testing on the last baseline day and on the day following LTP induction. Two examples are shown in Figure 4.8; one from the group in which only 400 Hz trains were delivered (left panel), and one from the group in which 400 Hz trains replaced the 6th pulses in the combined trains (right panel). Averaged I/O curves for the days before and after LTP induction show lasting enhancements in response amplitude at suprathreshold test-pulse intensities in all three groups (Figure 4.9). An ANOVA revealed a significant intensity by pre/post treatment effect ($F=11.24$, $p<0.001$), but there were no effects of group on the I/O measures.

The maintenance of the LTP effects in each group was assessed by plotting the mean evoked potential amplitudes in response to the test-pulse intensities used during LTP induction. While evoked potential amplitudes during the 5-day baseline period were stable, post-train responses were enhanced for a period of weeks in all groups (Figure 4.10). The curves for the

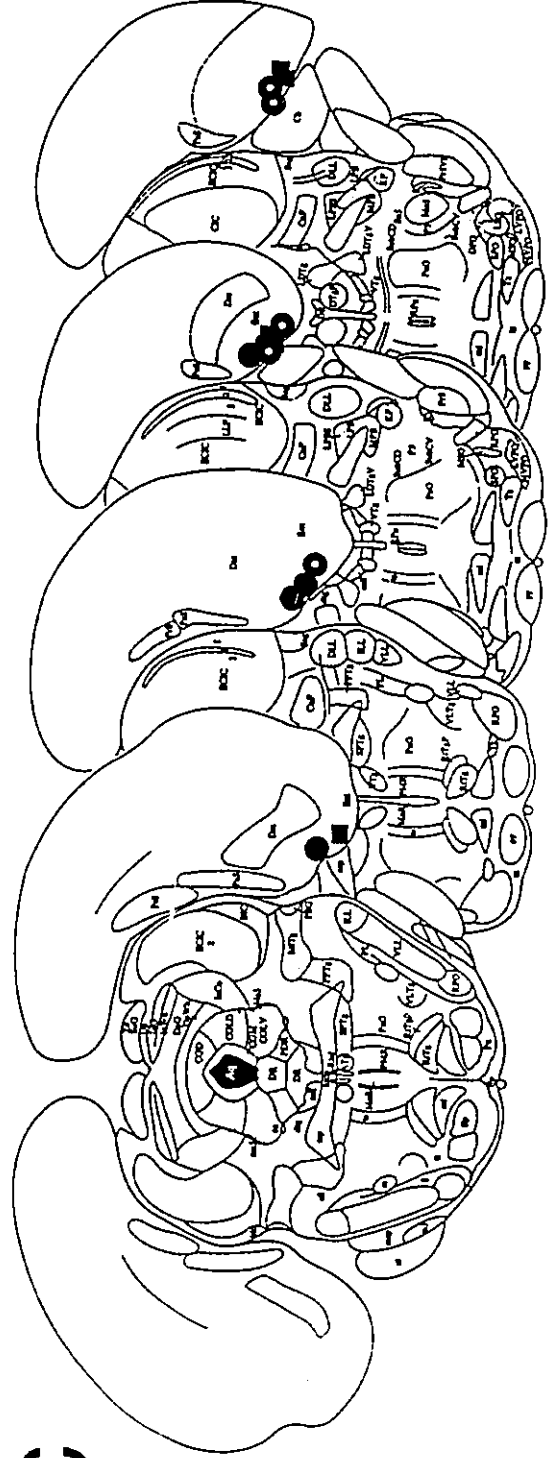
groups receiving combined train stimulation showed a greater amount of maintained LTP relative to the control group at these test-pulse intensities (Figures 4.9 & 4.10). Remarkably, in the group receiving combined trains in which the 400 Hz trains replaced the 6th pulse in the 15 Hz trains, there was no decay in response amplitude over a 10 week period (Figure 4.10B). Mean response amplitudes in the group receiving only 400 Hz trains returned to baseline values after 3 weeks of follow-up testing (Figure 4.10A). The primary objective of the third group was to contrast the amount of facilitation of LTP induced by trains when the 400 Hz trains replaced the 2nd rather than the 6th pulse in the frequency potentiating trains. Follow-up testing was not conducted for as long a period in this group, but this group also showed negligible decay of enhancement for up to two weeks post-treatment. Statistical analysis showed a significant group by days interaction between the control group and the group receiving 400 Hz trains as the 6th pulse ($F=2.60$, $p<0.05$). There was no significant group by days interaction for the two groups receiving combined train stimulations ($F=0.10$, $p=0.99$), indicating no significant difference between the lasting potentiation effects expressed in these two groups over the first two weeks post-treatment.

Figure 4.5

Figure 4.5. The locations of stimulating electrodes in the pyriform cortex (PY) and the entorhinal cortex (EC) are shown on representative coronal sections taken from the atlas of Paxinos and Watson (1986). Electrode positions are shown for groups of animals receiving 400 Hz stimulation either alone (**open circles**), or embedded as the 6th (**closed circles**), or as the 2nd (**closed squares**) pulse in 15 Hz stimulation trains.



PY



EC

Figure 4.6

Figure 4.6. The mean amplitudes of entorhinal cortex field responses evoked by pyriform cortex test-pulses during different phases of three LTP induction procedures are shown. Ten min periods, in which sets of stimulation trains were delivered to the pyriform cortex at the indicated frequencies, separated each of the 10 min testing periods shown. Thirty test-pulse responses were recorded during each 10 min testing period, and each point shown in the panels represents the group mean of the average of the amplitudes of three consecutively-recorded evoked potentials. Data are expressed as a percent of the average of the amplitudes of responses recorded during the baseline period. After the baseline period, sets of 400 Hz trains (**400**) were delivered repeatedly to the pyriform cortex until there was no further increment in response amplitude. Different animals required between 2 and 5 train deliveries to result in saturation, and the responses to the first two trains resulting in an asymptotic response increment for the 400 Hz trains are shown as occurring between the 10th and 30th min of testing. In **A**, two additional sets of 400 Hz trains were delivered to the pyriform cortex to confirm the saturation of the response enhancement. High-frequency trains at an increased intensity were then delivered. In **B** and **C**, sets of combined trains (**400+15**) were used in which 400 Hz trains replaced either the **6th pulse**, or the **2nd pulse** in 15 Hz trains.

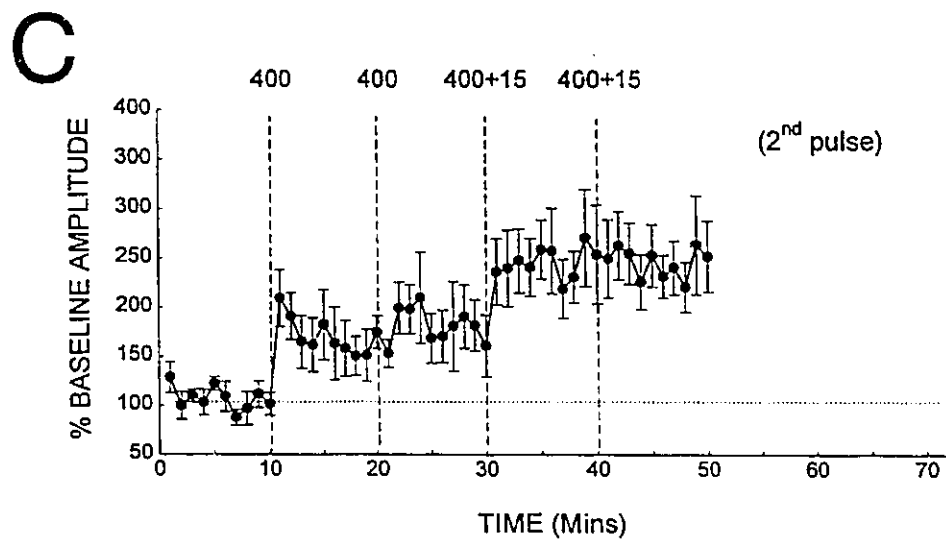
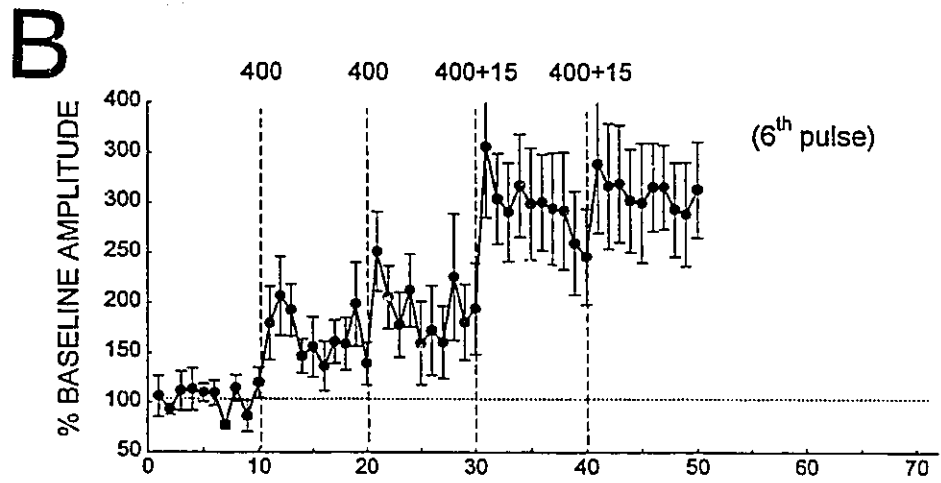
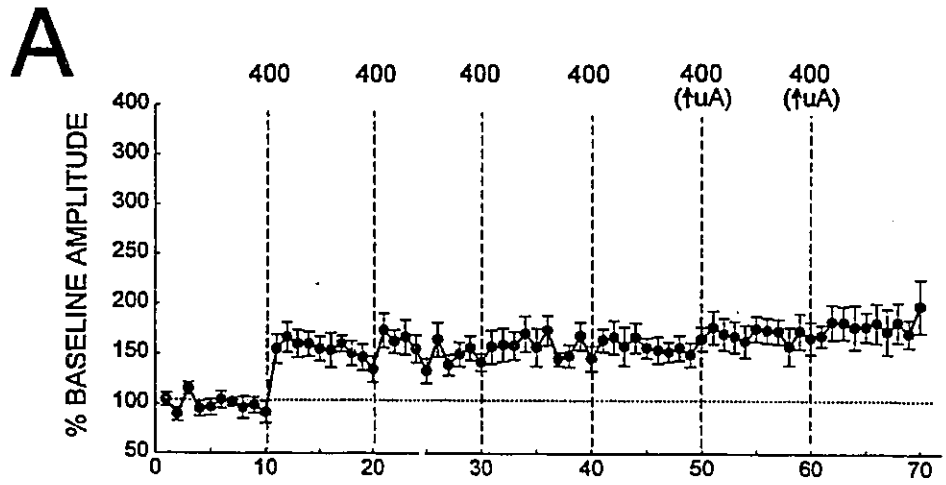
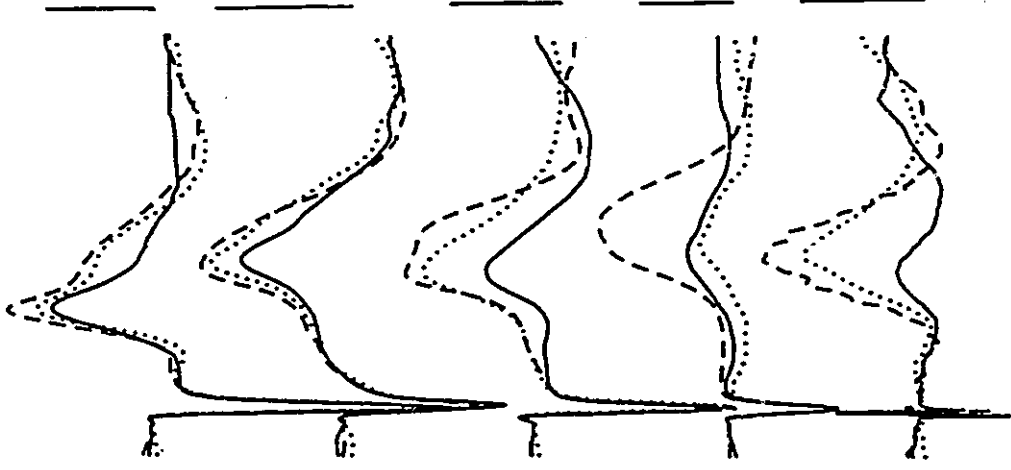


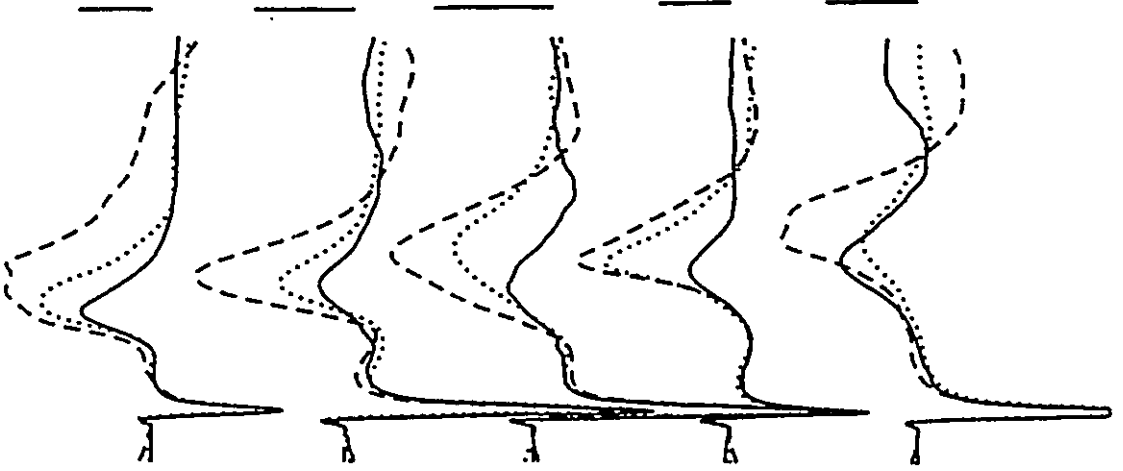
Figure 4.7

Figure 4.7. Averaged evoked potentials obtained during three different LTP induction procedures (**columns**) are shown for the five animals (**rows**) in each of three groups. All traces show the average of 10 field potentials in the entorhinal cortex evoked by pyriform cortex stimulation at the end of one phase of each test. **Solid traces** are the mean of potentials recorded at the end of 10 min baseline periods. **Dotted traces** are the mean of potentials recorded after repeated delivery of 400 Hz trains to the pyriform cortex. In the **left column**, **dashed traces** show recordings obtained after delivery of 400 Hz trains using an intensity higher than that initially required to induce a stable enhancement in the evoked potentials. In the **middle and right columns**, **dashed traces** show recordings obtained after delivering sets of combined 400 Hz and 15 Hz trains in which the 400 Hz train was embedded as either the 6th or as the 2nd pulse in the 15 Hz train. Field potential negativity is upward in this and all subsequent figures. Horizontal calibration, 10 msec; vertical calibration, 0.5 mV.

400Hz + 15Hz (2nd)



400Hz + 15Hz (6th)



400 Hz Only

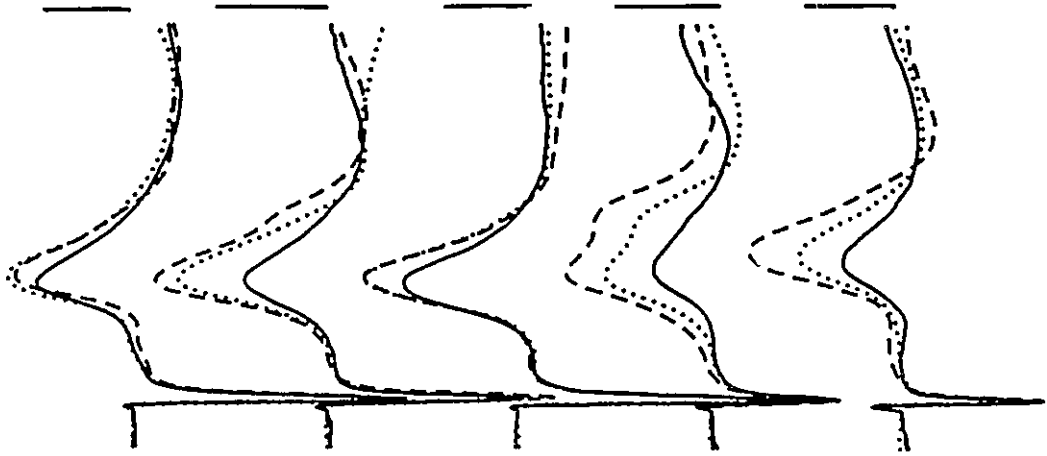


Figure 4.8

Figure 4.8. Two examples of field potentials in the entorhinal cortex evoked by pyriform cortex stimulation during input/output tests on the day before (**solid traces**), and the day after LTP induction (**dashed traces**). Test-pulse intensities are shown at left. Data from one animal receiving only 400 Hz trains (**A**), and from one animal receiving 400 Hz trains as the 6th pulse in a 15 Hz train (**B**) are shown. Horizontal calibration, 10 msec; vertical calibration 1.0 mV.

A

1259 μA

1000 μA

794 μA

501 μA

251 μA

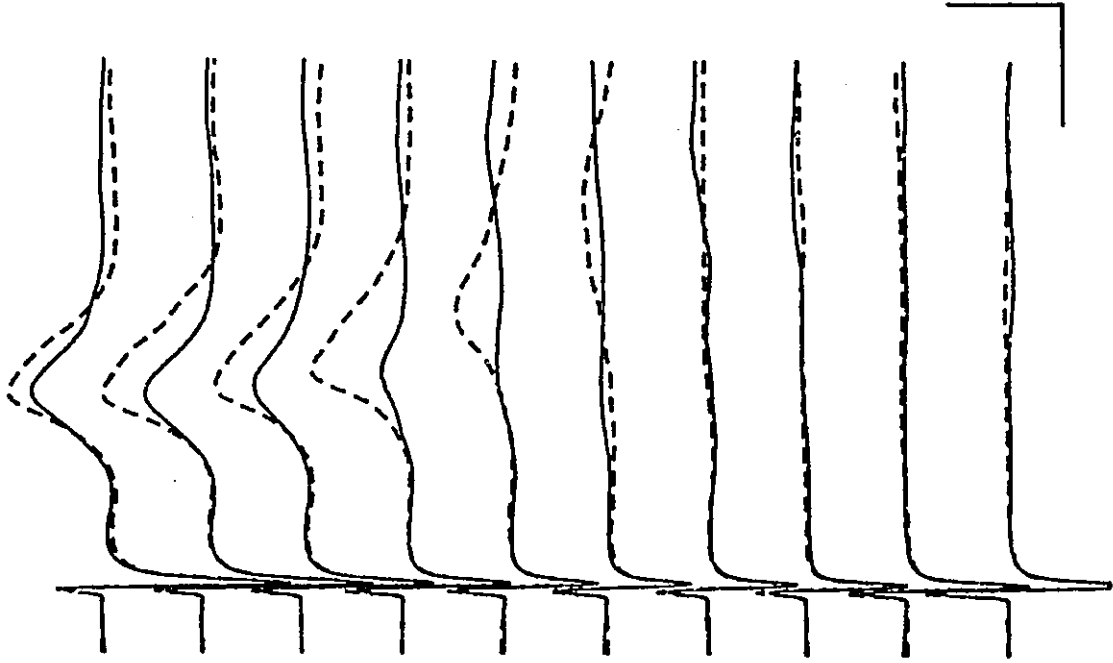
159 μA

100 μA

63 μA

32 μA

16 μA



B

Figure 4.9

Figure 4.9. Mean evoked potential peak amplitudes are shown as a function of stimulus intensity during I/O testing on the day before (**baseline**) and the day after (**post-LTP**) LTP induction. Data are shown for the group that received only high-frequency trains (**A**), and the groups that received 400 Hz trains as either the 6th (**B**), or the 2nd (**C**), pulse in the 15 Hz trains when combined trains were delivered. Data have been standardized to the peak amplitude of the response to the highest intensity response on the last baseline day.

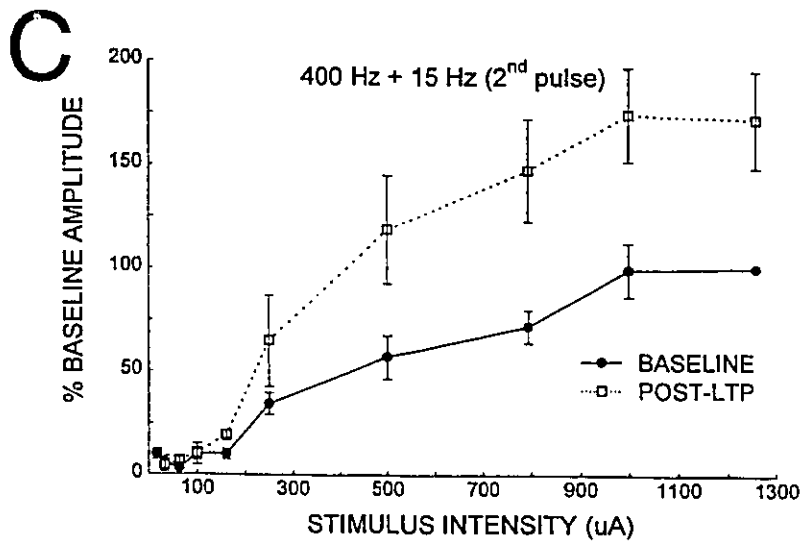
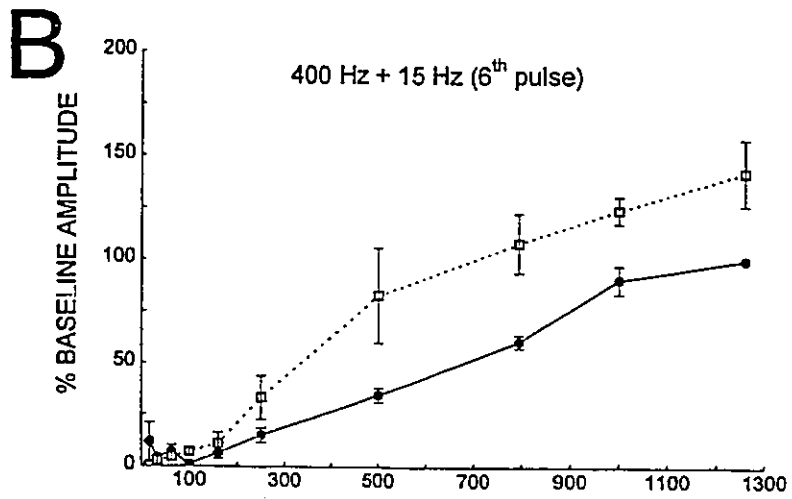
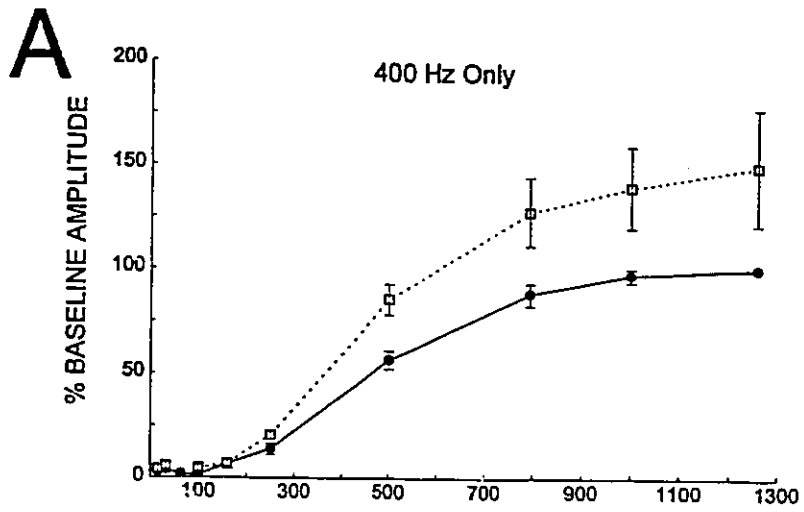
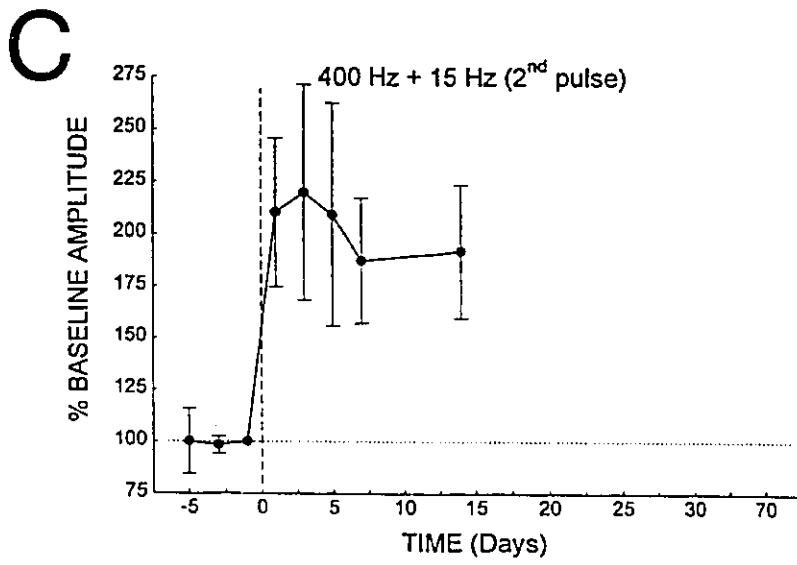
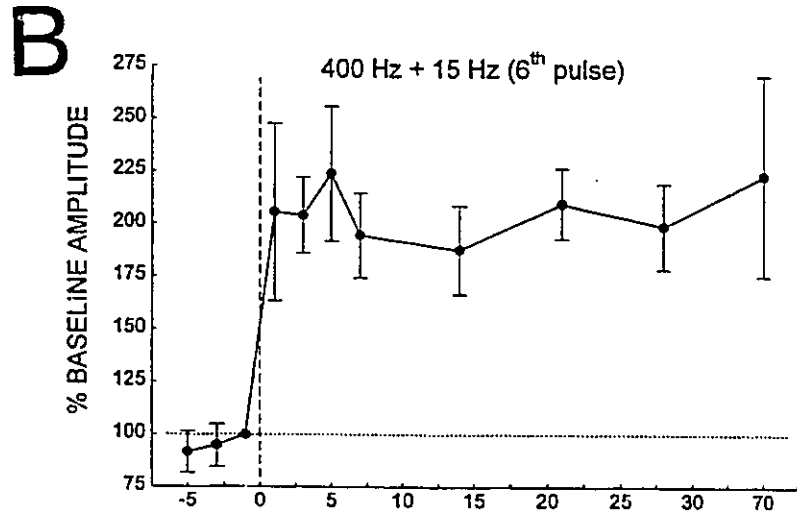
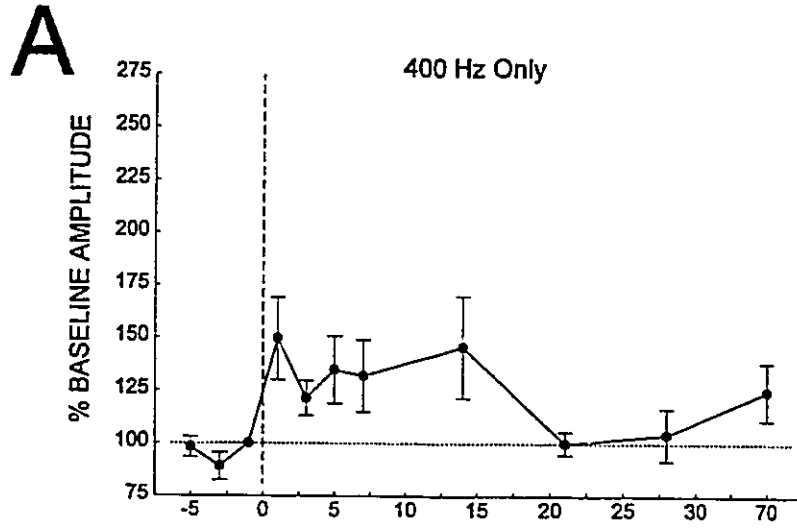


Figure 4.10

Figure 4.10. Mean evoked potential peak amplitude is shown as a function of days after LTP induction for the group that received only high-frequency trains (A), and the groups that received 400 Hz trains either as the 6th (B), or as the 2nd (C) pulse in 15 Hz trains when combined trains were delivered. Data are expressed as a percentage of the response amplitude observed during input/output testing on the last baseline day at the stimulus intensities used for test-pulses during LTP induction.



DISCUSSION

The monosynaptic projection from the pyriform cortex to the superficial layers of the entorhinal cortex in the chronically prepared rat was shown to support long-term synaptic potentiation in response to high-frequency, non-epileptogenic stimulation of the pyriform cortex. The LTP effects induced by high-frequency stimulation were enhanced when high-frequency induction stimuli were paired with 15 Hz stimulation trains. The resulting potentiation effects were large at intermediate test-pulse intensities, and were expressed as up to a tripling of response amplitudes over baseline levels. When observed, short term potentiation effects were expressed primarily only during the first 3 min after train delivery, and were inconsistently expressed across animals. The LTP effects were extremely long-lasting, with little decay in field potential amplitude over the course of weeks.

These results indicate that reliable LTP effects in the entorhinal cortex, previously observed only in *in vitro* preparations (Alonso et al., 1990; de Curtis & Llinas, 1993; Racine et al., 1983), can also be observed under more normal physiological conditions in the intact animal. The LTP effects can be induced in a graded manner by modifying stimulation parameters, making this an amenable experimental preparation for the examination of the rules which govern the induction of neuronal plasticity in the entorhinal cortex.

LTP induction in this pathway appears to require more intense stimulation than is sufficient for LTP induction in other pathways. Racine et al. (1983) demonstrated LTP effects in a variety of structures in the chronic rat, including the amygdala and intrinsic pathways of the hippocampal formation. These effects were induced by a series of 400 Hz, 8-pulse stimulation trains

delivered at an intensity which produced single-pulse responses 80% of asymptotic response amplitudes. This procedure was not sufficient, however, to reliably induce LTP in the entorhinal cortex response to pyriform cortex stimulation. The trains used in the present study were similar in amplitude and frequency to those used by Racine et al. (1983), but were longer in duration. These 16-pulse trains resulted in large and reliable LTP effects; only two animals showed no response enhancements following the delivery of 400 Hz trains alone.

The effectiveness of the longer trains used here in inducing LTP is likely to have resulted from the greater activation of NMDA-receptor-mediated currents which are critical for LTP induction in this pathway (Alonso et al., 1990; de Curtis & Llinas, 1993). Prolonged repetitive stimulation could have resulted in post-synaptic depolarization sufficient to induce enhanced NMDA-receptor-mediated currents either by temporal summation of monosynaptic EPSPs, and/or by a reduction in the effectiveness of inhibition in the entorhinal cortex during the course of the trains (Finch & Babb, 1980; Wouterlood et al., 1985; Finch et al., 1988; Jones & Heinemann, 1991; Jones, 1993). Effects of spatial summation among pyriform cortex efferents to the entorhinal cortex appear to play a lesser role in enhancing LTP once the initial LTP effect has been induced; when the train intensities were increased in the group receiving only 400 Hz trains, only 2 animals showed further increments in LTP.

Enhancement of LTP with Low-Frequency Stimulation.

Following saturation of LTP to the delivery of high-frequency trains alone, further increments in potentiation were produced by combining low- and high-frequency trains. The LTP effects in the experimental groups receiving combined train delivery were remarkably durable and showed negligible decay

over a 15 day follow-up period. Response enhancements were less consistently maintained in the group receiving only 400 Hz trains, but the greater decay of LTP in this group could be partly due to the smaller response enhancements which were induced.

The increments in LTP induction which followed combined train delivery must have been due to the *combination* of the low- and high-frequency trains. The delivery of the low-frequency trains alone is not sufficient to induce long-term changes in synaptic strength (Figure 3.3), and the combined trains were delivered after the LTP inducible by the repeated delivery of high-frequency trains alone had saturated. In the group in which 400 Hz trains replaced the 6th pulse in the 15 Hz trains, it was shown that high-frequency stimulation delivered at a time when frequency potentiation effects were well-developed can induce LTP which exceeds that induced by 400 Hz trains alone. However, when the 400 Hz trains replaced the 2nd pulse in each 15 Hz train, at a point when frequency potentiation was still weak, the response enhancements were only slightly smaller (Figure 4.6). The facilitation of LTP does not, therefore, depend on strong frequency potentiation effects.

Because the induction of LTP in this pathway is dependent on activation of the NMDA glutamate receptor subtype (Alonso et al., 1990; de Curtis & Llinas, 1993), the difference in the mean level of the increments in LTP induction between these two groups (Figure 4.6) is likely related to the degree to which the pulses preceding the 400 Hz trains enhanced the post-synaptic depolarization occurring during the 400 Hz trains. Paired-pulse stimulation of the pyriform cortex results in more than a doubling of the amplitude of entorhinal cortex field responses, and frequencies of stimulation near 15 Hz result in about a tripling of response amplitudes after the 5th pulse (Figures 3.5 &

3.14 top). Although the groups showed similar levels of LTP on the next day (Figure 4.10), differences between the facilitation induced by single pulses and by 15 Hz trains could underlie the slight difference in the amount of LTP initially induced in these groups (Figure 4.6).

The increased capacity of combined trains to induce LTP may also depend on reductions in the efficacy of inhibitory mechanisms. GABA-mediated inhibition is reduced during paired-pulse facilitation in the neocortex and hippocampus (Deisz & Prince, 1989; Davies et al., 1990; Mott et al., 1993; Wilcox & Dichter, 1994), and similar responses to single and repeated stimulation in the entorhinal cortex could result in similar increases in the net levels of post-synaptic depolarization induced by the high-frequency trains.

The mechanism of the enhancement observed when the high-frequency trains replaced the 2nd pulse in each low-frequency train could be similar to those which underlie "primed-burst" potentiation in the hippocampus (Ross & Dunwiddie, 1986, Davies et al., 1991). The development of the primed burst potentiation procedure resulted, in part, from attempts to determine the most minimal stimulation parameters that are sufficient to induce LTP effects. In this paradigm, each train of stimulation pulses is preceded by the delivery of a "priming" pulse. The delivery of the pulse approximately 200 msec prior to the high-frequency train has been found to greatly enhance the effectiveness of the trains in inducing LTP effects (Ross & Dunwiddie, 1986).

It is not known to what extent the *later* pulses in the 15 Hz trains may have contributed to the enhanced LTP following combined train delivery. The most effective pulse-train intervals and low-frequency stimulation rates for the enhancement of LTP could also be examined in further parametric studies. However, the apparent dependence of LTP induction in this pathway on the

degree of post-synaptic depolarization, and the finding that 15 Hz is near-optimal for frequency potentiation effects in this pathway, suggests that the low-frequency stimulation rate used here may also be optimal for the enhancement of LTP.

EXPERIMENT 4.3
ENHANCEMENT OF LONG-TERM POTENTIATION OF PYRIFORM CORTEX
EFFERENTS TO THE ENTORHINAL CORTEX BY COACTIVATION OF THE
MEDIAL SEPTUM

One aspect of LTP that makes it attractive as a memory model is that at least some of the pathways studied display interactions between input pathways in the induction of LTP (McNaughton et al., 1978; Levy & Steward, 1979; Robinson & Racine, 1982; Barrionuevo & Brown, 1983). Stimulation of the medial septum, which carries cholinergic afferents to the hippocampal formation (Mosko et al., 1973; Chandler & Crutcher, 1983; McNaughton & Miller, 1984), has been shown to enhance LTP in the dentate gyrus induced by tetanization of the perforant path input from the entorhinal cortex (Robinson & Racine, 1982; Robinson, 1986). The largest increments in the LTP effects observed were obtained when 400 Hz, 50 msec trains were delivered to the medial septum less than 100 msec prior to high-frequency stimulation of the perforant path (Robinson, 1986).

The role of the medial septum in enhancing plasticity in the dentate gyrus may be related to its putative involvement in the generation of oscillations in the hippocampus. Medial septal efferents are thought to contribute, in part, to theta rhythmicity in the hippocampus (Bland, 1986), and LTP is induced most effectively in the hippocampus when trains of stimulation are patterned to mimic the periodicity of the theta rhythm (Larson et al., 1986; Staubli & Lynch, 1987; Greenstein et al., 1988). The phase of the theta rhythm during which stimuli are

delivered appears to play an important role in LTP induction. In both the dentate gyrus and area CA1, LTP can be induced effectively when stimuli are delivered during the positive phase of the theta rhythm, but either no change or a response decrement is induced when stimuli are delivered during the negative phase (Pavrides et al., 1988; Huerta & Lisman, 1993). The cholinergic efferents from the medial septum to the hippocampus could underlie these effects since muscarinic agonists enhance LTP in the dentate gyrus (Burgard & Sarvey, 1990) and area CA1 (Blitzer et al., 1990), and acetylcholine enhances NMDA-receptor-mediated currents in CA1 neurons while not affecting responses to kainate and quisqualate (Markram & Segal, 1990).

The entorhinal cortex also receives inputs from the medial septum and, as in the hippocampus, they are believed to contribute to theta rhythm activity (Mitchell & Ranck, 1980; Alonso & Garcia-Austt, 1987a). These inputs are partly cholinergic (Segal, 1977; Alonso & Kohler, 1984; Insausti et al., 1987; Gaykema et al., 1990), and they terminate near the principal output neurons in layer II as well as in the deeper layers of the entorhinal cortex (Chapter 2; Alonso & Kohler, 1984; Witter et al., 1989; Gaykema et al., 1990). The possibility that medial septal activation may contribute to synaptic plasticity in the entorhinal cortex has, however, not been examined previously.

In the present study, the contribution of theta-frequency activation of the medial septum to LTP induction in pyriform cortex efferents to the entorhinal cortex was assessed using a procedure similar to that used in Experiment 4.2. Trains of high-frequency stimulation were first administered repeatedly to the pyriform cortex until no further enhancements in response amplitude to test-pulses were observed. After levels of LTP had saturated, the same trains were paired with 10 Hz stimulation trains applied to the medial septum, and test-pulse

responses were monitored for further increments in LTP. In addition to the comparison of input/output tests of pyriform cortex inputs to the entorhinal cortex before and after LTP induction, similar tests of the medial septal inputs were also conducted. This allowed the determination of whether heterosynaptic LTP effects could be induced in the septal inputs by the high-frequency trains applied to the pyriform cortex.

METHODS

Design. Eight animals were used in this experiment. The general design, materials, and methods used were similar to those described in Experiment 4.2. Bipolar electrodes were implanted into the same pyriform cortex and entorhinal cortex sites, and a third electrode was implanted in the medial septum (anterior 0.2 mm, lateral 0.0 - 0.2 mm, and 6.0 mm ventral to bregma). The vertical placement of this electrode was also modified during surgery to maximize the evoked entorhinal cortex response.

Input/Output Tests. Input/output tests were conducted over a 5 day baseline period prior to the LTP induction procedures on the next day. To determine the longevity of the LTP effect, evoked potentials were measured for up to two weeks post LTP induction. Two I/O runs were conducted on each test day; one in which test-pulses were delivered to the pyriform cortex, and one in which test-pulses were delivered to the medial septum. I/O tests in which the medial septum was stimulated allowed the assessment of heterosynaptic potentiation effects induced by the pyriform cortex trains, and the determination of pulse intensities resulting in $\approx 75\%$ asymptotic entorhinal cortex response amplitudes. These pulse intensities were used during cooperative LTP induction tests.

LTP Induction. Cooperative interactions between the pyriform cortex and medial septum in the induction of LTP in the pyriform cortex input to the entorhinal cortex were examined by determining if conjoint stimulation of the medial septum and the pyriform cortex could result in greater amounts of LTP than were inducible by pyriform cortex stimulation alone. Stable levels of LTP were first induced by repeated delivery of sets of 10 400 Hz trains to the pyriform cortex as in the previous experiment. As an additional control, however, responses to a series of test-pulses following delivery of a set of ten 10-pulse, 10 Hz medial septal trains were recorded prior to combined train delivery. During combined train delivery, high-frequency pyriform cortex trains were timed to arrive 100 msec after the last pulse in 10 Hz trains delivered to the medial septum. Pulses used for medial septal stimulation were set to an intensity that triggered responses approximately 75% of the asymptotic response amplitude during the I/O tests. After a 10 min series of test-pulses, a second set of combined trains was delivered, following which test-pulses were re-applied for a further 20 min.

Analysis. Data were normalized to baseline responses and averaged across animals for graphical display in the same way as reported in Experiment 4.2. Repeated measures ANOVAs were used to analyze changes in response amplitude. Responses recorded at the end of the baseline period, just prior to combined stimulation, and at the end of the follow-up period were analyzed to assess the effect of combined train delivery during the LTP induction procedure. Separate ANOVAs were used to assess changes in the I/O measures in response to medial septal and pyriform cortex stimulation.

RESULTS

Histology. The locations of electrode tips in the group of animals with medial septal electrodes are shown in Figure 4.11. All electrodes were located in targeted structures, and the pyriform cortex stimulating electrodes were all located near layer II pyramidal cells.

LTP Induction. All eight animals showed lasting enhancements in field potential amplitudes following the delivery of 400 Hz pyriform cortex trains alone. The degree of potentiation remained stable during subsequent delivery of 400 Hz trains, and following the delivery of a set of ten 10 Hz trains to the medial septum (Figure 4.12). The pyriform cortex train intensities used to induce these initial potentiation effects ranged between 501 and 1259 μA (mean=815 μA), and the 10 Hz medial septal trains were 501 to 1000 μA in intensity (mean=783 μA). The average baseline response was 0.30 mV (range= 0.16 to 0.60 mV), and there was an average increase to 178% of baseline response amplitudes (range= 139 to 291%).

Combined trains were subsequently applied in which a 400 Hz pyriform cortex train was delivered 100 msec following the last pulse in each of a set of 10-pulse, 10 Hz medial septal trains. Small but reliable additional enhancements were observed in all but one of the eight animals, and the mean evoked response amplitude increased from 178%, to 238% of baseline amplitudes (range= 160 to 432%; Figure 4.12). The means of the field potentials recorded at the end of the three major phases of the LTP induction procedure are shown in Figure 4.13 for the eight animals tested.

A 1-way repeated measures ANOVA of pulse-evoked responses recorded at the end of baseline testing, prior to combined train delivery, and at the end of the follow-up period, showed a significant difference in response

amplitudes at these times ($F=12.98$, $p<0.001$). A post-hoc Newman-Keuls test indicated significant differences for all three comparisons of the response amplitudes at these phases of the LTP induction procedure ($p<0.05$).

Input/Output Tests. Field potentials recorded during I/O testing in response to both pyriform cortex and medial septal stimulation were compared to assess the effects of LTP induction on field responses evoked by a range of test-pulse intensities. While the LTP induction procedure resulted in enhancements in entorhinal cortex field potentials in response to pyriform cortex stimulation, there were no increases in responses to medial septal stimulation (Figure 4.14; Figures 4.15A & 4.16A). Enhancements occurred in responses evoked by pyriform cortex test-pulses at all pulse-intensities above $100 \mu\text{A}$, although proportionally the greatest increments often occurred at the middle intensities (Figures 4.14 left, & 4.15A). The intensity by pre/post-LTP interaction was significant for pyriform cortex evoked responses ($F=4.08$, $p<0.001$), but was not significant for medial septum evoked responses ($F=1.08$, $p=0.38$).

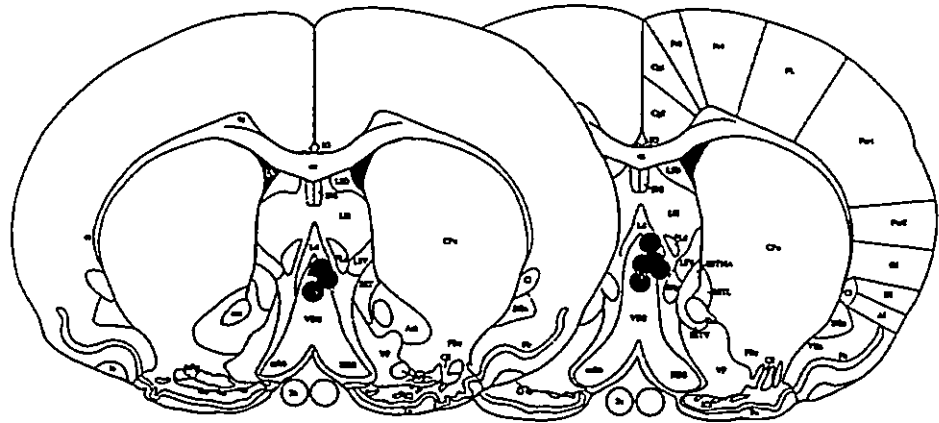
Response amplitudes showed considerable variability during the 5-day baseline period. However, while the amplitude of responses evoked by medial septal stimulation did not change systematically over the course of the experiment (Figure 4.16B), the enhancements in responses evoked by pyriform cortex stimulation were maintained for the duration of the two week follow-up period (Figure 4.15B). The main effect of days in 1-way ANOVAs on the decay data were significant for both pyriform cortex ($F=4.02$, $p<0.05$) and medial septal evoked responses ($F=2.9$, $p<0.05$), but post-hoc Newman-Keuls comparisons indicated significant differences between baseline and follow-up days only for the pyriform cortex evoked responses ($p<0.05$). The amount of potentiation observed during I/O tests on the day after LTP induction was

somewhat less than that observed at the end of the LTP induction procedure itself, indicating that much of the decay in the pyriform cortex evoked responses took place over the first 24 hr following LTP induction.

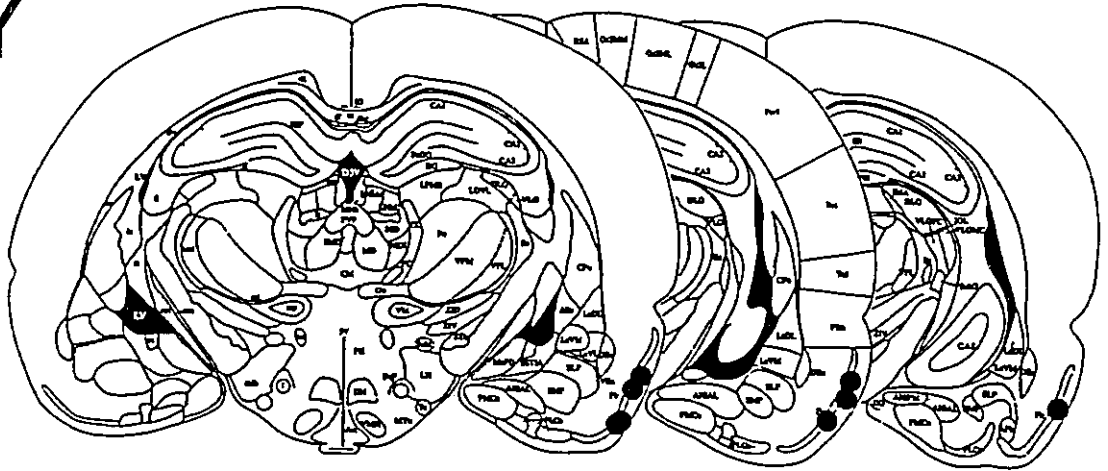
Figure 4.11

Figure 4.11. Histological results for experiments in which stimulation trains were delivered to both the medial septum (**MS**) and the pyriform cortex (**PY**). The locations of the stimulating electrodes and of the recording electrodes in the entorhinal cortex (**EC**), are shown on representative coronal sections taken from the atlas of Paxinos and Watson (1986).

MS



PY



EC

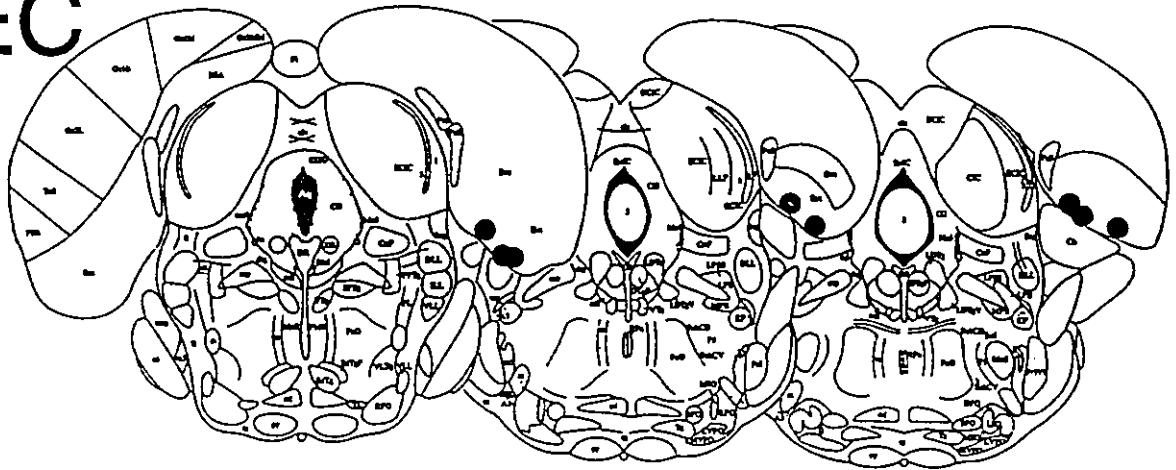


Figure 4.12

Figure 4.12. The mean amplitude of responses evoked in the entorhinal cortex by pyriform cortex test-pulses during tests of the effects of medial septal stimulation on the response enhancements produced by 400 Hz stimulation of the pyriform cortex (**PY 400**). The **upper panel** shows the averages of the changes in the evoked potential amplitudes which are presented as in Figure 4.6 (n=8). The **lower panel** shows a representative example of data from one of the animals. After the 20 min baseline period, sets of 400 Hz trains (**400**) were delivered repeatedly to the pyriform cortex until there was no further increment in response amplitude. Different animals required between 2 and 7 sets of trains to saturate. One set of 10 Hz trains was then delivered to the medial septum (**MS 10**), and then two sets of combined trains (**PY+MS**) were delivered in which the 400 Hz trains were applied to the pyriform cortex 100 msec after the end of the 10-pulse medial septal stimulation trains.

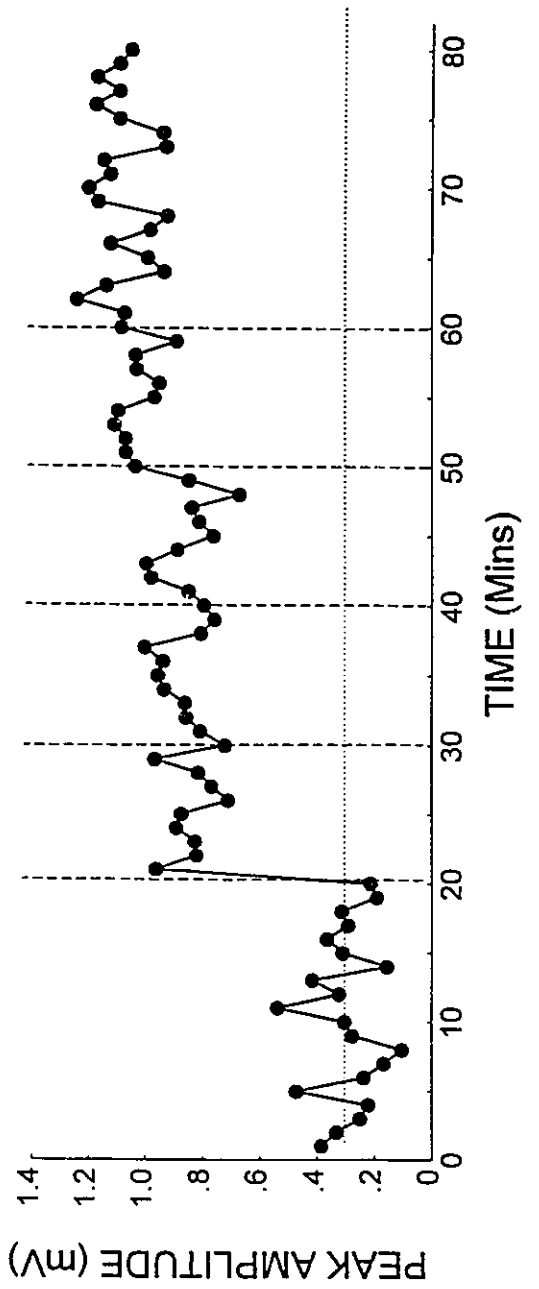
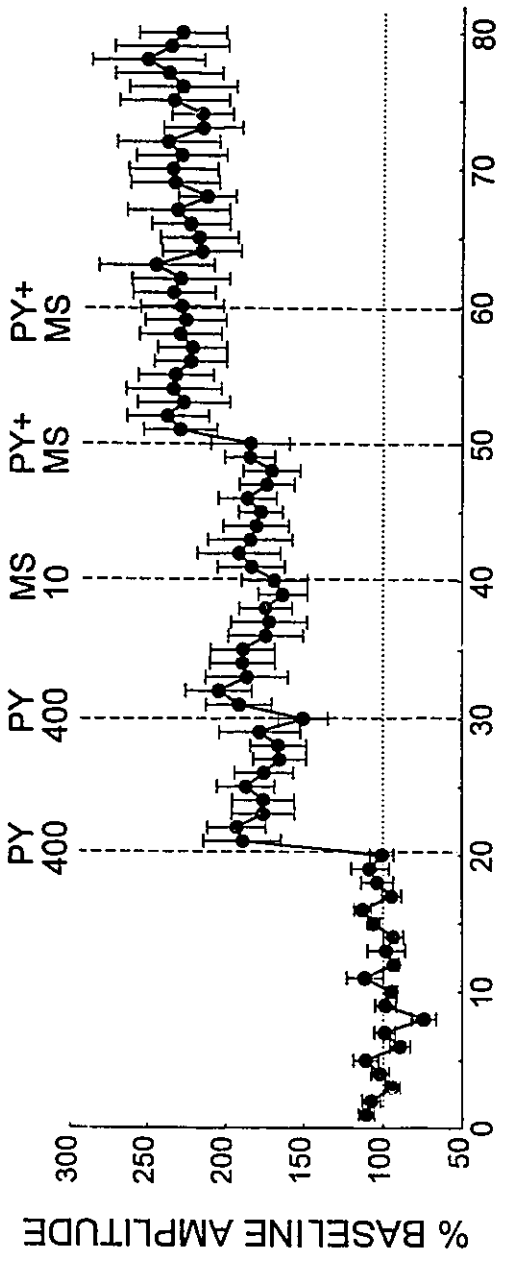


Figure 4.13

Figure 4.13. Averaged evoked potentials recorded from the eight animals (rows) used to test the effects of combined medial septal and pyriform cortex stimulation on LTP in the entorhinal cortex. Superimposed traces are the averages of 10 field potentials in the entorhinal cortex evoked by pyriform cortex stimulation at the end of three phases of the LTP induction procedure. Solid traces show the mean of potentials recorded at the end of the 20 min baseline periods (BL). Dotted traces show mean responses after repeated delivery of 400 Hz trains to the pyriform cortex, and the subsequent 10 Hz stimulation of the medial septum (400Hz). Dashed traces show recordings obtained 20 min after delivering combined sets of trains in which 400 Hz trains were applied to the pyriform cortex 100 msec after the end of a 10-pulse medial septal stimulation train (400Hz+10Hz). In only one of the 8 animals tested (top left) was there no further enhancement following combined stimulation. Horizontal calibration, 10 msec; vertical calibration, 0.5 mV.

— BL
..... 400Hz
- - - 400Hz
+ 10Hz

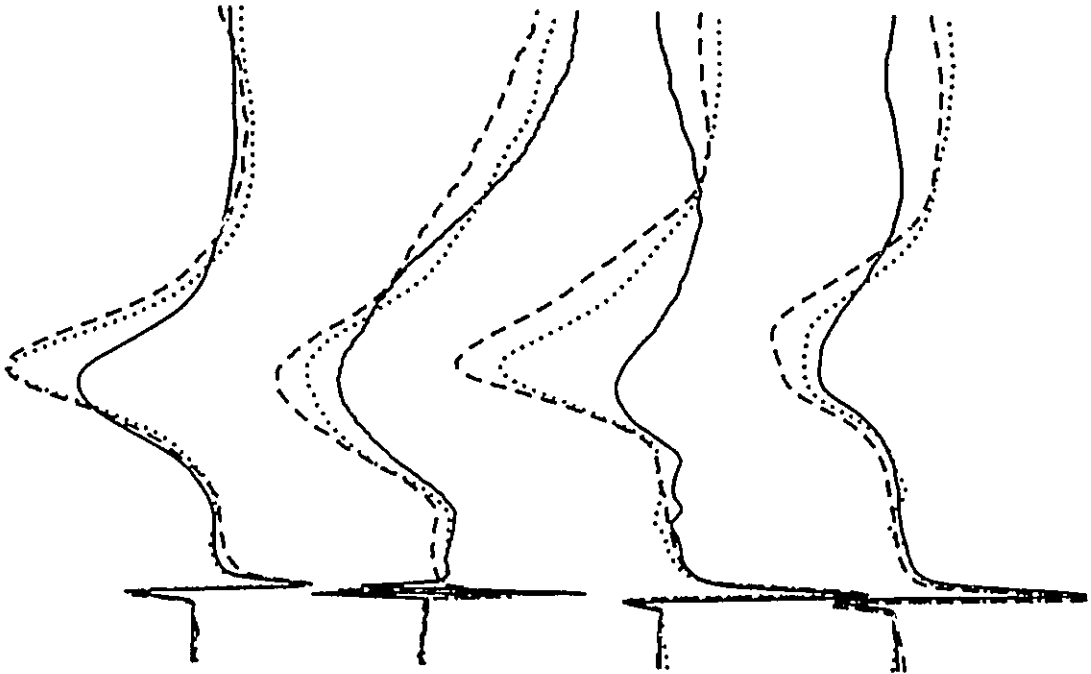
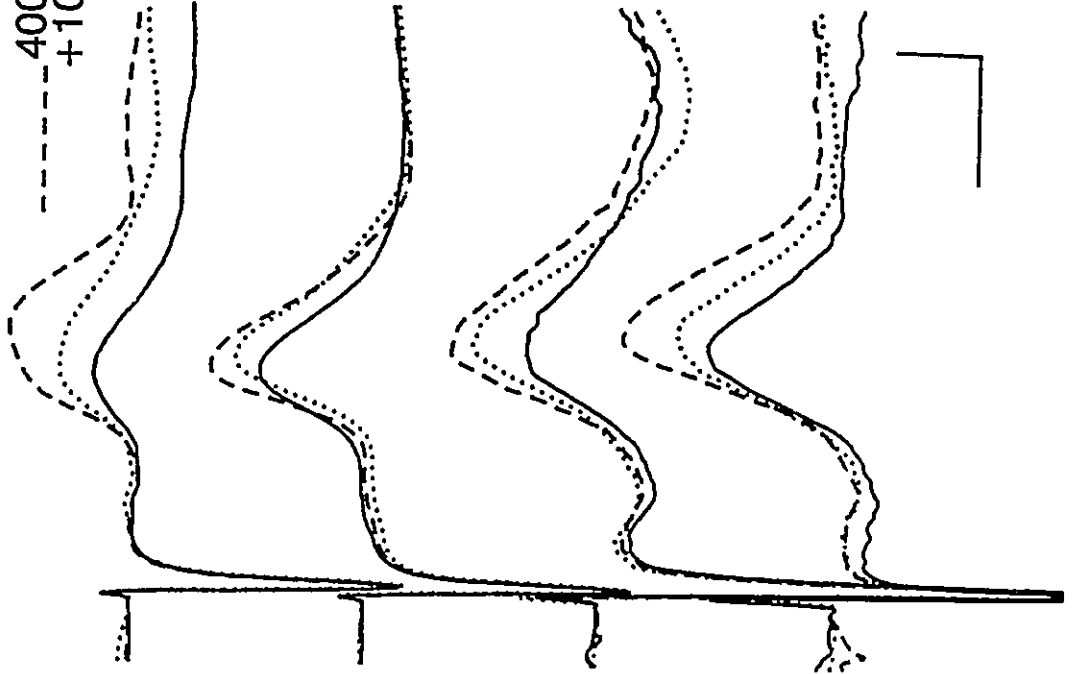
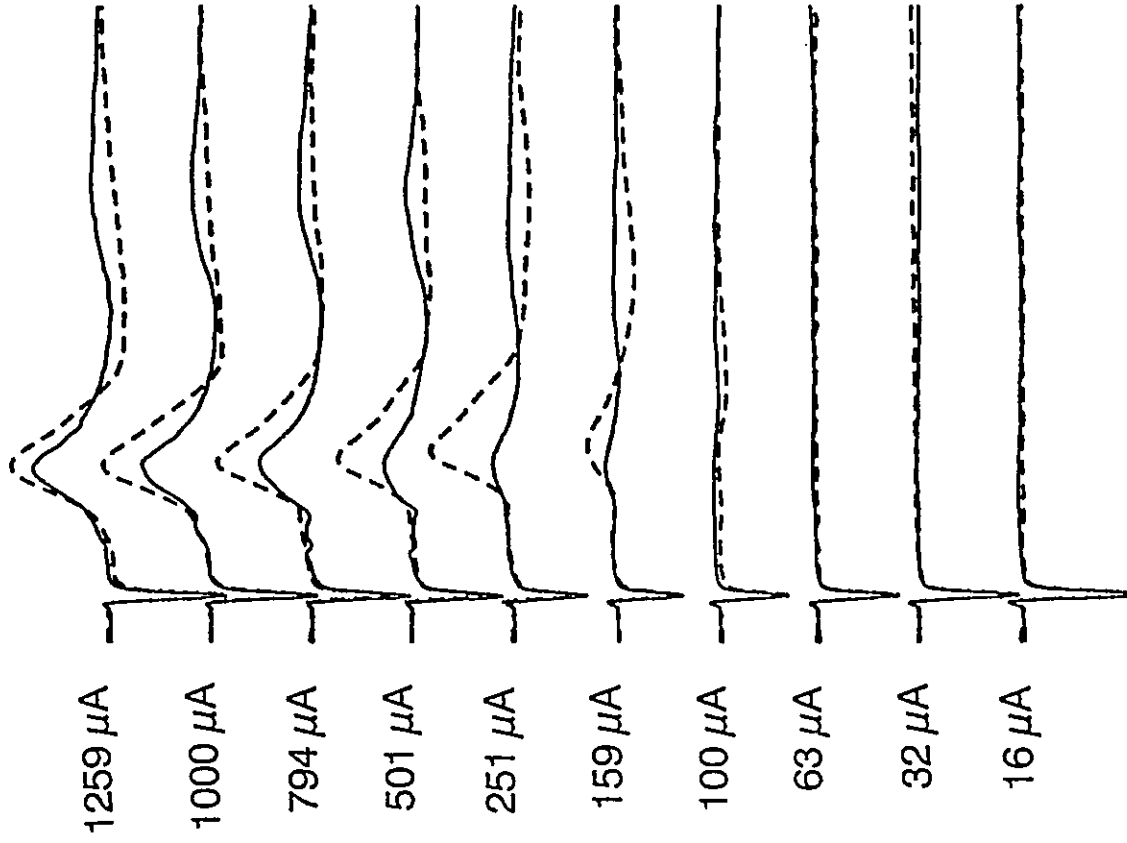


Figure 4.14

Figure 4.14. Examples of responses in the entorhinal cortex recorded on the day before (**solid traces**), and the day following LTP induction (**dashed traces**) in response to either the pyriform cortex or medial septal stimulation. Test-pulse intensities are shown at left. Horizontal calibration, 20 msec; vertical calibration 1.0 mV.

PYRIFORM STIMULATION



SEPTAL STIMULATION

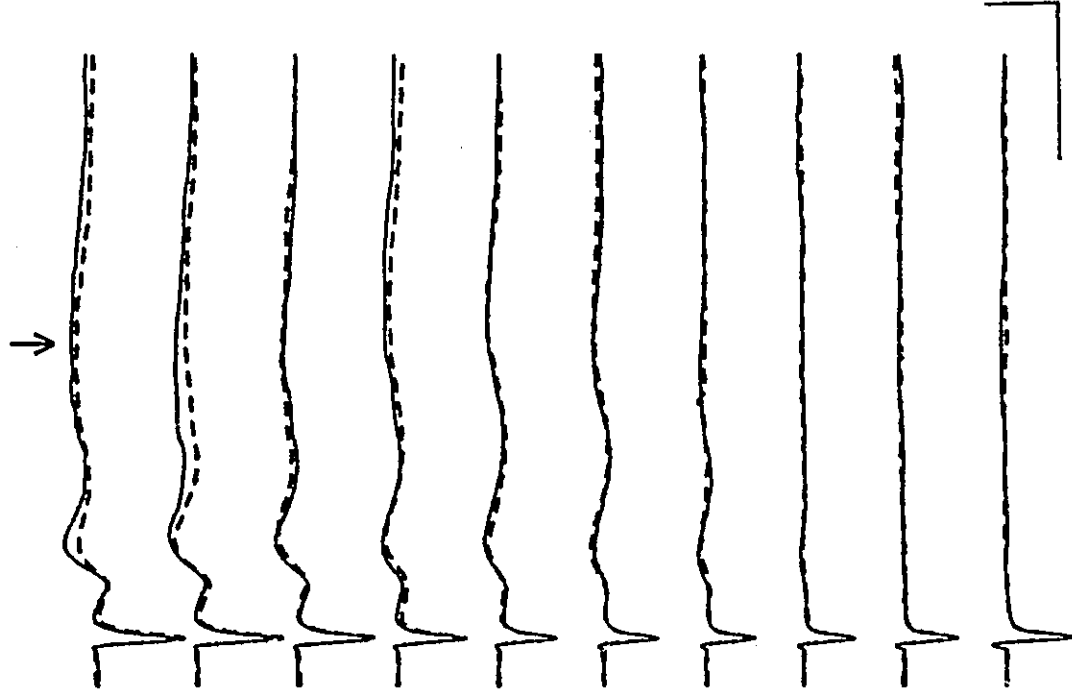


Figure 4.15

Figure 4.15. Mean evoked potential amplitudes in the entorhinal cortex evoked by pyriform cortex stimulation in the septal cooperativity experiment. In **A**, mean evoked potential peak amplitude is shown as a function of stimulus intensity on the day before (**pre**) and the day after (**post**) LTP induction. Data have been standardized to the response to the highest stimulus intensity on the last baseline day. In **B**, the mean evoked potential peak amplitude is shown as a function of days after LTP induction. Data are expressed as a percentage of the response amplitude observed during input/output testing on the last baseline day at the stimulus intensity used for test-pulses during LTP induction.

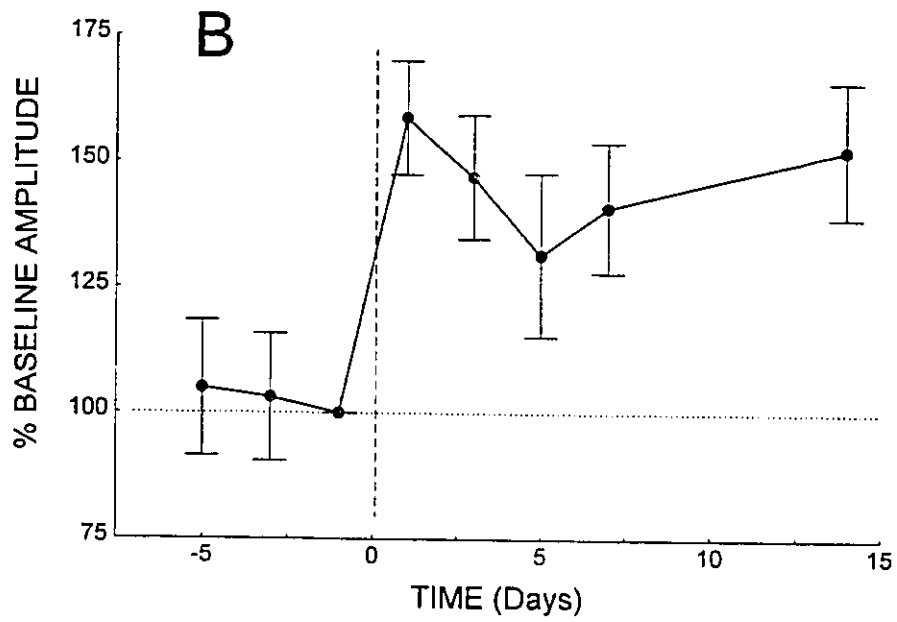
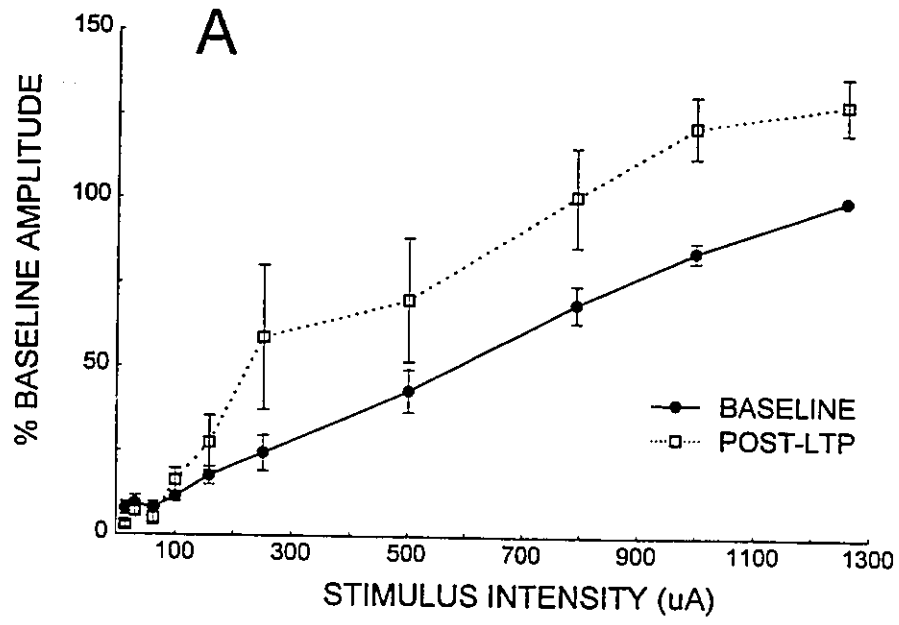
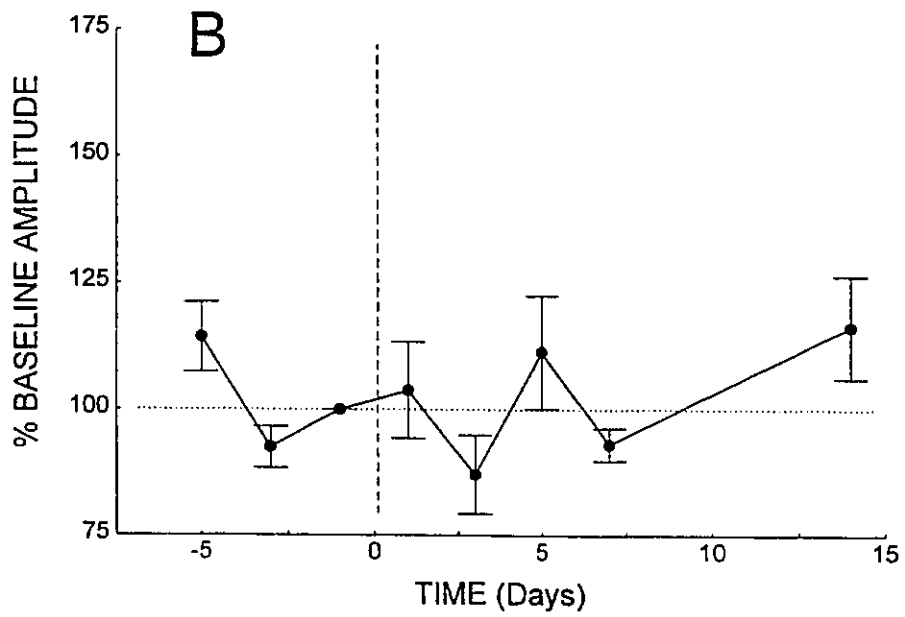
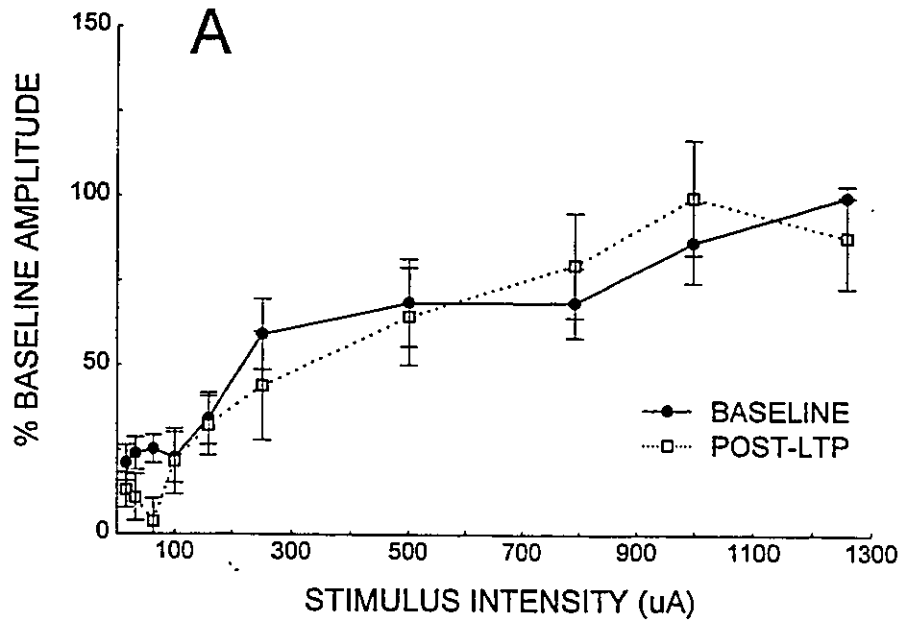


Figure 4.16

Figure 4.16. Mean evoked potential amplitudes in the entorhinal cortex evoked by medial septal stimulation in the septal cooperativity experiment. In **A**, mean evoked potential peak amplitude is shown as a function of stimulus intensity on the day before (**pre**) and the day after (**post**) LTP induction. Data have been standardized to the response to the highest stimulus intensity on the last baseline day. In **B**, the mean evoked potential peak amplitude for the two highest stimulus intensities are shown as a function of days after LTP induction. The responses to the two highest test-pulse intensities during input/output test were averaged, and standardized to the results for the last baseline day.



DISCUSSION

The results of this study have indicated that low-frequency stimulation of the medial septum can enhance LTP induced by stimulation of the pyriform cortex inputs to the entorhinal cortex. Ten Hz stimulation of the medial septum just prior to high-frequency stimulation of the pyriform cortex resulted in greater LTP effects than were inducible by pyriform cortex stimulation alone. Although the response enhancements following combined train delivery tended to be small, the effects were reliable, and were observed in all but one of the 8 animals tested.

The LTP induced by the stimulation protocol was specific to synapses activated by the high-frequency trains, and was not due to a general increase in cell excitability generalizing to synapses activated by septal inputs. Enhancements in the field potentials following the LTP induction procedure were specific to the synaptic responses evoked by pyriform cortex test-pulses, and were not observed in responses to medial septal stimulation (Figures 4.14, 4.15 & 4.16).

The LTP that was induced following combined train delivery showed no signs of decay over the 20 min follow-up period after the last set of trains was delivered, but there was some decay observed on the next day (Figures 4.12 & 4.15B). The amount of LTP expressed on the day following the LTP induction procedure, however, showed no signs of decay over the remainder of the follow-up period. A similar decay over the first 24 hr, and a durable maintenance of LTP over the testing period, were also observed in the groups receiving low- and high-frequency stimulation trains in Experiment 4.2.

The increments in LTP induced by combined train delivery must have been due to the combined effect of pyriform cortex and medial septal stimulation. First, the enhancements cannot have occurred due to the 10 Hz medial septal trains alone, since 1), eight to 18 Hz stimulation of the medial septum has been shown in previous experiments not to result in long-term changes in synaptic responses to either pyriform cortex or medial septal stimulation (Figure 3.3), and 2), in the present experiment, the delivery of medial septal trains alone (identical to those used in later combined stimulation) did not result in long-term changes in responses to pyriform cortex test-pulses (Figure 4.12). Second, the enhancements cannot have occurred due to the 400 Hz pyriform cortex trains alone since the combined trains were delivered after the LTP inducible by the repeated delivery of high-frequency trains alone had saturated.

The enhancing effects of medial septal stimulation on LTP in the projection from the pyriform cortex to the entorhinal cortex is likely to have occurred by enhancing the degree of post-synaptic depolarization and NMDA receptor activation induced by the pyriform cortex trains (Alonso et al., 1990; de Curtis & Llinas, 1993). The 10 Hz frequency of medial septal stimulation was chosen because it results in a frequency potentiation of post-synaptic responses in the entorhinal cortex (Figure 3.14), and is within the frequency range of the theta rhythm. Further, pyriform cortex trains were delivered 100 msec after each medial septal train. This interval was shown in Chapter 3 to result in paired-pulse heterosynaptic facilitation effects when single conditioning-pulses are delivered to the medial septum prior to the delivery of test-pulses to the pyriform cortex (Figure 3.9).

Medial septal projections terminate in layer II of the entorhinal cortex (Alonso & Kohler, 1984; Witter et al., 1989; Gaykema et al., 1990), and evoked sinks in the entorhinal cortex overlap with those evoked by pyriform cortex stimulation in the same animals (Figures 2.8 & 2.13). Consequently, an increased depolarization in the neurons activated by the pyriform cortex trains could have been mediated by direct monosynaptic inputs to these same cells from the medial septum. While the duration of field potentials evoked by medial septal activation is shorter than the 100 msec interval between the trains, activation of direct inputs from the medial septum could have much longer lasting effects on the excitability of entorhinal cortex neurons. Cholinergic inputs from the medial septum (Segal, 1977; Alonso & Kohler, 1984; Insausti et al., 1987; Gaykema et al., 1990) may have played a significant role. In the hippocampus, cholinergic agonists enhance LTP in the dentate gyrus and area CA1 (Burgard & Sarvey, 1990; Blitzer et al., 1990; Huerta & Lisman, 1993), and stimulation of the medial septum enhances LTP in the dentate gyrus (Robinson & Racine, 1983; Robinson, 1986). The induction of LTP in the sensorimotor (Lin & Phillis, 1991) and in the visual cortex (Brocher et al., 1992) is also facilitated by cholinergic agonists.

Although the effects of cholinergic drugs on the excitability of entorhinal neurons is not known, cholinergic agonists have been shown to reduce adaptation of repetitive firing in most cortical areas (Krnjevic & Phillis, 1963; Barkai & Hasselmo, 1994), and to result in a slow depolarization of resting membrane potential (Bernardo & Prince, 1982; Cole & Nicoll, 1984; Madison & Nicoll, 1984). These effects are due to attenuations of the Ca^{2+} -dependent K^+ conductance which mediates afterhyperpolarizations and the M-type K^+ -current (Madison & Nicoll, 1984; McCormick & Prince, 1986; Maddison et al., 1987).

Similar effects on entorhinal cortex neurons could result in an enhancement of evoked NMDA-receptor-mediated currents. Further, maintained depolarization of layer II stellate cells results in oscillations in membrane potential with a mean frequency of 8.6 Hz (Alonso & Klink, 1993). If similar oscillations at an elevated mean resting membrane potential were induced by 10 Hz medial septal stimulation, and maintained for at least 100 msec following the end of the train, the pyriform cortex volley could arrive in the entorhinal cortex at a time when stellate cells were partially depolarized and also engaged in a rhythmic state that may be conducive to LTP induction (Alonso et al., 1990).

Post-synaptic depolarization in entorhinal cortex neurons may also have been enhanced through a reduction of the inhibition of neurons in the superficial layers (Jones, 1993; Jones & Heinemann, 1991; Finch & Babb, 1980; Wouterlood et al., 1985; Finch et al., 1988). Although cholinergic projections typically activate GABA-ergic interneurons in hippocampal and neocortical target sites (McCormick & Prince, 1986; Pitler & Alger, 1992) repetitive stimulation markedly reduces inhibitory post-synaptic currents in the neocortex (Deisz & Prince, 1989), and hippocampus (Davies et al., 1990; Mott et al., 1993; Wilcox & Dichter, 1994). A similar mechanism in the entorhinal cortex could lead to a reduction in the feedforward or feedback inhibition normally evoked by pyriform cortex stimulation. Inhibitory interneurons in the superficial layers of the entorhinal cortex, where both pyriform cortex and medial septal inputs terminate, show extensive basket-like axonal arborizations (Jones & Buhl, 1993) so that a reduction in the inhibition mediated by these neurons could have widespread effects.

Activation of recurrent excitatory connections within the entorhinal cortex by medial septal stimulation could contribute to excitation in the

superficial layers (Jones & Heinemann, 1988; Jones, 1990). However, cholinergic agonists tend to *depress* synaptic transmission of *intrinsic* excitatory connections in cortical and hippocampal regions (Kahle & Cotman, 1989; Hasselmo & Schnell, 1994; Hasselmo, 1995).

Because of the prolonged duration of the medial septal trains, polysynaptic activation of other afferents to the entorhinal cortex may have contributed to the LTP effects induced by combined stimulation. Neuromodulatory systems, including dopaminergic inputs from the ventral tegmental area (Fallon et al., 1978), serotonergic inputs from the raphe nuclei (Kohler et al., 1981), noradrenergic inputs from the locus coeruleus (Moore & Card, 1984), reach the parahippocampal cortical regions via dorsal pathways distal to the medial septal stimulation site. The direct stimulation of cholinergic and non-cholinergic medial septal efferents is therefore more likely to have had effects in the entorhinal cortex sufficient to modify LTP induction. Direct medial septal stimulation, however, results in activation of neurons in the dentate gyrus (Andersen et al., 1961; Fantie & Goddard, 1982; Robinson & Racine, 1982, 1986; McNaughton & Miller, 1984). Additional entorhinal cortex activation could thus be added via the projection from the hippocampal formation to the entorhinal cortex via the subicular complex (Whitter et al., 1989). However, while field potential components attributable to entorhinal cortex activation grow during 10 Hz medial septal stimulation, the early field potential components attributable to dentate gyrus activation are attenuated (Figure 3.13 right), suggesting that frequency potentiating medial trains do not result in significant activation of the entorhinal cortex via the hippocampal formation.

In the following chapter, a neural network modelling approach was taken to the analysis of the possible roles that frequency potentiation may play in contributing to Hebbian learning processes in the entorhinal cortex.

CHAPTER 5
HETEROSYNAPTIC FACILITATION OF HEBBIAN LEARNING IN A NEURAL
NETWORK MODEL BY COACTIVATION OF FREQUENCY POTENTIATING
SYNAPTIC INPUTS

Neural network modelling offers a way of studying the possible ways in which neural systems perform computational functions and store information. Neuronal representations are thought to be instantiated by the firing patterns within highly distributed and interconnected neuronal assemblies, and to be determined by the strength of the synaptic connections between the individual neurons which compose the networks (Hebb, 1949; McClelland & Rumelhart, 1985, 1986). While existing neurophysiological techniques are inadequate for targeting a given cell assembly in the mammalian central nervous system in order to monitor the individual activities of the many component neurons, neural network modelling techniques have enabled the controlled study of the behaviour of artificial, mathematically formulated cell assemblies and the representations which they can support (Durbin, 1989).

An especially large branch of the modelling field is concerned with the capacity of neural networks to learn representations of sensory stimuli (McClelland & Rumelhart, 1986; Brown et al., 1990). In general, neural networks are composed of multiple neuron-like elements, or "units", and the activation level of a given unit is determined jointly by the activity of other network elements which project to it and the strength of the synapses, or "connection weights", which mediate these projections. Multiple layers of units

are often employed so that a distinct population of units can be activated by experimentally determined input stimuli, and so that the resulting activity in other populations of units can provide measures of the behaviour and of the output of the network. During learning, input patterns are presented to the network and algorithms are used to modify the connection weights depending on the activation values resulting from the input patterns. The processing and storage capacity of a neural network is partly related to the number of units in the network, the architecture of their connections, and the algorithms which control their interactions. A large number of learning algorithms have been developed for use in neural networks, and include Hebbian algorithms which modify connection weights in a purely local nature, depending on pre- and post-synaptic activation values specific to each connection in the network (McClelland & Rumelhart, 1986; Sejnowski & Tesauro, 1989; Brown et al., 1990; Gluck & Granger, 1993). Hebbian connection weight update algorithms have a strong theoretical (Hebb, 1949) and experimental (Bliss & Lomo, 1973; Bliss & Gardner-Medwin, 1973) basis, and are therefore attractive for use in models which are intended to be neurophysiologically realistic.

While a vast amount of modelling work has focussed on the spatial coding of long-term memories by Hebbian algorithms, there has also been a growing interest in modelling the temporal aspects of neuronal activity which may influence neuronal information processing. Short term memory mechanisms, for example, can be mediated by recurrent excitatory connections within single neuronal populations in Hopfield-type networks (Little & Shaw, 1975; Mezard et al., 1986; Abbott, 1990; Zipser, 1991). Further, there has been a growth in the number of network models which include sufficient physiological detail to allow a close resemblance between the temporal characteristics of the

units in the model, and those of the real neural network under study (Wilson & Bower, 1991, 1992; Cohen et al., 1992; Segev, 1992; Barkai et al., 1994).

Experimental studies of long-term potentiation (LTP) phenomena indicate that temporal aspects of neural activity play a critical role in Hebbian synaptic plasticity. In the hippocampal formation, electrical stimulation delivered at theta rhythm frequencies is particularly effective in inducing LTP (Staubli & Lynch, 1987; Greenstein et al., 1988; Larson & Lynch, 1989). One possible way in which theta-frequency activity may contribute to Hebbian learning is by setting a background of frequency potentiation. Frequency potentiation is a short-term enhancement of neuronal responses which occurs when the electrical stimuli evoking the responses repeat within a given frequency range (Anderson & Lomo, 1967, 1968; Deadwyler et al., 1975; Creager et al., 1980; Nickell & Shipley, 1988; Figures 3.13 & 3.14). Frequency potentiation in the hippocampal formation is observed most readily at frequencies corresponding to the theta rhythm (Andersen & Lomo, 1967; MacVicar & Dudek, 1979; Finch & Babb, 1980; Landfield, 1993), and the frequencies of both theta activity and optimal frequency potentiation effects are reduced from about 8-10 Hz to about 2-5 Hz under urethane anesthesia (Bland, 1986; Munoz et al., 1991; Jones & Heinemann, 1991). Although it is not clear whether frequency potentiation is actually induced during normal theta activity, such effects could provide a mechanism for the enhancement of LTP effects by increasing levels of post-synaptic depolarization (Experiments 4.2 & 4.3).

Although frequency potentiation effects in medial septal efferents to the entorhinal cortex are strongest for stimulation frequencies near 12 Hz, there are marked frequency potentiation effects at theta-related frequencies in the 8 to 10 Hz range (Figure 3.14 bottom). Further, frequency potentiating 10 Hz trains of

stimulation delivered to the medial septum, which is thought to play a role in the mediation of theta activity in the entorhinal cortex (Alonso & Garcia-Austt, 1987a; Mitchell & Ranck, 1980), results in an enhancement of the LTP induced by stimulating pyriform cortex inputs to the entorhinal cortex (Experiment 4.3). Stimulation of the medial septum with high-frequency trains, although not resulting in frequency potentiation, has also been shown to enhance LTP induction in the dentate gyrus (Robinson & Racine, 1983; Robinson, 1986).

The potential role of frequency potentiation of medial septal efferents to the entorhinal cortex in heterosynaptically amplifying Hebbian long-term synaptic enhancements in projections from the pyriform cortex to the entorhinal cortex has been studied here in a neural network simulation. Rhythmic stimulation which coincides with the positive phase of the theta rhythm contributes most strongly to LTP induction in both the dentate gyrus (Pavrides et al., 1988), and the CA1 region of the hippocampus (Huerta & Lisman, 1993), so that the phase of the theta rhythm during which afferent inputs arrive may also play an important role in longer-term changes in synaptic efficacy. Therefore, the effect of phase locking pyriform cortex activity with frequency potentiating input to the entorhinal cortex from the medial septum was also examined in a separate set of simulations. In a third set of network simulations, the effect of frequency potentiation on a Hebbian competitive learning algorithm was tested. This algorithm allowed for the *spatial* coding of different pyriform cortex input patterns in the entorhinal cortex (Plumbley, 1993; Oja, 1982).

Although frequency potentiation effects were first examined experimentally decades ago, and have potentially powerful effects on temporal processing in the nervous system, no previous neural network models have employed frequency potentiating synapses. It was therefore necessary to first

design a model synapse which displayed frequency potentiating characteristics by responding most strongly to intermediate frequencies of stimulation (Chapman & Becker, 1995).

5.1 SYNAPTIC MODELLING

Frequency Potentiating Synapses.

The modelling of frequency potentiation requires the algorithms which govern the behaviour of the synapse to be complex enough to act as if the enhanced output of the synapse is dependent on the output of a band pass filter; potentiated synaptic responses should result from intermediate frequencies of stimulation. The goal of the synaptic modelling described here was to implement a simple and biologically plausible mechanism which could reflect the time-course of experimentally observed frequency potentiation effects, and which could be incorporated with reasonable computational expense into a neural network containing multiple frequency potentiating synapses. The method used was to design a synapse with a connection weight strength which was dependent on the frequency of recent synaptic activation.

Short-term changes in the connection weight were controlled by three synaptic weight change components with correlates to physiological mechanisms that affect post-synaptic responses. The physiological correlates of the connection weight components are presynaptic facilitation of transmitter release, the activation of a fast inhibitory process, and late afterhyperpolarizations. The one facilitatory component, and early and late inhibitory components, are activated by presynaptic inputs, and decay with different time constants following synaptic input. Algorithms were chosen to

control the behaviour of the three connection weight components so that the connection weights depended on the activation of the synapse only during the preceding time step, and the synapse was not required to "remember" prior states of activation. In the model, the connection weight is modified at every time step depending on the summed value of the three components, so that,

$$W_{ij}(t+1) = F_{ij}(t) - I_{ij}(t) - \epsilon_0 H_{ij}(t) \quad (1)$$

where $W_{ij}(t+1)$ is the connection weight from unit j onto unit i on the next time step, F is the facilitatory component, I is an early inhibitory component, and H is a slower-decaying inhibition which is modified by the scalar $\epsilon_0=0.25$.

The three components are defined by:

$$F_{ij}(t) = \epsilon_1 F_{ij}(t-1) + (1-\epsilon_1) \text{input}_j(t) \quad (2)$$

$$I_{ij}(t) = \epsilon_2 I_{ij}(t-1) + (1-\epsilon_2) \text{input}_j(t) \quad (3)$$

$$H_{ij}(t) = \epsilon_3 H_{ij}(t-1) + (1-\epsilon_3) \text{input}_j(t) \quad (4)$$

where ϵ_1 , ϵ_2 and ϵ_3 are scalars which determine the decay of each component (left terms), and the added effect of new inputs (right terms).

Facilitation (F). Enhanced responses in the model synapse during repetitive stimulation are due largely to the facilitatory component, F . This component is modelled after the facilitation of Ca^{2+} -dependent neurotransmitter release which occurs when successive action potentials arrive at a presynaptic terminal (Katz & Miledi, 1968; White et al., 1979; Turner & Miller, 1982). Calcium entering the presynaptic terminal during repetitive stimulation is thought to sum with residual Ca^{2+} incompletely sequestered or inactivated following prior synaptic activation. Small amounts of residual Ca^{2+} can result in a large facilitation of transmitter release due to a non-linear relationship between transmitter release and free intracellular Ca^{2+} concentration near release sites (Barrett & Stevens, 1972; Stockbridge & Moore, 1984; Zucker, 1989). While

most of the evidence supporting the residual Ca^{2+} hypothesis for synaptic facilitation has been derived from peripheral nervous system preparations (Katz & Miledi, 1968; Zucker, 1989), facilitation effects at central synapses are also thought to result from the effects of residual presynaptic Ca^{2+} , and are roughly proportional to the amount of residual presynaptic Ca^{2+} (Hess & Kuhnt, 1992; Andreasen & Hablitz, 1994; Wu & Saggau, 1994).

Paired-pulse facilitation of synaptic transmission at the neuromuscular junction decays rapidly at first, with a time constant of roughly 20 to 35 msec, and then more slowly with a time constant of about 250 msec (Mallart & Martin, 1967; Barrett & Stevens, 1972; Magelby, 1973a, 1987; Zucker, 1989). Similar results are observed in paired-pulse facilitation curves obtained from the hippocampus (Racine & Milgram, 1983; Andreasen & Hablitz, 1994), and from the medial septal projection to the entorhinal cortex (Figure 3.7). These curves are affected by inhibition at short interpulse intervals, however, and decay to baseline values at intervals near 500 msec with a time-constant near 80 msec (Racine & Milgram, 1983; Figure 3.7). The time-course of decay in the facilitatory component in the synaptic model has been set to approximate the decay in the experimentally observed paired-pulse facilitation curve for the medial septal projection to the entorhinal cortex shown in Figure 3.7 by setting the parameter ϵ , to equal 0.75 (Figure 5.1A).

Inhibition (I). The early inhibitory weight-change component, I , is modelled after strong inhibitory mechanisms in the superficial layers of the entorhinal cortex (Finch & Babb, 1980; Colino & Fernandez de Molina, 1986; Finch et al., 1988; Jones & Heinemann, 1991; Jones, 1993). Synaptic inhibition in the entorhinal cortex, likely mediated by feedforward activation of fast-spiking interneurons (Wouterlood et al., 1985; Finch et al., 1988; Jones & Buhl, 1993),

has fast onset latencies in the range of about 5 to 25 msec following stimulation of input pathways and decays more quickly than synaptic facilitation (Finch & Babb, 1980; Finch et al., 1988; Jones, 1990; Jones & Heinemann, 1991). By setting the parameter ϵ_2 in Equation 3 to equal 0.55, the fast inhibitory component, I, responds more strongly to single inputs than F, and decays more quickly (Figure 5.1A).

Hyperpolarization (H). Inhibitory processes with much longer time-courses than those captured by the early inhibitory component have also been recorded from entorhinal cortex neurons. For example, the activation of entorhinal neurons by single stimuli delivered to the basolateral amygdaloid nucleus is followed by a period of 100 to 200 msec during which spontaneous activity is greatly reduced (Colino & Fernandez de Molina, 1986a&b). In studies of frequency potentiation in the hippocampus (Schwartzkroin, 1975; MacVicar & Dudek, 1979; Pitler & Landfield, 1985), and the *in vitro* and *in vivo* entorhinal cortex (Finch et al., 1986; Jones, 1990b), sustained hyperpolarizations during stimulation have been commonly observed. Shifts in membrane potential occur in layer II entorhinal cortex neurons during 11 Hz stimulation of the subicular complex (Finch et al., 1986; Jones, 1990b). While this prolonged hyperpolarization may be partly due to synaptic effects of recurrent inhibition (Colino & Fernandez de Molina, 1986a; Finch et al., 1986; Jones, 1990b), membrane afterhyperpolarizations are likely to play an important role (Alonso & Klink, 1993). Membrane afterhyperpolarizations follow the occurrence of spikes in stellate and non-stellate neurons in layer II of the entorhinal cortex, and the afterhyperpolarizations which follow spike *trains* in stellate cells can last for up to about 2.5 sec (Alonso & Klink, 1993). The late hyperpolarization in entorhinal cortex neurons has been modelled here with the synaptic component, H, which

is longer lasting than I and F . The prolonged time course of this component results from ϵ_3 in Equation 4 which has a value of 0.9. The parameter ϵ_0 in Equation 1 reduces the magnitude of the component so that it is relatively small compared to the faster inhibition mediated by I (Figure 5.1B).

Synaptic Frequency Response Characteristics. Two sets of simulations were run to assess the interactions between the three connection weight components. In all simulations, theta-frequency was assumed to be 10 Hz, or one cycle every 100 msec, and each discrete time step was taken to represent 20 msec so that five time steps correspond to one theta cycle. During early simulations, the frequency response characteristics of the model synapse in response to combinations of varying parameters, restricted by the relation $\epsilon_2 < \epsilon_1 < \epsilon_3$ described above, were examined. The final values of the parameters were chosen to provide a net facilitation of the connection weight (W) after 5 time steps, and to facilitate the response of the synapse most strongly at frequencies near 10 Hz ($\epsilon_2=0.55$, $\epsilon_1=0.75$ and $\epsilon_3=0.9$).

The behaviour of a synaptic model including only the facilitatory component, F , and the early inhibitory component, I , was compared to a model which also included the late inhibitory component H . The responses of the connection weight components in both synaptic models to a single input at $t=0$, and the sum of the components according to Equation 1, are shown in Figure 5.1. Both models responded similarly to a single input, and the values of W were affected most strongly by the components F and I . Immediately following an input, I is of larger absolute value than F , and the net effect of the two components is to render the potential connection strength, W , inhibitory. Because I decays faster than F , however, the amount of inhibition relative to facilitation decreases, and after 5 time steps a maximal facilitation of the

connection weight results (Figure 5.1). Although the effect of inhibition in the model synapse shortly after stimulation is stronger than that observed experimentally, the facilitation of the connection weight at 100 msec is similar to the paired-pulse facilitation effects in the entorhinal cortex following medial septum stimulation which peak at intervals between 50 and 100 msec (Figure 3.7).

In contrast to the synaptic response to a single input, the frequency response characteristics of the two models to multiple inputs were very different. In the model with only components F and I, the connection weight increased monotonically with stimulation frequency, and did not respond preferentially to intermediate input frequencies (Figure 5.2A). Although the synaptic output induced by theta-frequency stimulation was greater than that produced by 5 Hz stimulation, responses to 25 Hz stimulation reached similar values. The synaptic model including only F and I was therefore inadequate for modelling frequency potentiation effects in the medial septal projection to the entorhinal cortex since responding to 25 Hz stimulation in this pathway is much reduced compared to that induced by theta-frequency stimulation (Figure 3.14 bottom).

The effect of the slowly decaying late inhibitory component, H, on the frequency response characteristics of the synaptic model was marked. While part of the effect of adding this component was to reduce synaptic output across all stimulation frequencies, the effect was strongest in inhibiting synaptic output during high-frequency activation (Figure 5.2B). This effect is analogous to the increased afterhyperpolarizations observed in entorhinal cortex stellate cells following bursts of action potentials (Alonso & Klink, 1993). The connection weight of the model synapse containing all three synaptic components more closely resembled the frequency response characteristics

observed experimentally during frequency potentiation tests of the medial septal projection to the entorhinal cortex. It also reflects the inhibition in response amplitude observed during the highest frequencies of stimulation (Figure 3.14 bottom). This model synapse was incorporated into the neural network simulations described in the next section to provide frequency potentiating input from the medial septal units to the entorhinal cortex units.

Hebbian Synapses.

More conventional, Hebbian synapses were used to model plasticity in connections from the pyriform cortex to the entorhinal cortex in the network simulations (Sejnowski & Tesauro, 1989; Brown et al., 1990). Hebbian synaptic enhancements have been demonstrated in this pathway in response to tetanic stimulation of the pyriform cortex (Experiment 4.2; Alonso et al., 1990), and the amount of LTP induced can be enhanced by low-frequency stimulation of the medial septum (Experiment 4.3). The Hebbian connection weight changes in the model were implemented according to the algorithm:

$$W_{ij}(t+1) = W_{ij}(t) + \epsilon_L Y_i(t) Y_j(t) - \epsilon_D W_{ij}(t), \quad (5)$$

where ϵ_L controls the rate of learning, ϵ_D is a decay parameter which limits growth in the absolute values of the connection weights, and $Y_i(t)$ is the activation value of unit i at time t . Because changes in the connection weight depend in part on levels of post-synaptic activation, cooperative interactions between multiple inputs to the same unit can enhance weight changes (Sejnowski & Tesauro, 1989). The initial connection weights were set to small random values ranging between 0 and 0.1, and ϵ_L was set to 0.01. The activation value of each entorhinal cortex unit (Y_i) was the linear sum of its synaptic inputs which were defined by the product of the presynaptic activation value and the connection weight.

5.2 NETWORK MODELLING

Network Architectures. The network modelling performed here was used to assess the effects of frequency potentiation on Hebbian learning in two different network architectures. A simple architecture composed of three cellular populations was implemented for the first set of network simulations (Figure 5.3A). The layer of target cells in the entorhinal cortex received excitatory inputs from a layer of pyriform cortex units, and from a layer of medial septal units. There were 10 units in each layer, and both sets of afferents were fully connected with entorhinal cortex units. Medial septal units were connected to each of the entorhinal cortex units via frequency potentiating synapses, and pyriform cortex units were connected to each entorhinal cortex unit by Hebbian synapses.

In a second set of simulations, the entorhinal cortex layer was augmented with a layer of inhibitory inter-neurons (Figure 5.3B) to allow pattern specialization within the output layer by competitive interactions between the units. This network allowed an assessment of how frequency potentiation would modify learning in a network in which the entorhinal cortex units learned different *patterns* of activation in response to the input patterns. In this network, the number of pyriform cortex units was reduced to 4, and only 2 entorhinal cortex units and 2 recurrent units were used in order to assess the ability of the output layer to form distinct responses to different pyriform cortex input patterns with more limited computational resources. The pyriform cortex synapses were adapted using Equation 5, as were the connections from entorhinal units to inhibitory interneurons (V_{ij}), and the reverse connections from the inhibitory units to the entorhinal cortex units (V_{ij}). This part of the model is identical to the

skew-symmetric network proposed by Plumbley (1993) to which the frequency-potentiating medial septal inputs were added. Remarkably, Plumbley showed that for this type of network, a simple Hebb rule (Equation 5) will cause the output units to produce decorrelated output patterns in response to the training set. For the Hebbian synapses V_{ji} and V_{ij} , ϵ_a and ϵ_b were set to 0.03 and 0.1, respectively. For the connections from the pyriform cortex to the entorhinal cortex, the values were 0.01 and 0.4 (and 0.01 and 0 for the network in Figure 5.2A without inhibitory units).

In Plumbley's model, the following equations are applied to determine the activation values of the principal excitatory output units, and inhibitory interneuronal units, respectively:

$$Y_i(t) = \sum_j W_{ij} Y_j(t) - \sum_j V_{ij}(t) Z_j(t) \quad (6)$$

$$Z_j(t) = \sum_i V_{ji}(t) Y_i(t) \quad (7)$$

where Z_j are the inhibitory unit activation values, and V_{ij} are their synaptic weights. These equations were implemented in the present simulation through an iterative activation value update rule for the entorhinal cortex units' activities, Y_i , which allows the gradual approximation of Equations 6 and 7 over many cycles of training:

$$Y_i(t) = 0.75Y_i(t-1) + 0.25(\sum_j W_{ij} Y_j(t) - \sum_j V_{ij}(t) Z_j(t)) \quad (8)$$

Simulations. The contribution of theta-frequency input from the medial septum to plasticity in pyriform cortex inputs to the entorhinal cortex was assessed by testing the model in Figure 5.3A with four different pyriform cortex input patterns. Two of the patterns were presented to the network in the absence of septal input, and the other two patterns were presented concurrently

with theta-frequency medial septal inputs. Each pyriform cortex input pattern consisted of the activation of two of the 10 pyriform cortex units so that 2 units had an activation value of 1, and the rest had an activation values of 0. The patterns were,

- 1) Pyriform cortex units 1 and 2, with septal input,
- 2) Pyriform cortex units 5 and 6,
- 3) Pyriform cortex units 3 and 4, with septal input, and
- 4) Pyriform cortex units 7 and 8.

No pyriform cortex unit was activated during two different input patterns, and two of the 10 pyriform units (units 9 and 10) were never activated. The network was trained for 20 time steps during the presentation of each pattern and the four input patterns were presented to the network in the above order to complete one training cycle. When medial septal inputs were present, all 10 medial septal units were activated on every 5th time step with an activation value of 1. Allowing the network to run for the time needed for 4 theta cycles (20 time steps) resulted in the development of frequency potentiation of the medial septal inputs when they were active (Figure 5.2B). There were 10 training cycles in each simulation.

The network was tested under two conditions. In one set of simulations, the pyriform cortex inputs were presented on every time step during training. Then, in order to assess the effect of phase-locking the pyriform cortex inputs with the frequency potentiating medial septal inputs, the pyriform cortex input patterns were presented only on every 5th time step, in synchrony with the medial septal inputs during patterns in which medial septal inputs were activated. Five separate simulations were performed under each of the two conditions. To monitor learning during each simulation, the connection weights

for the pyriform cortex projections to the entorhinal cortex were recorded after each training cycle. The entorhinal cortex unit activation values resulting from the presentation of each pyriform cortex input pattern on one time step were also recorded after each training cycle (without changing the connection weights).

Two sets of simulations were performed using the network shown in Figure 5.3B. In one set of simulations the regular skew-symmetric network proposed by Plumbley was implemented without frequency potentiation, and in the other set of simulations two of the four pyriform cortex input patterns were paired with frequency potentiating medial septal input. Each input pattern consisted of the activation of one of the four pyriform cortex units, and the patterns were normalized to have zero means across the set of input units (Plumbley, 1993). The input patterns were each presented over 20 time steps in the following order to complete one training cycle:

- 1) Pyriform cortex unit 1, with septal input,
- 2) Pyriform cortex unit 2,
- 3) Pyriform cortex unit 3, with septal input, and
- 4) Pyriform cortex unit 4.

Septal inputs were included only in the second set of simulations, and in all simulations, the pyriform cortex input patterns were presented on every time step. On each time step the activation value equation (Equation 8) was iterated until the norm (i.e., root sum of squares) of changes in the entorhinal cortex unit activation values was reduced to a value less than 0.001. The output unit activities were thus permitted to gradually settle to a fixed point prior to calculating the Hebbian weight changes. The network was considered fully trained when the norm of the changes in the weights connecting pyriform cortex units to the entorhinal cortex units had decreased to a value below 0.01.

Network Modelling Results.

Enhanced Hebbian Learning During Septal Input. Cooperative enhancements of Hebbian synaptic plasticity were observed in both sets of simulations run using the network shown in Figure 5.4. During training, the connection weights of the pyriform cortex projections to the entorhinal cortex, and the activation values of the entorhinal cortex units were monitored after each training cycle. Because this network lacked inhibitory interneurons, changes in the connection weights from a given pyriform cortex input unit to all the entorhinal cortex units were very similar during training; the weights for each pyriform cortex unit were therefore averaged. This allowed the comparison of the results for the two different sets of simulations in which pyriform cortex input patterns were either presented constantly, or only on every 5th time step phase locked to the medial septal inputs (Figure 5.4).

In both simulations, the effect of adding theta-frequency medial septal inputs during some of the pyriform cortex input patterns was to greatly enhance the weights in the pyriform cortex projections which were coactive with the medial septal inputs (input units 1-4). Enhancements were not as large in the connection weights of pyriform cortex units when input patterns were not associated with septal input (input units 5-8). No weight increases were observed in units 9 and 10 which were never activated by any input pattern (Figure 5.4).

The weight changes were also affected by whether or not pyriform input patterns were presented to the network on every time step, or only on every 5th time step, in synchrony with medial septal input when present. When constant patterned input was presented, all weights reached larger values

(except for the inactive units 9 and 10). However, when the pyriform inputs were presented only on every 5th time step, the weights differentiated much more quickly depending on the presence of medial septal input, and reached proportionately more disparate values depending on whether the patterns were paired, or not paired, with medial septal input (Figure 5.4B).

These results were mirrored in the effect of training on entorhinal cortex activation values in response to the four pyriform cortex input patterns. Because the connection weights of a given pyriform cortex unit onto all of the entorhinal cortex units were similar, all entorhinal cortex units were activated to a similar extent by the presentation of a given pyriform cortex input pattern. The similarity in responding allowed the averaging of the entorhinal cortex activation values to provide a measure of the response to each input pattern (Figure 5.5). Similar to the results observed for the connection weights, the activation values showed larger increases when the patterns were paired with medial septal input and when constant pyriform cortex input was presented during training. Further, the responses to patterns either paired or not paired with medial septal stimulation were differentiated more quickly, and reached proportionately more disparate values, when the pyriform cortex inputs were phase-locked with the medial septal inputs (Figure 5.5).

Effects of Septal Input on Hebbian Decorrelation. In order to train entorhinal cortex units in the network to learn different spatial codes for the different pyriform cortex input patterns, and in order to test the effects of frequency potentiation on the learned patterns, the decorrelating network shown in Figure 5.3B, which includes recurrent inhibitory units, was used. Activation values in this network were able to reach negative values after training due to the effect of the inhibitory interneurons. When the network was trained on four

pyriform input patterns in the absence of medial septal input, the two entorhinal cortex output units tended to become uncorrelated by showing a different pattern of activation in response to the different input patterns (Plumbley, 1993). One input pattern resulted in large activation values in both output units, one pattern resulted in small activation values in both units, and the remaining patterns resulted in large activation values in only one of the two output units (Figure 5.6A). This general pattern was consistent, but the specific pattern preferences of the units varied across simulations due to the random initial weights.

In the second set of simulations in which two of the pyriform cortex input patterns were paired with frequency potentiating septal input during training, the patterns associated with the added input tended to produce positive outputs and the non-potentiated patterns tended to produce more negative outputs (Figure 5.6B). The spatial coding of the responses to the input patterns was still maintained, however, since, relative to each other, the output units responded more strongly to one of the patterns associated with medial septal input and one of the patterns not associated with medial septal input (Figure 5.6B). The effect of coactivating medial septal inputs with pyriform cortex input patterns in this network, then, was to separate the responses of the entorhinal cortex units into two distributions by increasing the amplitude of responses evoked by patterns which were paired with frequency potentiation. This occurred while preserving the ability of the entorhinal cortex units to learn distinct spatial representations for all of the input patterns. More training cycles were required for this network to settle to a solution (mean=37.2; range= 26 to 44) than were required by the network in which frequency potentiating inputs were not added (mean=6.4; range= 5 to 7).

Figure 5.1

Figure 5.1. Determination of the potential connection weight strength (**W**) by the effects of a single synaptic input on the synaptic weight change components at $t=0$. In **A**, the connection weight following activation of only the facilitatory (**F**) and early inhibitory (**I**) components is shown. In **B**, the added effect of the slow inhibitory (**H**) component on the potential connection weight is shown. In both cases in which a single input is presented at $t=0$, the potential weight strength is optimal after five time steps (simulated to represent 100 msec).

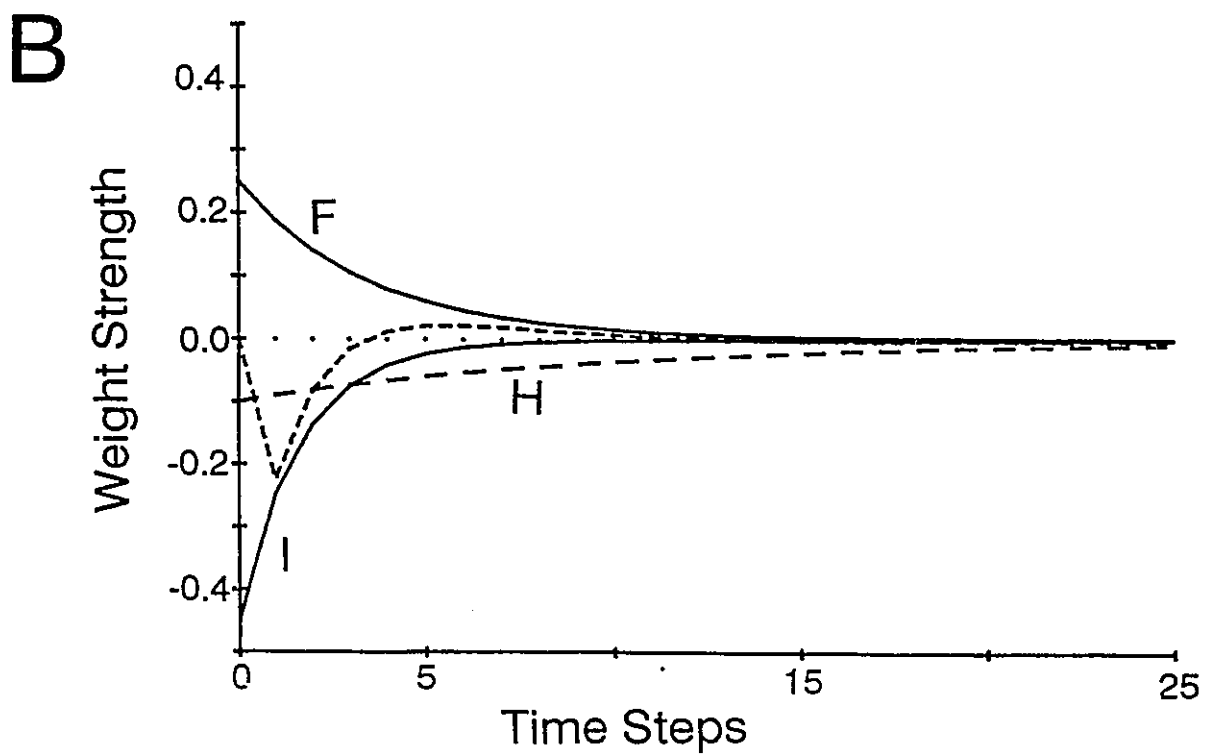
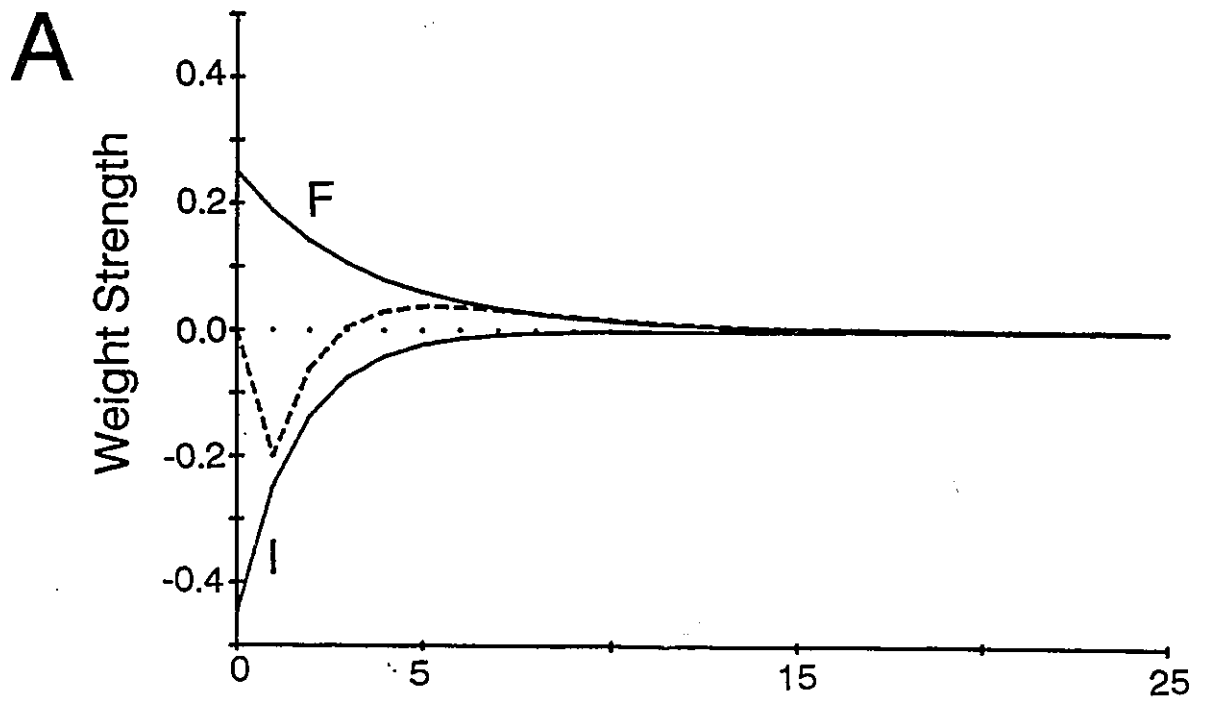


Figure 5.2

Figure 5.2. The frequency response characteristics of the potential connection weights of the two different synaptic models, one without the slow inhibitory component (**A**), and one including this component (**B**), are contrasted here by their responses to the delivery of multiple inputs at the three indicated frequencies. Each time step is modelled to represent 20 msec so that five time steps correspond to one 10 Hz theta cycle. The upper trace in each panel indicates the timing of the inputs which have a value of 0 or 1. Middle traces indicate the potential connection weight strength of the synapse. Lower traces are the product of the potential connection weight and the synaptic input, and represent the synaptic contribution to post-synaptic activation. In the synaptic model with only one inhibitory component (**A**), for all stimulation frequencies the synaptic output values are larger than in the synaptic model with two inhibitory components, and the synaptic output increases monotonically with stimulation frequency. In the synaptic model with two inhibitory components, the response of the synapse is optimal for frequencies of stimulation in the theta range, and are depressed at the highest stimulation frequencies. While synaptic outputs in the model are impulses occurring on discrete time steps, synaptic outputs are illustrated here by joining consecutive values for consecutive time steps. Horizontal calibration, 5 time steps (100 msec); vertical calibration 0.05.

A

5 Hz

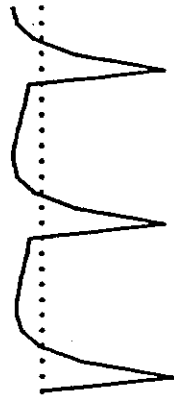
10 Hz

25 Hz

Synaptic
Input



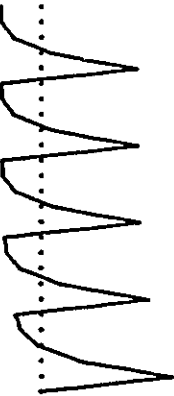
Potential
Weight



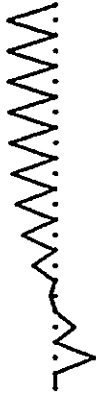
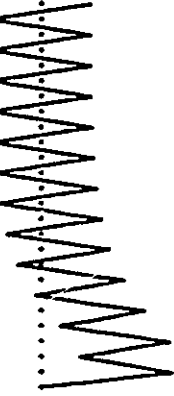
Synaptic
Output



Synaptic
Input



Synaptic
Input

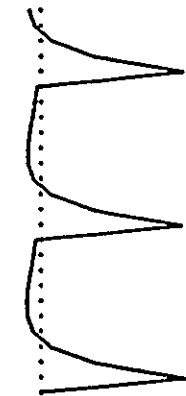


B

Synaptic
Input



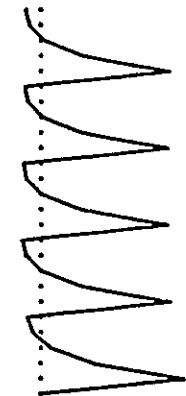
Potential
Weight



Synaptic
Output



Synaptic
Input



Synaptic
Input

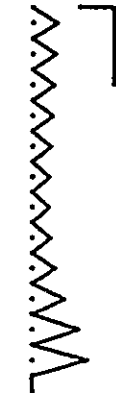
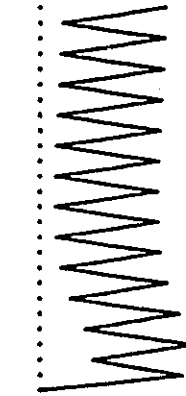
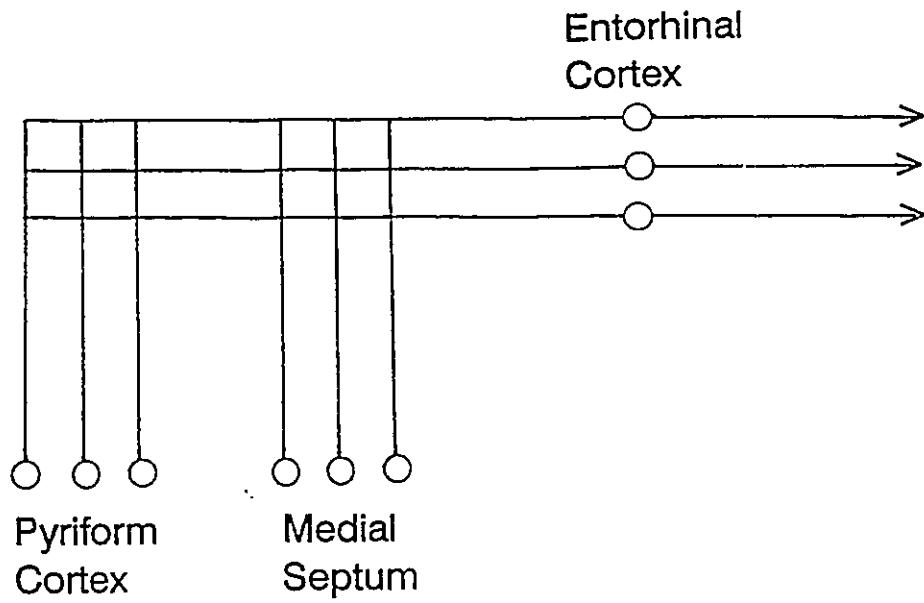


Figure 5.3

Figure 5.3. Schematic representations of the two network architectures used in separate simulations. In **A**, the units are fully connected in a feedforward manner, but only three of the ten units in each cellular population are shown. Synaptic connections from the pyriform cortex to the entorhinal cortex support Hebbian synaptic modification, and theta-frequency activation of medial septal afferents results in frequency potentiation of activation values in the entorhinal cortex. In **B**, fully-connected recurrent inhibitory units were added to the network for simulations using Plumbley's (1993) learning algorithms. There were 10 medial septal units in this network but all units in other layers of the network are shown.

A



B

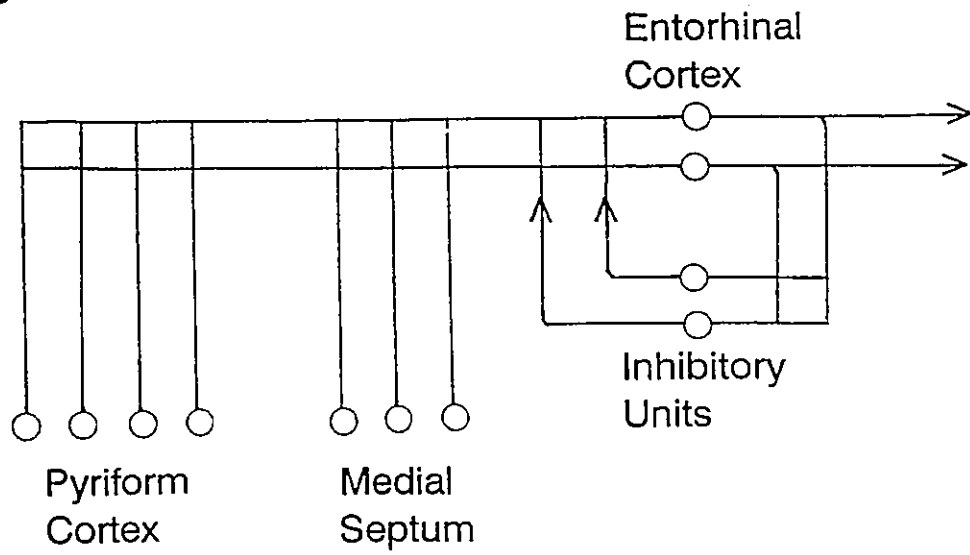
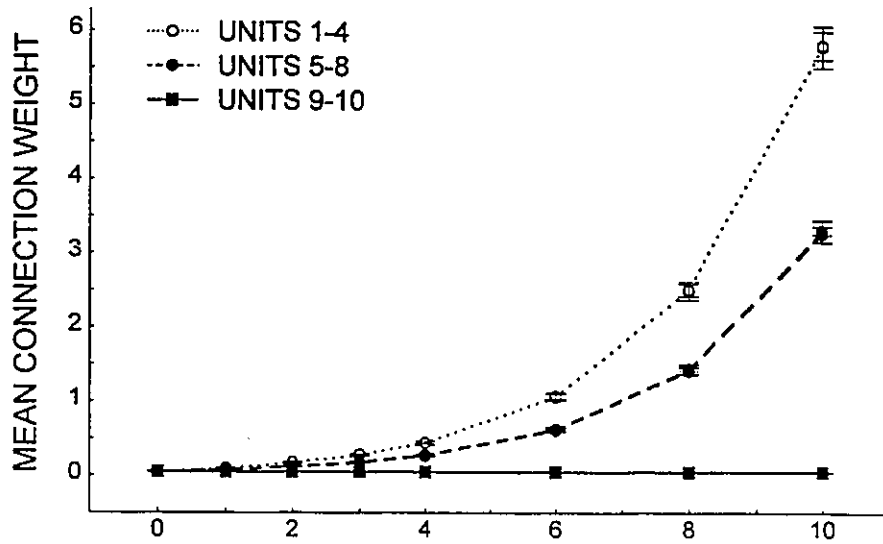


Figure 5.4

Figure 5.4. Changes during training in the mean of the connection weights associated with each pyriform cortex input unit. Results shown in **A** are from a set of simulations in which constant pyriform cortex input was presented at each time step. Results shown in **B** are from a second set of simulations in which pyriform cortex input patterns were presented only on every 5th time step, in synchrony with the frequency potentiating medial septal inputs when they were active. Bars indicate twice the standard error of the mean across 5 separate simulations.

A



B

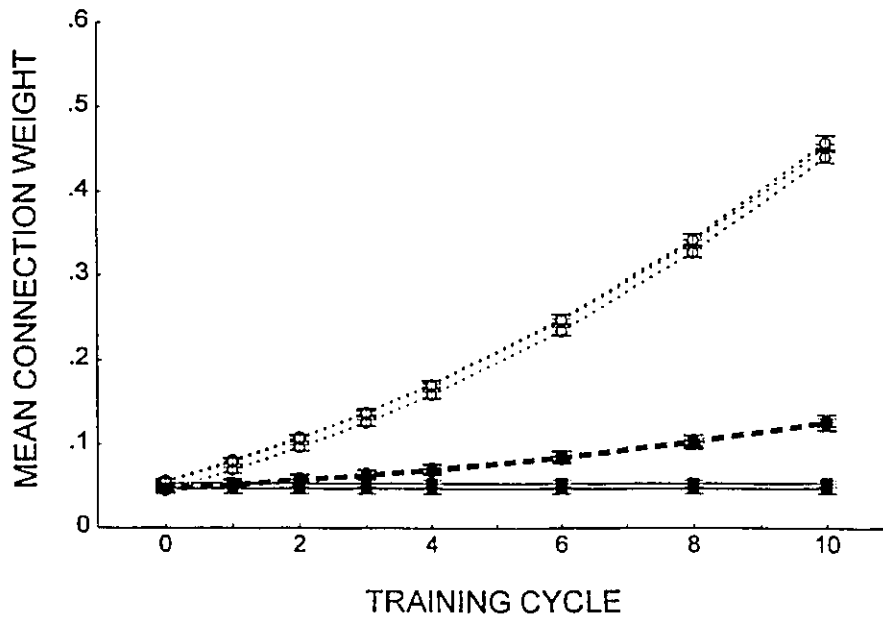
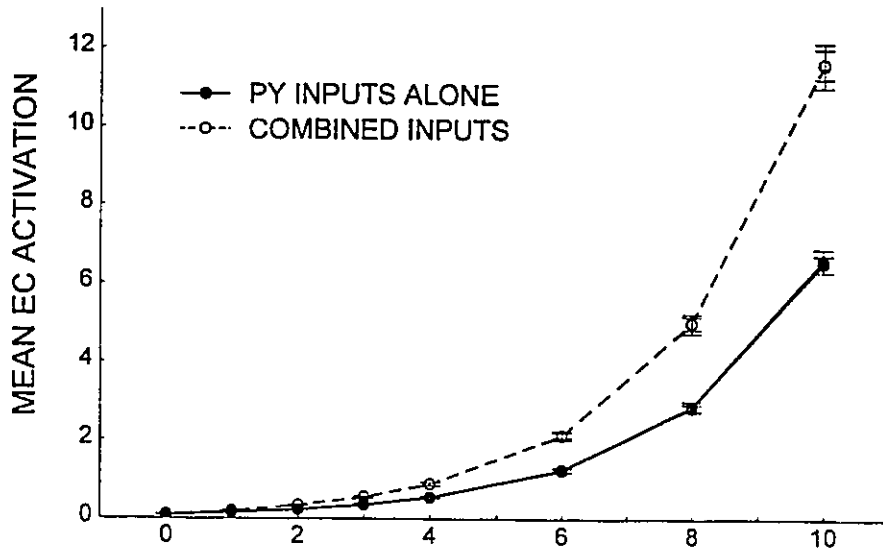


Figure 5.5

Figure 5.5. The average activation level of the 10 entorhinal cortex units in response to each of the 4 pyriform input patterns is shown as a function of training cycle. In **A** pyriform cortex input was present at each time step. In **B**, pyriform cortex input patterns were presented only on every 5th time step, in synchrony with medial septal activation. In both cases the **dashed lines** show the average responses to pyriform cortex input patterns which were associated with medial septal input, and **solid lines** show the average responses to patterns not associated with medial septal input. Values were obtained from the same 5 simulations used to provide measures of connection weight changes shown in Figure 5.4.

A



B

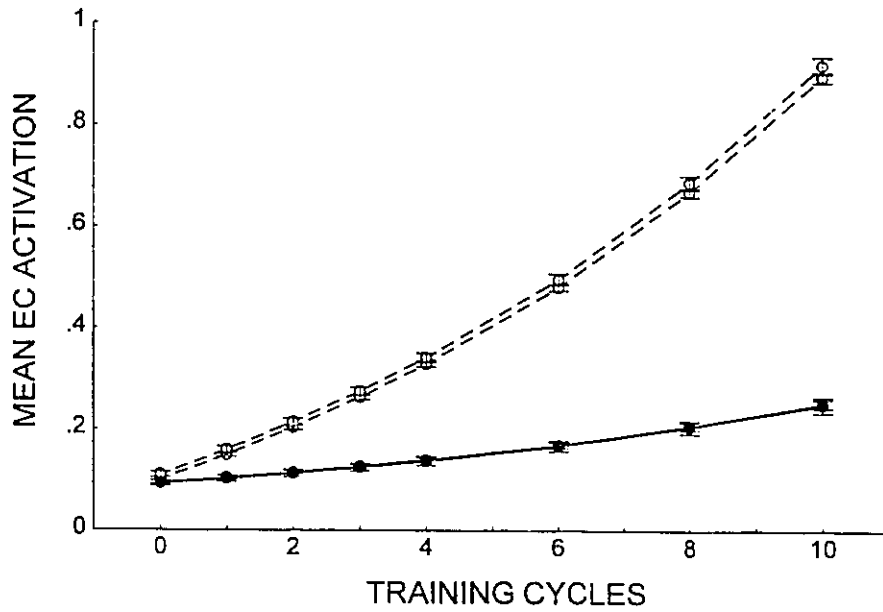
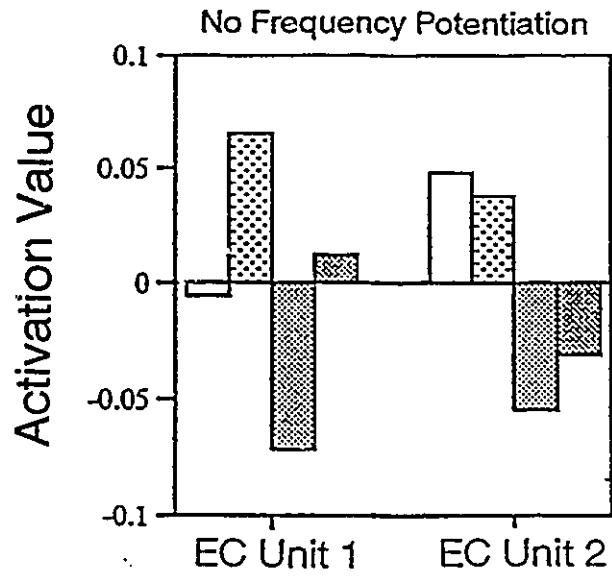


Figure 5.6

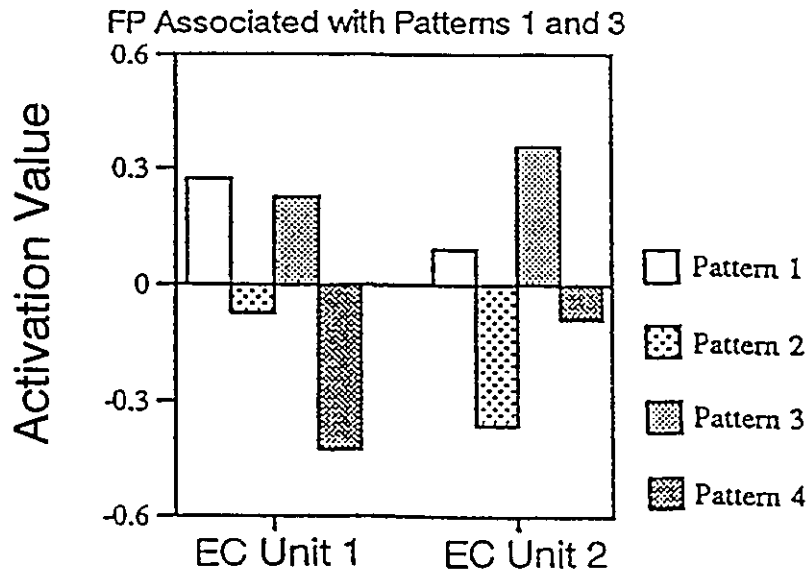
Figure 5.6. Entorhinal cortex unit activation values in response to each of the four pyriform cortex input patterns following training of the network model shown in Figure 5.3B. In **A**, response patterns following training of the decorrelating network without medial septal inputs are shown. In **B**, the response patterns following training of the network with frequency potentiating medial septal activation associated only with pyriform cortex input patterns 1 and 3 are shown.

Figure 5.6

A



B



DISCUSSION

The synaptic model presented here was used to formalize one possible way in which separate physiological mechanisms may combine to result in frequency potentiation in neural systems during low-frequency activation. The network models were used to explore the ways in which synapses with frequency potentiation characteristics can lead to cooperative interactions between separate populations of synaptic inputs to result in enhanced Hebbian learning. These computational simulations were partly based on facilitatory and inhibitory mechanisms believed to contribute to frequency potentiation effects in forebrain pathways including the projection from the medial septum to the entorhinal cortex (Figures 3.5 & 3.7). They were also based on the finding that low-frequency medial septal activation can cooperatively enhance the induction of long-term synaptic potentiation in pyriform cortex efferents to the entorhinal cortex (Experiment 4.3). The application of these modelling approaches has allowed the study of how frequency potentiation effects may contribute to Hebbian learning in a manner that is not possible using standard physiological techniques.

Synaptic Modelling. An important issue in the process of modelling neurons and neural systems is the extent to which detailed physiological characteristics of the neural system should be represented in the model (McClelland & Rumelhart, 1986; Durbin, 1989; Segev, 1992). While parameters affecting synaptic transmission and membrane conductances can be critical for models designed to investigate the mechanisms which control the dynamics of membrane potential and spiking behaviour (Segev, 1992), these parameters are often not known, can be computationally expensive to implement, and may be

superfluous to the computational function of the network as a whole (Cohen et al., 1992). Further, it may be impossible to know *a priori* which physiological characteristics are essential for the property of interest in the neural system.

In the synaptic modelling described here, the approach was to formulate a simple, autonomous set of algorithms which were modelled after known physiological phenomena, and which could capture the time-course of experimentally-observed frequency potentiation. In order to obtain the desired synaptic frequency response characteristics, it was necessary to include two inhibitory components in the synaptic model (Equations 1-4; Figure 5.2). The three synaptic weight change components have correlates to the physiological mechanisms which control the dynamics of Ca^{2+} -dependent neurotransmitter release (F), and the effects of inhibitory interneurons (I), and long-lasting hyperpolarizations (H). The inhibitory mechanisms controlling frequency potentiation could have been instantiated in the model through a separate layer of inhibitory interneurons (I), or through firing-related inhibition of the entorhinal cortex unit activation values (H). However, the Hebbian synaptic modifications reported here are dependent on total levels of postsynaptic depolarization, and if it is assumed that the strength of these alternate inhibitory mechanisms is linearly related to the number of septal fibers activated, then the use of these alternate instantiations of I and H would not have changed the modelled effects of frequency potentiation on Hebbian learning. Including the three components in a single set of synaptic update algorithms therefore provided a simple and adequate model suited for further investigations of the potential computational functions of frequency potentiating inputs.

Network Modelling. The set of simulations using the network architecture shown in Figure 5.3A formalized the mechanism proposed in

Experiment 4.3 through which low-frequency medial septal stimulation leads to cooperative enhancements of long-term potentiation in pyriform cortex efferents to the entorhinal cortex (Figures 3.14 bottom, & 4.12). In the model, synaptic strengthening was selectively enhanced in some pyriform cortex input patterns depending on the presence of the added post-synaptic activation caused by frequency potentiating medial septal inputs (Figure 5.4). The entorhinal cortex thereby learned to respond preferentially to pyriform cortex input patterns which had been previously paired with frequency-potentiating medial septal input (Figure 5.5). These simulations indicate a way in which activity in medial septal inputs to the entorhinal cortex can cause a selective enhancement of the response of the entorhinal cortex to certain olfactory inputs.

The contribution of phase-locking the pyriform cortex and medial septal inputs to the entorhinal cortex was assessed qualitatively by comparing the effects of constant pyriform cortex inputs with those of inputs synchronized with medial septal inputs. Proportionately greater weight increases occurred for patterns phase-locked to medial septal input (Figure 5.5). This result follows from differences in the proportion of time-steps on which pyriform cortex and medial septal inputs were coincident. There was a combined effect of both inputs on post-synaptic activation only on 20% of the time steps when constant pyriform cortex input was presented, and on 100% of the time-steps when theta-frequency pyriform cortex inputs were presented.

These results highlight the importance of temporal coincidence in multiple afferents in systems supporting cooperative Hebbian learning. Similarly, Singer (1993) has proposed that oscillatory activity may serve as a mechanism to increase the specificity with which use-dependent synaptic modifications may occur. Because temporal correlations between converging

inputs are so critical to Hebbian synaptic modification, and because the response of neurons to input may last hundreds of milliseconds, the determination of which synapses will be modified may be made much more specific by oscillatory activity (Singer, 1993). Frequency potentiating mechanisms contributing to rhythmic depolarization in the entorhinal cortex during periods of theta activity could provide one mechanism for the selective enhancement of synaptic inputs that are phase-locked to the depolarizing phase of the theta rhythm.

In the network in Figure 5.3A, a given input pattern resulted in similar levels of activation in all of the entorhinal cortex units, so that the spatial coding of the pyriform cortex input patterns was lost. The network shown in Figure 5.3B was then used to determine how frequency potentiating inputs could affect the formation of spatial representations in the entorhinal cortex based on the decorrelating activation value algorithms proposed by Plumbley (1993; Oja, 1982). The ability of this network to form distinct spatial representations of the input patterns results from competitive interactions between the principal output units mediated by recurrent inhibition in the added layer of interneurons. While inhibition in the entorhinal cortex is thought to be mediated mostly through feedforward connections (Finch et al., 1988), feedback inhibition is a common mechanism in cortical tissue. Also, inhibitory neurons in the superficial layers of the entorhinal cortex have the sort of extensive axonal arbourizations (Jones & Buhl, 1993) which could mediate the sort of competitive inhibition modelled in the decorrelating network.

The adaptation of the model proposed by Plumbley (1993) in the present simulations illustrates a computational role which could be played by the remarkably strong inhibitory mechanisms in the entorhinal cortex (Finch &

Babb, 1980; Colino & Fernandez de Molina, 1986; Jones 1990; 1993). Inhibitory interneurons in the entorhinal cortex could play a critical role in determining the form of the spatial representations which reach the hippocampal formation (Witter & Groenewegen, 1984; Kuro, 1995; Amaral & Witter, 1989; Witter et al., 1989). Further, the simulations in which frequency potentiating inputs were added to this network (Figure 5.6) suggest that such a competitive mechanism could operate in parallel with the training of the entorhinal cortex to respond strongly to patterns associated with medial septal inputs, and weakly to other patterns.

CHAPTER 6

GENERAL DISCUSSION

Several approaches have been used here to analyze activity-dependent synaptic enhancements in the monosynaptic projection from the pyriform cortex to the entorhinal cortex in the rat. The first experiments, reported in Chapter 2, provided a necessary foundation for the interpretation of evoked field potentials recorded from single cortical depths in later chapters. The results of current source density analyses indicated that there is an overlap of the current sinks generated by pyriform cortex and medial septal inputs in layers II and III of the entorhinal cortex. These results are shown in Figures 2.8 and 2.13, and are consistent with the known anatomy of these pathways (Luskin & Price, 1983; Gaykema et al., 1990). Later occlusion tests in chronic animals provided additional evidence for a convergence of pyriform cortex and medial septal inputs onto the same superficial entorhinal cortex neurons (Figure 3.12).

The identification of the synaptic currents evoked in the entorhinal cortex by pyriform cortex stimulation also provides the necessary groundwork for further studies of plasticity in this pathway in chronic preparations. The entorhinal cortex is of growing interest with regard to learning and memory (Squire & Zola-Morgan, 1991; Van Hoesen et al., 1991; Otto & Eichenbaum, 1992; Jones, 1993), and the projection from the pyriform cortex offers a model system for the study of plasticity in sensory afferents to the entorhinal cortex. The use of the chronic preparation affords a greater confidence that observed experimental results are not affected by the effects of more invasive

experimental procedures. Studies which have sought links between LTP effects and learning have focused on the hippocampus (McNaughton et al., 1986; Morris, 1989; Sakimura et al., 1995) and on the olfactory inputs to the pyriform cortex (Roman et al., 1987). The entorhinal cortex links these two systems and interactions between olfactory learning performance and LTP in pyriform cortex efferents to the entorhinal cortex might also be of interest. The chronic preparation could also be used for more exhaustive parametric testing of the optimal frequencies and patterns of stimulation for the induction of LTP, as well as pharmacological tests of neuromodulatory influences on LTP in this pathway.

The major experimental findings concerning synaptic plasticity reported here include both short-term facilitation effects and long-lasting potentiation effects. Also reported were enhancements of the LTP induced in the entorhinal cortex by intense pyriform cortex stimulation with concurrent frequency potentiating stimulation of either the pyriform cortex or the medial septum.

Short-Term Facilitation. Paired-pulse facilitation and frequency potentiation of responses evoked in the entorhinal cortex by stimulation of the pyriform cortex and/or medial septal area were reported in Chapter 3. Frequency potentiation has been used here as a measure of the responsiveness of the entorhinal cortex to rhythmic activity in these afferent pathways (Figure 3.13 & 3.14). Similar procedures have been used to monitor the frequency sensitivity of the afferent pathways of the olfactory bulb (Nickell & Shipley, 1988), pyriform cortex (Hasselmo & Bower, 1990; Mokrushin & Emel'yanov, 1991, 1993) and hippocampal formation (Anderson & Lomo, 1968; Deadwyler et al., 1975; Munoz et al., 1991). In the present study, it was found that frequency potentiation in the entorhinal cortex induced by pyriform cortex stimulation was optimal at frequencies between 12 and 16 Hz (Figure 3.14 top).

If *spontaneous* rhythmic activity in the pyriform cortex also leads to frequency-dependent enhancements of responses in the entorhinal cortex, then sensory representations carried by oscillatory activity at frequencies near 14 Hz may be processed preferentially by the entorhinal cortex, and may be transmitted preferentially to the hippocampal formation. Spectral power in spontaneous EEG is observed at frequencies between 6 and 18 Hz in the rat pyriform and entorhinal cortices, and power in these structures shows some coherence, or consistency in phase relationships at these frequencies ($C \approx 0.25$; Boeijinga & Lopes da Silva et al., 1988). Following either odour sampling or shock stimulations of olfactory afferents, however, bursts of oscillatory "gamma" activity at a frequency near 40 Hz spread from the olfactory bulb to the pyriform and entorhinal cortices (Freeman, 1978; Freeman & Schneider, 1982; Boeijinga & Lopez da Silva, 1988, 1989; Wilson & Bower, 1992; Kay & Freeman, 1994). Frequency potentiation in the tests reported here showed a decline at frequencies of stimulation above 16 Hz, but frequency potentiation was also observed during frequencies of stimulation at the low end of the gamma band (30 Hz) in the present study. While the frequency potentiation effects reported here are clearly not tuned to the gamma frequency band, frequency potentiation mechanisms may contribute to some extent to the transmission of gamma bursts to the entorhinal cortex.

The cellular mechanisms which result in frequency potentiation at central nervous system synapses are poorly understood, and more extensive intracellular studies are needed to directly measure the activities in principal entorhinal cortex neurons and inhibitory interneurons during different frequencies of stimulation. Presynaptic facilitation of neurotransmitter release likely contributes heavily to frequency potentiation (Turner & Miller, 1982;

Applegate & Landfield, 1988), but the contributions of inhibitory mechanisms are not clear. Field potential paired-pulse tests reflect the time course of net response facilitation and depression, but do not provide direct measures of frequency-dependent changes in inhibitory mechanisms such as IPSPs and afterhyperpolarizations. Intracellular recordings in the entorhinal cortex have been reported for only a few frequencies of stimulation (Finch et al., 1986; Jones, 1990b), and the responses of inhibitory neurons to low-frequency stimulation have not been characterized, partly because of difficulty of obtaining recordings from these sparsely distributed cells.

More detailed information about the frequency response characteristics of facilitatory and inhibitory systems could contribute to the construction of more physiologically realistic computational models of short-term plasticity in the entorhinal cortex. The synaptic model developed in Chapter 5 was used to explore certain computational functions which frequency potentiation may contribute to at the network level. As more information on the critical cellular mechanisms which underlie frequency potentiation becomes available, modelling efforts may begin to incorporate these elements and examine more exhaustively the conditions under which these mechanisms may contribute to spontaneous neuronal information processing, signal transmission and memory formation.

Long-Lasting Potentiation. Activity-dependent enhancements of synaptic strength in pyriform cortex efferents to the entorhinal cortex have been shown to result from both epileptogenic stimulation of the pyriform cortex (Experiment 4.1), and from high-frequency stimulation of the pyriform cortex (Experiment 4.2). The functional significance of synaptic plasticity in the entorhinal cortex is not known, but a contribution to the storage of some form of

olfactory memory in the entorhinal cortex is possible. Further, because the plasticity occurs in the same layers which contain cells that project to the hippocampal formation (Figure 2.8; Steward & Scoville, 1976), long-term changes in the transmission of olfactory information to the hippocampal formation could result from a strengthening of these synapses. Similar modifications in other sensory inputs to the entorhinal cortex have not been assessed.

The manipulations which have been used here to induce and to enhance LTP induction may offer some insights into the types of spontaneous neuronal activity which may contribute to learning-related synaptic modifications in the entorhinal cortex. Rather intense activation of the entorhinal cortex was necessary to induce these lasting synaptic potentiation effects. Large afterdischarges occurred in the entorhinal cortex during pyriform cortex kindling, and the long, high-frequency trains used to induce LTP also resulted in large *train*-evoked responses. Because LTP induction in this pathway depends on depolarization and NMDA receptor activation (Alonso et al., 1990, de Curtis & Llinas, 1993), the particularly intense stimulation required to induce LTP is likely due to high levels of inhibitory activity in the entorhinal cortex (Jones, 1993; Finch & Babb, 1980; Finch et al., 1988). The high levels of activation required to induce LTP in this pathway suggest that normally-occurring plasticity in this pathway is a highly-regulated process occurring only when inhibition is reduced. Once established, both the kindling-induced potentiation and the LTP effects were long-lasting, raising the possibility that learning-related synaptic plasticity in the entorhinal cortex is similarly durable.

The temporal pattern of activity in pyriform cortex efferents to the entorhinal cortex may contribute to plasticity in this pathway. LTP induction was

increased when low-frequency trains of stimulation resulting in short-term potentiation effects were paired with the high-frequency trains used to induce LTP (Figure 4.6). These enhancements occurred when the 400 Hz trains were preceded by either one or five pulses, so that the critical factor appears to be short-term enhancements in postsynaptic responses, rather than maintained repetitive stimulation. Rhythmic activity may be the primary endogenous cause of short-term synaptic enhancements, however, so that oscillatory activity in olfactory inputs in the theta and gamma bands, as described above with regard to short-term facilitation, may also contribute to conditions which are conducive to the endogenous induction of plasticity in the entorhinal cortex.

The finding that frequency potentiation phenomena can interact with the induction of LTP is consistent with the notion that frequency potentiation effects may play some role in enhancing longer-term changes in neuronal circuits during learning and memory (Andersen & Lomo, 1967; Brown et al., 1983; Landfield, 1988, 1993). Drugs that affect memory (lorazepam and scopolamine) delay the onset of frequency potentiation in CA1 and CA3 regions of the hippocampus (Brown et al., 1983), while not affecting paired-pulse facilitation or post-tetanic potentiation. Further, Landfield and colleagues have provided correlative evidence that some of the learning and memory deficits associated with aging in rats may be related to an impairment in frequency potentiation mechanisms. Frequency potentiation in the CA1 of aged animals rapidly decreases with prolonged (> 15 sec) stimulation at 4 to 12 Hz as compared to young rats (Landfield et al., 1978; Landfield, 1988). The depression in frequency potentiation may be due to enhanced Ca^{2+} -mediated inactivation of presynaptic Ca^{2+} currents (Eckert & Tillotson, 1981; Applegate & Landfield, 1988; Landfield et al., 1986), since aged animals show elevated

voltage-dependent Ca^{2+} influx (Pitler & Landfield, 1990), and reducing Ca^{2+} influx by elevating $\text{Mg}^{2+}/\text{Ca}^{2+}$ ratios in bathing medium enhances frequency potentiation responses in CA1 (Landfield et al., 1986). Aged animals with impaired hippocampal frequency potentiation also show impaired avoidance of foot-shock and place learning relative to young controls (Landfield, 1988; Diana et al., 1994). Aged animals placed on a high Mg^{2+} diet which elevates plasma Mg^{2+} levels and strengthens frequency potentiation *in vivo*, show improved avoidance performance on the reversal phase of a T-maze task (Landfield & Morgan, 1984). Therefore, a treatment which corrects deficits in frequency potentiation in aged rats also enhances their performance in a learning task (Landfield & Morgan, 1984; Landfield, 1988).

Buzsaki (1989) has also proposed a link between long-term information storage and short-term facilitation effects resulting from low frequencies of activity. In this model, theta activity is proposed to lead to transient, heterosynaptic enhancements of mossy fiber synapses onto CA3 pyramidal cells. Following theta activity, during large amplitude irregular EEG activity, the enhancements occurring during theta activity are proposed to result in synchronous population cell discharges in CA3 neurons which are expressed as sharp waves in the EEG record. Which CA3 cells are involved in the sharp wave discharge is thought to be determined by the pattern of afferent input during theta activity, and the discharge is proposed to result in longer-lasting synaptic enhancements in area CA1 which could mediate the storage of information (Buzsaki, 1986, 1989). Further, neurons in the deep layers of the entorhinal cortex, which receive hippocampal inputs and project to neocortical areas, fire in association with sharp waves (Chrobak & Buzsaki, 1994). This suggests that sharp waves may also provide a physiological mechanism for the transfer of hippocampal representations to the neocortex.

Medial Septal Stimulation and LTP Induction. The enhancement of synaptic responses in the entorhinal cortex during low-frequency medial septal stimulation (Figure 3.14 bottom), and the enhancement of LTP in pyriform cortex efferents to the entorhinal cortex by conjoint stimulation of the medial septum (Figures 4.12 & 4.13), have been demonstrated here. These findings add to a body of literature which suggest an important role of the medial septum, not only in learning and memory (Gray & McNaughton, 1982), but also in the modulation of LTP (Robinson & Racine, 1982; Robinson, 1986; Blitzer et al., 1990). The frequency of medial septal stimulation which was sufficient to enhance the LTP effects was within the range of the theta rhythm and induced frequency potentiation. This suggests that septally-driven short-term changes in excitability in the entorhinal cortex during periods of theta activity may also contribute to longer-term changes in information processing in the entorhinal cortex.

Medial septal stimulation may have led to the heterosynaptic facilitation of LTP via the neuromodulatory action of its cholinergic efferents to the entorhinal cortex (Gaykema et al., 1990). Electrical stimulation of the medial septum is likely to have activated both cholinergic and non-cholinergic efferents, however, so it is not clear what neurotransmitter was critical for the cooperativity effect. The hypothesis that the enhancement of LTP was due to the cholinergic inputs is consistent with the effects of cholinergic agonists on cellular responses (Markram & Segal, 1990), and LTP induction in other systems (Burgard & Sarvey, 1990; Blitzer et al., 1990). The contribution of cholinergic inputs to the effects reported here could be investigated by the slow infusion of cholinergic antagonists into the entorhinal cortex *in vivo* in an attempt to block the enhancement of LTP. Also, cholinergic agonists infused during stimulation of

the pyriform cortex might be expected to enhance the amount of LTP induced in this system. The cellular mechanisms mediating the effects of cholinergic agents on LTP induction could be examined through intracellular recordings *in vitro*.

In vitro studies could also contrast the effects of cholinergic agents on the intrinsic versus extrinsic excitatory synaptic inputs to the entorhinal cortex. In the pyriform cortex and area CA1 of the hippocampus, cholinergic activity has been proposed to contribute to associative memory processing by the selective *depression* of synaptic transmission at intrinsic associational synapses during learning (Hasselmo & Bower, 1992, 1993; Hasselmo & Schnell, 1994; Hasselmo, 1995). In neural models of associative memory, intrinsic recurrent connections between principal neurons are strengthened to form a network of mutually-exciting cells which represent the associative memory (McClelland & Rumelhart, 1986). Extrinsic inputs provide sensory inputs to the principal neurons, and multiple associative memories can be stored in different patterns of activation within the same group of principal cells. Hasselmo and Bower (1992, 1993) have shown in computational models of associative memory systems that a depression of synaptic transmission in the intrinsic synaptic connections during learning can reduce the concurrent reactivation of previously stored memories and the associated interference between the old memories and the storage of new memories. Cholinergic activity during learning may serve to reduce excitation at intrinsic synapses and lessen the degree of interference between previously stored memories and the representation being learned.

The enhancement of LTP induced by stimulating the medial septum may have been due in part to the temporal pattern of stimulation. The 10 Hz

stimulation used results in frequency potentiation in this pathway (Figure 3.14 bottom), and is also within the range of the theta rhythm which has been implicated in the enhancement of LTP in other systems (Larson et al., 1986; Staubli & Lynch, 1987; Greenstein et al., 1988; Lynch et al., 1990; Huerta & Lisman, 1993). Although the links between theta-frequency activity and learning and memory remain tenuous, the medial septum may contribute to learning-related synaptic plasticity in the entorhinal cortex by setting a background of temporal activity conducive to synaptic plasticity.

The findings that septal stimulation can enhance LTP in the entorhinal cortex and in the dentate gyrus (Experiment 4.3; Robinson & Racine, 1982; Robinson, 1986), and the putative role of the medial septum in theta activity (Bland, 1986; Alonso & Garcia-Austt, 1987a), suggest that the medial septum may play a central role in governing theta-related temporal processing and neuroplasticity in both of these structures. Theta activity in the entorhinal cortex and the hippocampal formation is highly coherent, that is, the relationship between the phases of theta activity in these sites is highly consistent (Alonso & Garcia-Austt, 1987a; Chapman & Racine, 1993; Xu et al., 1994). Coherence in theta activity may contribute to the transfer of neuronal activity between sites, so that rhythmically active entorhinal cortex inputs arrive in the hippocampal formation during periods when hippocampal neurons are more excitable. This could contribute to the enhancement of LTP-like effects in the hippocampus (Lynch et al., 1990), perhaps by the shorter-term synaptic enhancements which have been suggested by Buzsaki (1989) to coordinate sharp-wave activity. The medial septum, then, appears to contribute to the generation of a coherent rhythmic state that may be conducive to short- and long-term learning-related synaptic enhancements in both the entorhinal cortex and hippocampal formation.

Such a mechanism could also contribute to the interactions between the hippocampus and neocortex which have been proposed by Miller (1989) to mediate the consolidation of memory. In this theory, patterns of connectivity between the hippocampus and the neocortex are established during periods of theta activity. Because the conduction delays in the axonal pathways between the hippocampal formation, the prefrontal cortex, and the associational cortices sum to approximately the period of the theta rhythm, activity in neural loops between the hippocampus and these cortical sites could conceivably resonate during memory formation. If neocortical cells are tonically active during the theta rhythm, theta-frequency activity in hippocampo-cortical connections could lead to a Hebbian strengthening of these connections and an entrainment of cortical neurons to the theta rhythm. Reciprocal connections back to the hippocampal formation could, in turn, be strengthened if the cortical efferents arrive at an appropriate phase of the theta rhythm, and a resonant loop could be established (Miller, 1989). The data presented here are consistent with the idea that frequency potentiation mechanisms could contribute to the establishment of resonant loops by resulting in short-term enhancements in excitability, and that these enhancements could then contribute to more permanent synaptic potentiation effects.

REFERENCES

- Abbott, L.F. (1990) Modulation of function and gated learning in a network memory. Proceedings of the National Academy of Sciences; 87:9241-9245.
- Abraham, W.C., Mason, S.E., Demmer, J., Williams, J.M., Richardson, C.L., Tate, W.P., Lawlor, P.A., and Dragunow, M. (1993) Correlations between immediate early gene induction and the persistence of long-term potentiation. Neuroscience; 56:717-727.
- Adey, W.R., Sunderland, S., and Dunlop, C.W. (1957) The entorhinal area: electrophysiological studies of its interrelations with rhinencephalic structures and the brainstem. Electroencephalography and Clinical Neurophysiology; 9:309-324.
- Aigner, T.G., Walker, D.L., and Mishkin, M. (1991) Comparison of the effects of scopolamine administered before and after acquisition in a test of visual recognition memory in monkeys. Behavioural and Neural Biology; 55:61-67.
- Alonso, A., and Garcia-Austt, E. (1987a) Neuronal sources of theta rhythm in the entorhinal cortex of the rat. I. Laminar distribution of theta field potentials. Experimental Brain Research; 67:493-501.
- Alonso, A., and Garcia-Austt, E. (1987b) Neuronal sources of theta rhythm in the entorhinal cortex of the rat. II. Phase relations between unit discharges and theta field potentials. Experimental Brain Research; 67:502-509.
- Alonso, A., and Klink, R. (1993) Differential electroresponsiveness of stellate and pyramidal-like cells of medial entorhinal cortex layer II. Journal of Neurophysiology; 70:128-143.
- Alonso, A., and Kohler, C. (1984) A study of the reciprocal connections between the septum and the entorhinal area using anterograde and retrograde axonal transport methods in the rat brain. Journal of Comparative Neurology; 225:327-343.
- Alonso, A., de Curtis, M., and Llinas, R. (1990) Postsynaptic Hebbian and non-Hebbian long-term potentiation of synaptic efficacy in the entorhinal cortex in slices and in the isolated adult guinea pig brain. Proceedings of the National Academy of Sciences; 87:9280-9284.
- Alvarez-Leefmans, F.J., and Gardner-Medwin, A.R. (1975) Influences of the septum on the hippocampal dentate area which are unaccompanied by field potentials. Journal of Physiology; 249:14-15P.

- Amaral, D.G., and Kurz, J. (1985) An analysis of the origins of the cholinergic and noncholinergic septal projections to the hippocampal formation of the rat. Journal of Comparative Neurology; 240:37-59.
- Amaral, D.G., and Witter, M.P. (1989) The three-dimensional organization of the hippocampal formation: a review of anatomical data. Neuroscience; 31:571-591.
- Amaral, D.G., Insausti, R., and Cowan, W.M., (1987) The entorhinal cortex of the monkey. I. Cytoarchitectonic organization. Journal of Comparative Neurology; 264:326-355.
- Amaral, D.G., Insausti, R., and Cowan, W.M., (1983) Evidence for a direct projection from the superior temporal gyrus to the entorhinal cortex in the monkey. Brain Research; 275:263-277.
- Amaral, D.G., Dolorfo, C., and Alvarez-Royo, P. (1991) Organization of CA1 projections to the subiculum: a PHA-L analysis in the rat. Hippocampus; 1:415-436.
- Andersen, P., Bruland, H., and Kaada, B.R. (1961) Activation of the dentate area by septal stimulation. Acta Physiologica Scandinavia; 51:17-28.
- Andersen, P., and Lomo, T. (1967) Control of hippocampal output by afferent volley frequency. Progress in Brain Research; 27:400-412.
- Andersen, P., and Lomo, T. (1968) Counteraction of powerful recurrent inhibition in hippocampal pyramidal cells by frequency potentiation of excitatory synapses. In, Structure and Function of Inhibitory Neuronal Mechanisms; C. von Euler, S. Skogland, and U. Soderberg (Eds.), Permagon Press, Toronto, pp. 335-342.
- Andersen, P., Sundberg, S.H., Sveen, O., and Wigstrom, H. (1977) Specific long-lasting potentiation of synaptic transmission in hippocampal slices. Nature; 266:736-737.
- Andreasen, M., and Hablitz, J.J. (1994) Paired-pulse facilitation in the dentate gyrus: a patch-clamp study in rat hippocampus in vitro. Journal of Neurophysiology; 72:326-336.
- Applegate, M.D., and Landfield, P.W. (1988) Synaptic vesicle redistribution during hippocampal frequency potentiation and depression in young and aged rats. Journal of Neuroscience; 8:1096-1111.
- Artola, A., and Singer, W. (1987) Long-term potentiation and NMDA receptors in rat visual cortex. Nature; 330:649-652.
- Ascher, P., and Nowak, L. (1987) Electrophysiological studies of NMDA receptors. Trends in Neurosciences; 10:284-288.

- Barkai, E., Bergman, R.E., Horwitz, G., and Hasselmo, M.E. (1994) Modulation of associative memory function in a biophysical simulation of rat piriform cortex. Journal of Neurophysiology; 72:659-677.
- Barkai, E., and Hasselmo, M.E. (1994) Modulation of the input/output function of rat piriform cortex pyramidal cells. Journal of Neurophysiology; 72:644-658.
- Barnes, C.A. (1979) Memory deficits associated with senescence: a neurophysiological and behavioural study in the rat. Journal of Comparative and Physiological Psychology; 93:74-104.
- Barrett, E.F., and Stevens, C.F. (1972) The kinetics of transmitter release at the frog neuromuscular junction. Journal of Physiology; 277:691-708.
- Barrionuevo, and Brown, T.H. (1983) Associative long-term potentiation in hippocampal slices. Proceedings of the National Academy of Sciences; 80:7347-7351.
- Beckstead, R.M. (1978) Afferent connections of the entorhinal area in the rat as demonstrated by retrograde cell-labeling with horseradish peroxidase. Brain Research; 152:249-264.
- Bernardo, L.S., and Prince, D.A. (1982) Ionic mechanisms of cholinergic excitation in mammalian hippocampal pyramidal cells. Brain Research; 249:333-344.
- Berry, M.S., and Pentreath, V.W. (1976) Criteria for distinguishing between monosynaptic and polysynaptic transmission. Brain Research; 105:1-20.
- Bland, B.H. (1986) The physiology and pharmacology of hippocampal formation theta rhythms. Progress in Neurobiology; 26:1-54.
- Bland, B.H., and Colom, L.V. (1993) Extrinsic and intrinsic properties underlying oscillation and synchrony in limbic cortex. Progress in Neurobiology; 41:157-208.
- Bliss, T.V.P., and Collingridge, G.L. (1993) A synaptic model of memory: long-term potentiation in the hippocampus. Nature; 361:31-39.
- Bliss, T.V.P., and Gardner-Medwin, A.R. (1973) Long-lasting potentiation of synaptic transmission in the dentate area of the unanaesthetized rabbit following stimulation of the perforant path. Journal of Physiology; 232:357-374.
- Bliss, T.V.P., and Lomo, T. (1973) Long lasting potentiation of synaptic transmission in the dentate area of the anesthetized rabbit following stimulation of the perforant path. Journal of Physiology; 232:331-356.

- Blitzer, R.D., Gil, O., and Landau, E.M. (1990) Cholinergic stimulation enhances long-term potentiation in the CA1 region of rat hippocampus. Neuroscience Letters; 119:207-210.
- Boeijinga, P.H., and Lopes da Silva, F.H. (1988) Differential distribution of beta and theta EEG activity in the entorhinal cortex of the cat. Brain Research; 448:272-286.
- Boeijinga, P.H., and Lopes da Silva, F.H. (1989) Modulations of EEG activity in the entorhinal cortex and forebrain olfactory areas during odour sampling. Brain Research; 478:257-268.
- Boeijinga, P.H., Van Groen, T., Lopes da Silva, F.H., Room, P., and Russchen, F.T. (1982) Inputs from the primary olfactory cortex to the entorhinal area: an electrophysiological and anatomical tracing study. Neuroscience Letters (Supplement); 10:82.
- Boeijinga, P.H., and Van Groen, Th. (1984) Inputs from the olfactory bulb and olfactory cortex to the entorhinal cortex in the cat. II. Physiological studies. Experimental Brain Research; 57:40-48.
- Bouffard, J.-P., and Jarrard, L.E. (1988) Acquisition of a complex place task in rats with selective ibotenate lesions of hippocampal formation: combined lesions of subiculum and entorhinal cortex versus hippocampus. Behavioral Neuroscience; 102:828-834.
- Braak, H. (1990) Entorhinal lesions in dementia. Neurobiology of Aging; 11:226.
- Brankack, J., Stewart, M., and Fox, S.E. (1993) Current source density analysis of the hippocampal theta rhythm: associated sustained potentials and candidate synaptic generators. Brain Research; 615:310-327.
- Bressler, S.L. (1989) The gamma wave: a cortical information carrier? Trends in Neurosciences; 13:161-162.
- Brioni, J.D., Decker, M.W., Gamboa, L.P., Izquierdo, I., and McGaugh, J.L. (1990) Muscimol injections in the medial septum impair spatial learning. Brain Research; 522:227-234.
- Brocher, S., Artola, A., and Singer, W. (1992) Agonists of cholinergic and noradrenergic receptors facilitate synergistically the induction of long-term potentiation in slices of rat visual cortex. Brain Research; 573:27-36.
- Brown, M.W., Rose, D., and Ahlquist, J. (1983) Amnesia-producing drugs affect hippocampal frequency potentiation. Neuroscience; 10:697-706.
- Brown, T.H., Kairiss, E.W., and Keenan, C.L. (1990) Hebbian synapses: biophysical mechanisms and algorithms. Annual Review of Neuroscience; 13:475-511.

- Buno, W., and Velluti, J.C. (1977) Relationships of hippocampal theta cycles with bar pressing during self-stimulation. Physiology and Behaviour; 19:615-621.
- Burgard, E.C., and Sarvey, J.M. (1990) Muscarinic receptor activation facilitates the induction of long-term potentiation (LTP) in the rat dentate gyrus. Neuroscience Letters; 116:34-39.
- Buzsaki, G. (1986) Hippocampal sharp waves: their origin and significance. Brain Research; 398:242-252.
- Buzsaki, G. (1989) Two-stage model of memory trace formation: a role for "noisy" brain states. Neuroscience; 31:551-570.
- Buzsaki, G., Grastyan, E., Czopf, J., Kellenyi, L., and Prohaska, O. (1981) Changes in neuronal transmission in the rat hippocampus during behavior. Brain Research; 225:235-247.
- Buzsaki, G., Czopf, J., Kondakor, I., and Kellenyi, L. (1986) Laminar distribution of hippocampal rhythmic slow activity (RSA) in the behaving rat: current-source density analysis, effects of urethane and atropine. Brain Research; 365:125-137.
- Caballero-Bleda, M., and Witter, M.P. (1993) Regional and laminar organization of projections from the presubiculum and parasubiculum to the entorhinal cortex: an anterograde tracing study in the rat. Journal of Comparative Neurology; 328:115-129.
- Cain, D.P. (1977) Seizure development following repeated electrical stimulation of central olfactory structures. Annals of the New York Academy of Sciences; 290:200-216.
- Carmichael, S.T., Clugnet, M.-C., and Price, J.L. (1994) Central olfactory connections in the Macaque monkey. Journal of Comparative Neurology; 346:403-434.
- Castellucci, V.F., Carew, T.J., and Kandel, E.R. (1978) Cellular analysis of long-term habituation of the gill-withdrawal reflex of *Aplysia californica*. Science; 202:1306-1308.
- Chandler, J.P., and Crutcher, K.A. (1983) The septohippocampal projection in the rat: an electron microscopic horseradish peroxidase study. Neuroscience; 10:685-696.
- Chapman, C.A., and Becker, S. (1995) Model synapses with frequency potentiation characteristics can cooperatively enhance Hebbian learning. In, The Neurobiology of Computation; J. Bower (Ed.), Kluwer, Boston, pp. 197-202.

- Chapman, C.A., and Racine, R.J. (1993) Coherence and mutual information do not indicate altered relationships in spontaneous EEG between entorhinal cortex and dentate gyrus following LTP in dentate gyrus. Society for Neuroscience Abstracts; 19:805.
- Chapman, C.A., and Racine, R.J. (1994) Long-term potentiation and kindling-induced potentiation of field potentials in entorhinal cortex evoked by pyriform cortex stimulation. Society for Neuroscience Abstracts; 20:1559.
- Chapman, C.A., and Racine, R.J. (1995a) Spatial localization of current sinks in the superficial layers of the entorhinal cortex following pyriform cortex stimulation in the rat. Society for Neuroscience Abstracts; 21:805.
- Chapman, C.A., and Racine, R.J. (1995b) Long-term potentiation of pyriform cortex efferents to entorhinal cortex is enhanced by embedding the induction stimuli within low-frequency trains. Presented at the Southern Ontario Neuroscience Association Meeting, Hamilton, Ontario.
- Chrobak, J.J., and Buzsaki, G. (1994) Selective activation of deep layer (V-VI) retrohippocampal cortical neurons during hippocampal sharp waves in the behaving rat. Journal of Neuroscience; 14:6160-6170.
- Clower, R.P., Alvarez-Royo, A., Zola-Morgan, S., and Squire, L.R. (1991) Recognition memory impairment in monkeys with selective hippocampal lesions. Society for Neuroscience Abstracts; 17:338.
- Cohen, A.H., Ermentrout, G.B., Kiemel, T., Kopell, N., Sigvardt, K.A., and Williams, T.L. (1992) Modelling of intersegmental coordination in the lamprey central pattern generator for locomotion. Trends in Neurosciences; 15:434-438.
- Cole, A.E., and Nicoll, R.A. (1984) Characterization of a slow cholinergic postsynaptic potential recorded in vitro from rat hippocampal pyramidal cells. Journal of Physiology; 352:173-188.
- Colino, A., and Fernandez de Molina, A. (1986a) Inhibitory response in entorhinal and subicular cortices after electrical stimulation of the lateral and basolateral amygdala of the rat. Brain Research; 378:416-419.
- Colino, A., and Fernandez de Molina, A. (1986b) Electrical activity generated in subicular and entorhinal cortices after electrical stimulation of the lateral and basolateral amygdala of the rat. Neuroscience; 19:573-580.
- Colino, A., and Malenka, R.C. (1993) Mechanisms underlying induction of long-term potentiation in rat medial and lateral perforant paths in vitro. Journal of Neurophysiology; 69:1150-1159.
- Collier, T.J., and Routtenberg, A. (1978) Entorhinal cortex electrical stimulation disrupts retention performance when applied after, but not during, learning. Brain Research; 152:411-417.

- Collingridge, G.L., and Bliss, T.V.P. (1987) NMDA receptors - their role in long-term potentiation. Trends in Neurosciences; 10:288-293.
- Corkin, S. (1968) Acquisition of motor skill after bilateral medial temporal-lobe excision. Neuropsychologia; 6:255-265.
- Cragg, B.G. (1960) Responses of the hippocampus to stimulation of the olfactory bulb and of various afferent nerves in five mammals. Experimental Neurology; 2:547-572.
- Creager, R., Dunwiddie, T., and Lynch, G. (1980) Paired-pulse and frequency potentiation in the CA1 region of the in vitro rat hippocampus. Journal of Physiology; 299:409-424.
- Crow, T.J., Grove-White, I., and Ross, D.G. (1975) The specificity of the action of hyoscine on human learning. British Journal of Clinical Pharmacology; 2:367-368.
- Crutcher, K.A., Kesner, R.P., and Novak, J.M. (1983) Medial septal lesions, radial arm maze performance, and sympathetic sprouting: a study of recovery of function. Brain Research; 262:91-98.
- Davies, C.H., Davies, S.N., and Collingridge, G.L. (1990) Paired-pulse depression of monosynaptic GABA-mediated inhibitory postsynaptic responses in rat hippocampus. Journal of Physiology; 424:513-531.
- Davies, C.H., Starkey, S.J., Pozza, M.F., and Collingridge, G.L. (1991) GABA_B autoreceptors regulate the induction of LTP. Nature; 349:609-611.
- Davis, S., Butcher, S.P., and Morris, R.G.M. (1992) The NMDA receptor antagonist D-amino-5-phosphopentanoate (D-AP5) impairs spatial learning and LTP in vivo at intracerebral concentrations comparable to those that block LTP in vitro. Journal of Neuroscience; 12:21-34.
- Deacon, T.W., Eichenbaum, H., Rosenberg, P., and Eckmann, K.W. (1983) Afferent connections of the perirhinal cortex in the rat. Journal of Comparative Neurology; 220:168-190.
- Deadwyler, S.A., West, J.R., Cotman, C.W., and Lynch, G. (1975) Physiological studies of the reciprocal connections between the hippocampus and entorhinal cortex. Experimental Neurology; 49:35-57.
- de Curtis, M., and Llinas, R.R. (1993) Entorhinal cortex long-term potentiation evoked by theta-patterned stimulation of associative fibers in the isolated in vitro guinea pig brain. Brain Research; 600:327-330.
- de Curtis, M., Pare, D., and Nas, R.R. (1991) The electrophysiology of the olfactory-hippocampal circuit in the isolated and perfused adult mammalian brain in vitro. Hippocampus; 1:341-354.

- de Curtis, M., Arcelli, P., De Biasi, S., Spreafico, R., and Avanzini, G. (1994) Ultrastructural features of the isolated guinea-pig brain maintained in vitro by arterial perfusion. Neuroscience; 59:775-788.
- Deisz, R.A., and Prince, D.A. (1989) Frequency-dependent depression of inhibition in guinea-pig neocortex in vitro GABA_B receptor feedback on GABA release. Journal of Physiology; 412:513-541.
- de Jonge, M.C., and Racine, R.J. (1987) The development and decay of kindling-induced increases in paired-pulse depression in the dentate gyrus. Brain Research; 412:318-328.
- Del Castillo, J., and Katz, B. (1954) Statistical factors involved in neuromuscular facilitation and depression. Journal of Physiology; 124:574-85.
- DeOimos, J., Hardy, H., Heimer, L. (1978) The afferent connections of the main and the accessory olfactory bulb formation in the rat: and experimental HRP study. Journal of Comparative Neurology; 181:213-244.
- Diana, G., Scotti de Carlos, A., Frank, C., Domenici, M.R., and Sagratella, S. (1994) Selective reduction of hippocampal dentate frequency potentiation in aged rats with impaired place learning. Brain Research Bulletin; 35:107-111.
- Doyere, V., and Laroche, S. (1992) Linear relation between the maintenance of hippocampal long-term potentiation and retention of an associative memory. Hippocampus; 2:39-48.
- Drachman, D.A., and Leavitt, J. (1974) Human memory and the cholinergic system. Archives of Neurology; 30:113-121.
- Duckrow, R.B. and Spencer, S.S. (1992) Regional coherence and the transfer of ictal activity during seizure onset in the medial temporal lobe. Electroencephalography and Clinical Neurophysiology; 82:415-422.
- Dudek, F.E., Deadwyler, S.A., Cotman, C.W., and Lynch, G. (1976) Intracellular responses from granule cell layer in slices of rat hippocampus: perforant path synapse. Journal of Neurophysiology; 39:384-393.
- Dunwiddie, T.V., Roberson, N.L., and Worth, T. (1982) Modulation of long-term potentiation: effects of adrenergic and neuroleptic drugs. Pharmacology, Biochemistry and Behavior; 17:1257-1264.
- Durbin, R. (1989) On the correspondence between network models and the nervous system. In, The Computing Neuron; R. Durbin, C. Miall and G. Mitchison (Eds.), Addison-Wesley, Don Mills, pp. 1-10.
- Eckert, R., and Tillotson, D.L. (1981) Calcium-mediated inactivation of the calcium conductance in caesium-loaded giant neurones of *Aplysia californica*. Journal of Physiology; 314:265-280.

- Eichenbaum, H. (1992) The hippocampal system and declarative memory in animals. Journal of Cognitive Neuroscience; 4:217-231.
- Eichenbaum, H., Fagan, A., Mathews, P., and Cohen, N.J (1988) Hippocampal system dysfunction and odor discrimination learning in rats: impairment or facilitation depending on representational demands. Behavioural Neuroscience; 102:3531-3542.
- Eichenbaum, H., Otto, T., and Cohen, N.J. (1992) The hippocampus - what does it do? Behavioral and Neural Biology; 57:2-36.
- Entingh, D. (1971) Perseverative responding and hyperphagia following entorhinal lesions in cats. Journal of Comparative and Physiological Psychology; 75:50-58.
- Fallon, J.H., Koziell, D.A., and Moore, R.Y. (1978) Catecholamine innervation of the basal forebrain. II. amygdala, suprarhinal cortex and entorhinal cortex. Journal of Comparative Neurology; 180:509-532.
- Fantie, B.D., and Goddard, G.V. (1982) Septal modulation of the population spike in the fascia dentata produced by perforant path stimulation in the rat. Brain Research; 252:227-237.
- Ferreira, M.B.C., Da Silva, R.C., Medina, J.H., and Izquierdo, I. (1992) Late posttraining memory processing by entorhinal cortex: involvement of NMDA and GABAergic receptors. Pharmacology Biochemistry and Behavior; 41:767-771.
- Finch, D.M., and Babb, T.L. (1980) Inhibition in subicular and entorhinal principal; neurons in response to electrical stimulation of the fornix and hippocampus. Brain Research; 196:89-98.
- Finch, D.M., Wong, E.E., Derian, E.L., and Babb, T.L. (1986) Neurophysiology of limbic system pathways in the rat: projections from the subicular complex and hippocampus to the entorhinal cortex. Brain Research; 397:205-213.
- Finch, D.M., Tan, A.M., and Isokawa-Akesson, M. (1988) Feedforward inhibition of the rat entorhinal cortex and subicular complex. Journal of Neuroscience; 8:2213-2226.
- Flatman, J.A., Schwindt, P.C., Crill, W.E., and Stafstrom, C.E. (1983) Multiple actions of N-methyl-D-aspartate on cat neocortical neurons in vitro. Brain Research; 266:169-173.
- Flicker, C., Serby, M., and Ferris, S.H. (1990) Scopolamine effects on memory, language, visuospatial praxis and psychomotor speed. Psychopharmacology; 100:243-250.
- Fox, K., and Daw, N.W. (1993) Do NMDA receptors have a critical function in visual cortical plasticity? Trends in Neurosciences; 16:116-123.

- Freeman, J.A., and Nicholson, C. (1975) Experimental optimization of current source-density technique for anuran cerebellum. Journal of Neurophysiology; 38:369-371.
- Freeman, W.J. (1978) Spatial properties of an EEG event in the olfactory bulb and cortex. Electroencephalography and Clinical Neurophysiology; 44:586-605.
- Freeman, W.J., and Schneider, W. (1982) Changes in spatial patterns of rabbit olfactory EEG with conditioning to odors. Psychophysiology; 19:44-56.
- Frey, U., Schroeder, H., and Matthies, H. (1990) Dopaminergic antagonists prevent long-term maintenance of posttetanic LTP in the CA1 region of rat hippocampal slices. Brain Research; 522:69-75.
- Frey, U., Matthies, H., Reymann, K.G., and Matthies, H. (1991) The effect of dopaminergic D₁ receptor blockade during tetanization on the expression of long-term potentiation in the rat CA1 region in vitro. Neuroscience Letters; 129:111-114.
- Gauthier, M., and Soumireu-Mourat, B. (1981) Behavioral effects of bilateral entorhinal cortex lesions in the Balb/c mouse. Behavioral and Neural Biology; 33:419-436.
- Gauthier, M., Destrade, C., and Soumireu-Mourat, B. (1982) Late post-learning participation of entorhinal cortex in memory processes. Brain Research; 233:255-264.
- Gaykema, R.P.A., Luiten, P.G.M., Nyakas, C., and Traber, J. (1990) Cortical projection patterns of the medial septum-diagonal band complex. Journal of Comparative Neurology; 293:103-124.
- Germroth, P., Schwerdtfeger, W.K., and Buhl, E.H. (1989) Morphology of identified entorhinal neurons projecting to the hippocampus. A light microscopic study combining retrograde tracing and intracellular injection. Neuroscience; 30:683-691.
- Germroth, P., Schwerdtfeger, W.K., and Buhl, E.H. (1991) Ultrastructure and aspects of junctional organization of pyramidal and nonpyramidal entorhinal projection neurons contributing to the perforant path. Journal of Comparative Neurology; 305:215-231.
- Gluck, M.A., and Granger, R. (1993) Computational models of the neural bases of learning and memory. Annual Review of Neuroscience; 16:667-706.
- Goddard, G.V. (1967) Development of epileptic seizures through brain stimulation at low intensity. Nature; 214:1020-1021.

- Goddard, G.V., McIntyre, D.C., and Leech, C.K. (1969) A permanent change in brain function resulting from daily electrical stimulation. Experimental Neurology; 25:295-330.
- Gray, C.M. (1994) Synchronous oscillations in neuronal systems: mechanisms and functions. Journal of Computational Neuroscience; 1:1-38.
- Gray, C.M., and Singer, W. (1989) Stimulus-specific neuronal oscillations in orientation columns of cat visual cortex. Proceedings of the National Academy of Sciences; 86:1698-1702.
- Gray, J.A., and McNaughton, N. (1982) Comparison between the behavioural effects of septal and hippocampal lesions: a review. Neuroscience and Biobehavioral Reviews; 7:119-188.
- Green, J.D., and Arduini, A.A. (1954) Hippocampal electrical activity in arousal. Journal of Neurophysiology; 17:403-420.
- Greenstein, Y.J., Pavlides, C., and Winston, J. (1988) Long-term potentiation in the dentate gyrus is preferentially induced at theta rhythm periodicity. Brain Research; 438:331-334.
- Haberly, L.B., and Bower, J.M. (1984) Analysis of association fiber system in piriform cortex with intracellular recording and staining techniques. Journal of Neurophysiology; 51:90-112.
- Haberly, L.B., and Price, (1978) Association and commissural fiber systems of the olfactory cortex of the rat. I. Systems originating in the piriform cortex and adjacent areas. Journal of Comparative Neurology; 178:711-740.
- Haberly, L.B., and Shepherd, G.M. (1973) Current-density analysis of summed evoked potentials in Opossum prepyriform cortex. Journal of Neurophysiology; 36:789-802.
- Haberly, L.B., and Sutula, T.P. (1992) Neuronal processes that underlie expression of kindled epileptiform events in the piriform cortex in vivo. Journal of Neuroscience, 12:2211-2223.
- Habets, A.M.M.C., Lopes da Silva, F.H., and Mollevanger, W.J. (1980) An olfactory input to the hippocampus of the cat: field potential analysis. Brain Research; 182:47-64.
- Hagan, J.J., Jansen, J.H.M., and Broekkamp, C.L.E. (1987) Blockade of spatial learning by the M1 muscarinic antagonist pirenzepime. Psychopharmacology; 93:470-476.
- Hagan, J.J., Salamone, J.D., Simpson, J., Iversen, S.D., and Morris, R.G.M. (1988) Place navigation in rats is impaired by lesions of medial septum and diagonal band but not nucleus basalis magnocellularis. Behavioural Brain Research; 27:9-20.

- Hargreaves, E.L., Cain, D.P., and Vanderwolf, C.H. (1990) Learning and behavioral-long-term potentiation: importance of controlling for motor activity. Journal of Neuroscience; 10:1472-1478.
- Harley, C.W., and Milway, J.S. (1986) Glutamate ejection in the locus coeruleus enhances the perforant path-evoked population spike in the dentate gyrus. Experimental Brain Research; 63:143-150.
- Hasselmo, M.E. (1995) Neuromodulation and cortical function: modeling the physiological basis of behavior. Behavioural Brain Research; 67:1-27.
- Hasselmo, M.E., and Bower, J.M. (1990) Afferent and association fiber differences in short-term potentiation in piriform (olfactory) cortex of the rat. Journal of Neuroscience; 64:179-190.
- Hasselmo, M.E., and Bower, J.M. (1992) Cholinergic suppression specific to intrinsic not afferent fiber synapses in rat pyriform (olfactory) cortex. Journal of Neuroscience; 67:1222-1229.
- Hasselmo, M.E., and Bower, J.M. (1993) Acetylcholine and memory. Trends in Neurosciences; 16:218-222.
- Hasselmo, M.E., and Schnell, E. (1994) Laminar selectivity of the cholinergic suppression of synaptic transmission in rat hippocampal region CA1: computational modeling and brain slice physiology. Journal of Neuroscience; 14:3898-3914.
- Hebb, D.O. (1949) The Organization of Behavior: a Neuropsychological Theory. John Wiley, New York.
- Heinemann, W., Zhang, C.L., and Eder, C. (1993) Entorhinal cortex - hippocampal interactions in the normal and epileptic temporal lobe. Hippocampus; 3:89-98.
- Hess, G., and Kuhnt, U. (1992) Presynaptic calcium transients evoked by paired-pulse stimulation in the hippocampal slice. Neuroreport; 3:361-364.
- Holsheimer, J. (1987) Electrical conductivity of the hippocampal CA1 layers and application to current-source-density analysis. Experimental Brain Research; 67:402-410.
- Hopkins, W.F., and Johnston, D. (1984) Frequency-dependent noradrenergic modulation of long-term potentiation in the hippocampus. Science; 226:350-352.
- Huerta, P.T., and Lisman, J.E. (1993) Heightened synaptic plasticity of hippocampal CA1 neurons during a cholinergically induced rhythmic state. Nature; 364:723-725.
- Hunter, A.J., and Murray, T.K. (1989) Cholinergic mechanisms in a simple test of olfactory learning in the rat. Psychopharmacology; 99:270-275.

- Hyman, B.T., Van Hoesen, G.W., Kromer, L.J., and Damasio, A.R. (1986) Perforant pathway changes and the memory impairment of Alzheimer's disease. Annals of Neurology; 20:472-481.
- Insausti, R., Amaral, D.G., and Cowan, W.M. (1987) The entorhinal cortex of the Monkey. III. Subcortical afferents. Journal of Comparative Neurology; 264:396-408.
- Ishizuka, N, Weber, J., and Amaral, D.G. (1990) Organization of intrahippocampal projections originating from CA3 pyramidal cells in the rat. Journal of Comparative Neurology; 295:580-623.
- Izquierdo, I. (1989) Mechanism of action of scopolamine as an amnesic. Trends in Pharmacological Science; 10:175-177.
- Izquierdo, I., Medina, J.H. (1995) Correlation between the pharmacology of long-term potentiation and the pharmacology of memory. Neurobiology of Learning and Memory; 63:19-32.
- Izquierdo, I., da Cunha, C., Rosat, R., Jerusalinsky, D., Ferreira, M.B.C., and Medina, J.H. (1992) Neurotransmitter receptors involved in post-training memory processing by the amygdala, medial septum, and hippocampus of the rat. Behavioral and Neural Biology; 58:16-26.
- Izquierdo, I., Medina, J.H., Bianchin, M., Walz, R., Zanatta, M.S., Da Silva, R.C., E Silva, M.B., Ruschel, A.C., and Paczko, N. (1993) Memory processing by the limbic system: role of specific neurotransmitter systems. Behavioural Brain Research; 58:91-98.
- Jarrard, L.E., Okaichi, H., Steward, O., and Goldschmidt, R.B (1984) On the role of hippocampal connections in the performance of place and cue tasks: comparisons with damage to hippocampus. Behavioral Neuroscience; 98:946-954.
- Jellinger, K., Braak, H., Braak, E., and Fischer, P. (1991) Alzheimer lesions in the entorhinal region and isocortex in Parkinson's and Alzheimer's diseases. Annals of the New York Academy of Sciences; 640:203-209.
- Jibiki, I., Wakita, S., Kubota, t., Kurokawa, K., Fukushima, T., and Yamaguchi, N. (1993) Haloperidol-induced blockade of induction of long-term potentiation in perforant path-dentate gyrus pathway in chronically prepared rabbits. Pharmacology, Biochemistry and Behavior; 46:847-852.
- Johnston, D.L., and Kesner, R.P. (1994) The effects of lesions of the entorhinal cortex and the horizontal nucleus of the diagonal band of Broca upon performance of a spatial location recognition task. Behavioural Brain Research; 61:1-8.

- Johnston, D., Williams, S., Jaffe, D., and Gray, R. (1992) NMDA-receptor-independent long-term potentiation. Annual Review of Physiology; 54:489-505.
- Jones, R.S.G. (1987) Complex synaptic responses of entorhinal cortical cells in the rat to subicular stimulation in vitro: demonstration of an NMDA receptor-mediated component. Neuroscience Letters; 81:209-214.
- Jones, R.S.G. (1990a) Synaptic transmission between layers V-VI and layer II of the rat medial entorhinal cortex in vitro. Journal of Physiology; 429:47P.
- Jones, R.S.G. (1990b) Synaptic responses of neurones in layer II of the rat medial entorhinal cortex to stimulation of the para-subiculum in vitro. Journal of Physiology; 426:48P.
- Jones, R.S.G. (1993) Entorhinal-hippocampal connections: a speculative view of their function. Trends in Neurosciences; 16:58-64.
- Jones, R.S.G., and Buhl, E.H. (1993) Basket-like interneurons in layer II of the entorhinal cortex exhibit a powerful NMDA-mediated synaptic excitation. Neuroscience Letters; 149:35-39.
- Jones, R.S.G., and Heinemann, U. (1988) Synaptic and intrinsic responses of medial entorhinal cortical cells in normal and magnesium-free medium in vitro. Journal of Neurophysiology; 59:1476-1496.
- Jones, R.S.G., and Heinemann, U. (1991) Amino acid-mediated synaptic transmission in temporal lobe structures in vitro: implications for the generation and spread of epileptic activity. In, Excitatory Amino Acids and Synaptic Function; Academic Press, pp. 265-285.
- Jones, R.S.G., and Lambert, J.D.C. (1990) Synchronous discharges in the rat entorhinal cortex in vitro: site of initiation and the role of excitatory amino acid receptors. Neuroscience; 34:657-670.
- Kahle, J.S., and Cotman, C.W. (1989) Carbachol depresses synaptic responses in the medial but not the lateral perforant path. Brain Research; 482:159-163.
- Kano, M. (1995) Plasticity in inhibitory synapses in the brain: a possible mechanism that has been overlooked. Neuroscience Research; 21:177-182.
- Katz, B., and Miledi, R. (1968) The role of calcium in neuromuscular facilitation. Journal of Physiology; 195:481-492.
- Kay, L.M., and Freeman, W.J. (1994) Coherence of gamma oscillations throughout olfactory and limbic brain structures in rats. Society for Neuroscience Abstracts; 20:330.

- Kelsey, J.E., and Landry, B.A. (1988) Medial septal lesions disrupt spatial mapping ability in rats. Behavioral Neuroscience; 102:289-293.
- Kelso, S.R., and Brown, T.H. (1986) Differential conditioning of associative synaptic enhancement in hippocampal brain slices. 232:85-87.
- Kerr, D.I.B., and Dennis, B.J. (1972) Collateral projection of the lateral olfactory tract to entorhinal cortical areas in the cat. Brain Research; 36:399-403.
- Kesner, R.P. (1988) Reevaluation of the contribution of the basal forebrain cholinergic system to memory. Neurobiology of Aging; 9:609-616.
- Kesner, R.P., Crutcher, K., and Beers, D.R. (1988) Serial position curves for item (spatial location) information: role of the dorsal hippocampal formation and medial septum. Brain Research; 454:219-226.
- Ketchum, K.L., and Haberly, L.B. (1993a) Membrane currents evoked by afferent fiber stimulation in rat piriform cortex. I. Current source-density analysis. Journal of Neurophysiology; 69:248-260.
- Ketchum, K.L., and Haberly, L.B. (1993b) Membrane currents evoked by afferent fiber stimulation in rat piriform cortex. II. Analysis with a system model. Journal of Neurophysiology; 69:261-281.
- Kirkwood, A., and Bear, M.F. (1994) Hebbian synapses in visual cortex. Journal of Neuroscience; 14:1634-1645.
- Klink, R., and Alonso, A. (1993) Ionic mechanisms for the subthreshold oscillations and differential electroresponsiveness of medial entorhinal cortex layer II neurons. Journal of Neurophysiology; 70:144-156.
- Kohler, C. (1984) Morphological details of the projection from the presubiculum to the entorhinal area as shown with the novel PHA-L immunohistochemical tracing method in the rat. Neuroscience Letters; 45:285-290.
- Kohler, C. (1985) Intrinsic projections of the retrohippocampal region in the rat brain. I. The subicular complex. Journal of Comparative Neurology; 236:504-522.
- Kohler, C. (1986) Intrinsic connections of the retrohippocampal region in the rat brain. II. The medial entorhinal area. Journal of Comparative Neurology; 246:149-169.
- Kohler, C. (1988) Intrinsic connections of the retrohippocampal region in the rat brain. III. The lateral entorhinal area. Journal of Comparative Neurology; 271:208-228.
- Kohler, C., Chan-Palay, V., and Steinbusch, H. (1981) The distribution and orientation of serotonin fibers in the entorhinal and other retrohippocampal areas: an immunohistochemical study with anti-serotonin antibodies in the rat's brain. Anatomy and Embryology; 161:237-264.

- Kohler, C., Wu, J.-Y., Chan-Palay, V. (1985) Neurons and terminals in the retrohippocampal region in the rat's brain identified by anti-gamma-aminobutyric acid and anti-glutamic acid decarboxylase immunocytochemistry. Anatomy and Embryology; 173:35-44.
- Komisaruk, B.R. (1970) Synchrony between limbic system theta activity and rhythmical behaviors in rats. Journal of Comparative Physiology and Psychology; 70:482-492.
- Konopacki, J., Golebiewski, H. (1992) Theta rhythms in the rat medial entorhinal cortex in vitro: evidence for involvement of muscarinic receptors. Neuroscience Letters; 141:93-96.
- Konopacki, J., MacIver, M.B., Roth, S.H., and Bland, B.H. (1987) Carbachol-induced EEG theta activity in hippocampal brain slices. Brain Research; 405:196-198.
- Konopacki, J., Golebiewski, H., and Eckersdorf, B. (1992) Carbachol-induced theta-like activity in entorhinal cortex slices. Brain Research; 527:76-80.
- Kosel, K.C., Van Hoesen, G.W., and West, J.R. (1981) Olfactory bulb projections to the parahippocampal area of the rat. Journal of Comparative Neurology; 198:467-482.
- Kosel, K.C., Van Hoesen, G.W., and Rosene, D.L. (1982) Non-hippocampal cortical projections from the entorhinal cortex in the rat and rhesus monkey. Brain Research; 244:201-213.
- Kramis, R., Vanderwolf, C.H., and Bland, B.H. (1975) Two types of hippocampal rhythmical slow activity in both the rabbit and the rat: relations to behavior and effects of atropine, diethyl ether, urethane, and pentobarbitol. Experimental Neurology; 49:58-85.
- Krettek, J.E., and Price, J.L. (1977) Projections from the amygdaloid complex and adjacent olfactory structures to the entorhinal cortex and to the subiculum in the rat and cat. Journal of Comparative Neurology; 172:723-752.
- Krnjevic, K., and Phillis, J.W. (1963) Acetylcholine-sensitive cells in the cerebral cortex. Journal of Physiology; 166:296-327.
- Krug, M., Muler-Welde, P., Wagner, M., Ott, T., and Matthies, H. (1985) Functional plasticity in two afferent systems of the granule cells in the rat dentate area: frequency-related changes, long-term potentiation and heterosynaptic depression. Brain Research; 360:264-272.
- Lacaille, J.-C., and Harley, C.W. (1985) The action of norepinephrine in the dentate gyrus: beta-mediated facilitation of evoked potentials in vitro. Brain Research; 358:210-220.

- Landfield, P.W. (1988) Hippocampal neurobiological mechanisms of age-related memory dysfunction. Neurobiology of Aging; 9:571-579.
- Landfield, P.W. (1993) Impaired frequency potentiation as a basis for aging-dependent memory impairment: the role of excess calcium influx. Neuroscience Research Communications; 13:S19-22.
- Landfield, P.W., and Morgan, G. (1984) Chronically elevating plasma Mg^{2+} improves hippocampal frequency potentiation and reversal learning in aged and young rats. Brain Research; 322:167-171.
- Landfield, P.W., McGaugh, J.L., and Lynch, G. (1978) Impaired synaptic potentiation processes in the hippocampus of aged memory-deficient rats. Brain Research; 150:85-101.
- Landfield, P.W., Pitler, T.A., and Applegate, M.D. (1986) The effects of high Mg^{2+} -to- Ca^{2+} ratios on frequency potentiation in hippocampal slices of young and aged rats. Journal of Neurophysiology; 56:797-811.
- Larson, J., and Lynch, G. (1986) Induction of synaptic potentiation in the hippocampus by patterned stimulation involves two events. Science; 232:985-988.
- Larson, J., and Lynch, G. (1989) Theta pattern stimulation and the induction of LTP: the sequence in which synapses are stimulated determines the degree to which they potentiate. Brain Research; 439:49-58.
- Larson, J., Wong, D., and Lynch, G. (1986) Patterned stimulation at the theta frequency is optimal for the induction of hippocampal long-term potentiation. Brain Research; 368:347-350.
- Lashley, K. (1950) In search of the engram. Society of Experimental Biology; 4:454-482.
- Leung, L.S., and Fu, X.-W. (1994) Factors affecting paired-pulse facilitation in hippocampal CA1 neurons in vitro. Brain Research; 650:75-84.
- Leung, L.S., Shen, B., and Kaibara, T. (1992) Long-term potentiation induced by patterned stimulation of the commissural pathway to hippocampal CA1 region in freely moving rats. Neuroscience; 48:63-74.
- Levy, W.B., and Steward, O. (1979) Synapses as associative memory elements in the hippocampal formation. Brain Research; 175:233-245.
- Levy, W.B., and Steward, O. (1983) Temporal contiguity requirements for long-term associative potentiation/depression in the hippocampus. Neuroscience; 8:791-797.
- Lin, Y., and Phillis, W. (1991) Muscarinic agonist-mediated induction of long-term potentiation in rat cerebral cortex. Brain Research; 551:342-345.

- Lingenhol, K., and Finch, D.M. (1991) Morphological characterization of rat entorhinal neurons in vivo: soma-dendritic structure and axonal domains. Experimental Brain Research; 84:57-74.
- Little, W.A., and Shaw, G.L. (1975) A statistical theory of short and long term memory. Behavioral Biology; 14:115-133.
- Loesche, J., and Steward, O. (1977) Behavioral correlates of denervation and reinnervation of the hippocampal formation of the rat: recovery of alternation performance following unilateral entorhinal cortex lesions. Brain Research Bulletin; 2:31-39.
- Lopes da Silva, F. (1991) Neural mechanisms underlying brain waves: from neural membranes to networks. Electroencephalography and Clinical Neurophysiology; 79:81-93.
- Lopes da Silva, F.H., Witter, M.P., Boeijinga, P.H., and Lohman, A.H.M. (1990) Anatomical organization and physiology of the limbic cortex. Physiological Reviews; 70:453-511.
- Luskin, M.B., and Price, J.L. (1983) The laminar distribution of intracortical fibers originating in the olfactory cortex of the rat. Journal of Comparative Neurology; 216:292-302.
- Lynch, G., Kessler, M., Arai, A., and Larson, J. (1990) The nature and causes of hippocampal long-term potentiation. Progress in Brain Research; 83:233-250.
- Macrides, F., Eichenbaum, H.B., and Forbes, W.B. (1982) Temporal relationship between sniffing and the limbic theta rhythm during odor discrimination reversal learning. Journal of Neuroscience; 12:1705-1717.
- MacVicar, B.A., and Dudek, F.E. (1979) Intracellular recordings from hippocampal CA3 pyramidal cells during repetitive activation of the mossy fibers in vitro. Brain Research; 168:377-381.
- Madison, D.V., and Nicoll, R.A., (1984) Control of the repetitive discharge of rat CA1 pyramidal neurons in vitro. Journal of Physiology; 354:319-331.
- Madison, D.V., Lancaster, B., and Nicoll, R.A., (1987) Voltage clamp analysis of cholinergic action in the hippocampus. Journal of Neuroscience; 7:733-741.
- Madison, D.V., Malenka, R.C., and Nicoll, R.A. (1991) Mechanisms underlying long-term potentiation of synaptic transmission. Annual Review of Neuroscience; 14:379-397.
- Magelby, K.L. (1973a) The effect of repetitive stimulation on facilitation of transmitter release at the frog neuromuscular junction. Journal of Physiology; 234:327-352.

- Magelby, K.L. (1973b) The effect of tetanic and post-tetanic potentiation on facilitation of transmitter release at the frog neuromuscular junction. Journal of Physiology; 234:353-371.
- Magelby, K.L. (1987) Short-term changes in synaptic efficacy. In, Synaptic Function; W.E. Gall and W.M. Cowan (Eds.), John Wiley & Sons, Toronto, pp. 21-56.
- Magelby, K.L., and Zengel, J.E. (1975) A dual effect of repetitive stimulation on post-tetanic potentiation of transmitter release at the frog neuromuscular junction. Journal of Physiology; 245:163-182.
- Magelby, K.L., and Zengel, J.E. (1976) Augmentation: a process that acts to increase transmitter release at the frog neuromuscular junction. Journal of Physiology; 257:449-470.
- Magelby, K.L., and Zengel, J.E. (1982) A quantitative description of stimulation-induced changes in transmitter release at the frog neuromuscular junction. Journal of General Physiology; 80:613-638.
- Malenka, R.C. (1994) Synaptic plasticity in the hippocampus: LTP and LTD. Cell; 78:535-538.
- Malenka, R.C., and Nicoll, R.A. (1993) NMDA-receptor-dependent synaptic plasticity: multiple forms and mechanisms. Trends in Neurosciences; 16:521-527.
- Mallart, A., and Martin, A.R. (1967) An analysis of facilitation of transmitter release at the neuromuscular junction of the frog. Journal of Physiology; 193:697-694.
- Maren, S., and Baudry, M. (1995) Properties and mechanisms of long-term synaptic plasticity in the mammalian brain: relationships to learning and memory. Neurobiology of Learning and Memory; 63:1-18.
- Markram, J, and Segal, M. (1990) Acetylcholine potentiates responses to N-methyl-D-aspartate in the rat hippocampus. Neuroscience Letters; 113:62-65.
- Marr, D. (1971) Simple memory: a theory for archicortex. Philosophical Transactions of the Royal Society of London; 262:23-81.
- Marston, H.M., Everitt, B.J., and Robbins, T.W., (1993) Comparative effects of excitotoxic lesions of the hippocampus and septum diagonal band on conditional visual-discriminative and spatial learning. Neurophysiologia; 31:1099-1118.
- Matsuura, S., Hirayama, K., and Murata, R. (1993) Enhancement of synaptic facilitation during the progression of kindling epilepsy by amygdala stimulation. Journal of Neurophysiology; 70:602-609.

- McClelland, J.L. and Rumelhart, D.E. (1985) Distributed memory and the representation of general and specific information. Journal of Experimental Psychology: General; 114:159-188.
- McClelland, J.L., and Rumelhart, D.E. (1986) Parallel Distributed Processing: Explorations in the Microstructure of Cognition. MIT Press, Cambridge.
- McCormick, D.A., and Prince, D.A. (1986) Mechanisms of action of acetylcholine in the guinea-pig cerebral cortex in vitro. Journal of Physiology; 375:169-194.
- McIntyre, D.C., and Kelly, M.E. (1990) Is the pyriform cortex important for limbic kindling? In, Kindling 4; J.A. Wada (Ed.), Plenum Press, New York, pp. 21-32.
- McIntyre, D.C., and Plant, J.R. (1989) Pyriform cortex involvement in kindling. Neuroscience and Biobehavioral Reviews, 13:277-280.
- McLennan, H, and Miller, J.J. (1976) Frequency-related inhibitory mechanisms controlling rhythmical activity in the septal area. Journal of Physiology (London); 254:827-841.
- McNamara, R.K., and Skelton, R.W., (1992) Assessment of a cholinergic contribution to chlordiazepoxide-induced deficits of place learning in the Morris water maze. Pharmacology, Biochemistry and Behavior; 41:529-538.
- McNaughton, B.L. (1982) Long-term synaptic enhancement and short-term potentiation in rat fascia dentata act through different mechanisms. Journal of Physiology; 324:249-262.
- McNaughton, B.L. (1993) The mechanism of expression of long-term enhancement of hippocampal synapses: current issues and theoretical perspectives. Annual Review of Physiology; 55:375-396.
- McNaughton, N., & Miller, J.J. (1984) Medial septal projections to the dentate gyrus in the rat: electrophysiological analysis of distribution and plasticity. Experimental Brain Research; 56:243-256.
- McNaughton, B.L., Douglas, R.M., and Goddard, G.V. (1978) Synaptic enhancement in fascia dentata: cooperativity among coactive afferents. Brain Research; 157:277-293.
- McNaughton, B.L., Barnes, C.A., Rao, G., Baldwin, J., and Rasmussen, M. (1986) Long-term enhancement of hippocampal synaptic transmission and the acquisition of spatial information. Journal of Neuroscience; 6:563-571.
- Mezard, M., Nadal, J.P., and Toulouse, G. (1986) Solvable models of working memories. Journale de Physique; 47:1457-1462.
- Miller, R. (1989) Cortico-hippocampal interplay: self-organizing phase-locked loops for indexing memory. Psychobiology; 17:115-128.

- Mishkin, M. (1978) Memory in monkeys severely impaired by combined but not by separate removals of amygdala and hippocampus. Nature; 273:297-298.
- Mitchell, S.J., and Ranck, J.B. Jr. (1980) Generation of theta rhythm in medial entorhinal cortex of freely moving rats. Brain Research; 189:49-66.
- Mitchell, S.J., Rawlins, J.N.P., Steward, O., and Olton, D.S. (1982) Medial septal area lesions disrupt Θ rhythm and cholinergic staining in medial entorhinal cortex and produce impaired radial arm maze behavior in rats. Journal of Neuroscience; 2:292-302.
- Mitzdorf, U. (1985) Current source-density method and application in cat cerebral cortex: investigation of evoked potentials and EEG phenomena. Physiological Reviews; 65:37-100.
- Miyamoto, M., Kato, J., Narumi, S., and Nagaoka, A. (1987) Characteristics of memory impairment following lesioning of the basal forebrain and medial septal nucleus in rats. Brain Research; 419:19-31.
- Mizumori, S.J., Perez, G.M., Alvarado, M.C., Barnes, C.A., and McNaughton, B.L. (1990) Reversible inactivation of the medial septum differentially affects two forms of learning in rats. Brain Research; 528:12-20.
- Mody, I., Baimbridge, K.G., and Miller, J.J. (1984) Blockade of tetanic- and calcium-induced long-term potentiation in the hippocampal slice preparation by neuroleptics. Neuropharmacology; 23:625-631.
- Mokrushin, A.A, and Emel'yanov, N.A. (1991) Posttetanic and frequency potentiation in slices of rat olfactory cortex. Neuroscience and Behavioural Physiology; 21:349-352.
- Mokrushin, A.A, and Emel'yanov, N.A. (1993) Frequency-dependent plasticity of potentials evoked by repetitive stimulation of the lateral olfactory tract in rat olfactory cortex slices. Neuroscience Letters; 158:16-20.
- Moore, R.Y., and Card, J.P. (1984) Noradrenaline-containing neuron systems. In, Handbook of Chemical Neuroanatomy, Vol 2. Classical Transmitters in the CNS; A. Bjorklund and T. Hokfelt (Eds.), Elsevier, Amsterdam, pp. 123-156.
- Morris, R.G.M. (1989) Synaptic plasticity and learning: selective impairment of learning in rats and blockade of long-term potentiation in vivo by the N-methyl-D-aspartate receptor antagonist AP5. Journal of Neuroscience; 9:3040-3057.
- Morris, R.G.M., Garrud, P., Rawlins, J.N.P., and O'Keefe, J. (1982) Place navigation impaired in rats with hippocampal lesions. Nature; 297:681-683.

- Morris, R.G.M., Anderson, E., Lynch, G.S., and Baudry, M. (1986) Selective impairment of learning and blockade of long-term potentiation by an N-methyl-D-aspartate receptor antagonist, AP5. Nature; 319:774-776.
- Morris, R.G.M., Davis, S., and Butcher, S.P. (1990) Hippocampal synaptic plasticity and NMDA receptors: a role for information storage? Philosophical Transactions of the Royal Society of London B; 329:187-204.
- Moser, E., Mathiesen, I., and Andersen, P. (1993) Association between brain temperature and dentate field potentials in exploring and swimming rats. Science; 259:1324-1326.
- Moser, E., Moser, M.-B., and Andersen, P. (1994) Potentiation of dentate synapses initiated by exploratory learning in rats: dissociation from brain temperature, motor activity, and arousal. Learning and Memory; 1:55-73.
- Mosko, S., Lynch, G., and Cotman, C.W. (1973) The distribution of septal projections to the hippocampus of the rat. Journal of Comparative Neurology; 152:163-174.
- Moss, M., Mahut, H., and Zola-Morgan, S. (1981) Concurrent discrimination learning of monkeys after hippocampal, entorhinal, or fornix lesions. Journal of Neuroscience; 1:227-240.
- Mott, D.D., Xie, C.-W., Wilson, W.A., Swartzwelder, H.S., and Lewis, D.V. (1993) GABA_B autoreceptors mediate activity-dependent disinhibition and enhance signal transmission in the dentate gyrus. Journal of Neurophysiology; 69:674-691.
- Mumby, D.G., Wood, E.R., and Pinel, J.P.J. (1992) Object recognition memory is only mildly impaired in rats with lesions of the hippocampus and amygdala. Psychobiology; 20:18-27.
- Munoz, M.D., Nunez, A., and Garcia-Austt, E. (1991) Frequency potentiation in granule cells in vivo at theta frequency perforant path stimulation. Experimental Neurology; 113:74-78.
- Nathan, T., and Lambert, J.D.C. (1991) Depression of the fast IPSP underlies paired-pulse facilitation in area CA1 of the rat hippocampus. Journal of Neurophysiology; 66:1704-1715.
- Nathan, T., Jensen, M.S., and Lambert, J.D.C. (1990) GABA_B receptors play a major role in paired-pulse facilitation in area CA1 of the rat hippocampus. Brain Research; 531:55-65.
- Neuman, R.S., and Harley, C.W. (1983) Long-lasting potentiation of the dentate gyrus population spike by norepinephrine. Brain Research; 273:162-165.
- Nicholson, C., Freeman, J.A. (1975) Theory of current source density analysis and determination of conductivity tensor for anuran cerebellum. Journal of Neurophysiology; 38:356-368.

- Nickell, W.T., and Shipley, M.T. (1988) Neurophysiology of magnocellular forebrain inputs to the olfactory bulb in the rat: frequency potentiation of field potentials and inhibition of output neurons. Journal of Neuroscience; 8:4492-4502.
- Ning, T. and Bronzino, J.D. (1989) Bispectral analysis of the rat EEG during various vigilance states. IEEE Transactions on Biomedical Engineering; 36:497-499.
- Oja, E. (1982) A simplified neuron model as a principal component analyser. Journal of Mathematical Biology; 15:267-273.
- O'Keefe, J., and Nadel, L. (1979) Précis of O'Keefe & Nadel's The hippocampus as a cognitive map. Behavioral and Brain Sciences; 2:487-533.
- Olton, D.S., and Feustle, W.A. (1981) Hippocampal function required for non-spatial working memory. Experimental Brain Research; 41:380-389.
- Olton, D.S., Becker, J.T., and Handelmann, G.E. (1979) Hippocampus, space, and memory. Behavior and Brain Science; 2:313-365.
- Otto, T., Eichenbaum, H. (1992) Complimentary roles of the orbital prefrontal cortex and the perirhinal-entorhinal cortices in an odor-guided delayed-nonmatching-to-sample task. Behavioral Neuroscience; 106:762-775.
- Otto, T., Schottler, F., Staubli, U., Eichenbaum, H., and Lynch, G. (1991) Hippocampus and olfactory discrimination learning: effects of entorhinal cortex lesions on olfactory learning and memory in a successive-cue, go-no-go task. Behavioral Neuroscience; 105:111-119.
- Pavrides, C., Greenstein, Y.J., Grudman, M., and Winson, J. (1988) Long-term potentiation in the dentate gyrus is induced preferentially on the positive phase of theta-rhythm. Brain Research; 439:383-387.
- Paxinos, G., and Watson, C. (1986) The Rat Brain in Stereotaxic Coordinates, 2nd edn., Orlando, Academic Press.
- Penetar, D.M., and McDonough, J.H. (1983) Effects of cholinergic drugs on delayed match to sample performance of Rhesus monkeys. Pharmacology, Biochemistry and Behavior; 19:663-667.
- Penfield, W., and Milner, B. (1958) Memory deficit produced by bilateral lesions in the hippocampal zone. Archives of Neurology and Psychiatry; 79:475-497.
- Perio, A., Terranova, J.P., Worms, P., Bluthe, R.M., Dantzer, R., and Biziere, K. (1989) Specific modulation of social memory in rats by cholinomimetic and nootropic drugs, by benzodiazepine inverse agonists, but not by psychostimulants. Psychopharmacology; 97:262-268.

- Peterson, R.C. (1977) Scopolamine-induced learning failures in man. Psychopharmacologia; 52:283-289.
- Petsche, H., Stumpf, G., and Gogolak, G. (1962) The significance of the rabbit's septum as a relay station between the midbrain and the hippocampus. I. The control of hippocampus arousal activity by the septum cells. Electroencephalography and Clinical Neurophysiology; 19:25-33.
- Pitler, T.A., and Alger, B.E. (1992) Cholinergic excitation of GABAergic interneurons in the rat hippocampal slice. Journal of Physiology; 450:127-142.
- Pitler, T.A., and Landfield, P.W. (1987) Postsynaptic membrane shifts during frequency potentiation of the hippocampal EPSP. Journal of Neurophysiology; 58:866-882.
- Pitler, T.A., and Landfield, P.W. (1990) Aging-related prolongation of calcium spike duration in rat hippocampal slice neurons. Brain Research; 508:1-6.
- Plumbley, M.D. (1993) Efficient information transfer and anti-Hebbian neural networks. Neural Networks; 6:823-833.
- Press, G.A., Amaral, D.G., and Squire, L.R. (1989) Hippocampal abnormalities in amnesic patients revealed by high-resolution magnetic resonance imaging. Science; 341:54-57.
- Price, J.L., and Powell, T.P.S. (1971) Certain observations on the olfactory pathway. Journal of Anatomy; 110:105-126.
- Racine, R.J. (1972a) Modification of seizure activity by electrical stimulation. I. After-discharge threshold. Electroencephalography and Clinical Neurophysiology; 32:269-279.
- Racine, R.J. (1972b) Modification of seizure activity by electrical stimulation. II. Motor seizure. Electroencephalography and Clinical Neurophysiology; 32:281-294.
- Racine, R.J. (1975) Modification of seizure activity by electrical stimulation: cortical areas. Electroencephalography and Clinical Neurophysiology; 38:1-12.
- Racine, R.J. (1978) Kindling: the first decade. Neurosurgery, 3:234-252.
- Racine, R.J., and Burnham, W.M. (1984) The Kindling Model. In, Electrophysiology of Epilepsy; P.A. Schwartzkroin and H.V. Wheal (Eds.), Academic Press, London, England, pp. 153-171.
- Racine, R.J., and Cain, D.P. (1991) Kindling-induced potentiation. In, Kindling and Synaptic Plasticity; F. Morrell (Ed.), Birkhauser, Boston, pp. 38-53.

- Racine, R.J., and Kairiss, E.W. (1987) Long-term potentiation phenomena: the search for the mechanisms underlying memory storage processes. In, Neuroplasticity, Learning and Memory. Alan R. Liss, New York, pp. 173-197.
- Racine, R.J., and Milgram, N.W. (1983) Short-term potentiation phenomena in the rat limbic forebrain. Brain Research; 260:201-216.
- Racine, R.J., Gartner, J.G., and Burnham, W.M. (1972) Epileptiform activity and neural plasticity in limbic structures. Brain Research; 74:262-268.
- Racine, R.J., Newberry, F., and Burnham, W.M. (1975) Post-activation potentiation and the kindling phenomenon. Electroencephalography and Clinical Neurophysiology; 39:261-271.
- Racine, R.J., Milgram, N.W., and Hafner, S. (1983) Long-term potentiation phenomena in the rat limbic forebrain. Brain Research; 260:217-231.
- Racine, R.J., Mosher, M., and Kairiss, E.W. (1988) The role of the pyriform cortex in the generation of interictal spikes in the kindled preparation. Brain Research; 454:251-263.
- Racine R.J., Moore, K.-A, and Evans, C. (1991a) Kindling-induced potentiation in the piriform cortex. Brain Research; 556:218-225.
- Racine R.J., Moore, K.-A, and Wicks, S. (1991b) Activation of the NMDA receptor: a correlate in the dentate gyrus field potential and its relationship to long-term potentiation and kindling. Brain Research; 556:226-239.
- Racine, R.J., Teskey, G.C., Wilson, D., Seidlitz, E., and Milgram, N.W. (1994) Post-activation potentiation and depression in the neocortex of the rat. II. Chronic preparations. Brain Research; 637:83-96.
- Racine, R.J, Chapman, C.A., Teskey, G.C., and Milgram, N.W. (1995a) Post-activation potentiation in the neocortex. III. Kindling-induced potentiation in the chronic preparation. Brain Research; 702:77-86.
- Racine, R.J, Chapman, C.A., Trepel, C.D., Teskey, G.C., and Milgram, N.W. (1995b) Post-activation potentiation in the neocortex. IV. Multiple sessions required for induction of long-term potentiation in the chronic preparation. Brain Research; 702:87-93.
- Ramirez, J.J., and Stein, D.G. (1964) Sparing and recovery of spatial alternation performance after entorhinal cortex lesions in rats. Behavioral Brain Research; 13:53-61.
- Rasmussen, M., Barnes, C.A., and McNaughton, B.L. (1989) A systematic test of cognitive mapping, working-memory, and temporal discontinuity theories of hippocampal function. Psychobiology; 17:335-348.

- Rauch, S.L., and Raskin, L.A. (1984) Cholinergic mediation of spatial memory in the preweanling rat: application of the radial arm maze paradigm. Behavioral Neuroscience; 98:35-43.
- Ravel, N., Vigouroux, M., Elaagouby, A., and Gervais, R. (1992) Scopolamine impairs delayed matching in an olfactory task in rats. Psychopharmacology; 109:439-443.
- Rawlins, J.N.P., and Green, K.F. (1977) Lamellar organization in the rat hippocampus. Experimental Brain Research; 28:335-344.
- Robinson, G.B. (1986) Enhanced long-term potentiation induced in rat dentate gyrus by coactivation of septal and entorhinal inputs: temporal constraints. Brain Research; 379:56-62.
- Robinson, B.B. (1992) Maintained saturation of hippocampal long-term potentiation does not disrupt acquisition of the eight-arm radial maze. Hippocampus; 2:389-396.
- Robinson, G.B., and Racine, R.J. (1982) Heterosynaptic interactions between septal and entorhinal inputs to the dentate gyrus: long-term potentiation effects. Brain Research; 249:162-166.
- Robinson, G.B., and Racine, R.J. (1986) Interactions between septal and entorhinal inputs to the rat dentate gyrus: facilitation effects. Brain Research; 379:63-67.
- Rodriguez, R., and Haberly, L.B. (1989) Analysis of synaptic events in the Opossum piriform cortex with improved current source-density techniques. Journal of Neurophysiology; 61:702-718.
- Roman, F., Staubli, U., and Lynch, G. (1987) Evidence for synaptic potentiation in a cortical network during learning. Brain Research; 418:221-226.
- Room, P., Groenewegen, H.J. (1986) Connections of the parahippocampal cortex. I. Cortical afferents. Journal of Comparative Neurology; 251:415-450.
- Room, P., Groenewegen, H.J., and Lohman, A.H.M. (1984) Inputs from the olfactory bulb and olfactory cortex to the entorhinal cortex in the cat. II. Anatomical observations. Experimental Brain Research; 56:488-496.
- Ross, G.M., and Dunwiddie, T.V. (1986) Induction of hippocampal long-term potentiation using physiologically patterned stimulation. Neuroscience Letters; 69:244-248.
- Russell, R.D., and Stripling, J.S. (1985) Effect of olfactory bulb kindling on evoked potentials in the piriform cortex. Brain Research; 361:61-69.

- Sakimura, K., Kutsuwada, T., Ito, I., Manabe, T., Takayama, C., Kushiya, E., Yagi, T., Aizawa, S., Inoue, Y., Sugiyama, H., and Mishina, M. (1995) Reduced hippocampal LTP and spatial learning in mice lacking NMDA receptor $\epsilon 1$ subunit. Nature; 373:151-155.
- Sato, M., Racine, R.J., and McIntyre, D.C. (1990) Kindling: basic mechanisms and clinical validity. Electroencephalography and Clinical Neurophysiology; 76:459-472.
- Schenk, F., and Morris, R.G.M. (1985) Dissociation between components of spatial memory in rats after recovery from the effects of retrohippocampal lesions. Experimental Brain Research; 58:11-28.
- Schwartzkroin, P.A. (1975) Characteristics of CA1 neurons recorded intracellularly in the hippocampal in vitro slice preparation. Brain Research; 85:423-436.
- Schwerdtfeger, W.K., Buhl, E.H., and Germroth, P. (1990) Disynaptic olfactory input to the hippocampus mediated by stellate cells in the entorhinal cortex. Journal of Comparative Neurology; 292:163-177.
- Scoville, W.B., and Milner, B. (1957) Loss of recent memory after bilateral hippocampal lesions. Journal of Neurology, Neurosurgery and Psychiatry; 20:11-21.
- Segal, M. (1977) Afferents to the entorhinal cortex of the rat studied by the method of retrograde transport of horseradish peroxidase. Experimental Neurology; 57:750-765.
- Segev, I. (1992) Single neurone models: oversimple, complex and reduced. Trends in Neurosciences; 15:414-421.
- Sejnowski, T.J., and Tesauro, G. (1989) The Hebb rule for synaptic plasticity: algorithms and implementations. In, Neural Models of Plasticity; Academic Press, pp. 94-103.
- Semba, K., and Komisaruk, B.R. (1978) Phase of theta activity in relation to different limb movements in awake rats. Electroencephalography and Clinical Neurophysiology; 44:61-71.
- Shepherd, G.M. (1972) Synaptic organization of the mammalian olfactory bulb. Physiological Reviews; 52:864-917.
- Shiple, M.T. (1975) The topographical and laminar organization of the presubiculum's projection to the ipsi- and contralateral entorhinal cortex in the guinea pig. Journal of Comparative Neurology; 160:127-146.
- Singer, W. (1993) Synchronization of cortical activity and its putative role in information processing and learning. Annual Review of Physiology; 55:349-374.

- Singer, W., and Artola, a. (1991) The role of NMDA receptors in use-dependent synaptic plasticity of the visual cortex. In, Excitatory Amino Acids and Synaptic Function., Academic Press, pp. 333-359.
- Skelton, R.W., and McNamara, R.K. (1992) Bilateral knife cuts to the perforant path disrupt spatial learning in the Morris water maze. Hippocampus; 2:73-80.
- Soffie, M., and Lamberty, Y. (1988) Scopolamine effects on juvenile conspecific recognition in rats: possible interaction with olfactory sensitivity. Behavioural Processes; 17:181-190.
- Sorensen, K.E., and Shipley, M.T. (1979) Projections from the subiculum to the deep layers of the ipsilateral presubicular and entorhinal cortices. Journal of Comparative Neurology; 188:313-334.
- Spencer, S.S., and Spencer, D.D. (1994) Entorhinal - hippocampal interactions in medial temporal lobe epilepsy. Epilepsia; 35:721-727.
- Squire, L.R. (1992) Declarative and nondeclarative memory: multiple brain systems supporting learning and memory. Journal of Cognitive Neuroscience; 4:232-242.
- Squire, L.R., and Zola-Morgan, S. (1991) The medial temporal lobe memory system. Science; 253:1380-1386.
- Staubli, U., and Lynch, G. (1987) Stable hippocampal long-term potentiation elicited by "theta" pattern stimulation. Brain Research; 435:227-234.
- Staubli, U., Ivy, G., and Lynch, G. (1984) Hippocampal denervation causes rapid forgetting of olfactory information in rats. Proceedings of the National Academy of Sciences; 81:5885-5887.
- Staubli, U., Fraser, D., Kessler, M., and Lynch, G. (1986) Studies on retrograde and anterograde amnesia of olfactory memory after denervation of the hippocampus by entorhinal cortex lesions. Behavioural and Neural Biology; 46:432-444.
- Steriade, M., Gloor, P., Llinas, R.R., Lopes da Silva, F.H., and Mesulam, M.M. (1990) Basic mechanisms of cerebral rhythmic activities. Electroencephalography and Clinical Neurophysiology; 76:481-508.
- Stevens, R. (1981) Scopolamine impairs spatial maze performance in rats. Physiology and Behavior; 27:385-386.
- Steward, O. (1981) Evaluation of short-term cue recollection following entorhinal cortical lesions in rats. Behavioral and Neural Biology; 31:187-197.

- Steward, O., and Scoville, S.A. (1976) Cells of origin of entorhinal cortical afferents to the hippocampus and fascia dentata of the rat. Journal of Comparative Neurology; 169:347-370.
- Stewart, M., and Fox, S.E. (1990) Do septal neurons pace the hippocampal theta rhythm? Trends in Neurosciences; 13:163-168.
- Stockbridge, N., and Moore, J.W. (1984) Dynamics of intracellular calcium and its possible relationship to phasic transmitter release and facilitation at the frog neuromuscular junction. Journal of Neuroscience; 4:803-811.
- Stringer, J.L., and Lothman, E.W. (1992) Reverberatory seizure discharges in hippocampal - parahippocampal circuits. Experimental Neurology; 116:198-203.
- Stripling, J.S., and Patneau, D.K. (1990) Seizure mechanisms in the piriform cortex. In, Kindling 4; J.A. Wada (Ed.), Plenum Press, New York, pp. 45-57.
- Sutherland, R.J., and Rudy, J.W. (1989) Configural association theory: the role of the hippocampal formation in learning, memory, and amnesia. Psychobiology; 17:129-144.
- Sutherland, R.J., Whishaw, I.Q., and Regehr, J.C. (1982) Cholinergic receptor blockade impairs spatial localization by use of distal cues in the rat. Journal of Comparative Physiology and Psychology; 96:563-573.
- Sutherland, R.J., Dringenberg, H.C., and Hoelsing, J.M. (1993) Induction of long-term potentiation at perforant path dentate synapses does not affect place learning or memory. Hippocampus; 3:141-148.
- Sutula, T., and Steward, O.J. (1986) Quantitative analysis of synaptic potentiation during kindling of the perforant path. Neurophysiology; 56:732-746.
- Swanson, L.W., and Cowan, W.M. (1977) An autoradiographic study of the organization of the efferent connections of the hippocampal formation in the rat. Journal of Comparative Neurology; 172:49-84.
- Swanson, L.W., and Kohler, C. (1986) Anatomical evidence for direct projections from the entorhinal area to the entire cortical mantle in the rat. Journal of Neuroscience; 6:3010-3023.
- Taube, J.S., and Schwartzkroin, P.A. (1988) Mechanisms of long-term potentiation: a current source-density analysis. Journal of Neuroscience; 8:1645-1655.
- Terry, R.D., and Davies, P. (1980) Dementia of the Alzheimer type. Annual Review of Neuroscience; 3:77-95.
- Teskey, G.C., and Racine, R.J. (1993) Increased spontaneous unit discharge rates following electrical kindling in the rat. Brain Research; 624:11-18.

- Teyler, T.J., and DiScenna, P. (1984) Long-term potentiation as a candidate mnemonic device. Brain Research Reviews; 7:15-28.
- Teyler, T.J., and DiScenna, P. (1986) The hippocampal memory indexing theory. Behavioral Neuroscience; 100:147-154.
- Teyler, T.J., and DiScenna, P. (1987) Long-term potentiation. Annual Review of Neuroscience; 10:131-161.
- Thompson, A.M. and Deuchars, J. (1994) Temporal and spatial properties of local circuits in neocortex. Trends in Neuroscience; 17:119-126.
- Thompson, R. (1976) Entorhino-subicular lesions: amnesic effects on an assortment of learned responses in the white rat. Bulletin of the Psychonomic Society; 8:433-434.
- Thompson, S.M., and Gähwiler, B.H. (1989) Activity-dependent disinhibition. I. Repetitive stimulation reduces IPSP driving force and conductance in the hippocampus in vitro. Journal of Neurophysiology; 61:501-511.
- Turner, R.W., and Miller, J.J. (1982) Effects of extracellular calcium on low frequency induced potentiation and habituation in the in vitro hippocampal slice preparation. Canadian Journal of Physiology and Pharmacology; 60:266-275.
- Turner, R.W., Richardson, T.L., and Miller, J.J. (1983) Ephaptic interactions contribute to paired pulse and frequency potentiation of hippocampal field potentials. Experimental Brain Research; 54:567-570.
- Vanderwolf, C.H. (1969) Hippocampal electrical activity and voluntary movement in the rat. Electroencephalography and Clinical Neurophysiology; 26:407-418.
- Vanderwolf, C.H. (1988) Cerebral activity and behavior: control by central cholinergic and serotonergic systems. International Review of Neurobiology; 30:225-340.
- Vanderwolf, C.H. (1992) The electrocorticogram in relation to physiology and behavior: a new analysis. Electroencephalography and Clinical Neurophysiology; 82:165-175.
- Van Groen, T., and Wyss, M. (1990) The connections of presubiculum and parasubiculum in the rat. Brain Research; 518:227-243.
- Van Groen, T., Lopes da Silva, F.H., and Wadman, W.J. (1987) Synaptic organization of olfactory inputs and local circuits in the entorhinal cortex: a current source density analysis in the cat. Experimental Brain Research; 67:615-622.

- Van Hoesen, G.W., Pandya, D.N. (1975) Some connections of the entorhinal (area 28) and perirhinal (area 35) cortices of the Rhesus monkey. 1. Temporal lobe afferents. Brain Research; 95:1-24.
- Van Hoesen, G.W. (1982) The parahippocampal gyrus. New observations regarding its cortical connections in the monkey. Trends in Neurosciences; 5:345-350.
- Van Hoesen, G.W., Pandya, D.N., and Butters, N. (1972) Cortical afferents to the entorhinal cortex of the Rhesus monkey. Science; 175:1471-1473.
- Van Hoesen, G.W., Hyman, B.T., and Damasio, A.R. (1991) Entorhinal cortex pathology in Alzheimer's disease. Hippocampus; 1:1-8.
- Watts, J., Stevens, R., and Robinson, C. (1981) Effects of scopolamine on radial arm maze performance in rats. Physiology and Behavior; 26:845-851.
- White, T.D., Tan, A.M., and Finch, D.M. (1990) Functional reciprocal connections of the rat entorhinal cortex and subicular complex with the medial frontal cortex: an in vivo intracellular study. Brain Research; 533:95-106.
- White, W.F., Nadler, J.V., Cotman, C.W. (1979) Analysis of short-term plasticity at the perforant path - granule cell synapse. Brain Research; 178:41-53.
- Wilcox, K.S., and Dichter, M.A. (1994) Paired-pulse depression in cultured hippocampal neurons is due to a presynaptic mechanism independent of GABA_B autoreceptor activation. Journal of Neuroscience; 14:1775-1788.
- Wilson, M.A., and Bower, J.M. (1991) A computer simulation of oscillatory behavior in primary visual cortex. Neural Computation; 3:498-509.
- Wilson, M.A., and Bower, J.M. (1992) Cortical oscillations and temporal interactions in a computer simulation of piriform cortex. Journal of Neurophysiology; 67:981-995.
- Wilson, R.C., and Steward, O. (1978) Polysynaptic activation of the dentate gyrus of the hippocampal formation: an olfactory input via the lateral entorhinal cortex. Experimental Brain Research; 33:523-534.
- Winson, J. (1978) Loss of hippocampal theta rhythm results in spatial memory deficit in the rat. Science; 201:160-163.
- Winson, J., and Azbug, C. (1978) Dependence upon behavior of neuronal transmission from perforant pathway through entorhinal cortex. Brain Research; 147:422-427.
- Wise, R.A. (1989) The brain and reward. In, The Neuropharmacological Basis of Reward; J.M. Leibman and S.J. Cooper (Eds.), Carendon Press, Oxford, pp. 377-424.

- Whishaw, I.Q. (1989) Dissociating performance and learning deficits on spatial navigation tasks in rats subjected to cholinergic muscarinic blockade. Brain Research Bulletin; 23:347-358.
- Witter, M.P. (1993) Organization of the entorhinal-hippocampal system: a review of current anatomical data. Hippocampus; 3:33-44.
- Witter, M.P., Groenewegen, H.J. (1984) Laminar origin and septotemporal distribution of entorhinal and perirhinal projections to the hippocampus in the cat. Journal of Comparative Neurology; 224:371-385.
- Witter, M.P., Groenewegen, H.J., Lopes da Silva, F.H., and Lohman, H.M. (1989) Functional organization of the extrinsic and intrinsic circuitry of the parahippocampal region. Progress in Neurobiology; 33:161-253.
- Woolley, D.E., and Rarron, B.A. (1968) Hippocampal responses evoked by stimulation of the prepyriform cortex in the rat. Electroencephalography and Clinical Neurophysiology; 24:63-74.
- Wouterlood, F.G., and Nederlof, J. (1983) Terminations of olfactory afferents on layer II and III neurons in the entorhinal area: degeneration-Golgi-electron microscopic study in the rat. Neuroscience Letters; 36:105-110.
- Wouterlood, F.G., Mugnaini, E., and Nederlof, J. (1985) Projection of olfactory bulb efferents to layer I GABAergic neurons in the entorhinal area. Combination of anterograde degeneration and immunoelectron microscopy in rat. Brain Research; 343:283-296.
- Wouterlood, F.G., Saldana, E., and Witter, M.P. (1990) Projection from the nucleus reuniens thalami to the hippocampal region: light and electron microscopic tracing study in the rat with the anterograde tracer Phaseolus vulgaris-leucoagglutinin. Journal of Comparative Neurology; 296:179-203.
- Wu, L.G., and Saggau, P. (1994) Presynaptic calcium is increased during normal synaptic transmission and paired-pulse facilitation, but not in long-term potentiation in area CA1 of hippocampus. Journal of Neuroscience; 14:645-654.
- Wyss, J.M., (1981) An autoradiographic study of the efferent connections of the entorhinal cortex in the rat. Journal of Comparative Neurology; 199:495-512.
- Wyss, J.M., and Van Groen T., (1992) Connections between the retrosplenial cortex and the hippocampal formation in the rat: a review. Hippocampus; 2:1-12.
- Xu, Y., Haykin, S., Racine, R.J., and Chapman, C.A. (1994) Time-frequency analysis of EEG from entorhinal cortex and dentate gyrus. Society for Neuroscience Abstracts; 20:1434.

- Yamamoto, C. (1972) Activation of hippocampal neurons by mossy fiber stimulation in thin brain sections in vitro. Experimental Brain Research; 14:423-435.
- Yeckel, M.F., and Berger, T.W. (1990) Feedforward excitation of the hippocampus by afferents from the entorhinal cortex: redefinition of the role of the trisynaptic pathway. Proceedings of the National Academy of Sciences; 87:5832-5836.
- Zalutsky, R.A., and Nicoll, R.A. (1990) Comparison of two forms of long-term potentiation in single hippocampal neurons. Science; 248:1619-1624.
- Zengel, J.E., and Magelby, K.L. (1980) Differential effects of Ba^{2+} , Sr^{2+} , and Ca^{2+} on stimulation-induced changes in transmitter release at the frog neuromuscular junction. Journal of General Physiology; 76:175-211.
- Zengel, J.E., and Magelby, K.L. (1982) Augmentation and facilitation of transmitter release: a quantitative description at the frog neuromuscular junction. Journal of General Physiology; 80:583-611.
- Zipser, D. (1991) Recurrent network model of the neural mechanism of short-term active memory. Neural Computation; 3:179-193.
- Zola-Morgan, S., and Squire, L.R. (1986) Memory impairment in monkeys following lesions limited to the hippocampus. Behavioral Neuroscience; 100:155-160.
- Zola-Morgan, S., and Squire, L.R. (1990) The primate hippocampal formation: evidence for a time-limited role in memory storage. Science; 250:288-290.
- Zola-Morgan, S., Squire, L.R., Amaral, D.G. (1986) Human amnesia and the medial temporal region: enduring memory impairment following a bilateral lesion limited to field CA1 of the hippocampus. Journal of Neuroscience; 6:2950-2967.
- Zola-Morgan, S., Squire, L.R., and Amaral, D.G. (1989a) Lesions of the amygdala that spare adjacent cortical regions do not impair memory or exacerbate the impairment following lesions of the hippocampal formation. Journal of Neuroscience; 9:1922-1936.
- Zola-Morgan, S., Squire, L.R., Amaral, D.G., and Suzuki, W.A. (1989b) Lesions of perirhinal and parahippocampal cortex that spare the amygdala and hippocampal formation produce severe memory impairment. Journal of Neuroscience; 9:4355-4370.
- Zola-Morgan, S., Squire, L.R., Rempel, N.L., Clower, R.P., and Amaral, D.G. (1992) Enduring memory impairment in monkeys after ischemic damage to the hippocampus. Journal of Neuroscience; 12:2582-2596.
- Zucker, R.S. (1989) Short-term synaptic plasticity. Annual Review of Neuroscience; 12:13-31.

Zucker, R.S., and Stockbridge, N. (1983) Presynaptic calcium diffusion and the time courses of transmitter release and synaptic facilitation at the squid giant synapse. Journal of Neuroscience; 3:1263-1269.